

Copyright
by
Cynthia Ann Finley
2004

**The Dissertation Committee for Cynthia Ann Finley Certifies that this is the
approved version of the following dissertation:**

**Designing and Analyzing Test Program with Censored Data for Civil
Engineering Applications**

Committee:

Robert B. Gilbert, Supervisor

Philip C. Bennett

Daene C. McKinney

Ellen M. Rathje

Stephen G. Wright

**Designing and Analyzing Test Programs
with Censored Data for Civil Engineering Applications**

by

Cynthia Ann Finley, B.S., M.S.C.E.

Dissertation

Presented to the Faculty of the Graduate School of

The University of Texas at Austin

in Partial Fulfillment

of the Requirements

for the Degree of

Doctor of Philosophy

The University of Texas at Austin

May 2004

Dedication

This dissertation is dedicated to my faithful friend

Sarah F. O'Donnell

and to my husband

Sean W. O'Donnell

Acknowledgements

While pursuing this degree at the University of Texas at Austin, I received a vast amount of support from my professors, friends, and family. I am sincerely grateful to my advisor, Dr. Robert Gilbert, for his guidance in this research and the many opportunities he provided for me to learn. I would also like to thank the other members of my committee for reviewing this dissertation. My many fellow classmates over the years at UT made my time here immensely enjoyable, and my life has been enriched by knowing all of you. I appreciate all the love and support given to me by my mother during graduate school, and I thank my father for guiding me to study civil engineering.

Finally, I can never express my gratitude to my husband, Sean O'Donnell, who inspired me to pursue a Ph.D. and gave me a tremendous amount of encouragement, love, and understanding while I obtained this degree.

Designing and Analyzing Test Programs with Censored Data for Civil Engineering Applications

Publication No. _____

Cynthia Ann Finley, Ph.D.

The University of Texas at Austin, 2004

Supervisor: Robert B. Gilbert

The objective of this research was to develop a method for incorporating censored data into the design and analysis of test programs. In engineering applications, it is common to encounter censored data. The exact value of a censored data point is not known, only that it is above or below some specified threshold value. Existing methods for analyzing censored data are limited and usually involve assumptions about the data, such as normally-distributed or statistically independent data.

This research extends the First-Order Second-Moment (FOSM) Bayesian method (Gilbert 1999) to data sets that include censored data and have any type of distribution. This method is used for test program design and data analysis, allowing the Bayesian approach to be applied to practical engineering problems with large data sets and correlated data. The extension for censored data was validated through numerical experiments.

The method developed for analysis of censored data with a non-normal distribution was applied to a real site with contaminated groundwater. The concentration

measurements from the site, which were taken both before and after remediation, were calibrated with a groundwater model. The calibration resulted in reasonable estimates for the model parameters describing the physical characteristics of the site. The calibration also successfully fit the non-normal distribution of the measurements. The method was proven useful in considering all the complexities of the site: concentrations measured above and below the detection limit, the effects of remediation on the concentrations, measurements at many different times and locations, and correlations between concentrations that represent the heterogeneities at the site and the random errors in measurements. The method was also used to predict future contaminant concentrations at the site, which is helpful in making decisions regarding monitoring and remediation.

Table of Contents

List of Tables	xii
List of Figures	xiv
Chapter 1. Introduction	1
1.1 Background	1
1.2 Objectives and Approach of Research	2
1.3 Organization of Dissertation	4
Chapter 2: Censored Data Background Information	6
2.1 Introduction	6
2.2 Censored Data in Civil Engineering Applications	6
2.3 Parameter Estimator Methods for Censored Data	10
2.3.1 Analysis of Proof Load Tests	10
2.3.2 Analysis of Concentrations below the Detection Limit	11
2.4 Summary	12
Chapter 3. Bayesian Method with Point Measurements	13
3.1 Introduction	13
3.2 Bayesian Approach	13
3.3 Example Use of Bayes' Theorem	15
3.4 FOSM Bayesian Method	19
3.4.1 Example Application of the FOSM Bayesian Method	20
3.4.2 Notation used in FOSM Bayesian Method	22
3.4.3 Formulation of FOSM Bayesian Method for Data Analysis	23
3.4.4 Formulation of FOSM Bayesian Method for Test Program Design	27
3.4.5 Second Derivatives of the Natural Logarithm of the Likelihood Function	30
3.4.6 Likelihood Function for Normally-Distributed Data	32
3.4.6.1 Conditional Likelihood Function	33
3.4.6.2 Conditional Moments	34

3.4.7 Likelihood Function for Non-Normally Distributed Data	36
3.4.7.1 Hermite Polynomial Transform Function	37
3.4.7.2 Likelihood Function	41
3.4.7.3 Conditional Moments	43
3.5 Summary	44
Chapter 4. Bayesian Method with Censored Measurements	46
4.1 Introduction	46
4.2 Censored Data Points	46
4.3 Likelihood function for a Censored Data Point	50
4.3.1 Likelihood Function for a Normally-Distributed Censored Data Point	50
4.3.2 Likelihood Function for a Non-Normally Distributed Data Point	51
4.4 Conditional Moments for Censored Data	53
4.4.1 Conditional Moments for a Normally-Distributed Censored Data Point	53
4.4.1.1 Conditional Moments for One Known Data Point	54
4.4.1.2 Conditional Moments for Multiple Known Data Points	56
4.4.1.3 Conditional Moments for the Special Case of Independent Data	59
4.4.1.4 Moments for Censored Region of a Normally-Distributed Data Point	59
4.4.2 Moments for Censored Region of a Non-Normally-Distributed Data Point	60
4.5 Censored Data in Test Program Design	71
4.6 Summary	74
Chapter 5. Effect of Censored Measurements on Model Calibration	75
5.1 Introduction	75
5.2 Effect of Censored Data for Normally-Distributed Data	75
5.2.1 Simple Model	75
5.2.2 Method of Evaluation	77
5.2.3 Effect of Data Set Size	80
5.2.4 Effect of Censored Data on Estimated Mean Values	82

5.2.5	Effect of Censored Data on Estimated Standard Deviations of Model Parameters.....	84
5.2.6	Effect of Censored Data on Estimated Correlations between Model Parameters.....	92
5.3	Methods for Evaluating Expected Censored Data.....	95
5.3.1	Complete Numerical Integration.....	95
5.3.2	Using Prior Mean Model Parameters.....	96
5.3.3	Complete Analytical Approximation.....	97
5.4	Effect of Censored Data for Non-Normally-Distributed Data.....	101
5.5	Summary.....	109
Chapter 6. Case Study Application – Model for Measured Contaminant Concentrations		
		110
6.1	Introduction.....	110
6.2	French Limited Site.....	110
6.2.1	Site Description.....	111
6.2.2	Site Hydrogeology	111
6.2.3	Groundwater Investigation.....	113
6.2.4	Site Remediation.....	114
6.3	Model for Benzene Concentrations	116
6.3.1	Model for Mean Concentrations	117
6.3.2	Model Parameters for Remediation Effects.....	124
6.3.3	Model for Covariance of Data	128
6.3.4	Distribution for Natural Logarithm of Measurements.....	136
6.4	Summary.....	136
Chapter 7. Case Study Application – Calibration of Groundwater Model.....		
		137
7.1	Introduction.....	137
7.2	Model Calibration	137
7.2.1	Data from the French Limited Site	138
7.2.2	Model Parameters for Calibration.....	139
7.3	Calibration Process	143
7.4	Calibration Results.....	144

7.4.1 Updated Means and Standard Deviations of Model Parameters	145
7.4.2 Mean Model Parameters	147
7.4.3 Covariance Model Parameters	149
7.4.4 Data Distribution Parameters	152
7.4.5 Correlations between Model Parameters	154
7.4.6 Comparison of Model-Predicted and Measured Concentrations	156
7.5 Concentration Predictions	159
7.6 Summary	163
Chapter 8. Conclusions	164
8.1 Method Developed for Analyzing Censored Data	164
8.1.1 Conclusions	164
8.1.2 Recommendations for Future Work	166
8.2 Application of New Method to Contaminated Groundwater	167
8.2.1 Conclusions	168
8.2.2 Recommendations for Future Work	171
Appendix A. Derivation of Moments for Censored Normal Distribution	172
A.1 Mean of Censored Region	173
A.2 Variance of Censored Region	177
A.3 Mean of Non-Censored Region	179
A.4 Variance of Non-Censored Region	181
A.5 Alternative Expressions for Moments of Non-Censored Region	183
Appendix B. Example Calculation of Conditional Moments	186
Appendix C. Derivation of Analytical Method	190
Appendix D. Complete Results for Comparison of Methods to Calculate $E(-G'')$	196
Appendix E. Groundwater Monitoring Data from French Limited Site	205
Appendix F. Measured and Calculated Groundwater Concentrations	223
References	249
Vita	253

List of Tables

Table 5.1. Correlations between model parameters at varying censored levels, with significant correlations highlighted.....	93
Table 5.2. Results compared to exact solutions for independent, non-censored data. ..	96
Table 5.3. Expected updated standard deviation of mean model parameter, ϕ_μ , evaluated with different methods.....	98
Table 5.4. Updated standard deviation of the standard deviation model parameter, ϕ_σ , evaluated with different methods.....	99
Table 5.5. Updated standard deviation of correlation model parameter, ϕ_ρ , evaluated with different methods.	100
Table 5.6. Estimated mean values and 95 percent confidence intervals for the mean values for lognormal distributions.	104
Table 5.6. Confidence in 99 th percentile estimates for the standard lognormal distribution.	108
Table 6.1. Summary of parameters used in the Horizontal Plane Source model.....	118
Table 7.1. Prior values of model parameters used in calibration.....	142
Table 7.2. Constant values used during calibration.	143
Table 7.3. Updated values of model parameters used in calibration.	146
Table B1. Values for Measurements 1 through 4.	186
Table D1. Results of numerical simulations with $\bar{\phi}^* = \bar{\mu}_\phi$ for no censored data.	197
Table D2. Results of numerical simulations with $\bar{\phi}^* = \bar{\mu}_\phi$ for 25 percent censored data.	198
Table D3. Results of numerical simulations with $\bar{\phi}^* = \bar{\mu}_\phi$ for 50 percent censored data.	199

Table D4. Results of numerical simulations with $\bar{\phi}^* = \bar{\mu}_{\bar{\phi}}$ for 75 percent censored data.....	200
Table D5. Results of numerical simulations with $\bar{\phi}^*$ maximizing the likelihood function for no censored data.....	201
Table D6. Results of numerical simulations with $\bar{\phi}^*$ maximizing the likelihood function for 25 percent censored data.....	202
Table D7. Results of numerical simulations with $\bar{\phi}^*$ maximizing the likelihood function for 50 percent censored data.....	203
Table D8. Results of numerical simulations with $\bar{\phi}^*$ maximizing the likelihood function for 75 percent censored data.....	204
Table E1. Wells at the French Limited site sampled before remediation.....	206
Table E2. Wells at the French Limited site sampled after remediation.....	207
Table E3. Benzene concentration measurements at the French Limited site	208

List of Figures

Figure 2.1. Censoring with a proof-load test.	7
Figure 2.2. Definition of method detection limit.	8
Figure 2.3. Censored and point measurements of benzene from a real site.....	9
Figure 3.1. Illustration and example of the Bayesian approach.....	16
Figure 3.2. Components required for the FOSM Bayesian approach.....	21
Figure 3.3. Effect of the magnitude of $g(\phi)$ on the variance reduction for a single model parameter.....	31
Figure 3.4. Hermite Polynomials, order zero through two.	38
Figure 3.5. Hermite Polynomials, order three through five.	39
Figure 3.6. Linear relationship between two data points, y_i and y_j	44
Figure 4.1. Normally-distributed data point with censoring between $y_{i,l}$ and $y_{i,u}$	48
Figure 4.2. Normally-distributed data point censored in the lower tail of the distribution.	48
Figure 4.3. Normally-distributed data point censored in the upper tail of the distribution.	49
Figure 4.4. Finding the probability that a data point is censored for non-normally distributed data.....	52
Figure 4.5. Censored region of a lognormal distribution approximated with the censored region of a normal distribution with the same mean and standard deviation.....	62
Figure 4.6. Exact mean and variance for censored regions in the lower portion of a uniform distribution compared to an equivalent normal distribution.	65

Figure 4.7. Exact mean and variance for censored regions in the upper portion of a uniform distribution compared to an equivalent normal distribution.	66
Figure 4.8. Exact mean and variance for censored regions in the lower portion of a slightly skewed lognormal distribution compared to an equivalent normal distribution.	67
Figure 4.9. Exact mean and variance for censored regions in the upper portion of a slightly skewed lognormal distribution compared to an equivalent normal distribution.	68
Figure 4.10. Exact mean and variance for censored regions in the lower portion of a highly skewed lognormal distribution compared to an equivalent normal distribution.	69
Figure 4.11. Exact mean and variance for censored regions in the upper portion of a highly skewed lognormal distribution compared to an equivalent normal distribution.	70
Figure 5.1. Effect of data set size for the simple model.	81
Figure 5.2. Estimated mean values of the mean, $\mu_{\mu \bar{y}}$, with 95 percent confidence intervals.	83
Figure 5.3. Estimated mean values of the standard deviation, $\mu_{\sigma \bar{y}}$ with 95 percent confidence intervals.	85
Figure 5.4. Estimated mean values of the correlation between adjacent data points, $\mu_{\rho \bar{y}}$ with 95 percent confidence intervals.	86
Figure 5.5. Expected updated standard deviations for the mean of the simple model.	88
Figure 5.6. Expected updated standard deviations for the standard deviation of the simple model.	89

Figure 5.7. Expected updated standard deviations for the correlation between adjacent points for the simple model.....	91
Figure 5.8. Illustration of the negative correlation between mean and standard deviation with 75 percent censored data.....	94
Figure 5.9. Comparison of standard normal distribution and standard lognormal distribution.	102
Figure 5.10. Probability distribution for Case 1, a standard lognormal distribution with no censored data and statistically independent data.	105
Figure 5.11. Probability distribution for Case 2, a standard lognormal distribution with no censored data and correlated data.	106
Figure 5.12. Probability distribution for Case 3, a standard lognormal distribution with censored and correlated data.....	107
Figure 6.1. Map of French Limited site and vicinity (from Applied Hydrology Associates, 1989).	112
Figure 6.2. Monitoring wells at French Limited site.	115
Figure 6.3. Geometric parameters of the Horizontal Plane Source model.	120
Figure 6.4. Conceptual illustration of convolution integral for calculating contaminant concentration.....	123
Figure 6.5. Illustration of remediation factors used to calculate contaminant concentration.....	127
Figure 6.6. Correlation coefficients for longitudinal, transverse, and temporal dimensions.	132
Figure 6.7. T parameters for vertical averaging correlation coefficient.	133
Figure 6.8. Correlation reduction due to random variability or remediation status.....	135

Figure 7.1. Summary of benzene concentration data available from the French Limited site.....	139
Figure 7.2. Updated source size, source location, and groundwater flow direction for the French Limited site.	148
Figure 7.3. Calibrated correlation with time for French Limited site.....	151
Figure 7.4. Measured data distribution compared to calibrated distribution.	153
Figure 7.5. Correlations between model parameters for the means and covariances of the benzene concentrations at the French Limited site.	155
Figure 7.6. Comparison of measured and model-predicted concentrations for well ERT-21, sampled prior to remediation.	157
Figure 7.7. Comparison of measured and model-predicted concentrations for well INT-101, sampled after remediation.....	158
Figure 7.8. Probability distribution of predicted benzene concentration for well INT-26.....	161
Figure 7.9. Probability distribution of predicted benzene concentration for well S1-108A.....	162
Figure F1. Comparison of measured and calculated benzene concentrations for well ERT-1.....	224
Figure F2. Comparison of measured and calculated benzene concentrations for well ERT-1A.....	224
Figure F3. Comparison of measured and calculated benzene concentrations for well ERT-2.....	225
Figure F4. Comparison of measured and calculated benzene concentrations for well ERT-5.....	225

Figure F5. Comparison of measured and calculated benzene concentrations for well ERT-4.....	226
Figure F6. Comparison of measured and calculated benzene concentrations for well ERT-4A.....	226
Figure F7. Comparison of measured and calculated benzene concentrations for well ERT-6.....	227
Figure F8. Comparison of measured and calculated benzene concentrations for well ERT-7.....	227
Figure F9. Comparison of measured and calculated benzene concentrations for well ERT-7A.....	228
Figure F10. Comparison of measured and calculated benzene concentrations for well ERT-8.....	228
Figure F11. Comparison of measured and calculated benzene concentrations for well ERT-8A.....	229
Figure F12. Comparison of measured and calculated benzene concentrations for well ERT-9.....	229
Figure F13. Comparison of measured and calculated benzene concentrations for well ERT-9A.....	230
Figure F14. Comparison of measured and calculated benzene concentrations for well ERT-10.....	230
Figure F15. Comparison of measured and calculated benzene concentrations for well ERT-20.....	231
Figure F16. Comparison of measured and calculated benzene concentrations for well ERT-21.....	231

Figure F17. Comparison of measured and calculated benzene concentrations for well ERT-22.....	232
Figure F18. Comparison of measured and calculated benzene concentrations for well ERT-23.....	232
Figure F19. Comparison of measured and calculated benzene concentrations for wells ERT-24, ERT-25, ERT-27, ERT-28, and ERT-29.	233
Figure F20. Comparison of measured and calculated benzene concentrations for well REI-10-2.	233
Figure F21. Comparison of measured and calculated benzene concentrations for well REI-10-3.	234
Figure F22. Comparison of measured and calculated benzene concentrations for well REI-10-4.	234
Figure F23. Comparison of measured and calculated benzene concentrations for well FLTG-13.	235
Figure F24. Comparison of measured and calculated benzene concentrations for well FLTG-14.	235
Figure F25. Comparison of measured and calculated benzene concentrations for well INT-22.....	236
Figure F26. Comparison of measured and calculated benzene concentrations for well INT-26.....	236
Figure F27. Comparison of measured and calculated benzene concentrations for well INT-60-P3.....	237
Figure F28. Comparison of measured and calculated benzene concentrations for well INT-101.....	237

Figure F29. Comparison of measured and calculated benzene concentrations for well INT-106.....	238
Figure F30. Comparison of measured and calculated benzene concentrations for well INT-108.....	238
Figure F31. Comparison of measured and calculated benzene concentrations for well INT-118.....	239
Figure F32. Comparison of measured and calculated benzene concentrations for well INT-120.....	239
Figure F33. Comparison of measured and calculated benzene concentrations for well INT-123.....	240
Figure F34. Comparison of measured and calculated benzene concentrations for well INT-127.....	240
Figure F35. Comparison of measured and calculated benzene concentrations for well INT-134.....	241
Figure F36. Comparison of measured and calculated benzene concentrations for well INT-135.....	241
Figure F37. Comparison of measured and calculated benzene concentrations for well INT-144.....	242
Figure F38. Comparison of measured and calculated benzene concentrations for well INT-214.....	242
Figure F39. Comparison of measured and calculated benzene concentrations for well INT-217.....	243
Figure F40. Comparison of measured and calculated benzene concentrations for well INT-233.....	243

Figure F41. Comparison of measured and calculated benzene concentrations for well S1-31.....	244
Figure F42. Comparison of measured and calculated benzene concentrations for well S1-33.....	244
Figure F43. Comparison of measured and calculated benzene concentrations for well S1-51-P3.	245
Figure F44. Comparison of measured and calculated benzene concentrations for well S1-106A.	245
Figure F45. Comparison of measured and calculated benzene concentrations for well S1-108A.	246
Figure F46. Comparison of measured and calculated benzene concentrations for well S1-118.....	246
Figure F47. Comparison of measured and calculated benzene concentrations for well S1-121.....	247
Figure F48. Comparison of measured and calculated benzene concentrations for well S1-123.....	247
Figure F49. Comparison of measured and calculated benzene concentrations for well S1-131.....	248
Figure F50. Comparison of measured and calculated benzene concentrations for well S1-135.....	248

Chapter 1. Introduction

1.1 BACKGROUND

In engineering applications, it is common to encounter censored data. The exact value of a censored data point is not known, only that it is above or below some specified value. An example of a censored data point is a proof load test where the structure does not fail under the maximum applied load. The capacity of the tested structure is proven to be greater than the applied load, but the exact capacity is unknown. Another example of a censored data point is a contaminant concentration in a groundwater sample that is reported as below the detection limit. The actual concentration is uncertain, since the contaminant may be present in the sample at a concentration below the detection limit, or the contaminant may be absent in the sample.

Existing methods to analyze situations where censored data have been obtained or are expected are limited in their applications. A typical method used in structural engineering is to treat load and resistance as random variables; however, the data are assumed to have a normal distribution, or a transformation of the normal distribution, and to be uncorrelated. Another common method is Bayesian updating. While non-normal data may be incorporated with these methods, the amount of data that can be considered is limited and the data must again be uncorrelated.

In the Bayesian approach, model parameters are considered to be random variables, so that both the expected value of the parameter and the uncertainty in that value can be quantified. Any type of information can be incorporated in estimating model parameters, including indirect data, such as empirical correlations, and actual measurements. The model parameters are updated by accounting for prior beliefs about the model parameters and for collected data. While the classical Bayesian method is

useful for including all relevant information and accounting for uncertainty in model parameters, it is difficult to apply analytically to practical problems.

The First-Order Second-Moment (FOSM) Bayesian method developed by Gilbert (1999) is an analytical approximation for analyzing data and designing test programs. The FOSM Bayesian method provides a framework to apply the Bayesian method to practical problems. Data that have already been collected may be used in this method to calibrate model parameters. Test programs for collecting data to achieve the greatest reduction of uncertainty in the model parameters may also be designed with this method. The FOSM Bayesian method overcomes some of the problems with the other methods presented in literature, since it does not require numerical integration, Monte Carlo simulations, or assumptions regarding the value of the censored data, and it allows for correlations between censored and non-censored data. It has been used successfully for data analysis both with and without censored data that are normally distributed (McBrayer 2000). It has also been used for designing test programs without censored data (Muchard 1996), and for data analysis with non-censored, non-normally distributed data (Wang 2002). This research will expand the FOSM Bayesian method to incorporate censored data of any distribution type into data analysis and test program design.

1.2 OBJECTIVES AND APPROACH OF RESEARCH

The objectives of this research are to:

1. Extend the FOSM Bayesian method for test design to include censored data that are correlated and have a normal or non-normal distribution.
2. Extend the FOSM Bayesian method for data analysis to include censored data are correlated and have a non-normal distribution.

3. Determine the effects of censored data on the updated means and covariances of model parameters.
4. Demonstrate the new methods through application to a contaminated groundwater problem that includes censored data.

Since the exact value of a censored data point is not known, the method for including censored data in the FOSM Bayesian method considers this uncertainty. For data analysis, the method considers the likelihood of a censored data point, given the model parameters, based on the conditioned mean and standard deviation of the censored point. In extending the method to test program design, the likelihood that an expected data point is censored, and the likelihood that it is not censored, are both considered appropriately.

When considering data that are not normally distributed, a Hermite polynomial transform function is used to fit a general distribution to a normal distribution. With both data analysis and test program design, the characteristics of the transformed non-normal distribution are used to find the probability that a data point is censored.

Censored data is prominent in the real contaminated site that is used as an application for the FOSM Bayesian method. The method is used both to calibrate a groundwater model to existing groundwater data and to develop site investigation and monitoring plans. The contamination at the site resulted from petrochemical and wood preservative wastes that were placed in an unlined lagoon approximately twenty years prior to investigation of the site. A variety of remediation methods were used at the site, including active bioremediation of the waste lagoon, active remediation of groundwater consisting of pump-and-treat with injection of oxygen and nutrients, and natural

attenuation of groundwater. The groundwater monitoring data available for the site is extensive, both before and after remediation.

The FOSM Bayesian method is advantageous because uncertainty can be considered in the highly variable parameters used in the groundwater model. The parameters included in the groundwater model involve the source (size, location, time of release), groundwater flow (seepage velocity, dispersivity), and contaminant properties (half-life, concentration at source). The variance in the contaminant concentrations is also modeled, as are the correlations between concentration measurements (based on location and time of measurements). The non-normal distribution of the measurements is also modeled. For all of these model parameters, the uncertainty in the parameters is quantified, instead of using deterministic values for them.

All of the complexities of the site are included in the model calibration and test program design with the method developed in this study. The large amount of groundwater concentration measurements over time and space, including both censored and point measurements, are accounted for in the method. The correlation of the data points and the non-normal distribution of the data set are also included. The method is able to quantify the uncertainty in all of the model parameters, including the effect of the remediation on the groundwater conditions. This type of analysis would not be possible with other available methods.

1.3 ORGANIZATION OF DISSERTATION

A description of censored data, particularly as it relates to groundwater applications, is contained in Chapter 2. Literature dealing with censored data and model calibration in civil engineering applications involving censored data is also summarized in Chapter 2.

The basic framework of the FOSM Bayesian method, without censored data, is outlined in Chapter 3. Chapter 4 explains how censored data are incorporated into the FOSM Bayesian method. The method developed for including censored data in data analysis is derived, then extended for test program design for data with either a normal distribution or a general distribution. The use of censored data in data analysis with generally-distributed data is also covered in Chapter 4. The effects of including censored data in a test program design and in data analysis are explored in Chapter 5.

The FOSM Bayesian analysis is applied to a groundwater contamination problem in Chapters 6 and 7. The history of the site and the groundwater model used for the site are described in Chapter 6. The groundwater model is calibrated to the groundwater concentration data collected both before and after remediation of the site, and the results of the calibration are discussed in Chapter 7.

Conclusions and contributions of this research are presented in Chapter 8.

Chapter 2: Censored Data Background Information

2.1 INTRODUCTION

In the field of civil engineering, censored data are commonly encountered in the area of proof load tests and groundwater contaminant concentrations below the detection limit. The concept of censored data is introduced in this chapter through these two examples of censored data. A brief survey is also provided of several methods of analysis using censored data in these civil engineering applications for calibrating models with data and designing test programs.

2.2 CENSORED DATA IN CIVIL ENGINEERING APPLICATIONS

Censored data occurs when the exact value of a measured quantity is unknown, and it is only known that the value is above or below a certain threshold value. A common type of censored data encountered in civil engineering are proof load tests. With this type of test, a load is applied to a structure, such as a pile for a foundation or a bridge, and the structure either withstands the load or fails. If the structure withstands the load, the true capacity of the structure is still unknown. The capacity is only known to be more than the applied load. This is illustrated in Figure 2.1 for a capacity with a normal distribution. The expected capacity is greater than the maximum applied load, but the actual capacity could be anywhere in the censored region. The capacity of the structure is therefore censored.

Another frequently encountered type of censored data occurs in groundwater sampling when a contaminant concentration is reported as below the detection limit. The

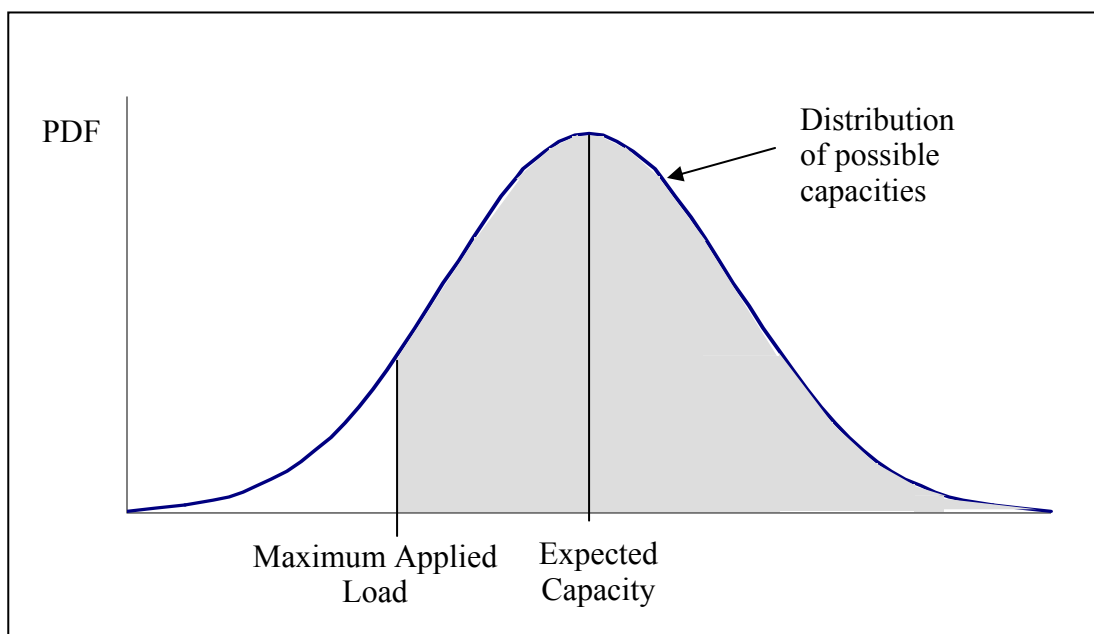


Figure 2.1. Censoring with a proof-load test.

method detection limit (MDL) is a statistical concept and is defined by the U.S. Environmental Protection Agency as “the minimum concentration of a substance that can be measured and reported with 99 percent confidence that the analyte concentration is greater than zero and is determined from analysis of a sample in a given matrix containing the analyte” (U.S. EPA 2003a). This confidence is illustrated in Figure 2.2. A sample with a concentration at the MDL will be measured as greater than zero 99 percent of the times it is tested. The MDL is estimated from testing data and is therefore not an exact quantity (Berthouex 1993). It may be defined with a mean and a variance, but it is often treated as an absolute value.

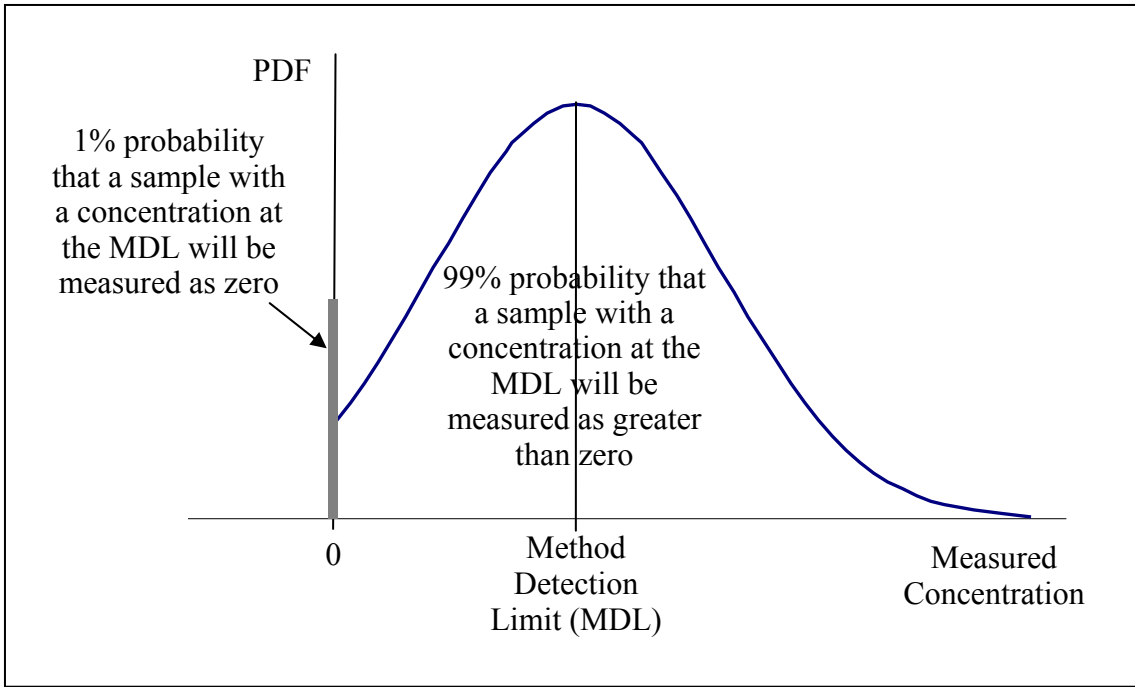


Figure 2.2. Definition of method detection limit.

Concentrations below the MDL are usually reported only as “not detected”, although more information would be conveyed with a numerical result and its precision (Porter et al. 1988). A “non-detect” measurement is frequently misunderstood to be a concentration of zero or a concentration that is too small to measure. Censored data, or contaminant concentrations below the detection limit, are expected and usually required in groundwater investigations. The extent of contamination and the effect of remediation efforts are evaluated by determining where contaminants are absent in the groundwater. Since contaminant concentrations will only be reported as below the detection limit, not as zero, censored data are necessary for defining areas of contaminated groundwater.

Engineers typically deal with censored groundwater measurements by making assumptions about the values of concentrations. One common assumption is that a non-

detect measurement indicates no contaminant present in the sample, and the concentration is set to zero. Another common assumption is to assign an arbitrary, non-zero value to the non-detect measurement, such as the value of the detection limit or half of the detection limit. Non-detect concentrations are also sometimes excluded from an analysis of groundwater contamination. All of these assumptions may lead to errors in estimating the mean and variance of contamination in the groundwater.

An example of how these types of assumptions can lead to errors is illustrated in Figure 2.3. This figure shows both censored measurements and non-censored, or point,

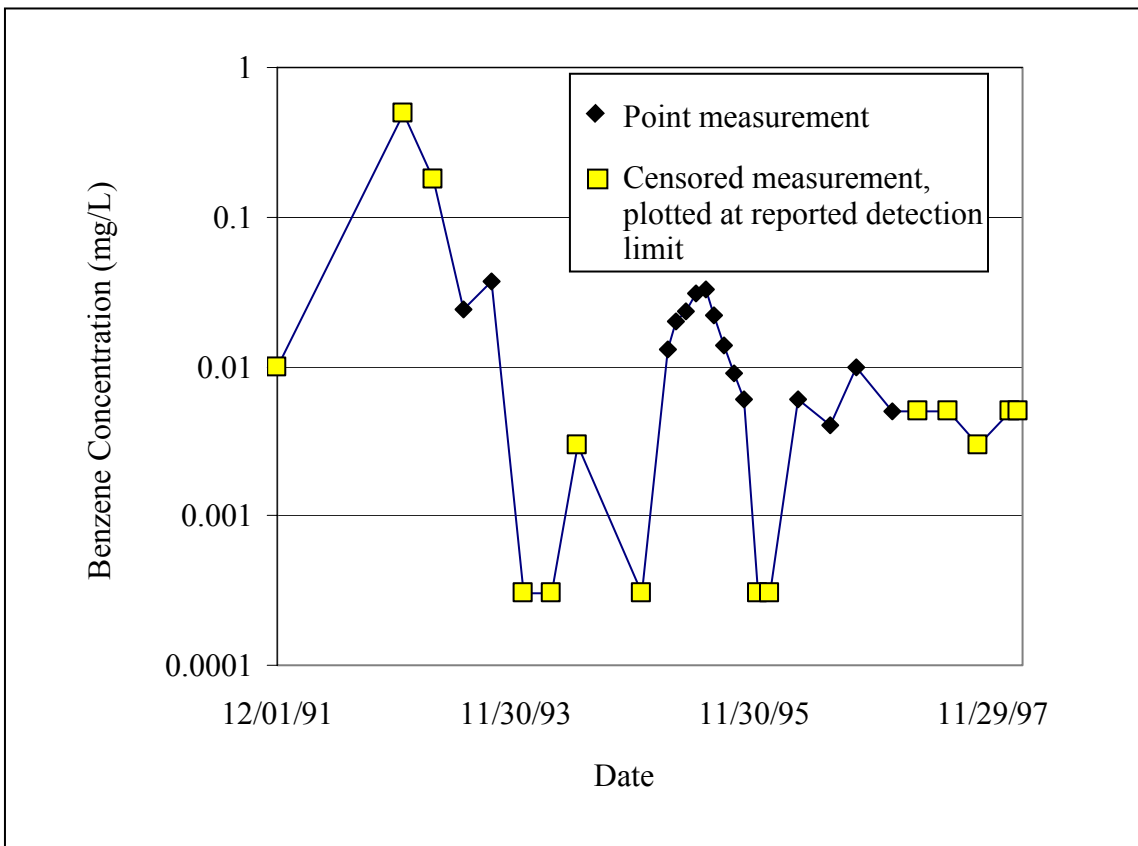


Figure 2.3. Censored and point measurements of benzene from a real site.

measurements of benzene from a well at the real site studied in this dissertation. The censored data points are plotted at the concentration reported as the detection limit. The detection limit was different at different sampling times, and was especially large at the beginning of the sampling period. At one of these large detection limits, assuming a concentration of zero or half the detection limit might lead to a much smaller estimate of concentration present in the sample than actually exists. Even at the smaller detection limits, assuming there is no benzene in the sample for a non-detect measurement may be erroneous. A measurement of benzene in the sample was obtained, but the measured value could not be reported with 99 percent confidence that it was greater than zero.

2.3 PARAMETER ESTIMATOR METHODS FOR CENSORED DATA

This section provides a brief overview of previously applied methods of analysis for the censored data that occurs in proof load tests and contaminated groundwater concentrations.

2.3.1 Analysis of Proof Load Tests

The testing of bridges is commonly addressed as a proof load test problem; however, the methods are applicable to proof loads on other types of structures. Fujino and Lind (1977) describe the traditional method of analyzing proof load tests, which is treating the resistance of the structure and the applied load as normally or lognormally-distributed random variables. The proof load test gives a higher reliability by eliminating the lower tail of the reliability distribution. A probability of failure may then be calculated, as well as a reliability index. Nowak and Tharmabala (1988) also use this method and discuss the difference between analytical results and actual test results. Fu

and Tang (1995) address the target proof loads to minimize costs and maximize benefits from test data. With all of these methods, the data are assumed to have a normal distribution, or a transformation of the normal distribution, and to be uncorrelated.

Stewart and Val (1999) and Rodriguez et al. (1998) used Monte Carlo simulations to update the distribution of a structure's resistance and determine the probability of failure based on service and proof loads. Numerical approximations were necessary in these methods, and data were assumed to be normal and uncorrelated. Umble et al. (1999) developed a Bayesian approach that can be used with any probability distribution to estimate the probability of failure under two different proof loads. While non-normal data may be used in this method, the amount of data that can be considered is limited and the data must be uncorrelated.

2.3.2 Analysis of Concentrations below the Detection Limit

Liu et al. (1996) uses a maximum likelihood method to analyze groundwater contaminant concentrations reported as below the detection limit. The censored data are assumed to have a normal or log-normal distribution. Gilliom and Helsel (1986), Haas and Scheff (1990), and El-Shaarawi and Esterby (1992) evaluated and compared different techniques for analyzing concentrations below the detection limit, including log-normal regression, maximum likelihood estimator, and assigning a constant value to censored data points, such as one-half the detection limit. Gilliom and Helsel (1986) consider different distributions for the censored data, while Haas and Scheff (1990) and El-Shaarawi and Esterby (1992) consider only normally-distributed and log-normally-distributed data. The conclusions about the best method vary, depending on the degree of censoring and the distribution assumed for the data. A disadvantage of these methods is that all the data are assumed to be uncorrelated. Also, they only consider the censored

data obtained, and do not consider non-censored data that may also have been collected and may be correlated to the censored data.

McBrayer (1999) proposes a technique for the First-Order Second-Moment (FOSM) Bayesian method (Gilbert 1999) to use in analyzing censored data, such as the kind obtained from water concentrations and from load tests. This proposed method overcomes some of the problems with the other methods presented in the literature for analyzing censored data, since it does not require assumptions regarding the value of the censored data and it allows for correlations between censored and non-censored data. However, the proposed method only uses normally-distributed data, and it may only be used for data analysis, not for designing test programs.

2.4 SUMMARY

In this chapter, the concept of censored data was introduced. Two common types of censored data in civil engineering, proof load tests and contaminant concentrations below the detection limit, were described. A brief survey of methods used to analyze both of these types of problems was presented. The previously used methods generally make assumptions about the data, such as statistically independent data or normally-distributed data. The FOSM Bayesian method does not require these assumptions, and was therefore chosen as the basis for this research. The research presented in this dissertation develops the method proposed by McBrayer (1999) so that normally-distributed or non-normally-distributed censored data may be used in both data analysis and test program design. The framework of the FOSM Bayesian method is described in the next chapter, then the method to include generally-distributed censored data for use in data analysis and test program design is derived in Chapter 4.

Chapter 3. Bayesian Method with Point Measurements

1.1 INTRODUCTION

The Bayesian approach is a framework for including all available information in a decision analysis. Data that is based on physical principles or prior experience may be updated with data from observations or measurements. The Bayesian approach is particularly useful in updating parameters that are used to model physical processes. The mean values of the parameters and the uncertainty in those values may be updated as new knowledge is gained. However, the Bayesian approach is difficult to apply analytically to situations involving multiple model parameters. The FOSM Bayesian method (Gilbert 1999) was developed to provide a practical Bayesian method for problems with multiple model parameters, large data sets, and various data distributions. This chapter describes the theory behind the Bayesian approach, gives an example of its application, then summarizes the FOSM Bayesian method for use with data sets that have only point (non-censored) measurements.

3.2 BAYESIAN APPROACH

The basis of all Bayesian methods is Bayes' theorem (Greene 1997, Ang and Tang 1975), which is expressed in terms of the probabilities of two events, A and B. The probability of event A is updated with the knowledge that event B has occurred:

$$P(A|B) = \frac{P(B|A)P(A)}{P(B)} \quad (3.1)$$

The probability of A given that event B occurs, $P(A|B)$, is referred to as the posterior or updated probability of A. The probability of event A before it is known if event B occurs, $P(A)$, is the prior probability of A. The probability of event B, regardless of whether event A occurs or not, is $P(B)$. The probability of event B given that event A occurs is $P(B|A)$.

Bayes' theorem is useful for updating model parameters with new data that are collected. Each parameter is treated as a random variable, which has an expected value, a variance, and a probability distribution. In terms of updating model parameters, Bayes' theorem can be paraphrased as follows (Greene 1997):

$$P(\text{parameters}|\text{data}) = \frac{1}{P(\text{data})} [P(\text{data}|\text{parameters})P(\text{parameters})] \quad (3.2)$$

where:

$P(\text{data}|\text{parameters})$ = joint distribution of the observed random variables (data) given the model parameters (this is also referred to as the likelihood function)

$P(\text{parameters})$ = prior beliefs about the model parameters

$P(\text{parameters}|\text{data})$ = updated distribution of the parameters given the current data

$P(\text{data})$ = probability of the observed random variables (the data)

Note that the term $\frac{1}{P(\text{data})}$ may be thought of as a normalizing constant so that the updated distribution, $P(\text{parameters}|\text{data})$, has an area of 1.0. This term is obtained with a summation over all of the possible parameter values:

$$P(\text{data}) = \sum_{\text{all possible parameter values}} P(\text{data}|\text{parameters})P(\text{parameters})$$

The updated probability of the parameters may be thought of as a “mixture” of the prior information about the parameters and the current information that the data provide about the parameters.

3.3 EXAMPLE USE OF BAYES’ THEOREM

An example of Bayesian updating is shown in Figure 3.1. In this example, a normal distribution is used to model the variability in a random variable Y with a mean value of ϕ_μ and a known standard deviation of 5.0. This model describes the probability or likelihood of measuring a particular value of y_i . The likelihood is the height of the curve at any point in Figure 3.1(a), which is equal to the probability density function (PDF) for y_i , denoted $PDF(y_i)$. Multiple data points are modeled as statistically independent, so the correlation coefficient between data points is zero ($\rho_{y_i, y_j} = 0$). Therefore, the probability or likelihood of measuring multiple data points, y_1, y_2, \dots, y_n , is the product of the probabilities for each y_i :

$$P(\text{measuring data points } y_1, y_2, \dots, y_n) = PDF(y_1) \times PDF(y_2) \times \dots \times PDF(y_n) \quad (3.3)$$

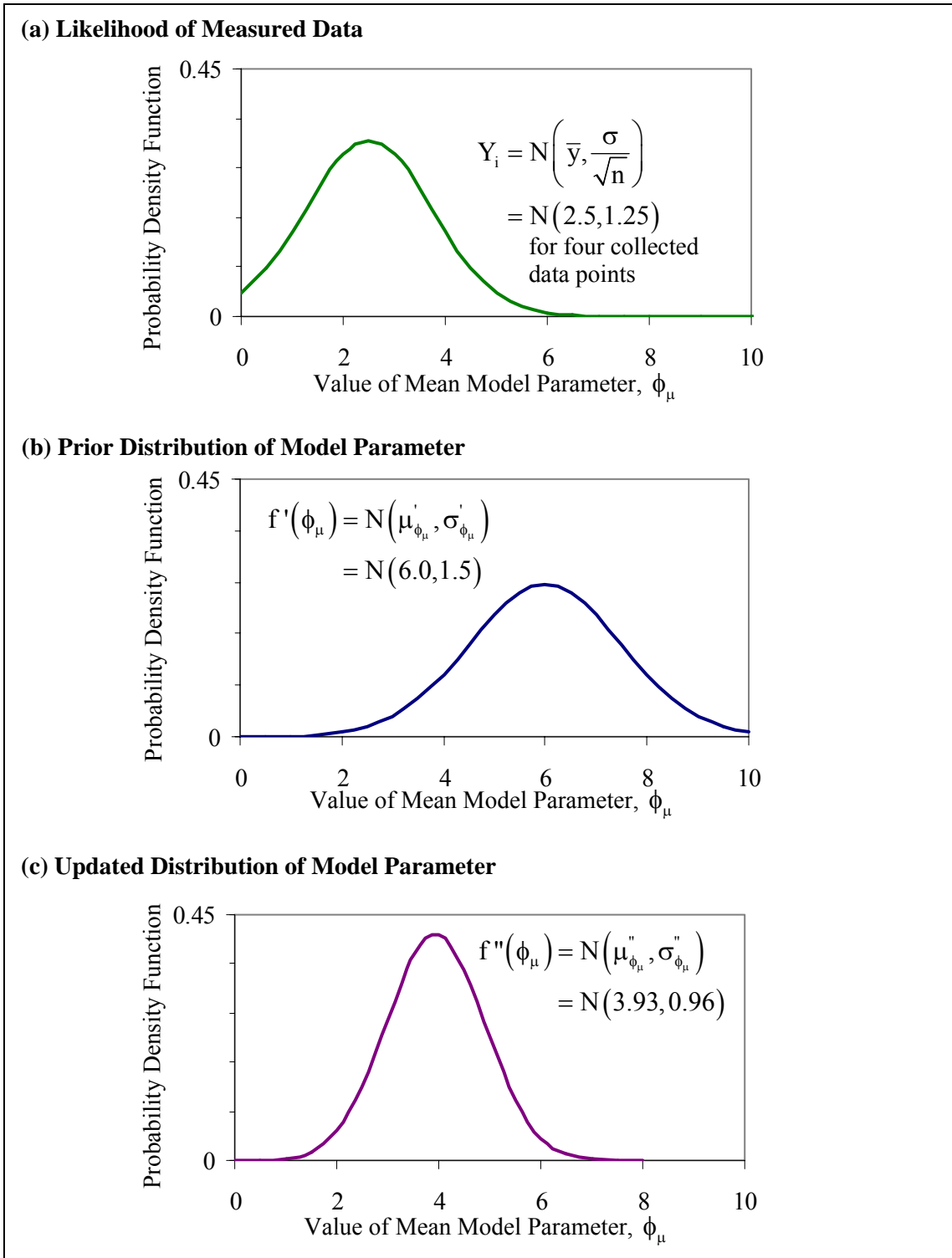


Figure 3.1. Illustration and example of the Bayesian approach.

Each $\text{PDF}(y_i)$ value depends on the mean value, ϕ_μ , for the normal distribution in Figure 3.1(a). This relationship between the data, y_1 to y_i , and the model parameter, ϕ_μ , is expressed as follows:

$$\begin{aligned} P(\text{measuring data points } y_1, y_2, \dots, y_n | \phi_\mu) &= \text{PDF}(y_1 | \phi_\mu) \times \text{PDF}(y_2 | \phi_\mu) \\ &\times \dots \times \text{PDF}(y_n | \phi_\mu) \end{aligned} \quad (3.4)$$

Since y_i has a normal distribution with a mean of ϕ_μ and a standard deviation of 5.0, the PDF is $\phi\left(\frac{y_i - \phi_\mu}{5.0}\right)$. Therefore, the term $P(\text{data} | \text{parameters})$ in Equation 3.2 is given by the following for this example:

$$\begin{aligned} P(\text{data} | \text{parameters}) &= \text{PDF}(y_1 | \phi_\mu) \times \text{PDF}(y_2 | \phi_\mu) \times \dots \times \text{PDF}(y_n | \phi_\mu) \\ &= \phi\left(\frac{y_1 - \phi_\mu}{5.0}\right) - \phi\left(\frac{y_2 - \phi_\mu}{5.0}\right) - \dots - \phi\left(\frac{y_n - \phi_\mu}{5.0}\right) \end{aligned} \quad (3.5)$$

where there are n data points and there is one model parameter to be calibrated, ϕ_μ .

The next step is to represent prior information in the model parameter that will be calibrated with the data. Previous information indicates that the prior mean value of ϕ_μ is 6.0, the prior standard deviation of ϕ_μ is 1.5, and the prior distribution of ϕ_μ is normal. The probability of a particular value of ϕ_μ is therefore obtained from a normal distribution, and the distribution in Figure 3.1(b) provides the $P(\text{parameters})$ term in Equation 3.2.

For the next step, four data points are collected. The collected data have a sample mean of 2.5. The likelihood of obtaining these data, given the prior model parameters, is calculated using Equation 3.4 and is shown in Figure 3.1(a).

The prior value of the model parameter is updated with the observed data using Bayes' Theorem. The updated distribution of the model parameter, $P(\text{parameter}|\text{data})$ in Equation 3.2, is calculated by integrating the product of $P(\text{data}|\text{parameters}) \times P(\text{parameters})$ to find $P(\text{data})$ and then plugging it into Equation 3.2. The result is that ϕ_μ has a normal distribution with a mean and standard deviation equal to:

$$\mu_{\phi_\mu}'' = (\sigma_{\phi_\mu}'')^2 \left[\mu_{\phi_\mu}' \left(\frac{1}{(\sigma_{\phi_\mu}')^2} \right) + \bar{y} \left(\frac{n}{\sigma_y^2} \right) \right] \quad (3.6)$$

$$(\sigma_{\phi_\mu}'')^2 = \left[\frac{1}{(\sigma_y^2/n)} + \frac{1}{(\sigma_{\phi_\mu}')^2} \right]^{-1} \quad (3.7)$$

where:

μ_{ϕ_μ}'' = updated mean of the model parameter

σ_{ϕ_μ}'' = updated standard deviation of the model parameter

μ_{ϕ_μ}' = prior mean of the model parameter = 6.0

σ_{ϕ_μ}' = prior standard deviation of the model parameter = 1.5

\bar{y} = sample mean of the collected data = 2.5

σ_y = sample standard deviation of the collected data = 5.0

n = number of measured data values = 4

This application of Bayes' theorem (Equations 3.3 and 3.4) results in an updated expected value ($\mu_{\phi_{\mu}}''$) of 3.93, which is between the prior mean value and the mean of the observed data, and an updated standard deviation ($\sigma_{\phi_{\mu}}''$) of 0.96, which is smaller than the standard deviation of both the prior value and the observed data. These results are shown in Figure 3.1(c) with the "Updated" distribution. The updated distribution for the mean lies between the prior distribution and the likelihood function, and it is narrower than the prior distribution or likelihood function because of its reduced variance.

In this example, the Bayesian updating was easy to perform because it involved only one model parameter and both the model parameter and the data had normal distributions. Applying Bayes' Theorem analytically to more complicated situations, with more model parameters and various distributions, is difficult and usually not attempted or, in rare cases, accomplished through numerical simulation.

3.4 FOSM BAYESIAN METHOD

The basic formulation of the FOSM Bayesian method will be described in this section. A more detailed derivation may be found in Gilbert (1999). The FOSM Bayesian Method is an analytical Bayesian technique that is able to incorporate multiple model parameters, large sets of data, and different distributions of data. The method may be used for data analysis or for test program design. In data analysis, the model parameters are calibrated with data that has been collected, and updated distributions for the model parameters are determined. For test program design, the expected reduction in variance of the model parameters is determined with the data that are expected to be obtained from a potential test program.

3.4.1 Example Application of the FOSM Bayesian Method

The basic procedure of the FOSM Bayesian method is presented here through an example, which is illustrated in Figure 3.2. In this example, the physical problem of concern is groundwater contamination caused by a leaking underground storage tank. The data that have been or will be collected are concentrations of various contaminants in the groundwater at three monitoring wells. The plume is in a steady-state condition, meaning that the concentrations at each well are not changing appreciably with time.

The FOSM Bayesian method is used to describe the relationship between a model and the measured data. The expected or mean values of the concentrations at the locations of the measurements are modeled with a simple, steady-state plume model (Charbeneau 2000). This model contains seven model parameters: ϕ_R , ϕ_n , ϕ_{Dyy} , ϕ_m , ϕ_b , ϕ_λ , and ϕ_v (retardation, porosity, dispersivity, contaminant mass, aquifer thickness, contaminant half-life, and seepage velocity, respectively). Throughout this dissertation, the symbol “ ϕ ” will be used for model parameters.

The standard deviation of a concentration measurement is modeled as a constant for all measurement locations, and it is represented by the exponent of the model parameter ϕ_σ . This exponential representation insures that the standard deviation will have a positive value regardless of the value of the model parameter. The correlation between data points at different measurement times is modeled with the parameter ϕ_ρ to decrease exponentially with distance in time between the measurements, since measurements are more likely to be correlated if they are made near one another. Finally, the distribution of data about the mean is modeled as a normal distribution. For problems analyzed with the FOSM Bayesian method, these components of data and models for the mean, variance, correlation, and distribution of the data are calibrated. Calibration means

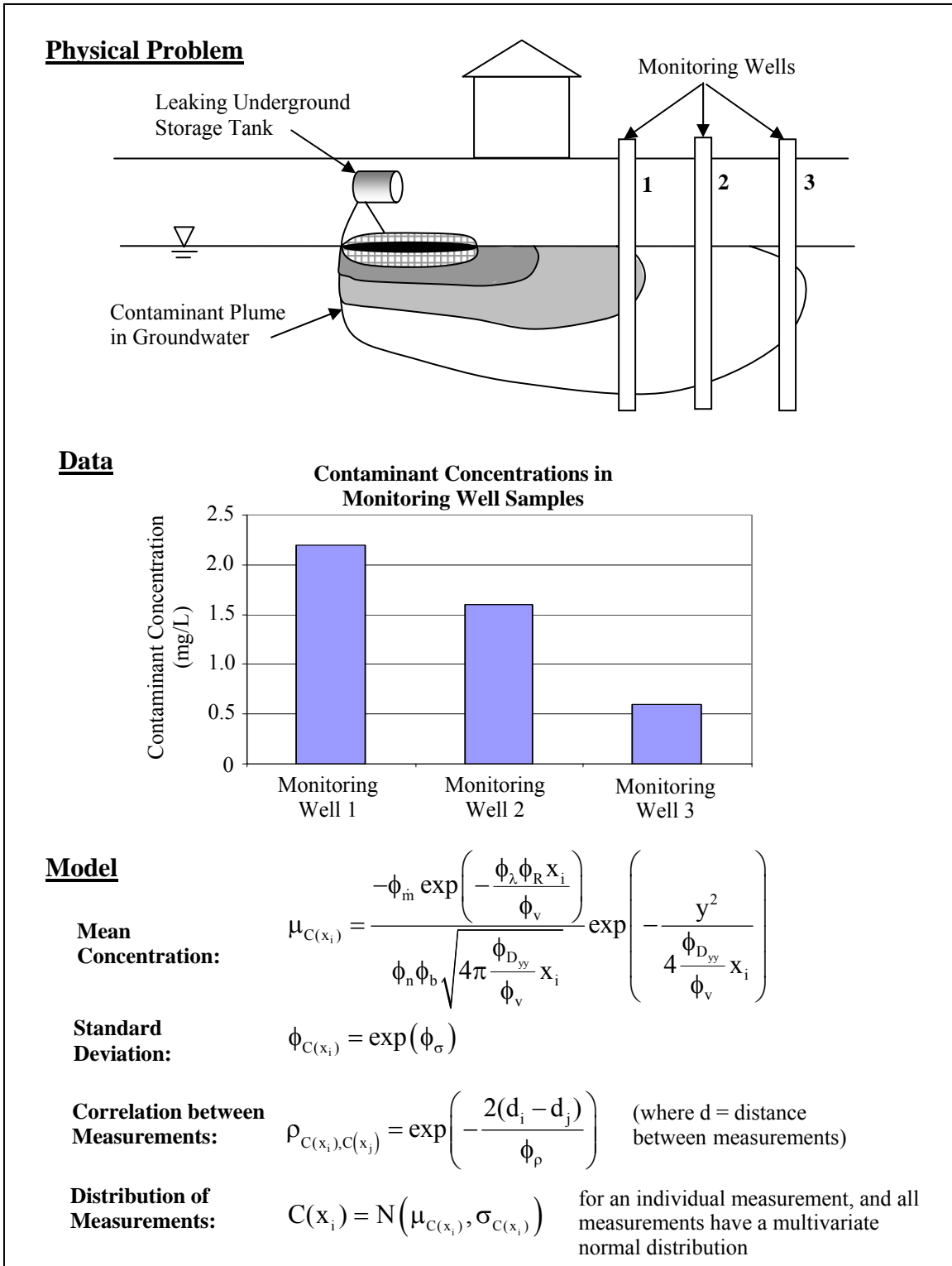


Figure 3.2. Components required for the FOSM Bayesian method.

that the expected values and covariances for all of the parameters ($\phi_R, \phi_n, \phi_{Dyy}, \phi_m, \phi_b, \phi_\lambda, \phi_v, \phi_\sigma,$ and ϕ_ρ) are updated based on the measured data.

3.4.2 Notation used in FOSM Bayesian Method

In the remainder of this dissertation, the following notations will be used:

$\bar{\Phi}$ = vector of random variables that are the model parameters

$\bar{\phi}$ = vector of mean values for each model parameter

\bar{Y} = vector of random variables that are the data

\bar{y} = vector of numeric values of the data that are measured or expected

In these terms, Bayes' Theorem is expressed as follows:

$$f_{\bar{\phi}}(\bar{\phi}|\bar{y}) = k \cdot L(\bar{y}|\bar{\phi}) \cdot f_{\bar{\phi}}(\bar{\phi}) \quad (3.8)$$

where:

$f_{\bar{\phi}}(\bar{\phi}|\bar{y})$ = the updated probability density function for the model parameters, given the current data

$L(\bar{y}|\bar{\phi})$ = the likelihood of obtaining the current data, given the set of model parameters (the likelihood that the model parameters describe the actual data)

$f_{\bar{\phi}}(\bar{\phi})$ = the prior probability density function of the model parameters, before data are obtained

k = a normalizing constant that makes $f_{\bar{\phi}}(\bar{\phi}|\bar{y})$ a probability density function, with an integral of 1.0 over all possible model parameter values.

Note that Equation 3.8 is the same as the paraphrased version of Bayes' Theorem of Equation 3.2. The probability density functions and the likelihood function in Equation 3.8 are functions of vectors that produce scalar values.

3.4.3 Formulation of FOSM Bayesian Method for Data Analysis

For data analysis using the FOSM Bayesian method, the model parameters are calibrated with the measured data to maximize the likelihood that the model parameters describe the observed data. The prior means and covariances of the model parameters may then be updated with the calibrated parameters. The full derivation of the FOSM Bayesian method for data analysis is described by Gilbert (1999) and Muchard (1997). The steps of the derivation of the FOSM Bayesian method, which result in approximations for the updated mean and covariance of the model parameters, are summarized below:

1. Define $g(\bar{\phi})$ as the natural logarithm of the likelihood function:

$$g(\bar{\phi}) = \ln(L(\bar{y}|\bar{\phi})) \quad (3.9)$$

2. Use a second-order Taylor series, with an expansion point of $\bar{\phi}^*$, to approximate the natural logarithm of the likelihood function:

$$g(\bar{\phi}) \cong g(\bar{\phi}^*) + \left\{ \frac{\partial g}{\partial \phi_i} \bigg|_{\bar{\phi}^*} \right\} + \frac{1}{2} \{ \bar{\phi} - \bar{\phi}^* \}^T \left[\frac{-\partial^2 g}{\partial \phi_i \partial \phi_j} \bigg|_{\bar{\phi}^*} \right] \{ \bar{\phi} - \bar{\phi}^* \} \quad (3.10)$$

where:

$\left\{ \frac{\partial \mathbf{g}}{\partial \phi_i} \Big|_{\bar{\phi}^*} \right\}$ = a vector of the first derivatives of the natural logarithm of the likelihood function with respect to each parameter, evaluated at the Taylor series expansion point

$\left[\frac{-\partial^2 \mathbf{g}}{\partial \phi_i \partial \phi_j} \Big|_{\bar{\phi}^*} \right]$ = a matrix of the negative of the second derivatives of the natural logarithm of the likelihood function with respect to all parameters, evaluated at the Taylor series expansion point

3. Assume that the prior model parameters have a multivariate normal distribution:

$$f_{\bar{\phi}}(\bar{\phi}) \cong \frac{1}{(2\pi)^{n/2} |\mathbf{C}_{\bar{\phi}}|^{1/2}} \exp \left[-\frac{1}{2} \{ \bar{\phi} - \bar{\mu}_{\bar{\phi}} \}^T \mathbf{C}_{\bar{\phi}}^{-1} \{ \bar{\phi} - \bar{\mu}_{\bar{\phi}} \} \right] \quad (3.11)$$

then take the natural logarithm of this distribution:

$$\ln(f_{\bar{\phi}}(\bar{\phi})) \cong \ln \left(\frac{1}{(2\pi)^{n/2} |\mathbf{C}_{\bar{\phi}}|^{1/2}} \right) - \frac{1}{2} \{ \bar{\phi} - \bar{\mu}_{\bar{\phi}} \}^T \mathbf{C}_{\bar{\phi}}^{-1} \{ \bar{\phi} - \bar{\mu}_{\bar{\phi}} \} \quad (3.12)$$

4. Take the natural logarithm of Bayes' Theorem (Equation 3.8):

$$\begin{aligned} \ln[f_{\bar{\phi}}(\bar{\phi}|\bar{y})] &= \ln(k) + \ln[L(\bar{y}|\bar{\phi})] + \ln[f_{\bar{\phi}}(\bar{\phi})] \\ &= \ln(k) + g(\bar{\phi}) + \ln[f_{\bar{\phi}}(\bar{\phi})] \end{aligned} \quad (3.13)$$

5. By substituting the Taylor series approximation of the natural logarithm of the likelihood function (Equation 3.10) and the natural logarithm of the prior model parameters (Equation 3.12) into the natural logarithm of Bayes' Theorem (Equation 3.13), the updated distribution of the model parameters is found:

$$\ln \left[f_{\bar{\phi}|\bar{y}}(\bar{\phi}|\bar{y}) \right] \cong \ln(k) - \frac{1}{2} \left\{ \bar{\phi} - \bar{\mu}_{\bar{\phi}|\bar{y}} \right\}^T C_{\bar{\phi}|\bar{y}}^{-1} \left\{ \bar{\phi} - \bar{\mu}_{\bar{\phi}|\bar{y}} \right\} \quad (3.14)$$

where $\bar{\mu}_{\bar{\phi}|\bar{y}}$ and $C_{\bar{\phi}|\bar{y}}$ contain the updated means and covariances of the model parameters, respectively, and have the following approximations:

$$\bar{\mu}_{\bar{\phi}|\bar{y}} \cong \left[\left[\frac{-\partial^2 \mathbf{g}}{\partial \phi_i \partial \phi_j} \Big|_{\bar{\phi}^*} \right] + C_{\bar{\phi}}^{-1} \right]^{-1} \left\{ \left[\frac{-\partial^2 \mathbf{g}}{\partial \phi_i \partial \phi_j} \Big|_{\bar{\phi}^*} \right] \bar{\phi}^* - \left\{ \frac{\partial \mathbf{g}}{\partial \phi_i} \Big|_{\bar{\phi}^*} \right\} + C_{\bar{\phi}}^{-1} \bar{\mu}_{\bar{\phi}} \right\} \quad (3.15)$$

$$C_{\bar{\phi}|\bar{y}} \cong \left[\left[\frac{-\partial^2 \mathbf{g}}{\partial \phi_i \partial \phi_j} \Big|_{\bar{\phi}^*} \right] + C_{\bar{\phi}}^{-1} \right]^{-1} \quad (3.16)$$

These are the updated moments for the model parameters that are used in a data analysis application of the FOSM Bayesian method.

6. The expansion point for the Taylor series approximation of Equation 3.10 is chosen so that the likelihood function is maximized and therefore the natural logarithm of the likelihood function, $g(\bar{\phi})$, is also maximized. At this point, $\left\{ \frac{\partial \mathbf{g}}{\partial \phi_i} \Big|_{\bar{\phi}^*} \right\}$ is zero and Equation 3.15 becomes:

$$\bar{\mu}_{\bar{\phi}|\bar{y}} \cong [C_{\bar{\phi}|\bar{y}}] \left\{ \left[\frac{-\partial^2 \mathbf{g}}{\partial \phi_i \partial \phi_j} \Big|_{\bar{\phi}^*} \right] \bar{\phi}^* + C_{\bar{\phi}}^{-1} \bar{\mu}_{\bar{\phi}} \right\} \quad (3.17)$$

The updated means and covariances of the model parameters (Equations 3.17 and 3.16, respectively) depend on the prior means and covariances of the model parameters, the maximum likelihood point, and the second derivatives of the natural logarithm of the likelihood function. The effects of the magnitudes of the second derivatives will be discussed in Section 3.4.5.

One challenge in implementing Equations 3.16 and 3.17 is when the natural logarithm of the likelihood function is discontinuous near the expansion point. In this case, the second derivatives in $\left[\frac{-\partial^2 \mathbf{g}}{\partial \phi_i \partial \phi_j} \Big|_{\bar{\phi}^*} \right]$ are difficult or impossible to obtain. An alternative formulation of this approach is to use the first and second moments of the natural logarithm of the likelihood function:

$$C_{\bar{\phi}|\bar{y}} = \left[[C_G]^{-1} + [C_{\bar{\phi}}]^{-1} \right]^{-1} \quad (3.18)$$

$$\bar{\mu}_{\bar{\phi}|\bar{y}} = C_{\bar{\phi}|\bar{y}} \left[[C_G]^{-1} \bar{\mu}_G + [C_{\bar{\phi}}]^{-1} \bar{\mu}_{\bar{\phi}} \right] \quad (3.19)$$

where $[C_G]$ is a matrix with the second central moments of the natural logarithm of the likelihood function and $\bar{\mu}_G$ is a vector with the first central moment (center of mass) of the natural logarithm of the likelihood function. Therefore, $\left[\frac{-\partial^2 \mathbf{g}}{\partial \phi_i \partial \phi_j} \Big|_{\bar{\phi}^*} \right]$ is replaced with $[C_G]^{-1}$ and $\bar{\phi}^*$ is replaced with $\bar{\mu}_G$. The advantage of this alternative formulation is that

maximizing the natural logarithm of the likelihood function to get $\bar{\phi}^*$ and then calculating the second derivatives to get $\left[\frac{-\partial^2 \mathbf{g}}{\partial \phi_i \partial \phi_j} \Big|_{\bar{\phi}^*} \right]$, which can be difficult and even impossible in some cases, is not necessary. The disadvantage of the alternative formulation is that numerical integration is generally required to obtain $\bar{\mu}_G$ and $[C_G]$.

3.4.4 Formulation of FOSM Bayesian Method for Test Program Design

For test program design, data have not been collected yet, and therefore the updated means and covariances of the model parameters are uncertain. Numerical simulation is usually used to estimate the expected values of the updated moments; however, the FOSM Bayesian Method can make use of analytical approximations to obtain the expected values. When designing a test program with the FOSM Bayesian method, the amount and type of data that will be collected are first determined, then the expected covariances of the model parameters are updated. By trying different test programs, the expected reductions in the variances of model parameters may be compared. The best program may be selected by balancing the cost or difficulty of the test program with the benefit of variance reduction provided by the test program for the model parameters. The full derivation of the FOSM Bayesian method for test program design is contained in Gilbert (1999) and summarized by Muchard (1997). The steps of this derivation, which result in an approximation for the expected covariance of the model parameters, are summarized below:

1. Obtain first-order approximations of the expected mean and covariance of the updated model parameters from Equations 3.15 and 3.16:

$$\begin{aligned}
E_{\bar{Y}}(\bar{\mu}_{\Phi|\bar{Y}}) &\cong \left[E_{\bar{Y}} \left[\frac{-\partial^2 \mathbf{g}}{\partial \phi_i \partial \phi_j} \Big|_{\bar{\phi}^*} \right] + \mathbf{C}_{\bar{\Phi}}^{-1} \right]^{-1} \\
&\quad \left\{ E_{\bar{Y}} \left[\frac{-\partial^2 \mathbf{g}}{\partial \phi_i \partial \phi_j} \Big|_{\bar{\phi}^*} \right] E_{\bar{Y}}(\bar{\phi}^*) - E_{\bar{Y}} \left\{ \frac{\partial \mathbf{g}}{\partial \phi_i} \Big|_{\bar{\phi}^*} \right\} + \mathbf{C}_{\bar{\Phi}}^{-1} \bar{\mu}_{\bar{\Phi}} \right\}
\end{aligned} \tag{3.20}$$

$$E_{\bar{Y}}(\mathbf{C}_{\Phi|\bar{Y}}) \cong \left[E_{\bar{Y}} \left[\frac{-\partial^2 \mathbf{g}}{\partial \phi_i \partial \phi_j} \Big|_{\bar{\phi}^*} \right] + \mathbf{C}_{\bar{\Phi}}^{-1} \right]^{-1} \tag{3.21}$$

where:

$E_{\bar{Y}}(\)$ = the expected value with respect to the data that will be collected

2. Use an approximation for the expected Taylor series expansion point (derived in Gilbert 1999):

$$E(\bar{\phi}^*) \cong \bar{\mu}_{\Phi|\bar{Y}} \tag{3.22}$$

This approximation indicates that the prior parameter mean values are the most likely values and will maximize the likelihood function. Therefore,

$E \left\{ \frac{\partial \mathbf{g}}{\partial \phi_i} \Big|_{\bar{\phi}^*} \right\}$ is zero.

3. Substituting the approximation of Equation 3.22 into Equations 3.20 and 3.21, the expected mean and covariances for the model parameters become:

$$E_{\bar{y}}(\bar{\mu}_{\bar{\phi}|\bar{y}}) \cong \bar{\mu}_{\bar{\phi}} \quad (3.23)$$

$$E_{\bar{y}}(C_{\bar{\phi}|\bar{y}}) \cong \left[E_{\bar{y}} \left[\left. \frac{-\partial^2 \mathbf{g}}{\partial \phi_i \partial \phi_j} \right|_{\bar{\mu}_{\bar{\phi}}} \right] + C_{\bar{\phi}}^{-1} \right]^{-1} \quad (3.24)$$

where the expected value of the second derivative of $\mathbf{g}(\bar{\phi})$ is evaluated by integrating over all possible values of the data vector, \bar{y} :

$$E_{\bar{y}} \left[\left. \frac{-\partial^2 \mathbf{g}}{\partial \phi_i \partial \phi_j} \right|_{\bar{\mu}_{\bar{\phi}}} \right] = \int_{-\infty}^{\infty} \dots \int_{-\infty}^{\infty} \left. \frac{-\partial^2 \mathbf{g}}{\partial \phi_i \partial \phi_j} \right|_{\bar{\mu}_{\bar{\phi}}} L(\bar{y}|\bar{\mu}_{\bar{\phi}}) dy_1 \dots dy_n \quad (3.25)$$

The expected values for the updated means of the model parameters are the same as the prior means of the model parameters. Since the prior mean values are the parameter values that are expected to be obtained with data, it is reasonable that the expected updated parameters are the same as the prior values. The expected values for the updated covariances of the model parameters depend on the expected values of the second derivatives of the natural logarithm of the likelihood function evaluated at the prior means. These second derivatives are discussed in the section below.

3.4.5 Second Derivatives of the Natural Logarithm of the Likelihood Function

The effect of the data on the updated covariances of the model parameters is determined by the matrix of second derivatives of the natural logarithm of the likelihood function. To simplify notation, the matrix of second derivatives of the natural logarithm of the likelihood function will also be referred to as G'' . If the likelihood function is maximized, the vector of first derivatives is zero and G'' must be negative definite. This is equivalent to the second derivative test for a local maximum of a single-parameter function, $f(x)$: at a local maximum, $\frac{df(x)}{dx} = 0$ and $\frac{d^2f(x)}{dx^2} < 0$.

Equations 3.16 and 3.24 show that the updated covariances (for data analysis) and the expected updated covariances (for test program design) depend on the prior covariances of the model parameters and on G'' . The magnitudes of the second derivatives in G'' indicates how much is learned about the model parameters from the measured or expected data. When the absolute magnitudes of the second derivatives are large compared to the inverse of the prior covariance matrix, G'' will dominate the updated covariances or expected updated covariances of the model parameters. In this case, the data provide a large amount of information about the model parameters and the updated covariances are therefore reduced significantly from the prior covariances. When the absolute magnitudes of the second derivatives are small compared to the inverse of the prior covariance matrix, the prior covariances will dominate the updated covariances or expected updated covariances of the model parameters. In this case, the data do not provide much information about the model parameters, and the updated covariances are not reduced significantly from the prior.

The effect of the magnitude of the second derivatives is illustrated for the case of one model parameter in Figure 3.3. The updated variance of the model parameter is

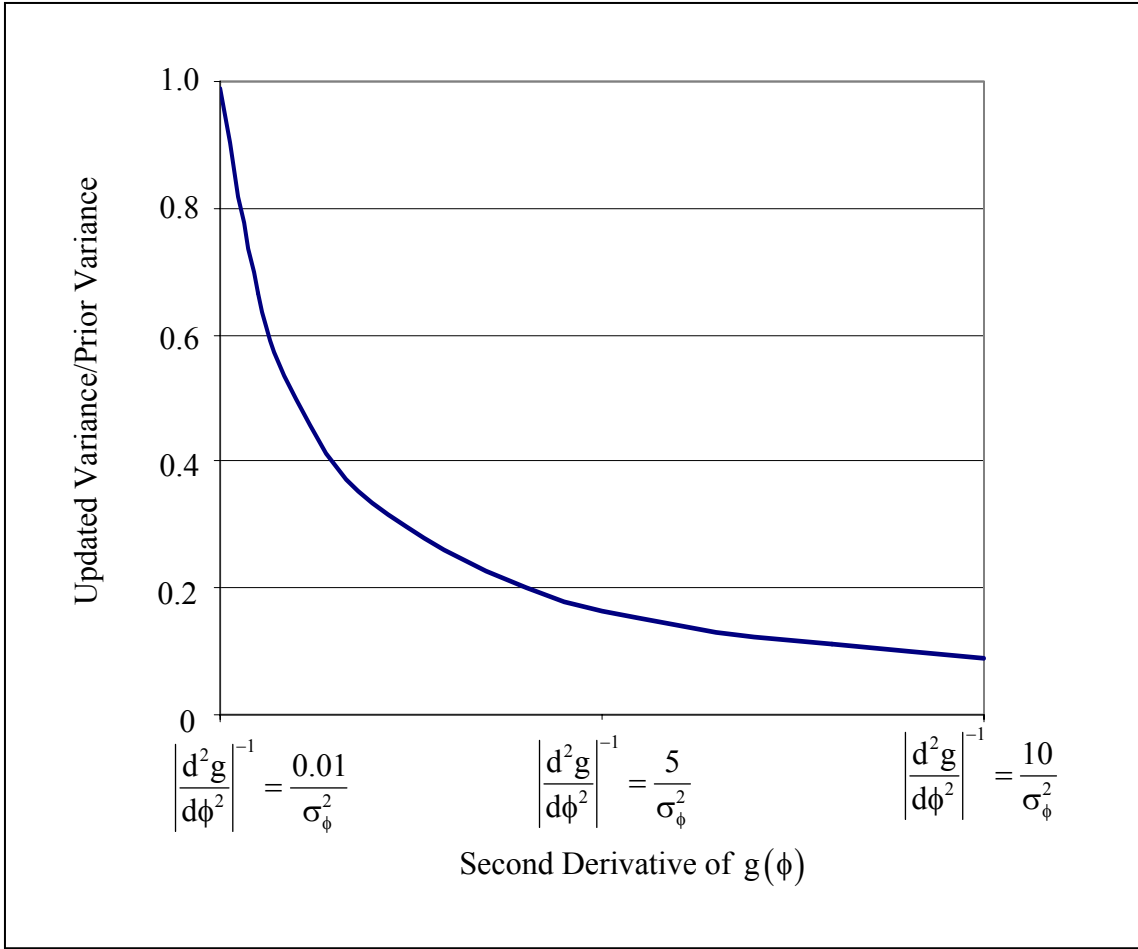


Figure 3.3. Effect of the magnitude of $g(\phi)$ on the variance reduction for a single model parameter.

calculated with Equation 3.16, which reduces to the following for only one model parameter:

$$C_{\phi|y} \cong \frac{1}{\frac{-\partial^2 g}{\partial \phi^2} \Big|_{\phi^*} + \sigma_\phi^2} \quad (3.26)$$

In Figure 3.3, the updated variance divided by the prior variance is plotted as a function of the second derivative of natural logarithm of the likelihood function. As the value of this ratio of updated to prior variance decreases, the variance of the model parameter is reduced more from the prior variance and therefore more is learned about the model parameter. The value of the second derivative is expressed as a function of the inverse of the prior variance of the model parameter. When the second derivative is 0.01 of the inverse of the prior variance of the parameter, there is virtually no variance reduction for the model parameter. However, the variance of the model parameter is reduced rapidly as the magnitude of the second derivative increases in comparison to the inverse of the prior variance.

3.4.6 Likelihood Function for Normally-Distributed Data

The choice of the likelihood function, $L(\bar{y}|\bar{\phi})$, to use in the FOSM Bayesian method depends on the distribution of the data that have been collected or are expected. When the data are described by a normal distribution, or can be easily transformed to a normal distribution, the likelihood function has a multivariate normal distribution:

$$L(\bar{y}|\bar{\phi}) = \frac{1}{(2\pi)^{n/2} |\mathbf{C}_{\bar{Y}}|^{1/2}} \exp\left[-\frac{1}{2} \{\bar{y} - \bar{\mu}_{\bar{Y}}\}^T \mathbf{C}_{\bar{Y}}^{-1} \{\bar{y} - \bar{\mu}_{\bar{Y}}\}\right] \quad (3.27)$$

The natural logarithm of the likelihood function is then:

$$\mathbf{g}(\bar{\phi}) = -\ln\left[(2\pi)^{n/2}\right] - \frac{1}{2} \ln\left(|\mathbf{C}_{\bar{Y}}|^{1/2}\right) - \frac{1}{2} \{\bar{y} - \bar{\mu}_{\bar{Y}}\}^T \mathbf{C}_{\bar{Y}}^{-1} \{\bar{y} - \bar{\mu}_{\bar{Y}}\} \quad (3.28)$$

where:

n = the number of data points measured or expected

$\bar{\mu}_{\bar{y}}$ = the vector of the mean data values predicted by the model that depends on $\bar{\phi}$

$C_{\bar{y}}$ = the covariance matrix of the data points predicted by the model that depends on $\bar{\phi}$

The derivation of the first and second derivatives, and the expected first and second derivatives, of this likelihood function are presented in Muchard (1997) and Gilbert (1999).

3.4.6.1 Conditional Likelihood Function

For a set of y_n measurements of the variable y , the likelihood function is the joint distribution of the data:

$$L(\bar{y}|\bar{\phi}) = f_{Y_1, Y_2, \dots, Y_n}(y_1, y_2, \dots, y_n) dy_1 dy_2 \dots dy_n \quad (3.29)$$

which can also be expressed in terms of conditional probabilities:

$$\begin{aligned} L(\bar{y}|\bar{\phi}) &= L(y_n | y_1, y_2, \dots, y_{n-1}) \\ &\quad \times L(y_{n-1} | y_1, y_2, \dots, y_{n-2}) \\ &\quad \times \dots \times L(y_2 | y_1) \times L(y_1) \\ &= f_{Y_n | Y_1, Y_2, \dots, Y_{n-1}}(y_n | y_1, y_2, \dots, y_{n-1}) \\ &\quad \times f_{Y_{n-1} | Y_1, Y_2, \dots, Y_{n-2}}(y_{n-1} | y_1, y_2, \dots, y_{n-2}) \\ &\quad \times \dots \times f_{Y_2 | Y_1}(y_2 | y_1) \times f_{Y_1}(y_1) \times dy_1 dy_2 \dots dy_n \end{aligned} \quad (3.30)$$

The natural logarithm of the likelihood function is then:

$$\begin{aligned}
g(\bar{\phi}) = & \ln \left[f_{Y_n|Y_1, Y_2, \dots, Y_{n-1}}(y_n | y_1, y_2, \dots, y_{n-1}) \right] \\
& + \ln \left[f_{Y_{n-1}|Y_1, Y_2, \dots, Y_{n-2}}(y_{n-1} | y_1, y_2, \dots, y_{n-2}) \right] \\
& + \dots + \ln \left[f_{Y_2|Y_1}(y_2 | y_1) \right] + \ln \left[f_{Y_1}(y_1) \right] + \ln \left[dy_1 dy_2 \dots dy_{n_y} \right]
\end{aligned} \tag{3.31}$$

The natural logarithm of the likelihood function may therefore be calculated sequentially for each data point using the conditional likelihood. For each normally-distributed data point, the conditional likelihood is:

$$L(y_i | y_1, y_2, \dots, y_{i-1}) = \text{PDF} \left(\frac{y_i - \mu_{Y_i|y_1, y_2, \dots, y_{i-1}}}{\sigma_{Y_i|y_1, y_2, \dots, y_{i-1}}} \right) \tag{3.32}$$

where $\text{PDF}(\)$ is the probability distribution function for a normal distribution and $\mu_{Y_i|y_1, y_2, \dots, y_{i-1}}$ and $\sigma_{Y_i|y_1, y_2, \dots, y_{i-1}}$ are the moments of y_i conditioned on the previously known data points, y_1, y_2, \dots, y_{i-1} . These conditional moments are presented in the next section.

3.4.6.2 Conditional Moments

The likelihood function for normally-distributed data depends on the conditional mean and standard deviation of each data point, as shown in Equations 3.32. Since the conditional probability function is calculated sequentially for each data point (Equation 3.31), each data point is conditioned on the previously known data points. The following subscripts will be used to denote the current data point and the known data points:

A = the current data point under consideration, y_i

B = the set of known data points, y_1, y_2, \dots, y_{i-1}

The mean value for Y_i conditioned on multiple known data points y_1 through y_{i-1} is then:

$$\mu_{Y_i|y_1, y_2, \dots, y_{i-1}} = \mu_{Y_A|Y_B} = \mu_{Y_A} + C_{Y_{AB}} \left\{ \bar{y}_B - \bar{\mu}_{Y_B} \right\} \quad (3.33)$$

$$\sigma_{Y_i|y_1, y_2, \dots, y_{i-1}}^2 = \sigma_{Y_A|Y_B}^2 = \sigma_{Y_A}^2 - C_{Y_{AB}} C_{Y_{BB}}^{-1} C_{Y_{AB}}^T \quad (3.34)$$

where:

μ_{Y_A} and $\sigma_{Y_A}^2$ are the model-predicted moments for the data point currently under evaluation:

$$\mu_{Y_A} = \mu_{Y_i} \quad (3.35)$$

$$\sigma_{Y_A}^2 = \sigma_{Y_i}^2 \quad (3.36)$$

\bar{y}_B is the vector of previous data measurements:

$$\bar{y}_B = \left\{ \begin{array}{c} y_1 \\ \vdots \\ y_{i-1} \end{array} \right\} \quad (3.37)$$

$\bar{\mu}_{Y_B}$ is the vector of model-predicted mean values for the previous data points:

$$\bar{\mu}_{Y_B} = \begin{Bmatrix} \mu_{Y_1} \\ \vdots \\ \mu_{Y_{i-1}} \end{Bmatrix} \quad (3.38)$$

$C_{Y_{BB}}$ is the covariance matrix for the previous data points:

$$C_{Y_{BB}} = \begin{bmatrix} \text{Cov}(Y_1, Y_1) & \text{Cov}(Y_1, Y_2) & \cdots & \text{Cov}(Y_1, Y_{i-1}) \\ \text{Cov}(Y_2, Y_1) & \text{Cov}(Y_2, Y_2) & \cdots & \text{Cov}(Y_2, Y_{i-1}) \\ \vdots & \vdots & \vdots & \vdots \\ \text{Cov}(Y_{i-1}, Y_1) & \text{Cov}(Y_{i-1}, Y_2) & \cdots & \text{Cov}(Y_{i-1}, Y_{i-1}) \end{bmatrix} \quad (3.39)$$

and $C_{Y_{AB}}$ is the covariance between the current data point and the previous data points:

$$C_{Y_{AB}} = [\text{Cov}(Y_i, Y_1) \quad \cdots \quad \text{Cov}(Y_i, Y_{i-1})] \quad (3.40)$$

3.4.7 Likelihood Function for Non-Normally Distributed Data

A method for including measured data that do not have a normal distribution into the FOSM Bayesian Method is described in Gilbert and Wang (2003) and will be outlined in this section. The method uses Hermite Polynomials to transform the data to a normal distribution, and the coefficients of the Hermite Polynomial transform function are treated as model parameters in the data analysis. Two assumptions are made regarding the non-normally-distributed data: (1) the probability density function has the same normalized shape for each data point (that is, $\frac{Y_i - \mu_{Y_i}}{\sigma_{Y_i}}$ has the same distribution for all i), and (2) statistical relationships between all data points are linear (described by the

first and second moments). The likelihood function used for the transformed data is a conditional likelihood function, with each data point conditioned on the previous data points as shown in the previous section.

3.4.7.1 Hermite Polynomial Transform Function

Hermite Polynomials are derived from the cumulative density function for a standard normal distribution and are defined as follows (Journal and Huijbregts 1978):

$$H_i(u) = e^{\frac{u^2}{2}} \frac{d^i}{du^i} \left(e^{-\frac{u^2}{2}} \right) \quad (3.41)$$

where:

u = a variable with a standard normal distribution

i = the order of the Hermite Polynomial

Equations and graphs for Hermite Polynomials from the zero through fifth order are presented in Figures 3.4 and 3.5. Notice that the scale of the x-axis is the same in each plot and that although the scale of the y-axis varies, the gridlines cross the y-axis at the same interval on each plot. As the order of the Hermite Polynomial increases, the tails of the polynomial become more sensitive to the value of u when u is small or large. This indicates that a higher order of Hermite Polynomial will be required to fit the tails of non-normal distributions.

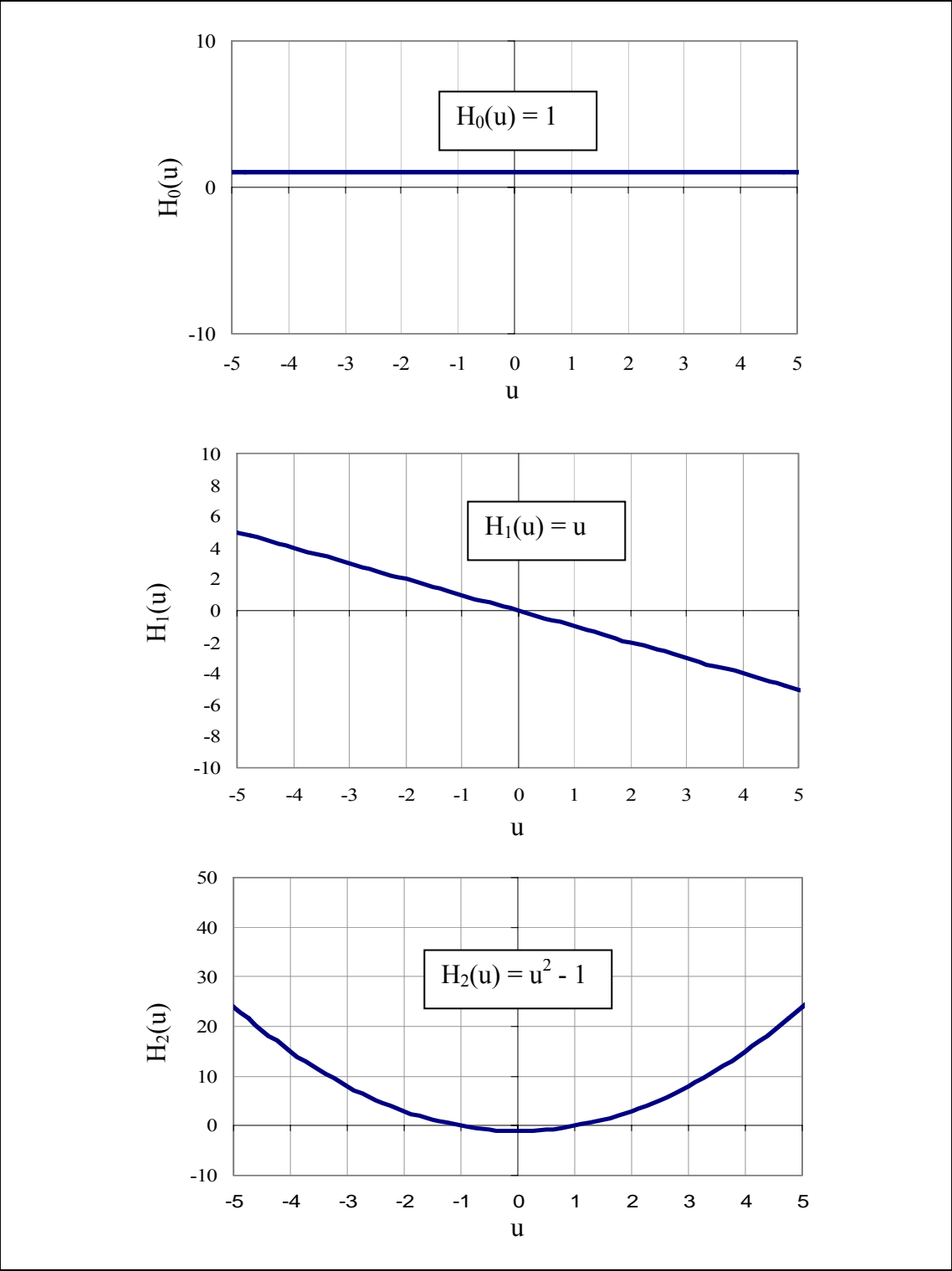


Figure 3.4. Hermite Polynomials, order zero through two.

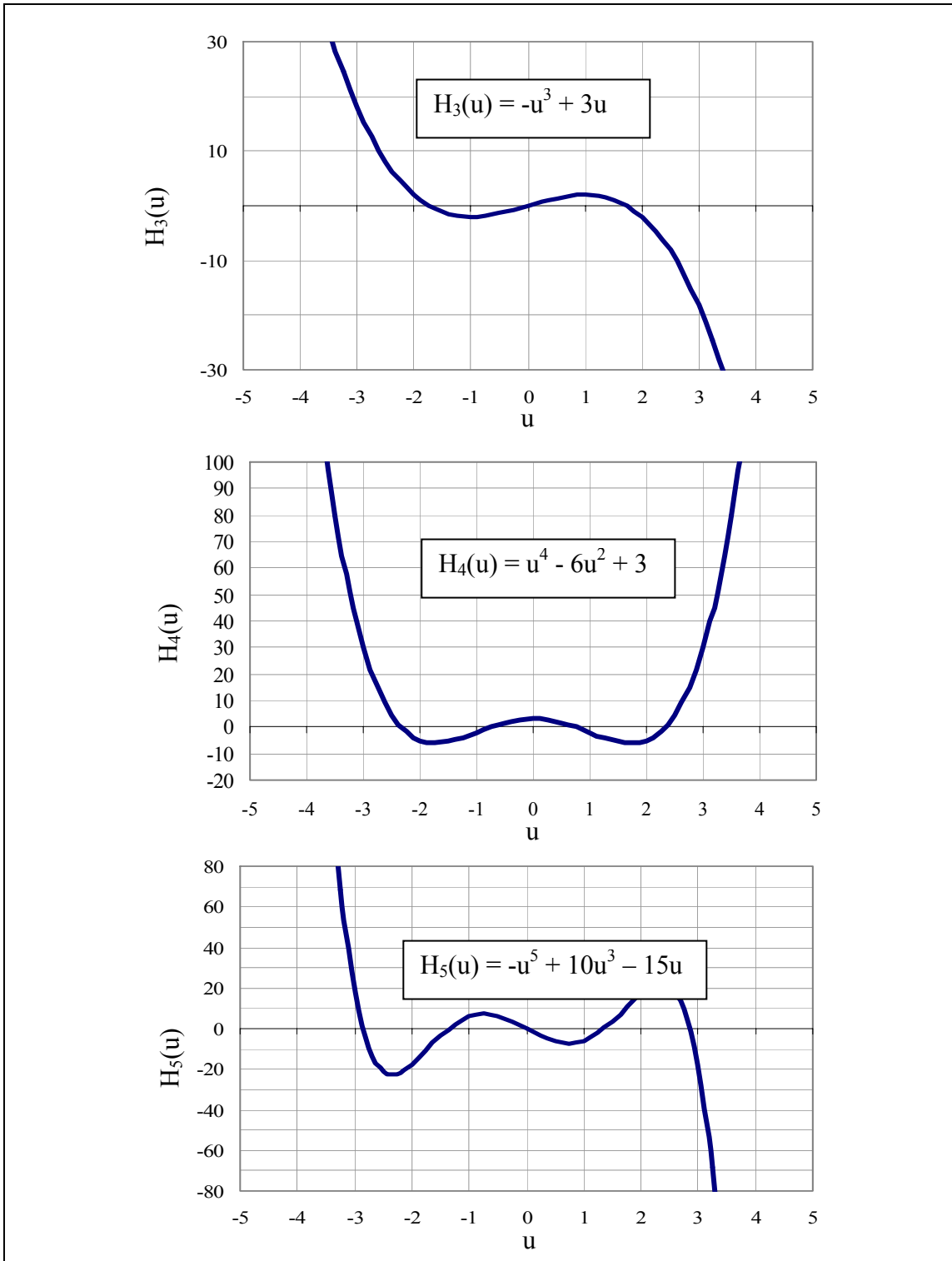


Figure 3.5. Hermite Polynomials, order three through five.

To fit data with a non-normal probability distribution to a standard normal distribution, a transform function is used:

$$Y = \varphi_Y (U) \tag{3.42}$$

where:

Y = a general random variable, with non-normal distribution

U = a standard normal variable

φ_Y = the transform function

A transform function using Hermite Polynomials is presented by Journal and Huijbergts (1978) and may be expressed as follows:

$$Y = \varphi_Y (U) \cong \sum_{i_\psi=0}^{n_\psi} \frac{\Psi_{i_\psi}}{i_\psi!} H_{i_\psi} (U) \tag{3.43}$$

where:

n_ψ = the order of the transform

Ψ_i = the coefficient of the transform

The first two coefficients of the transform function are related to the mean and standard deviation of the random variable, Y :

$$\Psi_0 = \mu_Y \tag{3.44}$$

$$\Psi_1 = \frac{\sigma_Y}{\sqrt{1 + \sum_{i=2}^n \frac{(\Psi_i')^2}{i!}}} \quad (3.45)$$

where:

$$\Psi_i' = \frac{\Psi_i}{\Psi_1}$$

The transform function may then be expressed as follows:

$$\frac{Y - \mu_Y}{\sigma_Y} \cong \frac{1}{\sqrt{1 + \sum_{i_\psi=2}^{n_\psi} \frac{(\Psi_{i_\psi}')^2}{i_\psi!}}} \left[H_1(U) + \sum_{i_\psi=2}^{n_\psi} \frac{\Psi_{i_\psi}'}{i_\psi!} H_{i_\psi}(U) \right] \quad (3.46)$$

The transform function is therefore described by the parameters μ_Y , σ_Y , and Ψ_2' through Ψ_{n_ψ}' .

3.4.7.2 Likelihood Function

As for normally-distributed data, the likelihood function for non-normally-distributed data is expressed in terms of conditional probability density functions (Equation 3.30). The conditional probability density functions for non-normally distributed data are evaluated as follows:

$$f_{Y_i|y_1, y_2, \dots, y_{i-1}}(y_{i_y} | y_1, y_2, \dots, y_{i-1}) = \sum_{r=1}^{n_r} f_U(u_r) \left(\left| \frac{dy}{du} \right|_{u_r} \right)^{-1} \quad (3.47)$$

where $f_U(u_r)$ is the standard normal probability density function and each u_r is one of n_r real roots of u for the transformed data point y_{i_y} , conditioned on the previous data points:

$$y_i = \mu_{Y_i|y_1, y_2, \dots, y_{i-1}} \frac{\sigma_{Y_i|y_1, y_2, \dots, y_{i-1}}}{-\sqrt{1 + \sum_{i_\psi=2}^{n_\psi} \frac{(\psi'_{i_\psi})^2}{i_\psi!}}} \left[H_1(u) + \sum_{i_\psi=2}^{n_\psi} \frac{\psi'_{i_\psi}}{i_\psi!} H_{i_\psi}(u) \right] \quad (3.48)$$

The roots are the values of u that will result in the value of y_i from the Hermite Polynomial transform. The derivative of the above equation, evaluated at each root u_r , is $\left. \frac{dy}{du} \right|_{u_r}$ in Equation 3.47:

$$\left. \frac{dy}{du} \right|_{u_r} = \frac{\sigma_{Y_i|y_1, y_2, \dots, y_{i-1}}}{-\sqrt{1 + \sum_{i_\psi=2}^{n_\psi} \frac{(\psi'_{i_\psi})^2}{i_\psi!}}} \left[\frac{dH_1(u_r)}{du} + \sum_{i_\psi=2}^{n_\psi} \frac{\psi'_{i_\psi}}{i_\psi!} \frac{dH_{i_\psi}(u_r)}{du} \right] \quad (3.49)$$

The derivatives of the Hermite Polynomials, $\frac{dH_1(u_r)}{du}$, are as follows:

$$\frac{dH_{i_\psi}(u)}{du} = \begin{cases} 0 & \text{for } i_\psi = 0 \\ -1 & \text{for } i_\psi = 1 \\ -H_{i_\psi-1}(u) - u \frac{dH_{i_\psi-1}(u)}{du} - (i_\psi - 1) \frac{dH_{i_\psi-2}(u)}{du} & \text{for } i_\psi > 1 \end{cases} \quad (3.50)$$

The first and second derivatives of the likelihood function are presented in Gilbert and Wang (2003). The conditional moments for each data point that are used in Equations 3.48 and 3.49 are described in the next section.

3.4.7.3 *Conditional Moments*

The likelihood function for non-normally-distributed data depends on the conditional mean and standard deviation of each data point, as shown in Equations 3.48 and 3.49. Since the conditional probability function is calculated sequentially for each data point (Equation 3.31), each data point is conditioned on the previously known data points.

In order to calculate the conditional moments for non-normally distributed data points, a linear relationship is assumed between data points. A linear relationship for two data points, y_i and y_j , is shown in Figure 3.6. The mean value of y_i is modeled to increase as the value of y_j increases according to a linear trend (Ang and Tang 1975):

$$\mu_{Y_i|y_j} = \alpha + \beta y_j \quad (3.51)$$

where α is the intercept of the line and β is the slope.

For data points with normal distributions, this linear relationship is an inherent property and the values of α and β are (Ang and Tang 1975):

$$\alpha = \mu_{Y_i} - \beta \mu_{y_j} \quad (3.52)$$

$$\beta = \rho_{Y_i, Y_j} \frac{\sigma_{Y_i}}{\sigma_{Y_j}} \quad (3.53)$$

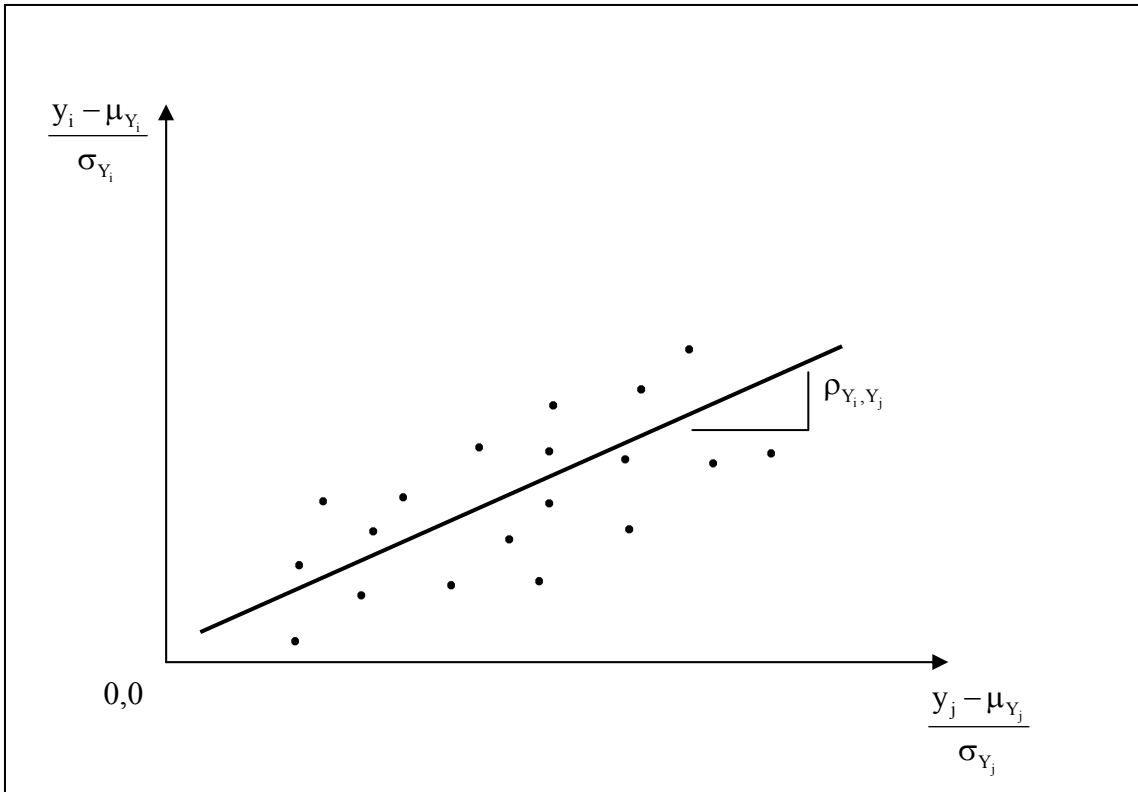


Figure 3.6. Linear relationship between two data points, y_i and y_j .

For data points with non-normal distributions, this linear relationship is still assumed to apply. With this assumption, Equation 3.33 and Equation 3.34 describe the conditional mean and variance, respectively, of a non-normally distributed data point Y_i .

3.5 SUMMARY

The basic framework of the FOSM Bayesian method was outlined in this chapter for data sets with only point measurements (no censored data points). The methodology for the two uses of the FOSM Bayesian method, data analysis and test program design, were summarized. The distribution of the data is accounted for in the likelihood function,

which describes the likelihood that the data are observed given a set of model parameters. For normally distributed data, a multivariate normal distribution is used for the likelihood function. For non-normally distributed data, a conditional distribution is used that includes a Hermite polynomial transformation of the data to a multivariate normal distribution. These cases provide the basis for the extension of the FOSM Bayesian method to include censored data, which is presented in the next chapter.

Chapter 4. Bayesian Method with Censored Measurements

4.1 INTRODUCTION

The FOSM Bayesian method has been applied thus far for data analysis for both normally-distributed and generally-distributed data sets with no censoring. It has also been used in test program design for normally-distributed data sets with no censoring. The method was outlined briefly for these cases in the last chapter. This research develops an approach proposed by McBrayer (2000) to include censored data in the FOSM Bayesian method. In this chapter, the methods for including censored data in both data analysis and test program design are derived for normally-distributed and non-normally-distributed data. The definition of a censored data point is first discussed, then the likelihood functions used for normally-distributed and non-normally distributed data points are presented. The conditional moments of the censored data points, which are used in the likelihood functions, and the moments of the censored region of the data points, which are used in the conditional moments, are derived.

4.2 CENSORED DATA POINTS

When a data point is censored, its precise value is uncertain, as discussed in Section 2.2. The value of the data point is only known to lie within a censored region, which is generally above or below a fixed threshold. The censored region for a data point y_i is defined in the remainder of this dissertation as follows:

$y_{i,l}$ = lower bound of censored region for data point y_i

$y_{i,u}$ = upper bound of censored region for data point y_i

The subscript “ul” will be used to denote the censored region between $y_{i,l}$ and $y_{i,u}$.

A censored data point is illustrated in Figure 4.1 for a data point with a normal distribution. In this example, the censored region is in the middle of the distribution. Data values between $y_{i,l}$ and $y_{i,u}$ are censored, so that their exact values are not known. The mean, $\mu_{Y_i,ul}$, and standard deviation, $\sigma_{Y_i,ul}$, of Y_i in the censored region are also shown in Figure 4.1. Note that a point (non-censored) measurement may be thought of as a censored measurement when $y_{i,l}$ approaches $y_{i,u}$ and there is no censored region for that data point.

It is rare for a censored region to occur in the middle of a distribution for engineering applications. The censored region is usually in a tail of the distribution, as shown in Figures 4.2 and 4.3. In Figure 4.2, $y_{i,l}$ is negative infinity and $y_{i,u}$ is a threshold value below which data are censored. An example of this case is a contaminant concentration in water that is below the detection limit. In Figure 4.3, $y_{i,u}$ is positive infinity and $y_{i,l}$ is a threshold value above which data are censored. An example of this case is a proof load test. The expected value of the data point may be inside or outside the censored region. In Figure 4.2, the expected value of the data point is not in the censored region, and the data point is not expected to be censored. In Figure 4.3, the censored region includes more of the distribution. In this case, the expected value is within the censored region and this data point is therefore expected to be censored.

The procedure for including censored data in the FOSM Bayesian method for data analysis follows the same steps as the procedure described in Section 3.4. However, the likelihood function changes when a data point is censored. The probability of obtaining a censored data point is the area of the censored region in the distribution of the data point:

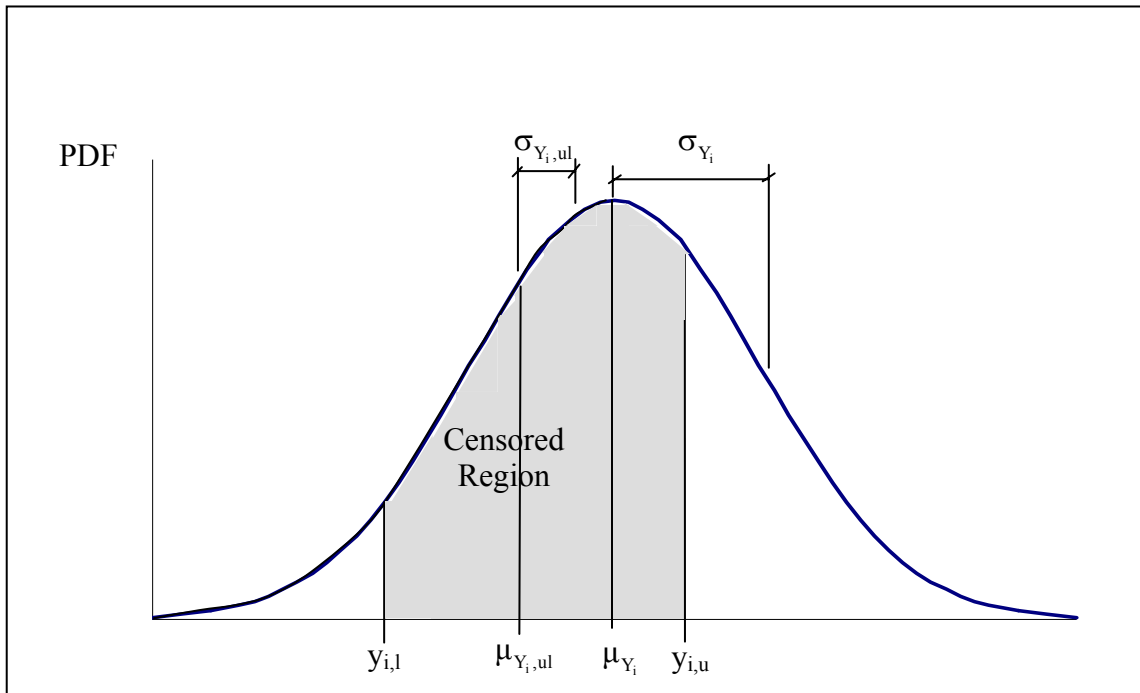


Figure 4.1. Normally-distributed data point with censoring between $y_{i,l}$ and $y_{i,u}$.

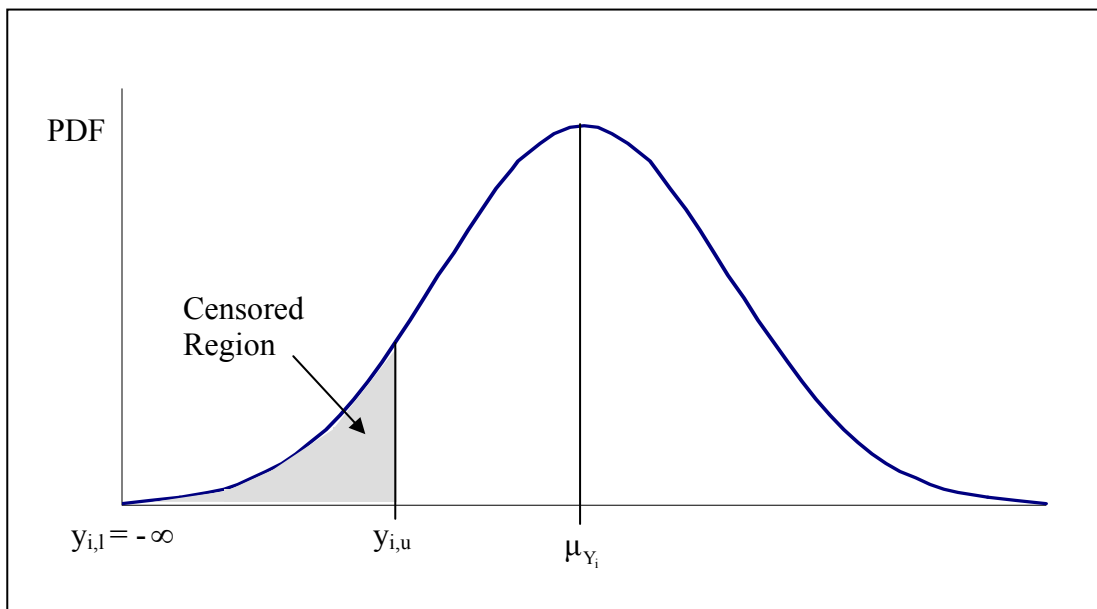


Figure 4.2. Normally-distributed data point censored in the lower tail of the distribution.

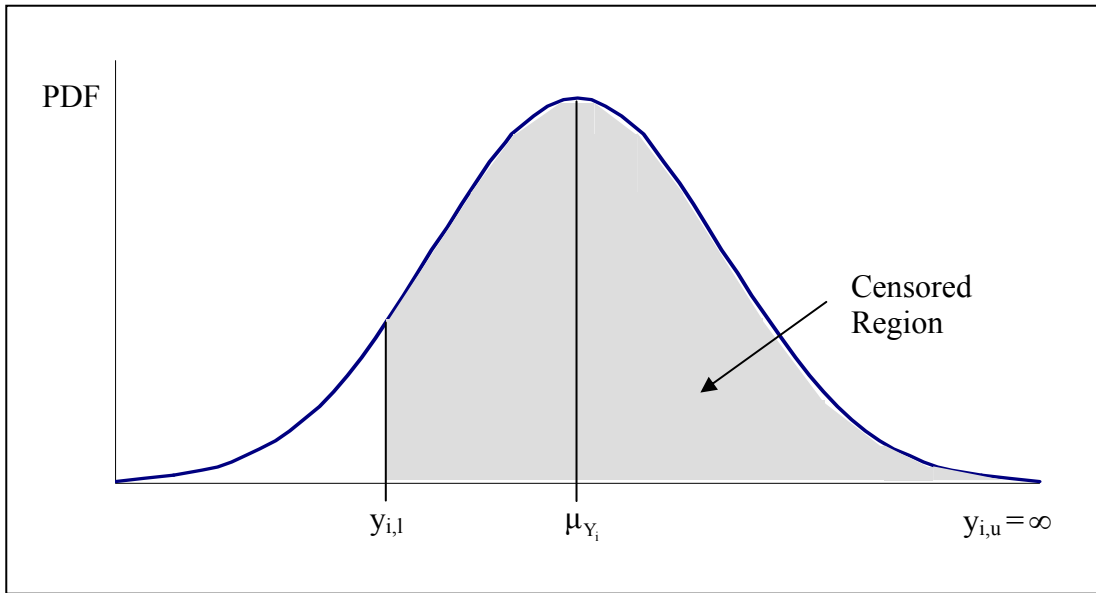


Figure 4.3. Normally-distributed data point censored in the upper tail of the distribution.

$$P(y_{i,l} < Y_i \leq y_{i,u}) = F_Y(y_{i,u}) - F_Y(y_{i,l}) \quad (4.1)$$

where $F_Y(\cdot)$ is the cumulative distribution function (CDF) for the data point. Therefore, the likelihood function for a data point that is censored is:

$$L(y_i | \bar{y}_B) = F_{Y|\bar{y}_B}(y_{i,u} | \bar{y}_B) - F_{Y|\bar{y}_B}(y_{i,l} | \bar{y}_B) \quad (4.2)$$

where \bar{y}_B is defined in Chapter 3 (Equation 3.37) to be the set of all available data, y_1, y_2, \dots, y_{i-1} . Note that for a point measurement:

$$P\left(y_i - \frac{dy}{2} < Y_i \leq y_i + \frac{dy}{2}\right) = \frac{dF_Y(y_i)}{dy} = \text{PDF}(y_i) \quad (4.3)$$

The next section describes how to calculate $F_{Y_i|\bar{y}_B}(y_{i,u}|\bar{y}_B)$ and $F_{Y_i|\bar{y}_B}(y_{i,l}|\bar{y}_B)$ when data point y_i is censored.

4.3 LIKELIHOOD FUNCTION FOR A CENSORED DATA POINT

When a data point is censored, the likelihood function is the probability that the value will be within the censored region, which is found from the cumulative distribution function for the data point. In this section, the likelihood function for a normally-distributed censored data point, which is obtained from the standard normal function, is first described. The likelihood function for a non-normally-distributed censored data point is then presented. This likelihood function uses the Hermite Polynomial transform function (Section 3.4.7.1) to evaluate the cumulative distribution function.

4.3.1 Likelihood Function for a Normally-Distributed Censored Data Point

The cumulative distribution function for a normally-distributed data point is obtained from the standard normal function as follows:

$$F_{Y|\bar{y}_B}(y_i|\bar{y}_B) = F_{Y|\bar{y}_B}(y_A|Y_B) = \Phi\left(\frac{y_A - \mu_{Y_A|Y_B}}{\sigma_{Y_A|Y_B}}\right) \quad (4.4)$$

where:

$\mu_{Y_A|Y_B}$ = the mean value of Y_A conditioned on the known measurements, Y_B

$\sigma_{Y_A|Y_B}$ = the standard deviation of Y_A conditioned on the known measurements, Y_B

$\Phi()$ = the standard normal function

The conditional likelihood function in Equation 3.30 for a normally-distributed censored data point is therefore:

$$L(y_i | \bar{y}_B) = L(Y_A | Y_B) = \Phi\left(\frac{y_{i,u} - \mu_{Y_A|Y_B}}{\sigma_{Y_A|Y_B}}\right) - \Phi\left(\frac{y_{i,l} - \mu_{Y_A|Y_B}}{\sigma_{Y_A|Y_B}}\right) \quad (4.5)$$

Note that this is similar to the conditional likelihood of Equation 3.32 for a non-censored point. The probability density function for a normal distribution is used for non-censored data, while the cumulative distribution function is used for censored data.

4.3.2 Likelihood Function for a Non-Normally Distributed Data Point

From the Hermite Polynomial transform function described in Section 3.4.7.1, the cumulative distribution function is obtained as follows:

$$F_{Y|Y_B}(y_i | Y_B) = \sum_{k=1}^{n_k} [\Phi(u_{t,k}) - \Phi(u_{-\infty,k})] \quad (4.6)$$

where n_k is the number of regions where $u_{-\infty} < u \leq u_t$ gives a value of $y \leq y_i$. The relationship between y_i and u is obtained from Equation 3.48. Therefore, additional model parameters, ψ_{i_ψ} for $i_\psi = 1$ to n_ψ , describe the likelihood function in addition to those that describe $\mu_{Y_A|Y_B}$ and $\sigma_{Y_A|Y_B}$.

The calculation of the likelihood function for a non-normally-distributed, censored data point is illustrated in Figure 4.4. The Hermite Polynomial transform function for the data point is shown, and in this case y has one root at u_t . Because there is

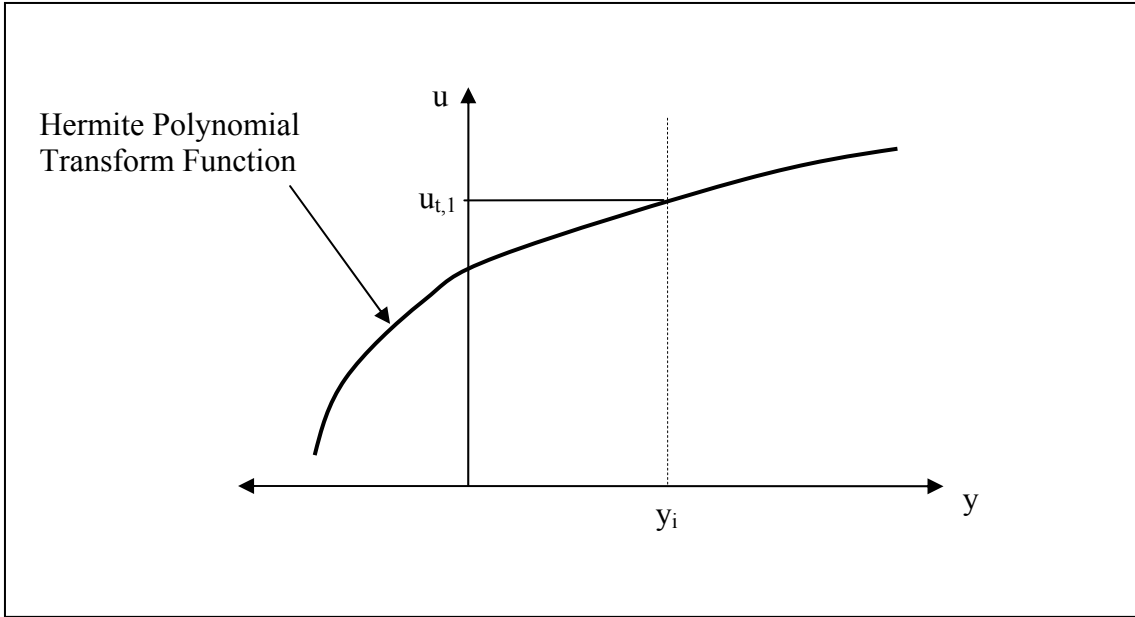


Figure 4.4. Finding the probability that a data point is censored for non-normally distributed data.

only one root, there is only one region where $u_{-\infty} < u \leq u_t$ results in $y \leq y_i$. The value of this root is found first, then it is used in Equation 4.5 to calculate the likelihood function:

$$F_{Y|Y_B}(y_i | Y_B) = \Phi(u_t) - \Phi(u_{-\infty}) \quad (4.7)$$

where $u_{-\infty} = -\infty$, and then $\Phi(-\infty) = 0$.

Note that a normal distribution is a special case of the Hermite Polynomial transform function. For a normal distribution, the number of additional model parameters to describe the likelihood function, n_ψ , is zero. Since $H_1(u)$ is equal to u (Figure 3.4), this reduces Equation 3.48 to:

$$\frac{y_i - \mu_{Y_A|Y_B}}{\sigma_{Y_A|Y_B}^2} = u \quad (4.8)$$

which is the definition of a standard normal variate.

4.4 CONDITIONAL MOMENTS FOR CENSORED DATA

The likelihood functions for both normally-distributed and non-normally-distributed censored data points depend on the conditional moments of the data point, as shown in Equations 4.4 and 4.5. Each data point is related to the data points measured previously by using a conditional mean and standard deviation for the current data point. The conditional mean for a data point, $\mu_{Y_A|Y_B}$, is the model-predicted expected value for that point given the known measurements, and the conditional standard deviation, $\sigma_{Y_A|Y_B}$, is the model-predicted uncertainty for that point given the known measurements. The conditional mean may be inside or outside the censored region. In this section, the conditional moments for a normally-distributed censored data point are derived. These moments are used as an approximation for the non-normal case, and this approximation is evaluated.

4.4.1 Conditional Moments for a Normally-Distributed Censored Data Point

The conditional moments for a normally-distributed censored data point are calculated from the multivariate normal distribution. Because the derivation of the conditional moments is shown most easily if \bar{y}_B only contains one known measurement, the conditional moments are first derived for this case of two data points. The general case of multiple data points in \bar{y}_B is then shown, followed by the special case of

independent data. The equations for calculating the mean and variance of the censored region are also presented, since these quantities are necessary to calculate the conditional moments.

4.4.1.1 Conditional Moments for One Known Data Point

For the case where \bar{y}_B contains only one known data point, the joint distribution between Y_A and \bar{y}_B is a bivariate normal distribution if both data points are normally distributed. When \bar{y}_B is not censored, the conditional mean is obtained from the conditional form of the bivariate normal distribution (Ang and Tang 1975):

$$\mu_{Y_A|Y_B=y_B} = \mu_{Y_A} + \rho_{Y_A, Y_B} \frac{\sigma_{Y_A}}{\sigma_{Y_B}} (y_B - \mu_{Y_B}) \quad (4.9)$$

where:

μ_{Y_A} = the model-predicted mean for the data point currently under evaluation

μ_{Y_B} = the model-predicted mean for the known data point

ρ_{Y_A, Y_B} = the correlation coefficient between Y_A and Y_B

y_B = the measured value of Y_B

If the measured value of Y_B is censored, its exact value is not known and the conditional mean is therefore uncertain. Since Y_B is between the upper and lower bounds of the censored region, an integral between $y_{B,l}$ and $y_{B,u}$ is applied to Equation 4.9 to find the expected value of the conditional mean:

$$E\left(\mu_{Y_A|(y_{B,l} \leq Y_B < y_{B,u})}\right) = \mu_{Y_A} + \rho_{Y_A, Y_B} \frac{\sigma_{Y_A}}{\sigma_{Y_B}} \int_{y_{B,l}}^{y_{B,u}} (y_B - \mu_{Y_B}) dy_B \quad (4.10)$$

which gives the following result for the conditional mean when Y_B is censored:

$$E\left(\mu_{Y_A|Y_B=y_B}\right) = \mu_{Y_A} + \rho_{Y_A, Y_B} \frac{\sigma_{Y_A}}{\sigma_{Y_B}} (\mu_{Y_B|ul} - \mu_{Y_B}) \quad (4.11)$$

If Y_B is not censored, the conditional variance is the variance of the bivariate normal distribution:

$$\sigma_{Y_A|Y_B=y_B}^2 = (1 - \rho_{Y_A}^2) \sigma_{Y_A}^2 \quad (4.12)$$

If Y_B is censored, then additional uncertainty is added because the conditional mean (Equation 4.11) is uncertain. The total variance is equal to the expected value of the conditional variance plus the variance of the conditional mean (Ang and Tang 1975):

$$\sigma_{Y_A|Y_B=y_B}^2 = E\left(\sigma_{Y_A|Y_B=y_B}^2\right) + \text{Var}\left(\mu_{Y_A|Y_B=y_B}\right) \quad (4.13)$$

The variance of the conditional mean is the variance of Equation 4.9:

$$\text{Var}_{ul}\left(\mu_{Y_A|Y_B=y_B}\right) = \text{Var}\left[\mu_{Y_A} + \rho_{Y_A, Y_B} \frac{\sigma_{Y_A}}{\sigma_{Y_B}} Y_B\right] \quad (4.14)$$

Since all of the terms in the equation above are constant except for Y_B , the variance of the conditional mean is:

$$\text{Var}_{\text{ul}}\left(\mu_{Y_A|(y_{B,l} \leq Y_B < y_{B,u})}\right) = \left[\rho_{Y_A, Y_B} \frac{\sigma_{Y_A}}{\sigma_{Y_B}} \right]^2 \sigma_{Y_B, \text{ul}}^2 \quad (4.15)$$

where $\sigma_{Y_B, \text{ul}}^2$ is the total conditional variance when Y_B is censored and is therefore:

$$\sigma_{Y_A|(y_{B,l} \leq Y_B < y_{B,u})}^2 = (1 - \rho_{Y_A}^2) \sigma_{Y_A}^2 + \left[\rho_{Y_A, Y_B} \frac{\sigma_{Y_A}}{\sigma_{Y_B}} \right]^2 \sigma_{Y_B, \text{ul}}^2 \quad (4.16)$$

Because $\sigma_{Y_B, \text{ul}}$ will be zero when the data are not censored and the censored region is infinitesimally small, Equation 4.9 may be used to generally express the conditional variance of Y_A , regardless of whether Y_B is censored or not:

$$\sigma_{Y_A|Y_B}^2 = (1 - \rho_{Y_A}^2) \sigma_{Y_A}^2 + \left[\rho_{Y_A, Y_B} \frac{\sigma_{Y_A}}{\sigma_{Y_B}} \right]^2 \sigma_{Y_B, \text{ul}}^2 \quad (4.17)$$

4.4.1.2 Conditional Moments for Multiple Known Data Points

The results of the previous derivation of the moments for Y_A conditioned on a single data point Y_B may be easily extended to the case where \bar{y}_B contains multiple data points. When a data point is conditioned on multiple known data points, the conditional mean from Equations 4.9 is expressed as:

$$\mu_{Y_A|Y_B} = \mu_{Y_A} + \left\{ \left[C_{Y_{BB}} \right]^{-1} \left[C_{Y_{AB}} \right] \right\}^T \left\{ \bar{y}_B - \bar{\mu}_{Y_B} \right\} \quad (4.18)$$

The values used in \bar{y}_B are determined by whether each data point in Y_B is censored or non-censored. The total variance of Y_A from Equation 4.16 is expressed as follows for multiple known data points in Y_B :

$$\sigma_{Y_A|Y_B}^2 = \sigma_{Y_A}^2 - \left\{ \left[C_{Y_{AB}} \right]^T \left[C_{Y_{BB}} \right]^{-1} \left[C_{Y_{AB}} \right] \right\} + \left\{ \left[C_{Y_{BB}} \right]^{-1} \left[C_{Y_{AB}} \right] \right\}^T \left[C_{Y_{BB,ul}} \right] \left\{ \left[C_{Y_{BB}} \right]^{-1} \left[C_{Y_{AB}} \right] \right\} \quad (4.19)$$

The third term in this equation accounts for the uncertainty in the conditional mean value of Y_A when data points in Y_B are censored. The vectors and matrices used in Equations 4.10 and 4.11 are defined as follows:

- The $(i-1) \times 1$ vector \bar{y}_B is the vector of values for the known data points:

$$\bar{y}_B = \begin{Bmatrix} y_1 \\ \vdots \\ y_{i-1} \end{Bmatrix} \quad (4.20)$$

and the value used for each y_j , where $j=1$ to $i-1$, depends on if the known data point is censored or not. If the data point is not censored, the measured value is used in this vector. If the data point is censored, the expected value of the censored region for a censored measurement, $\mu_{Y_i,ul}$, is used.

- The $(i-1) \times (i-1)$ matrix $\left[C_{Y_{BB}} \right]$ contains the model-predicted covariances between known data points:

$$C_{Y_{BB}} = \begin{bmatrix} \text{Cov}(Y_1, Y_1) & \text{Cov}(Y_1, Y_2) & \cdots & \text{Cov}(Y_1, Y_{i-1}) \\ \text{Cov}(Y_2, Y_1) & \text{Cov}(Y_2, Y_2) & \cdots & \text{Cov}(Y_2, Y_{i-1}) \\ \vdots & \vdots & \vdots & \vdots \\ \text{Cov}(Y_{i-1}, Y_1) & \text{Cov}(Y_{i-1}, Y_2) & \cdots & \text{Cov}(Y_{i-1}, Y_{i-1}) \end{bmatrix} \quad (4.21)$$

- The $1 \times (i-1)$ matrix $[C_{Y_{AB}}]$ contains the model-predicted covariances between the current data point and all previous data points:

$$C_{Y_{AB}} = [\text{Cov}(Y_i, Y_1) \quad \cdots \quad \text{Cov}(Y_i, Y_{i-1})] \quad (4.22)$$

- The $(i-1) \times 1$ vector $\bar{\mu}_{Y_B}$ is the vector of model-predicted mean values for the previous data points:

$$\bar{\mu}_{Y_B} = \begin{Bmatrix} \mu_{Y_1} \\ \vdots \\ \mu_{Y_{i-1}} \end{Bmatrix} \quad (4.23)$$

- The $(i-1) \times (i-1)$ matrix $[C_{Y_{BBul}}]$ is the model-predicted covariance matrix which adds variability to Y_A only for the censored data points in the previously known measurements. This matrix is calculated as follows:

$$[C_{Y_{BBul}}] = [\sigma_{Y_1, ul} \quad \cdots \quad \sigma_{Y_{i-1}, ul}] \begin{bmatrix} \rho_{Y_1, Y_1} & \cdots & \rho_{Y_1, Y_{i-1}} \\ \vdots & \ddots & \vdots \\ \rho_{Y_{i-1}, Y_1} & \cdots & \rho_{Y_{i-1}, Y_{i-1}} \end{bmatrix} \begin{bmatrix} \sigma_{Y_1, ul} \\ \vdots \\ \sigma_{Y_{i-1}, ul} \end{bmatrix} \quad (4.24)$$

where the value of $\sigma_{Y_i,ul}$ depends on censoring. For uncensored data points, the variance of the censored region is zero and no extra variability is added due to these points. For censored data points, the variance of the censored region, $\sigma_{Y_i,ul}^2$ will have a value greater than zero and will therefore increase the variance of Y_A .

An example of how to calculate the conditional mean and variance is shown in Appendix B.

4.4.1.3 Conditional Moments for the Special Case of Independent Data

The special case of independent data is presented to show the effect of assuming no correlation between data points on the calculation of the conditional moments. In both the conditional moments, $[C_{Y_{AB}}]$ is zero and all the non-diagonal components of $[C_{Y_{BB}}]$ are zero if the data points are not correlated. The conditional moments of Equations 4.18 and 4.19 therefore reduce to:

$$\mu_{Y_A|Y_B} = \mu_{Y_A} \quad (4.25)$$

$$\sigma_{Y_A|Y_B} = \sigma_{Y_A} \quad (4.26)$$

4.4.1.4 Moments for Censored Region of a Normally-Distributed Data Point

The mean and standard deviation of Y_i in the censored region, $\mu_{Y_i,ul}$ and $\sigma_{Y_i,ul}$, are illustrated in Figure 4.1. The values for these moments are found by integrating over the probability density function from the lower bound to the upper bound of the censored region. These moments are derived in Appendix A for a normally distributed data point. The resulting mean of Y_i in the censored region is:

$$\mu_{Y_i,ul} = \mu_{Y_A} + \left[\frac{\sigma_{Y_A}}{\sqrt{2\pi}} \left(e^{-\frac{1}{2}\left(\frac{y_{i,l}-\mu_{Y_A}}{\sigma_{Y_A}}\right)^2} - e^{-\frac{1}{2}\left(\frac{y_{i,u}-\mu_{Y_A}}{\sigma_{Y_A}}\right)^2} \right) \right] \frac{1}{P(y_{i,l} \leq Y_i < y_{i,u})} \quad (4.27)$$

and the standard deviation of Y_i in the censored region is:

$$\begin{aligned} \sigma_{Y_i,ul}^2 &= \mu_{Y_A}^2 - \mu_{Y_i,ul}^2 + \frac{2\mu_{Y_A}\sigma_{Y_A}}{\sqrt{2\pi}} \left(e^{-\frac{1}{2}\left(\frac{y_{i,l}-\mu_{Y_A}}{\sigma_{Y_A}}\right)^2} - e^{-\frac{1}{2}\left(\frac{y_{i,u}-\mu_{Y_A}}{\sigma_{Y_A}}\right)^2} \right) \frac{1}{P(y_{i,l} \leq Y_i < y_{i,u})} \\ &+ \frac{\sigma_{Y_A}^2}{\sqrt{2\pi}} \left[\left(\frac{y_{i,l}-\mu_{Y_A}}{\sigma_{Y_A}} \right) e^{-\frac{1}{2}\left(\frac{y_{i,l}-\mu_{Y_A}}{\sigma_{Y_A}}\right)^2} - \left(\frac{y_{i,u}-\mu_{Y_A}}{\sigma_{Y_A}} \right) e^{-\frac{1}{2}\left(\frac{y_{i,u}-\mu_{Y_A}}{\sigma_{Y_A}}\right)^2} \right] \frac{1}{P(y_{i,l} \leq Y_i < y_{i,u})} \\ &+ \frac{\sigma_{Y_A}^2}{\sqrt{2\pi}} \left[\sqrt{\frac{\pi}{2}} \operatorname{erf}\left(\frac{y_{i,u}-\mu_{Y_A}}{\sigma_{Y_A}\sqrt{2}}\right) - \sqrt{\frac{\pi}{2}} \operatorname{erf}\left(\frac{y_{i,l}-\mu_{Y_A}}{\sigma_{Y_A}\sqrt{2}}\right) \right] \frac{1}{P(y_{i,l} \leq Y_i < y_{i,u})} \end{aligned} \quad (4.28)$$

where $P(y_{i,l} \leq Y_i < y_{i,u})$ is the probability that the censored data point is in the censored region:

$$P(y_{i,l} \leq Y_i < y_{i,u}) = \Phi\left(\frac{y_{i,u}-\mu_{Y_A}}{\sigma_{Y_A}}\right) - \Phi\left(\frac{y_{i,l}-\mu_{Y_A}}{\sigma_{Y_A}}\right) \quad (4.29)$$

4.4.2 Moments for Censored Region of a Non-Normally-Distributed Data Point

In order to calculate the conditional moments with non-normally distributed censored data, the same assumption is made as for point data: a linear relationship exists between the data points, as described in Section 3.4.7.3. With this assumption, the

conditional moments for non-normally distributed data points may be calculated in the same way as the conditional moments for normally-distributed data points, as described in Section 4.4.1.2.

Evaluating $\mu_{Y_i,ul}$ and $\sigma_{Y_i,ul}^2$ is generally not possible for a non-normal distribution without numerical integration. As an approximation, the moments of the censored region for a data point with a non-normal distribution may be approximated with the censored region of a normal distribution. The normal distribution used for the approximation has the same mean and standard deviation as the non-normal distribution, and the censored region of the normal distribution is between the same upper and lower bounds as the censored region of the non-normal distribution. In Figure 4.5, the censored region of a lognormal distribution is shown, as well as the corresponding censored region of the normal distribution used in the approximation.

The accuracy of this approximation was tested with three different non-normal distributions: a uniform distribution, a slightly skewed log-normal distribution, and a highly skewed log-normal distribution. The procedure for testing the approximation was as follows:

1. Calculate the mean and standard deviation, μ_{Y_i} and σ_{Y_i} , of the non-normal distribution.
2. Set the bounds of the censored region, $y_{i,l}$ and $y_{i,u}$, for the non-normal distribution. This was done for a total of ten censored regions in each distribution. For five of the censored regions, $y_{i,l}$ was set to negative infinity and $y_{i,u}$ was determined for probabilities of 0.01, 0.1, 0.25, 0.5, and 0.75 that the data point was censored. For the other five censored

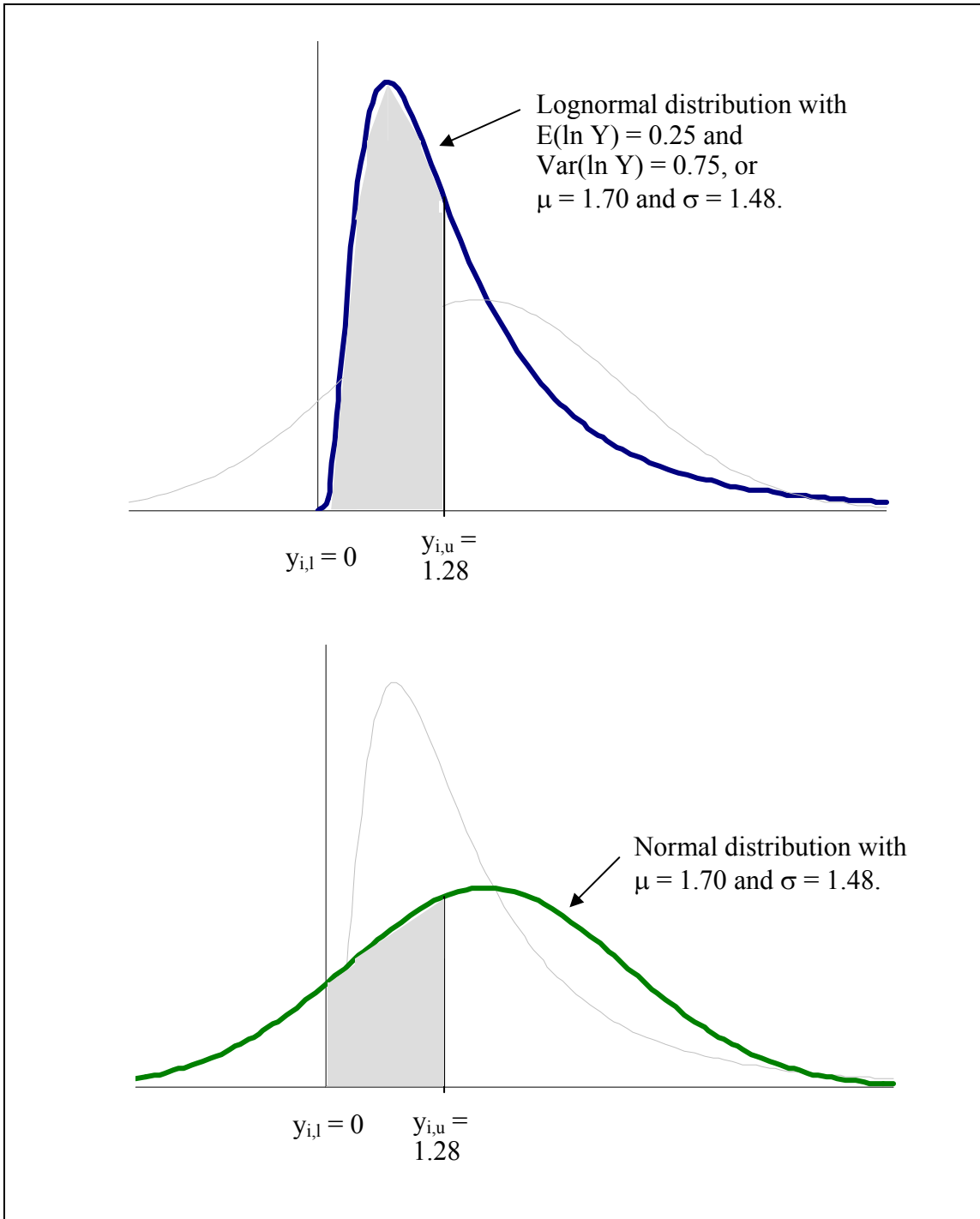


Figure 4.5. Censored region of a lognormal distribution approximated with the censored region of a normal distribution with the same mean and standard deviation.

regions, $y_{i,u}$ was set to positive infinity and $y_{i,l}$ was determined for probabilities of 0.01, 0.1, 0.25, 0.5, and 0.75 that the data point was censored.

3. Calculate the exact mean and variance of each censored region of the non-normal distribution using the following integrals:

$$\mu_{Y_i|y_{i,l} \leq Y_i < y_{i,u}} = \frac{1}{P(y_{i,l} \leq Y_i < y_{i,u})} \int_{y_{i,l}}^{y_{i,u}} y \cdot f_{Y_i}(y) dy \quad (4.30)$$

$$\sigma_{Y_i|y_{i,l} \leq Y_i < y_{i,u}}^2 = \frac{1}{P(y_{i,l} \leq Y_i < y_{i,u})} \int_{y_{i,l}}^{y_{i,u}} \left(y - \mu_{Y_i|y_{i,l} \leq Y_i < y_{i,u}} \right)^2 f_{Y_i}(y) dy \quad (4.31)$$

For the uniform distribution, these integrals can be solved analytically and the moments are as follows:

$$\mu_{Y_i|y_{i,l} \leq Y_i < y_{i,u}} = y_{i,l} + \frac{y_{i,u} - y_{i,l}}{2} \quad (4.32)$$

$$\sigma_{Y_i|y_{i,l} \leq Y_i < y_{i,u}} = \frac{(y_{i,u} - y_{i,l})^2}{12} \quad (4.33)$$

For log-normal distributions, these integrals are evaluated numerically.

4. Calculate the approximate mean and variance of each censored region of the non-normal distribution. Using Equations 4.27 and 4.28, calculate the

mean and variance of each censored region for a normal distribution with mean μ_{Y_i} and standard deviation σ_{Y_i} . The censored region is defined by the same $y_{i,l}$ and $y_{i,u}$ as for the non-normal distribution. (The probability that the data point is censored is therefore different for the normal distribution than for the non-normal distribution.)

The accuracy of the approximation for the mean and variance of the censored region depends on how well the censored region of the non-normal distribution corresponds to the censored region of the normal distribution. The results for the uniform distribution are shown in Figures 4.6 and 4.7. The difference between the approximate and exact values is shown for each censored region. The approximate values are generally very close to the exact values for all cases. The approximation is better for both the mean and the variance when the censored region is small. As the probability that the data point is censored increases, the difference between the approximate mean and variance also increases.

The results of the slightly skewed lognormal distribution are shown in Figures 4.8 and 4.9. The shape of this lognormal distribution is very similar to the shape of the normal distribution used to approximate the mean and variance of the censored region. The approximate and exact values for the mean of the censored region are therefore almost identical for censoring in both tails of the distribution. The approximate values for the variance of the censored region are slightly greater than the exact values for all cases.

The results for the highly skewed lognormal distribution are shown in Figures 4.10 and 4.11. The approximations are generally very similar to the exact values, especially when the lognormal distribution is censored in the lower tail (Figure 4.10).

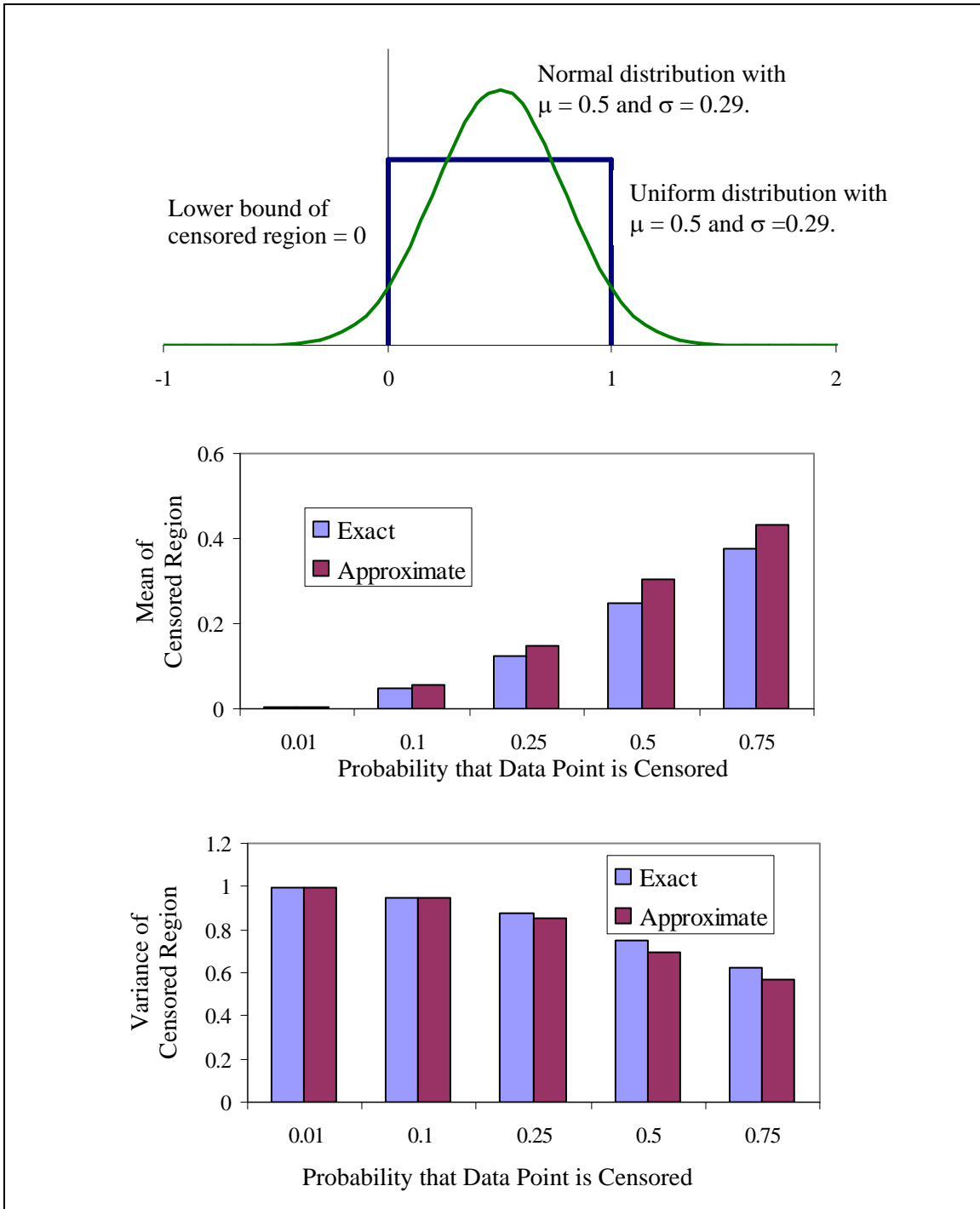


Figure 4.6. Exact mean and variance for censored regions in the lower portion of a uniform distribution compared to an equivalent normal distribution.

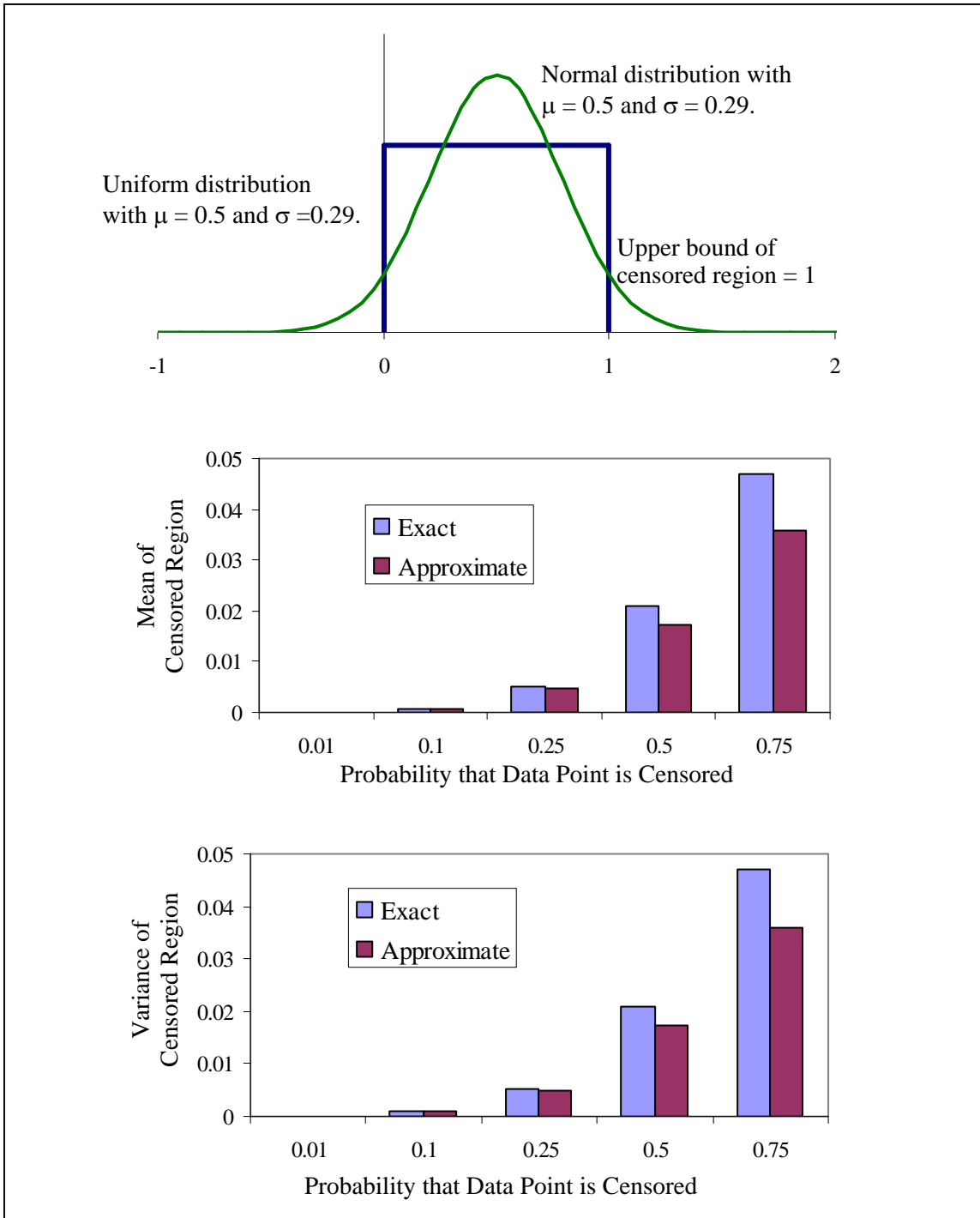


Figure 4.7. Exact mean and variance for censored regions in the upper portion of a uniform distribution compared to an equivalent normal distribution.

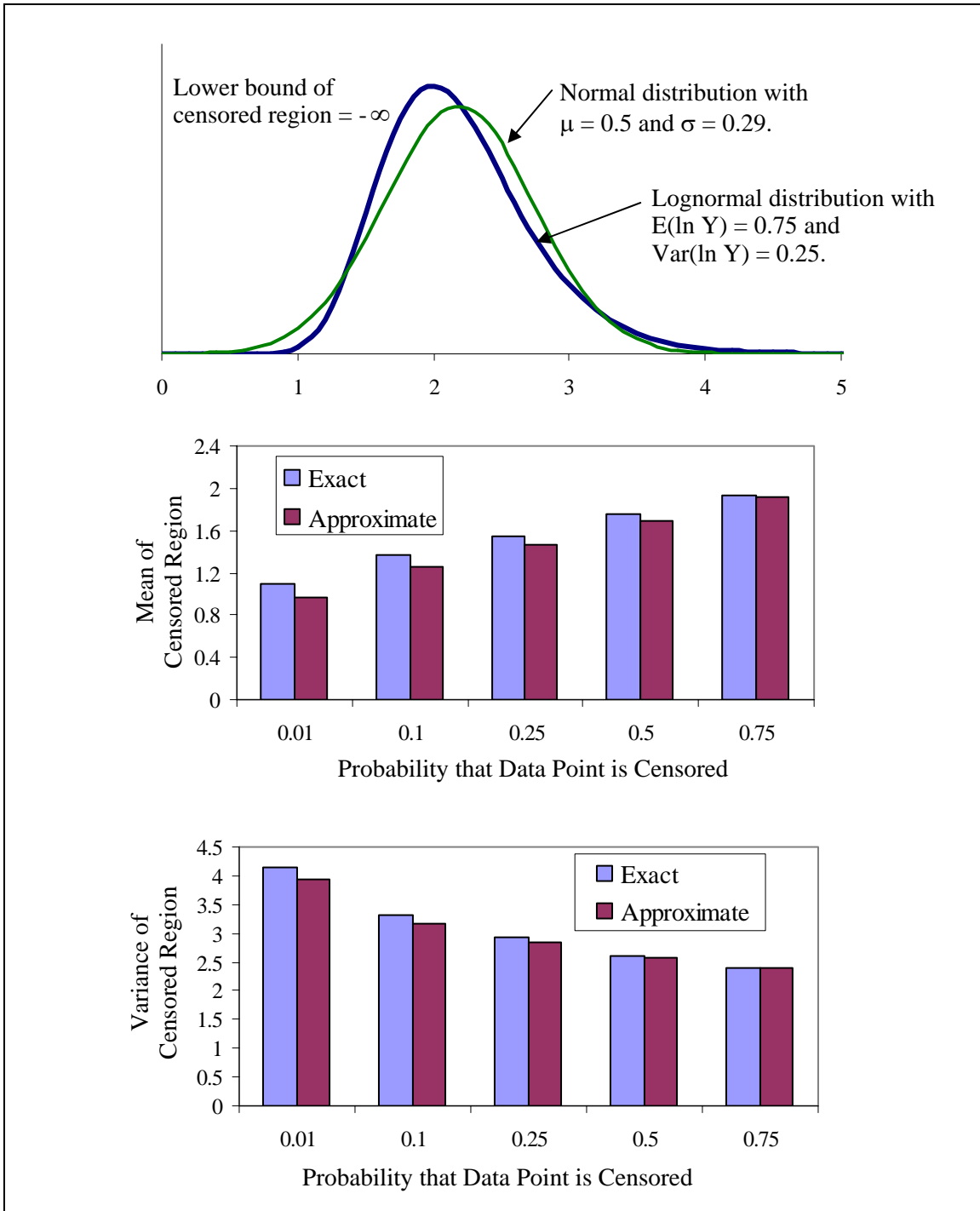


Figure 4.8. Exact mean and variance for censored regions in the lower portion of a slightly skewed lognormal distribution compared to an equivalent normal distribution.

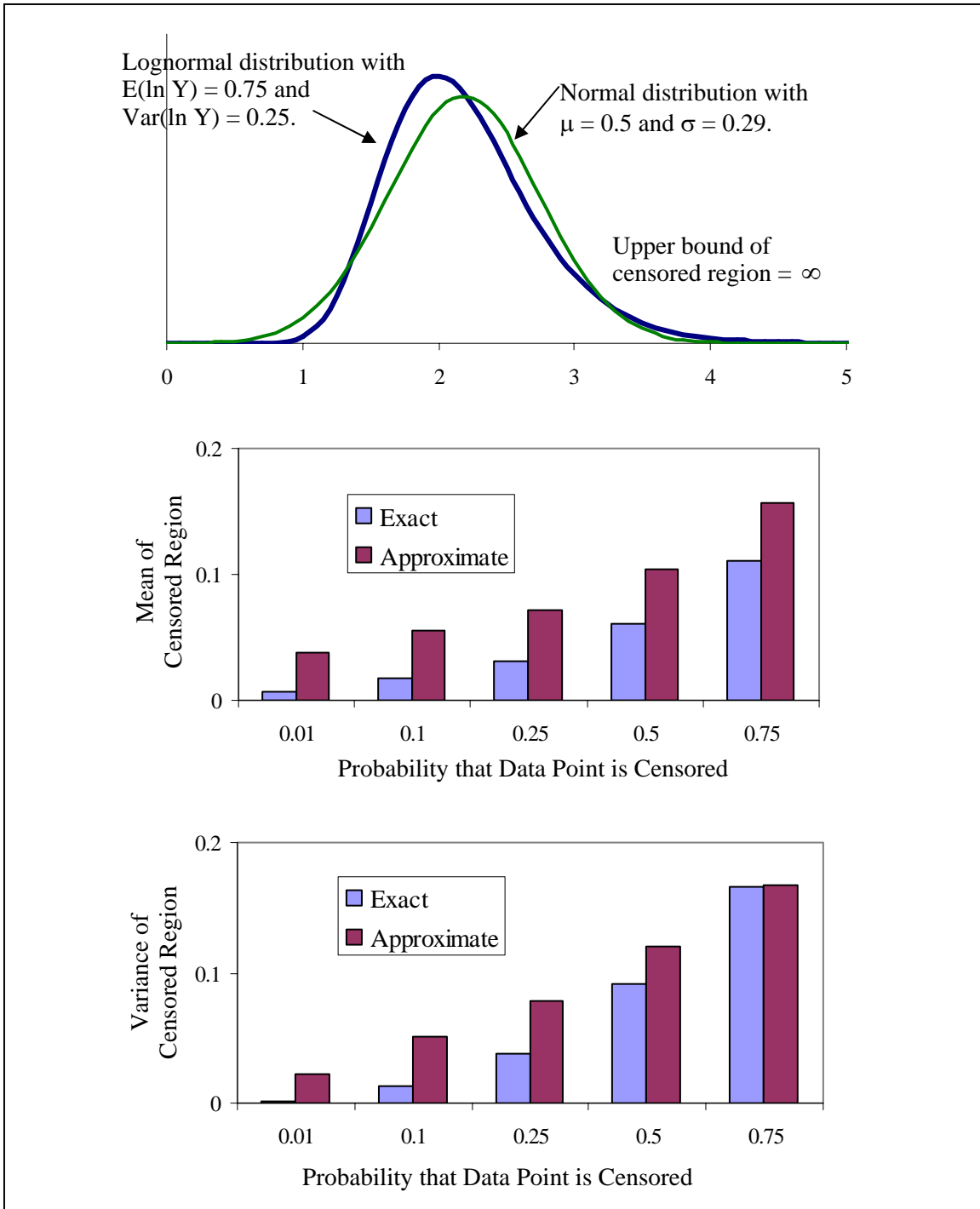


Figure 4.9. Exact mean and variance for censored regions in the upper portion of a slightly skewed lognormal distribution compared to an equivalent normal distribution.

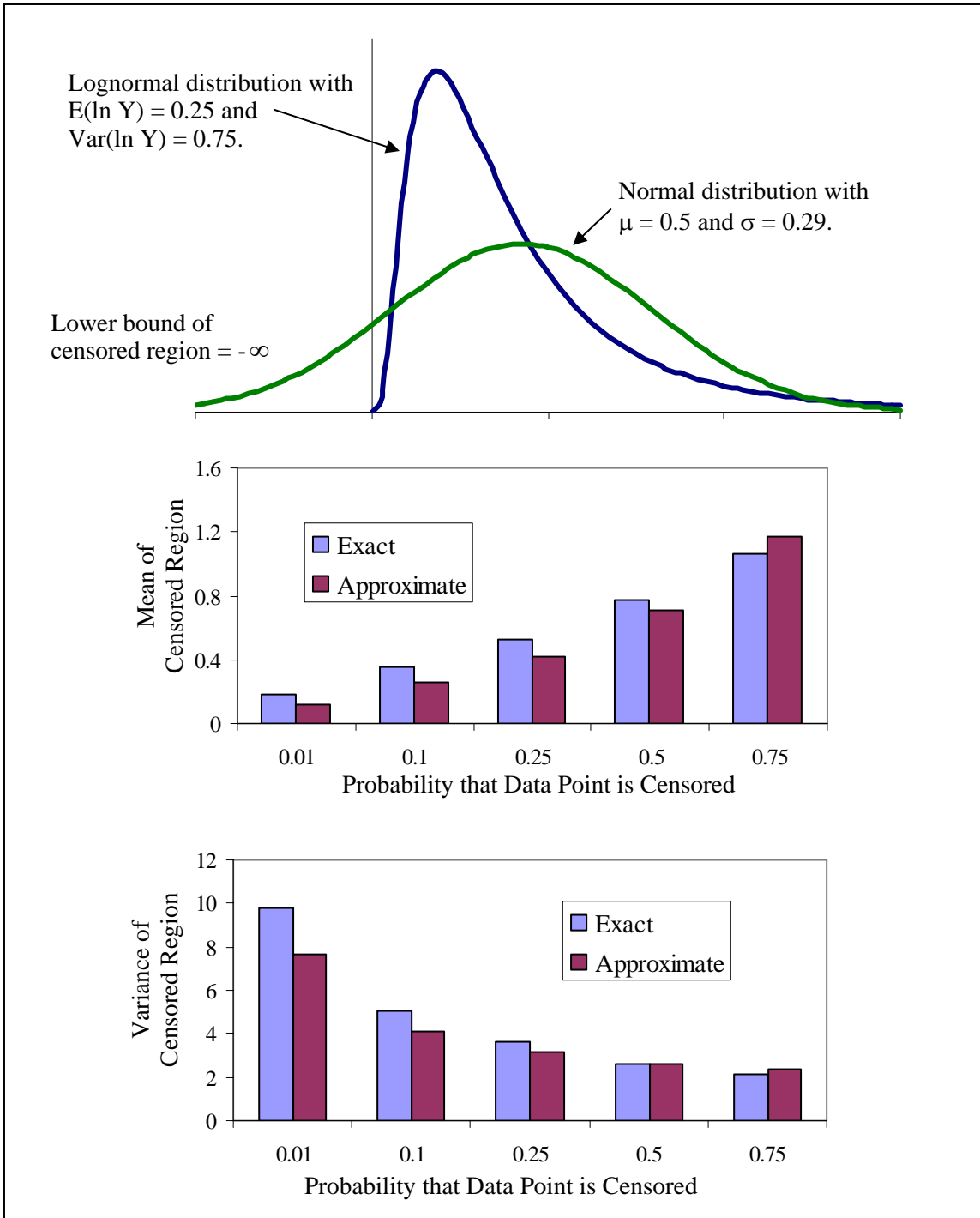


Figure 4.10. Exact mean and variance for censored regions in the lower portion of a highly skewed lognormal distribution compared to an equivalent normal distribution.

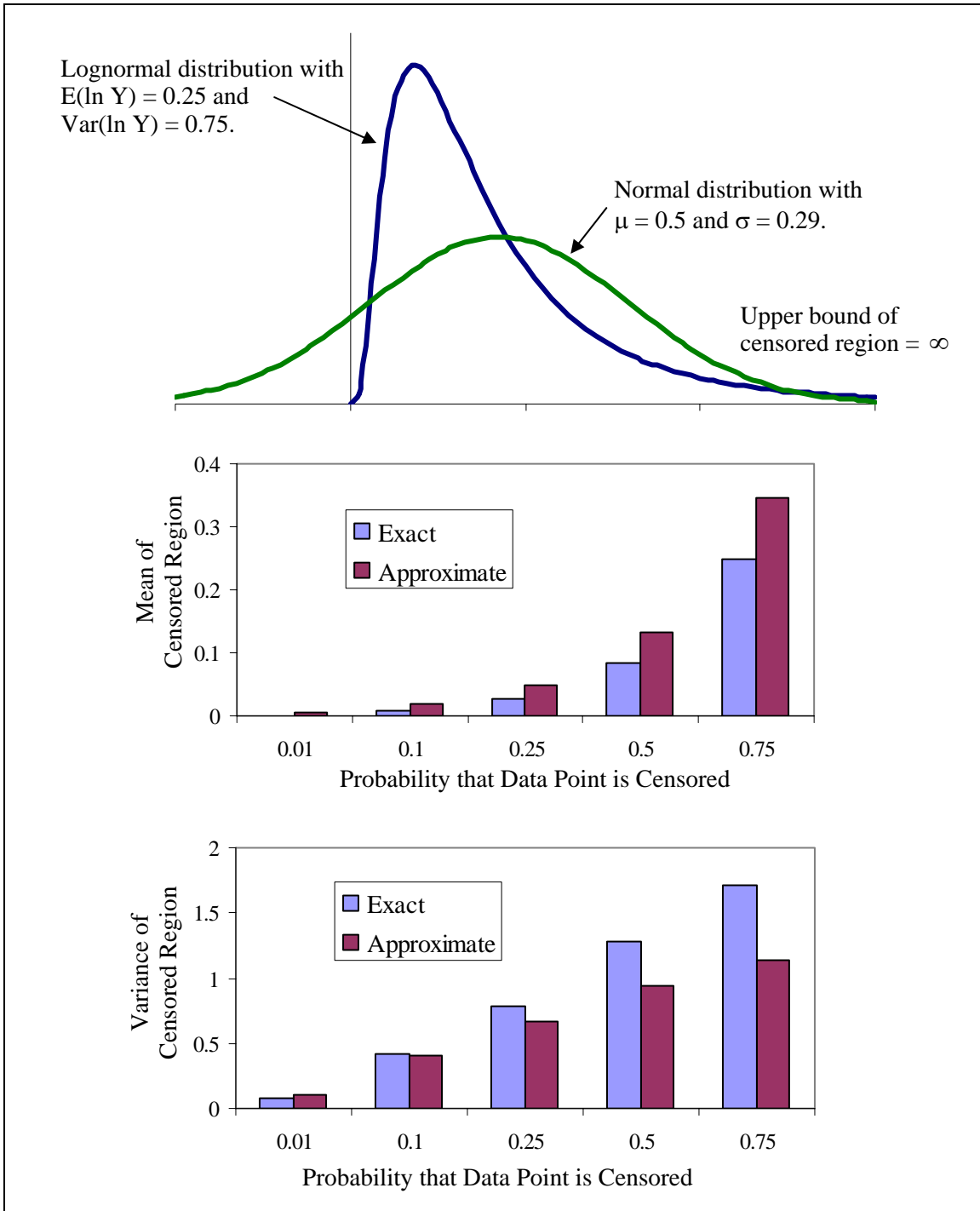


Figure 4.11. Exact mean and variance for censored regions in the upper portion of a highly skewed lognormal distribution compared to an equivalent normal distribution.

The differences between the approximate and the exact values for the variance increase as the size of the censored region increases. When censoring is in the lower tail of the distribution, the approximate variance is greater than the exact value. When censoring is in the upper tail of the distribution, the approximate variance is less than the exact value, except for the smallest probability that the data point is censored.

These examples show that the approximation for the mean and variance of the censored region for a non-normally distributed data point are reasonable, even for cases with a highly non-normal distribution, such as a uniform distribution with finite upper and lower bounds and a highly skewed lognormal distribution. The accuracy of the approximation depends on the shape of the non-normal distribution and the size of the censored region.

4.5 CENSORED DATA IN TEST PROGRAM DESIGN

When designing a test program with the FOSM Bayesian method, the amount and type of data that will be collected are determined and the variance of the model parameters may then be updated. Test program designs are compared by determining how much each test program reduces the variance in the model parameters. As derived in Section 3.4.4, the expected updated covariances of the model parameters depend on the prior covariances and the expected value of the second partial derivatives of the natural logarithm of the likelihood function:

$$E_{\bar{y}}(C_{\phi|\bar{y}}) = \left[E_{\bar{y}} \left[\frac{-\partial^2 \mathbf{g}}{\partial \phi_i \partial \phi_j} \Big|_{\bar{\phi}^*} \right] + C_{\bar{\phi}}^{-1} \right]^{-1} \quad (4.34)$$

The following notation will be used for the expected value of the negative second derivative of the natural logarithm of the likelihood function, evaluated at the Taylor series expansion point:

$$E(-G'') = E_Y \left(\left. \frac{-\partial^2 \mathbf{g}}{\partial \phi_i \partial \phi_j} \right|_{\bar{\phi}^*} \right) \quad (4.35)$$

When $E(-G'')$ is much larger than the prior covariances, the updated covariances depend mostly on the data that are expected. When $E(-G'')$ is much smaller than the inverse of the prior covariances, $C_{\bar{\phi}}^{-1}$, the updated covariances depend mostly on the prior covariances, and therefore the reduction in the variance of the model parameters will be small. Since $C_{\bar{\phi}}^{-1}$ is a constant, $E(-G'')$ is the quantity required to evaluate the reduction of variance for a test program design, as described in Section 3.4.5.

Since the likelihood function is the product of the likelihoods of each individual data point given the known data points, the natural logarithm of the likelihood function is the sum of these individual likelihoods. The second derivative of the natural logarithm of the likelihood function is therefore:

$$\left. \frac{\partial^2 \mathbf{g}}{\partial \phi_i \partial \phi_j} \right|_{\bar{\phi}^*} = \sum_{i=1}^n \left. \frac{\partial^2 \mathbf{g}(y_i | y_1, y_2, \dots, y_{i-1})}{\partial \phi_i \partial \phi_j} \right|_{\bar{\phi}^*} \quad (4.36)$$

and the expected value, $E(G'')$, is then:

$$E_Y \left(\left. \frac{\partial^2 \mathbf{g}}{\partial \phi_i \partial \phi_j} \right|_{\bar{\phi}^*} \right) = \sum_{i=1}^n E_Y \left[\left. \frac{\partial^2 \mathbf{g}(y_i | y_1, y_2, \dots, y_{i-1})}{\partial \phi_i \partial \phi_j} \right|_{\bar{\phi}^*} \right] \quad (4.37)$$

Each expected value term in the summation of Equation 4.36 is found by considering both the possibility that the data point will be censored and the possibility that the data point will not be censored. As described in Section 4.3, the likelihood function is different if the point is in the censored region of the distribution than if it is in the non-censored region. The expectation integral is therefore taken separately over the censored region and the non-censored region, using the appropriate likelihood function for each region:

$$\begin{aligned}
E_{\bar{y}} \left(\frac{\partial^2 \mathbf{g}}{\partial \phi_i \partial \phi_j} \right) &= \int_{y_{i,l}}^{y_{i,u}} \left(\frac{\partial^2 \mathbf{g}(y_i | y_1, y_2, \dots, y_{i-1})_C}{\partial \phi_i \partial \phi_j} \right) \Bigg|_{\bar{\phi}^* | \bar{y}} L(y_i | \bar{\phi}^*)_C dy \\
&+ \int_{-\infty}^{y_{i,l}} \left(\frac{\partial^2 \mathbf{g}(y_i | y_1, y_2, \dots, y_{i-1})_{NC}}{\partial \phi_i \partial \phi_j} \right) \Bigg|_{\bar{\phi}^* | \bar{y}} L(y_i | \bar{\phi}^*)_{NC} d\bar{y} \\
&+ \int_{y_{i,u}}^{+\infty} \left(\frac{\partial^2 \mathbf{g}(y_i | y_1, y_2, \dots, y_{i-1})_{NC}}{\partial \phi_i \partial \phi_j} \right) \Bigg|_{\bar{\phi}^* | \bar{y}} L(y_i | \bar{\phi}^*)_{NC} d\bar{y}
\end{aligned} \tag{4.38}$$

where:

\mathbf{g}_{NC} = natural logarithm of the likelihood function if the point is non-censored

\mathbf{g}_C = natural logarithm of the likelihood function if the point is censored

$L(y_i | \bar{\phi}^*)_{NC}$ = likelihood function if the point is non-censored

$L(y_i | \bar{\phi}^*)_C$ = likelihood function if the point is censored

The expected value in Equation 4.38 may only be solved analytically if approximations are made regarding the evaluation of the likelihood function. For the

general case with any type of data distribution and correlated data, numerical integration must be used. The evaluation of Equation 4.38 will be further discussed in Chapter 5.

4.6 SUMMARY

The method for including censored data in the FOSM Bayesian method was derived in this chapter. The method follows the same framework as the method outlined in Chapter 3 for both normally-distributed and non-normally-distributed data, except that different likelihood functions are used for censored data points and censored data points are considered differently when data points are conditioned on them. For censored data points, the likelihood function is the probability that the data point is actually in the censored region for the conditional distribution of that data point. This probability is calculated directly with the standard normal cumulative density function for a normally-distributed data point. For a data point that does not have a normal distribution, this probability is calculated using the roots of the Hermite Polynomial transform function. The moments of the censored region of a non-normally-distributed data point, which are used to find the conditional moments of that data point, are approximated with the moments of the equivalent censored region of a normal distribution. This approximation was tested for three different non-normal distributions, and the approximated moments were found to be reasonably close to the exact values.

Chapter 5. Effect of Censored Measurements on Model Calibration

5.1 INTRODUCTION

The method for including censored data in the FOSM Bayesian method was derived in the previous chapter. In this chapter, the effects of censored data in an analysis using the FOSM Bayesian method are determined. The case of normally-distributed data is first presented, with an examination of the effects of censoring on the updated mean, variance, and correlation of model parameters. Different methods for calculating the variance reduction achieved in test program design for normally-distributed data are then compared. Finally, the effects of censoring with non-normally-distributed data are discussed.

5.2 EFFECT OF CENSORED DATA FOR NORMALLY-DISTRIBUTED DATA

In this section, a simple model is evaluated to illustrate the effects of censored data in applying the FOSM Bayesian method. First, the estimated mean values of the model parameters are examined for bias. Next, the effect of censored data on the standard deviation of the model parameters is determined. Finally, the effect of censored data on the correlations between the model parameters is found.

5.2.1 Simple Model

The simple model used in this analysis consists of normally-distributed, statistically independent data points, or measurements, with the same censoring level for each measurement. Three parameters, ϕ_μ , ϕ_σ , and ϕ_ρ , model the mean, the standard deviation, and the correlation of the measurements:

$$\mu = \phi_{\mu} \quad (5.1)$$

$$\sigma = \exp(\phi_{\sigma}) \quad (5.2)$$

$$\rho = \exp\left(-\frac{\tau}{\phi_{\rho}}\right) \quad (5.3)$$

The form of the standard deviation equation insures that the standard deviation will be a positive number. In the correlation coefficient, τ is the separation distance between measurements. This equation form insures that the correlation coefficient will remain between -1.0 and 1.0, regardless of the value of ϕ_{ρ} .

The actual or true values for the model parameters are defined so that each expected measurement has a standard normal distribution with a mean of zero and a standard deviation of one. The actual values of ϕ_{μ} and ϕ_{σ} are therefore both zero.

The actual value of ϕ_{ρ} varies depending on the desired correlation between measurements. For all cases, measurements are separated by a distance of 10.0. Values of 0.1, 1.98, 2.67, and 3.55 were used for the correlation model parameter, ϕ_{ρ} , resulting in correlations between adjacent measurements, ρ_{adj} , of 0.0, 0.25, 0.50, and 0.75, respectively. Four different censoring levels were used for each correlation case. The distribution was censored in the lower tail, so that $y_{i,l}$ was negative infinity for each case. The censoring level determines the amount of censored data expected, with the amount of expected censored data equal to $P(y_i \leq y_{i,u})$. Censoring levels of $-\infty$, -0.6745, 0, and 0.6745 were used, resulting in 0, 25, 50 and 75 percent of the measurements expected to be censored, respectively.

5.2.2 Method of Evaluation

The updated covariances of the model parameters depend only on the negative second derivatives of the natural logarithm of the likelihood function, $E(-G'')$, and the prior covariances, $C_{\bar{\phi}}$, of the model parameters (Equation 3.21). When there is no prior information about the model parameters, the prior covariance matrix is infinite and the inverse of the prior covariance matrix, $C_{\bar{\phi}}^{-1}$, is a zero matrix. The expected updated means and covariances of the model parameters (Equation 3.20 and 3.21) therefore reduce to:

$$E_{\bar{Y}}(\bar{\mu}_{\bar{\phi}|y}) = E_Y \left(\left[C_{\bar{\phi}|y} \right] \left\{ \left[\frac{-\partial^2 \mathbf{g}}{\partial \phi_i \partial \phi_j} \Big|_{\bar{\phi}^*} \right] \bar{\phi}^* \right\} \right) \quad (5.4)$$

$$E_{\bar{Y}}(C_{\bar{\phi}|y}) = \left[E_{\bar{Y}} \left(\frac{-\partial^2 \mathbf{g}}{\partial \phi_i \partial \phi_j} \Big|_{\bar{\phi}^*} \right) \right]^{-1} \quad (5.5)$$

For the alternative formulation described in Section 3.4.3, an infinite prior covariance matrix makes the expected updated means and covariances of the model parameters (Equations 3.18 and 3.19) reduce to:

$$E_{\bar{Y}}(\bar{\mu}_{\bar{\phi}|y}) = E_{\bar{Y}}(\bar{\mu}_G) \quad (5.6)$$

$$E_{\bar{Y}}(C_{\bar{\phi}|y}) = E_{\bar{Y}}(C_G) \quad (5.7)$$

As discussed in Section 4.5, the natural logarithm of the likelihood function is the sum of the individual likelihoods for each data point. The expected value of the second derivative of the natural logarithm of the likelihood function for an individual data point is given in Equation 4.38. For test program design, values for the individual data point and the data points on which it is conditioned are unknown. Therefore, all possible data sets must be considered in calculating $E(-G'')$ as follows:

$$E_{\bar{y}} \left(\frac{-\partial^2 \mathbf{g}}{\partial \phi_i \partial \phi_j} \right) = \int_{\text{all } \bar{y}} \dots \int \left[\frac{-\partial^2 \mathbf{g}}{\partial \phi_i \partial \phi_j} \Big|_{\bar{\phi}^*} \right] L(\bar{y} | \bar{\phi}^*) dy_1 dy_2 \dots dy_n \quad (5.8)$$

or, using the alternative formulation in Equations 5.6 and 5.7:

$$E_{\bar{y}} (C_G) = \int_{\text{all } \bar{y}} \dots \int [C_G] L(\bar{y} | \bar{\phi}^*) dy_1 dy_2 \dots dy_n \quad (5.9)$$

The integral of Equation 5.8 is approximated with the following steps:

1. Consider a possible data set, \bar{y}_i .
2. Find the set of model parameters, $\bar{\phi}^*$, that maximizes the likelihood function for this data set.
3. Evaluate the negative second derivative of the natural logarithm of the likelihood function at $\bar{\phi}^*$, $\left(\frac{-\partial^2 \mathbf{g}}{\partial \phi_i \partial \phi_j} \Big|_{\bar{\phi}^*} \right)$, for each data set using the Taylor series approximation for the likelihood function shown in Chapter 3.

4. Weight $\left(\frac{-\partial^2 \mathbf{g}}{\partial \phi_i \partial \phi_j} \Big|_{\bar{\phi}^*} \right)$ by the probability of obtaining that data set with the model parameters set to the expansion point, $L(\bar{y} | \bar{\phi}^*)$.
5. Calculate $\bar{\mu}_{\phi | \bar{y}} = \bar{\mu}_G$ and $C_{\phi | \bar{y}} = C_G$.
6. Repeat Steps 1 through 4 for all possible data sets.

These steps may be performed numerically with a Monte Carlo simulation. The Monte Carlo simulation randomly generates data sets for Step 1 based on the prior means and standard deviations of the model parameters. For this study of normally-distributed data, 1000 sets of data were simulated for each censoring and correlation case. Since the 1000 sets of generated data do not represent all possible data sets, the average result found with the Monte Carlo simulation is an approximation. One way to consider the accuracy of this approximation is with confidence intervals. The 95-percent confidence interval about the average result is calculated as follows:

$$\langle \mu \rangle_{0.95} = \left(\bar{x} - \frac{1.96\sigma}{\sqrt{n}}, \bar{x} + \frac{1.96\sigma}{\sqrt{n}} \right) \quad (5.10)$$

where:

$\langle \mu \rangle_{0.95}$ = 95-percent confidence bounds

\bar{x} = average value of the Monte Carlo simulation results

σ = standard deviation of the Monte Carlo simulation results

n = number of data sets used in the Monte Carlo simulation

The 95-percent confidence bounds indicate that there is a 95 percent probability that the true mean value will be within this interval around the average value found with the Monte Carlo simulations.

5.2.3 Effect of Data Set Size

The effect of the data set size used in the Monte Carlo simulations was determined by calculating the expected variance for the mean of the simple model, $E_{\bar{y}}(\sigma_{\mu}^2|\bar{y})$, for data sets of 25, 50, and 100 points. The amount of censored data was varied between 0 percent and 100 percent for each data set size. The expected updated variance was smallest for the case of no censored data and 100 data points, meaning that more was learned about the mean with this case than with any other case. To compare the different cases and show how data set size and censoring affects the amount learned about the mean, a ratio was calculated as follows:

$$\frac{E_{\bar{y}}(\sigma_{\mu}^2|\bar{y}_{100 \text{ pts, Non-Cens}})}{E_{\bar{y}}(\sigma_{\mu}^2|\bar{y})} \quad (5.11)$$

As the expected updated variance increases in comparison to the case of 100 data points and no censored data, the amount learned about the mean decreases.

The results of the comparison between data set sizes are shown in Figure 5.1. The amount learned about the mean decreases as the size of the data set decreases, since more can be learned with more data points. However, the size of the data set matters less as the amount of censored data increases. The amount learned about the mean decreases as the amount of censored data increases. This is because the exact value of a censored data

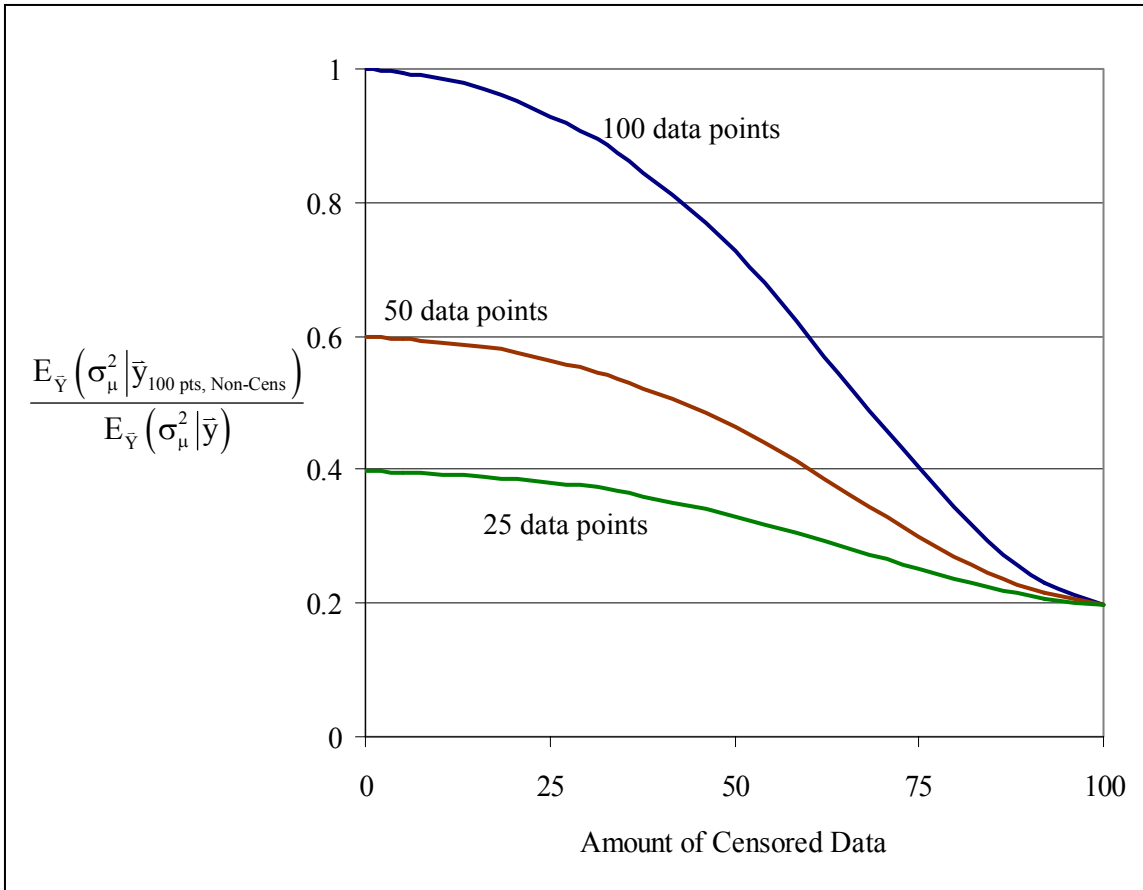


Figure 5.1. Effect of data set size for the simple model.

point is not known, and it provides less information than a non-censored data point. At 100 percent censored data, nothing new is learned about the mean regardless of the size of the data set, and the expected updated variance is equal to the prior variance.

Because the effects of censored data are most dramatic with larger data sets, a data set of 100 points was chosen to examine the effect of censored data on the estimated means, variances, and correlations of the model parameters.

5.2.4 Effect of Censored Data on Estimated Mean Values

To determine if the method described in Chapter 4 for including censored data in the FOSM Bayesian method is biased, the expected mean values of the mean (μ), standard deviation (σ), and correlation (ρ) of the simple model (Equation 5.1 through 5.3) are compared to the true means. If the expected mean and true mean are the same at all censoring levels, then censoring does not cause bias (systematic overestimation or underestimation) of the mean model parameters.

The expected means of the modeled variables (μ , σ , and ρ) are found with first-order approximations as follows:

$$E(\mu) = E_{\bar{y}}(\phi_{\mu} | \bar{y}) \quad (5.12)$$

$$E(\sigma) = \exp[E_{\bar{y}}(\phi_{\sigma} | \bar{y})] \quad (5.13)$$

$$E(\rho) = \exp\left[\frac{-\tau}{\exp[E_{\bar{y}}(\phi_{\rho} | \bar{y})]}\right] \quad (5.14)$$

The results at different censoring and correlation levels for the mean, μ , are shown in Figure 5.2. The estimated mean values are very close to the true mean value of zero for all cases. At a high level of correlation (correlation coefficient of 0.75 between adjacent data points), the estimate of the mean value of the parameter moves slightly further away from the true mean with increasing censored data than at lower levels of correlation. However, the 95-percent confidence bounds on the estimated mean values include the true mean in all cases.

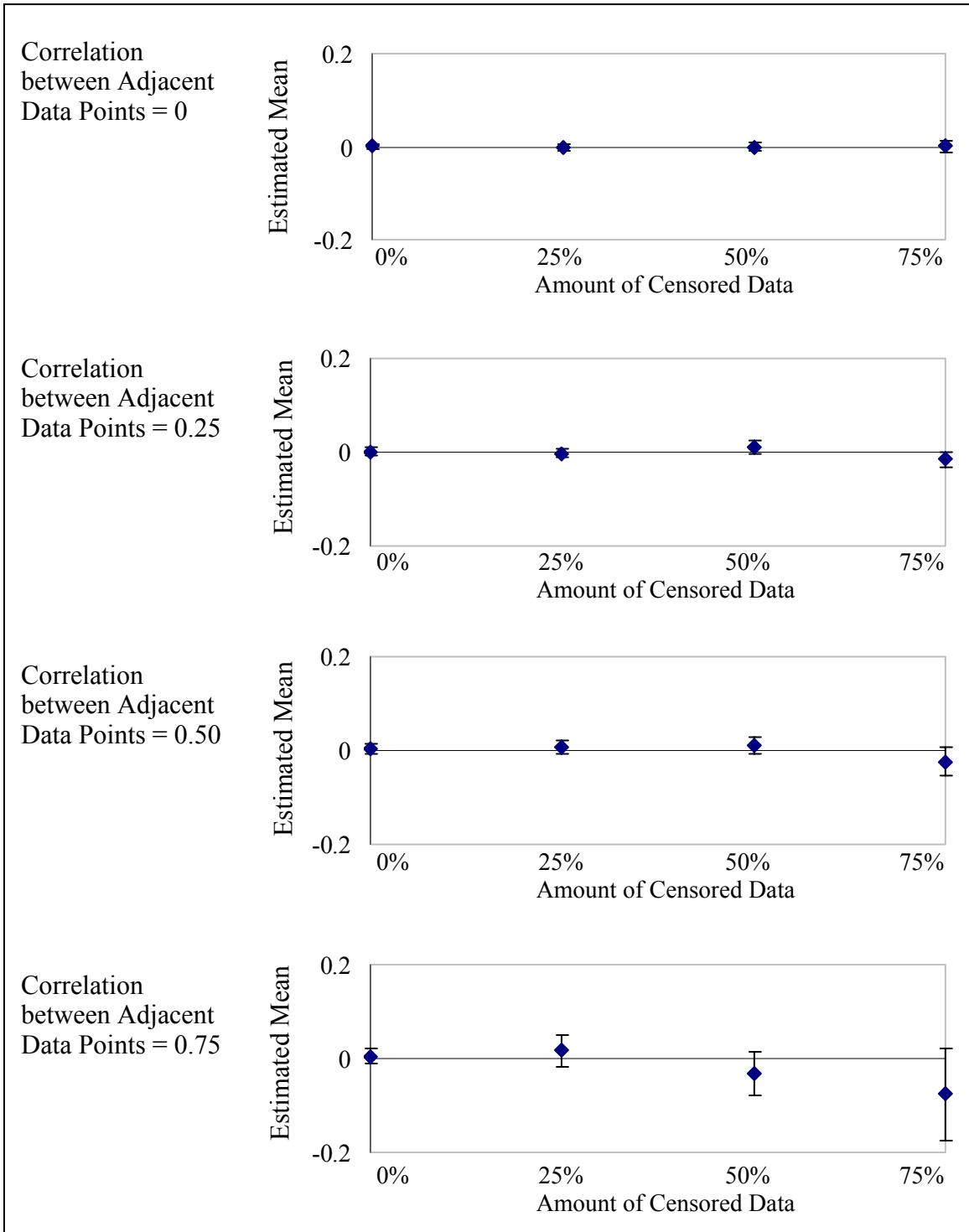


Figure 5.2. Estimated mean values of the mean, $\mu_{\mu|y}$, with 95 percent confidence intervals.

Similar results were obtained for the estimated mean values of the standard deviation, σ , as shown in Figure 5.3. The 95-percent confidence bounds for the standard deviation are so close to the estimated mean values that they are not visible with the scale of the graphs in Figure 5.3. The estimated mean values are very close to the true mean value of 1.0 for all cases. However, for the case of a correlation coefficient of 0.75 between adjacent data points, the 95-percent confidence bounds of the estimated mean value do not include the true mean value. This is an error caused by the correlation, not by the censoring, since the error does not consistently increase with censoring.

The same effect is found for the estimated mean values of the correlation between adjacent data points, ρ_{adj} , which are shown in Figure 5.4. As the correlation coefficient increases, the discrepancies between the estimated and true mean values increases. However, it is important to note the scale of the vertical axes in both Figure 5.3 and Figure 5.4. The differences between the estimated and true mean values are very small in all cases.

5.2.5 Effect of Censored Data on Estimated Standard Deviations of Model Parameters

Censored data affects how much is expected to be learned about the model variables, μ , σ , and ρ . The expected standard deviation of a model variable indicates how much is learned about the variable from the data. The magnitude of the expected standard deviation is proportional to the uncertainty in the value of the model parameter. Lower values of the expected standard deviation therefore indicate that more has been learned about the model variable. The expected standard deviations of the model parameters are calculated with first-order approximations as follows:

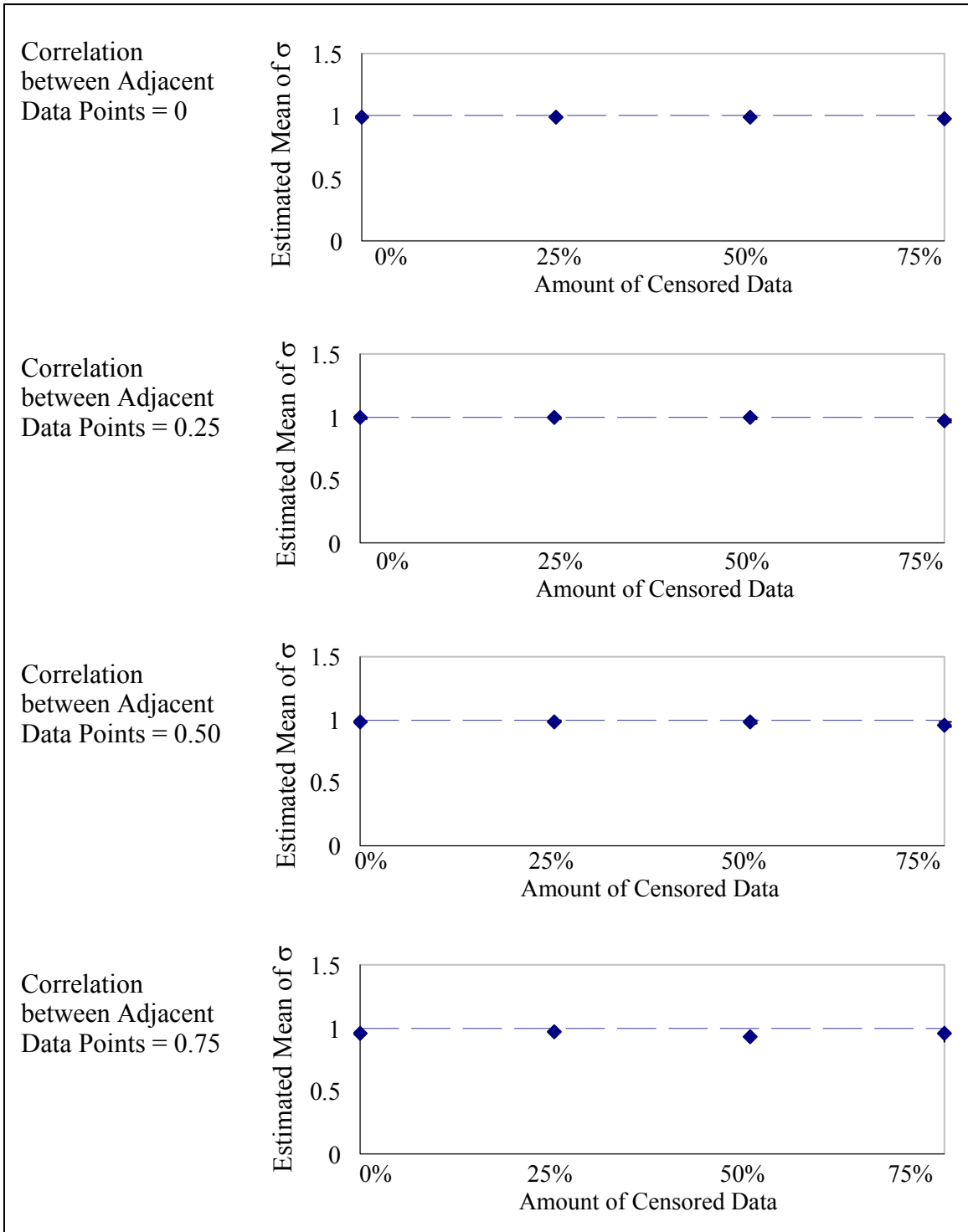


Figure 5.3. Estimated mean values of the standard deviation, $\mu_{\sigma|y}$ with 95 percent confidence intervals.

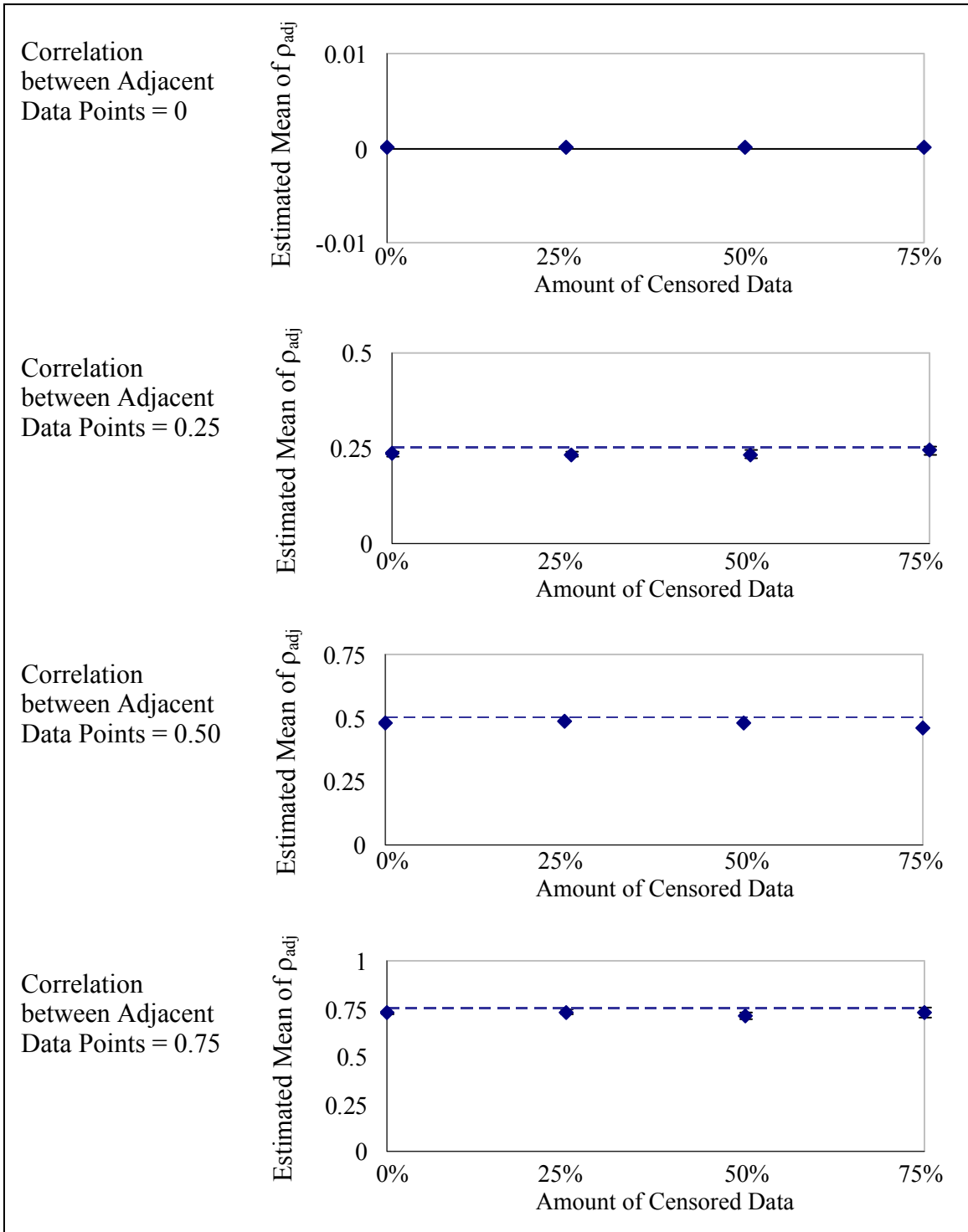


Figure 5.4. Estimated mean values of the correlation between adjacent data points, $\mu_{\rho|y}$ with 95 percent confidence intervals.

$$E_{\bar{y}}(\sigma_{\mu}|\bar{y}) = E_{\bar{y}}(\sigma_{\phi_{\mu}}|\bar{y}) \quad (5.15)$$

$$E_{\bar{y}}(\sigma_{\sigma}|\bar{y}) = E_{\bar{y}}(\sigma_{\phi_{\sigma}}|\bar{y}) \exp[E_{\bar{y}}(\phi_{\sigma}|\bar{y})] \quad (5.16)$$

$$E_{\bar{y}}(\sigma_{\rho}|\bar{y}) = 10 \cdot E_{\bar{y}}(\sigma_{\phi_{\rho}}|\bar{y}) \cdot \exp\left[\frac{-10}{E_{\bar{y}}(\phi_{\rho}|\bar{y})}\right] \cdot \exp[E_{\bar{y}}(\phi_{\rho}|\bar{y})] \quad (5.17)$$

The value of $E_{\bar{y}}(\sigma_{\mu}|\bar{y})$ for the case of no censored data and statistically independent data is used to determine how censoring and correlation affects the amount learned about μ . A ratio is calculated as follows:

$$\frac{E_{\bar{y}}(\sigma_{\mu}|\bar{y}_{\text{Non-Cens, SI}})}{E_{\bar{y}}(\sigma_{\mu}|\bar{y})} \quad (5.18)$$

As $E_{\bar{y}}(\sigma_{\mu}|\bar{y})$ becomes larger in comparison to the case of no censored data and statistically independent data, the value of this ratio decreases and the amount learned about μ also decreases. The same ratio is also calculated for the expected standard deviation for σ :

$$\frac{E_{\bar{y}}(\sigma_{\sigma}|\bar{y}_{\text{Non-Cens, SI}})}{E_{\bar{y}}(\sigma_{\sigma}|\bar{y})} \quad (5.19)$$

The results of this comparison for the mean of the simple model, μ , and the standard deviation of the simple model, σ , are shown in Figures 5.5 and 5.6, respectively.

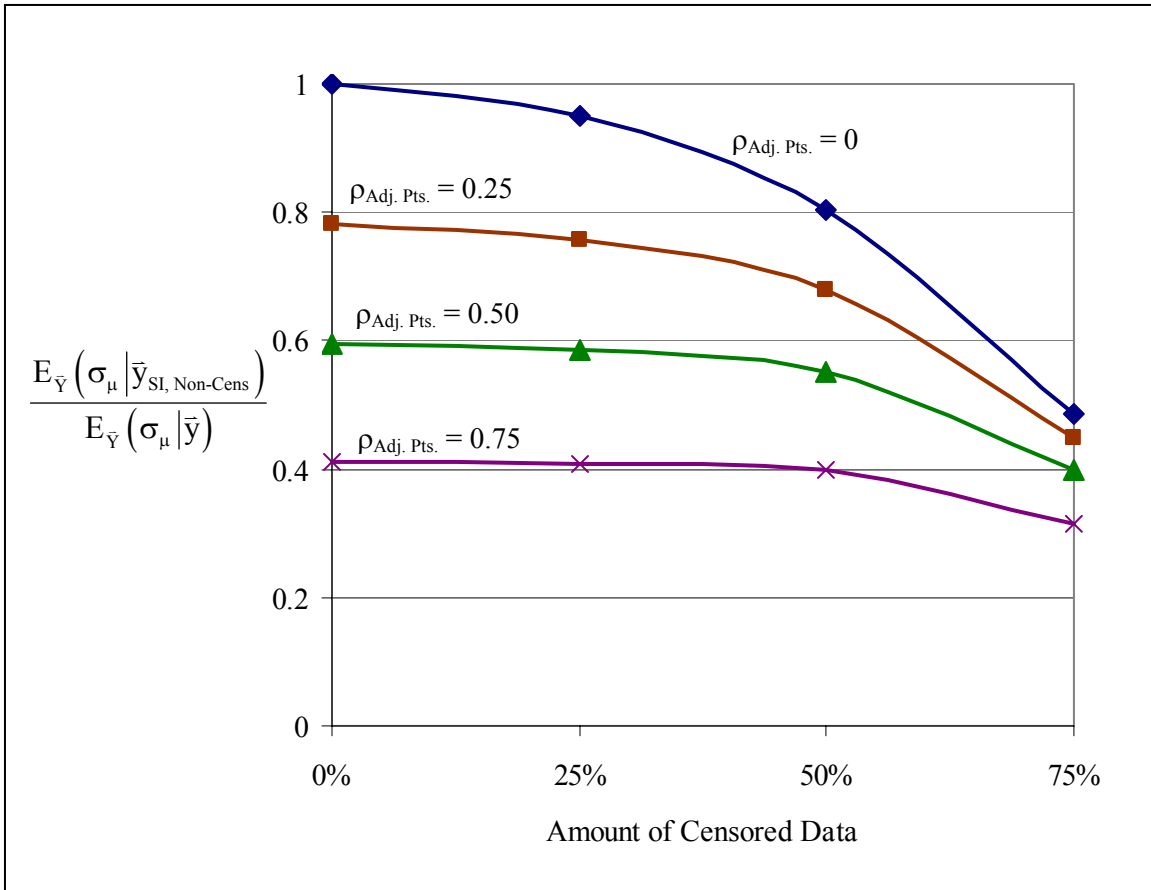


Figure 5.5. Expected updated standard deviations for the mean of the simple model.

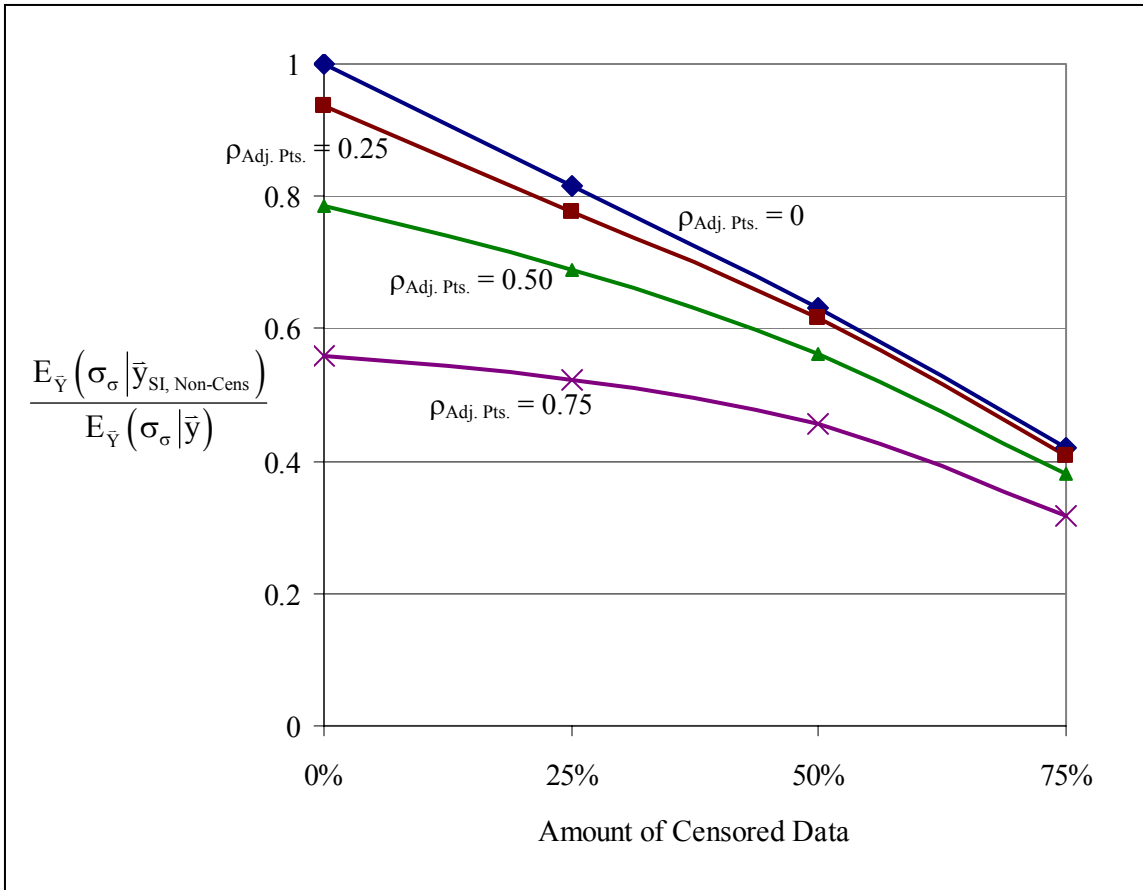


Figure 5.6. Expected updated standard deviations for the standard deviation of the simple model.

As the level of censoring increases, less is learned about the mean and standard deviation. This is because the exact value of a censored measurement is not known, and it provides less information than a point measurement. As the correlation between data points increases, less is learned about each model parameter. This is because a data point that is correlated with other data points provides less information than a statistically independent data point. Correlation between data points essentially reduces the amount of data available, causing the same effect seen by decreased data set size in Figure 5.1.

A similar ratio is used to compare the effects of censoring on the correlation between adjacent data points, ρ_{adj} :

$$\frac{E_{\bar{Y}}\left(\sigma_{\rho_{\text{adj}}}\left|\bar{Y}_{\text{Non-Cens}, \rho_{\text{adj}}=0.25}\right.\right)}{E_{\bar{Y}}\left(\sigma_{\rho_{\text{adj}}}\left|\bar{Y}\right.\right)} \quad (5.20)$$

For the case of statistically independent data, there is no correlation between data points and nothing new can be learned about the correlation; therefore, the expected updated standard deviations are all zero. For this comparison, the value of the numerator in Equation 5.20 was $E_{\bar{Y}}\left(\sigma_{\rho_{\text{adj}}}\left|\bar{Y}_{\text{No Cens}, \rho_{\text{adj}}=0.25}\right.\right)$, which is the expected value of the standard deviation of the correlation for the case of the correlation between adjacent data points equal to 0.25. The results of the comparison for the correlation between adjacent points for the simple model, ρ_{adj} , are shown in Figure 5.7. With correlations between data points, the amount learned about the correlation decreases as the amount of censoring increases. This is again because the exact value of a censored measurement is not known, and it provides less information than a non-censored measurement.

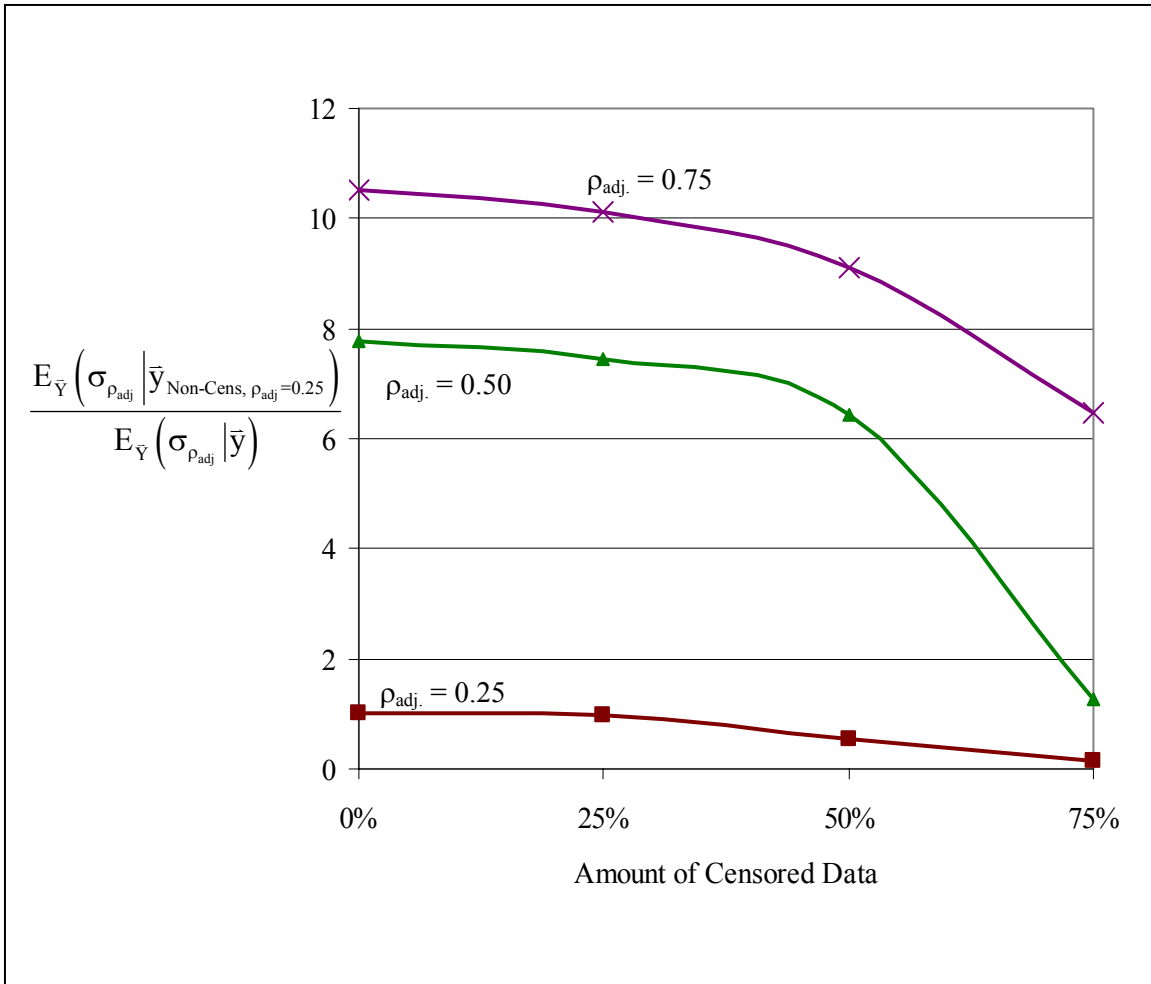


Figure 5.7. Expected updated standard deviations for the correlation between adjacent points for the simple model.

5.2.6 Effect of Censored Data on Estimated Correlations between Model Parameters

The effects of censoring on the correlation coefficients between the model parameters are shown in Table 5.1. The significant correlation coefficients ($|\rho| > 0.75$) are shaded in this table. A significant negative correlation between ϕ_μ and ϕ_σ occurs with 75 percent censored data for statistically independent data. This negative correlation occurs because the standard deviation of a distribution with a set amount of censored data must be decreased if the mean is increased to keep the same amount of censored data in the distribution. This is illustrated in Figure 5.8 with three normal distributions that have 75 percent censored data. As the value of the distribution is increased, the standard deviation must decrease so that the censored region remains in the lower 75 percent of the distribution. As the amount of censored data is reduced, the negative correlation between ϕ_μ and ϕ_σ becomes less significant, since the censored region of the distribution will be smaller and shifting the mean will have less effect on the amount of censored data in the distribution for the same standard deviation.

Significant positive correlations between ϕ_σ and ϕ_ρ occurred with no censored data and with 25 percent censored data for a correlations of 0.75 between adjacent measurements, indicating that the standard deviation and correlation parameters tend to increase together. With less correlation between measurements, the model that is fit to the measurements has more freedom to adjust to the measurements, and therefore the standard deviation in the model will be smaller. With more correlated measurements, the standard deviation parameter must be larger to explain the variability in the measurements.

Table 5.1. Correlations between model parameters at varying censored levels, with significant correlations highlighted.

Amount of Censored Data	$\rho_{\phi_{\mu}, \phi_{\sigma}}$	$\rho_{\phi_{\mu}, \phi_{\rho}}$	$\rho_{\phi_{\sigma}, \phi_{\rho}}$
Correlation between Adjacent Data Points = 0			
0%	0	0	0
25%	-0.17	0	0
50%	-0.44	0	0
75%	-0.76	0	0
Correlation between Adjacent Data Points = 0.25			
0%	0	0	0.32
25%	-0.13	0	0.27
50%	-0.36	-0.02	0.23
75%	-0.71	-0.06	0.17
Correlation between Adjacent Data Points = 0.50			
0%	0	0	0.60
25%	-0.07	0.02	0.53
50%	-0.25	-0.01	0.47
75%	-0.58	-0.01	0.41
Correlation between Adjacent Data Points = 0.75			
0%	0	0	0.81
25%	0.02	0.07	0.76
50%	-0.16	-0.01	0.68
75%	-0.52	-0.24	0.64

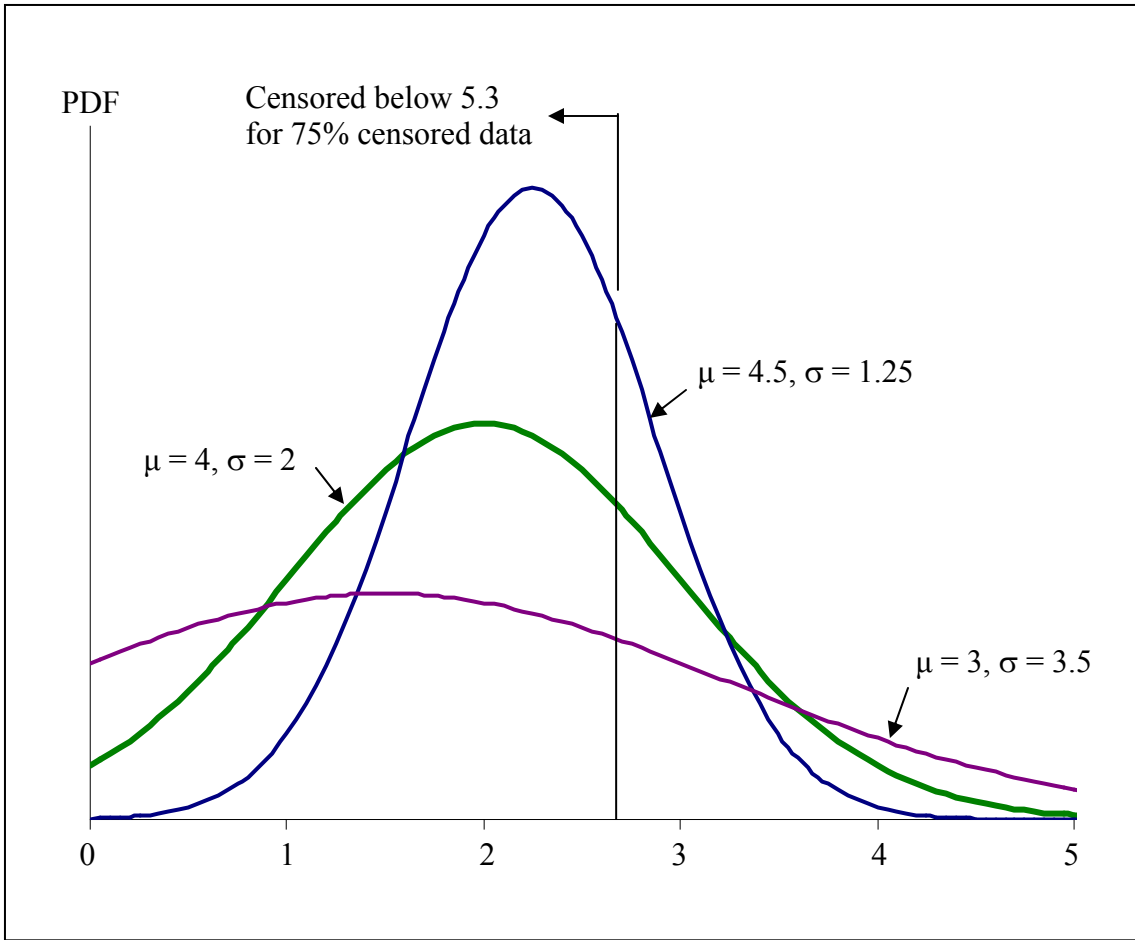


Figure 5.8. Illustration of the negative correlation between mean and standard deviation with 75 percent censored data.

5.3 METHODS FOR EVALUATING EXPECTED CENSORED DATA

In the previous section, the updated moments of the model parameters were calculated using a Taylor series approximation for the natural logarithm of the likelihood function, as described in Section 5.2.2. Alternative methods for calculating the moments are compared in this section.

5.3.1 Complete Numerical Integration

One alternative method to evaluating the updated covariances of the model parameters follows the same procedure outlined in Section 5.2.2, except the $\left(\frac{-\partial^2 \mathbf{g}}{\partial \phi_i \partial \phi_j} \Big|_{\bar{\phi}^*} \right)$ terms in Equations 5.4 and 5.5 are evaluated with numerical integration instead of using the Taylor series approximation for the natural logarithm of the likelihood function. This numerical integration method was compared to the Taylor series approximation method with a data set consisting of 100 normally-distributed, statistically independent, non-censored data points. The simple model of Equations 5.1 through 5.3 was used for the mean, standard deviation, and correlation coefficient. For each method, 1000 data sets were generated for the Monte Carlo simulation. The numerical integration was performed with a Monte Carlo simulation using 1000 model parameters generated for each data set. The resulting updated standard deviations for each model parameter for the two methods are presented in Table 5.2. The two methods gave the same results. The major difference between the two methods is the required computation time. The large number of simulations required for the numerical integration, which is more exact, greatly increases the computation time of this method. The computation time for the numerical integration is about 10 times greater than for the Taylor series approximation.

Table 5.2. Results compared to exact solutions for independent, non-censored data.

	Numerical Integration of Likelihood Function	Taylor series approximation of Likelihood Function
$E_Y(\sigma_{\phi_\mu} \bar{y})$	0.10	0.10
$E_Y(\sigma_{\phi_\sigma} \bar{y})$	0.07	0.07
$E_Y(\sigma_{\phi_p} \bar{y})$	100.0	100.0

The Taylor series approximation is therefore preferable to the numerical integration method for finding $\bar{\phi}^*$ to maximize the likelihood function.

5.3.2 Using Prior Mean Model Parameters

Another method of evaluating $E(-G'')$ in Equations 5.4 and 5.5 is available by assuming that $\bar{\phi}^*$ does not depend on the data, \bar{y} , and is equal to the prior mean values of the model parameters, $\bar{\mu}_{\bar{\phi}}$. The same procedure outlined in Section 5.2.2 is followed, except that $\left(\frac{-\partial^2 g}{\partial \phi_i \partial \phi_j} \Big|_{\bar{\phi}^*} \right)$ is evaluated at $\bar{\phi}^* = \bar{\mu}_{\bar{\phi}}$. Although this approximate method still requires simulation of numerous sets of measurements in order to obtain a reasonable estimate of G'' , the computation time is less than for the Taylor series approximation. This is because the values of $\bar{\phi}^*$ are assumed and the step of finding $\bar{\phi}^*$ to maximize the likelihood function is eliminated. These two methods were compared with the simple model described in Section 5.2.2. For each method, 1000 sets of 100 data points were simulated. The expected updated standard deviations for each of the three model parameters were calculated to compare the two methods, and the results are shown in Tables 5.3 through 5.5. The discrepancies between the two methods tend to increase with increasing correlation coefficient and increasing amount of censored data. Therefore, the

Taylor series approximation method is preferable to using the prior mean values of the model parameters.

5.3.3 Complete Analytical Approximation

An analytical approximation may be developed by making two assumptions: (1) $\bar{\phi}^*$ does not depend on the data, \bar{y} , and is equal to the prior mean values of the model parameters, $\bar{\mu}_{\phi}$, and (2) censored data points are equal to the mean of the censored region for that data point, $\mu_{Y_j,ul}$, when calculating the conditional moments. The derivation of the analytical method using these assumptions is presented in Appendix D. The advantage of this analytical method is that it does not involve any numerical simulations, therefore greatly reducing the required computation time.

The complete analytical method and the Taylor series approximation method were compared using the simple model described in Section 5.2.2. The expected updated standard deviations for each of the three model parameters were calculated to compare the two methods, and the results are shown in Tables 5.3 through 5.5. The discrepancy of the complete analytical approximation results compared to the Taylor series approximation increases with increasing correlation coefficient and increasing amount of censored data. Therefore, the Taylor series approximation is preferable for all cases except non-censored, statistically independent data.

Table 5.3. Expected updated standard deviation of mean model parameter, ϕ_μ , evaluated with different methods.

Amount of Censored Data	Correlation between Adjacent Measurements	Numerical Simulation with $\bar{\phi}^*$ Maximizing Likelihood	Numerical Simulation with $\bar{\phi}^* = \bar{\mu}_{\bar{\phi}}$	Analytical Approximation
0%	0.0	0.1	0.1	0.10
	0.25	0.13	0.13	0.12
	0.50	0.17	0.17	0.16
	0.75	0.26	0.26	0.22
25%	0.0	0.10	0.10	0.10
	0.25	0.13	0.13	0.13
	0.50	0.18	0.17	0.16
	0.75	0.26	0.25	0.21
50%	0.0	0.12	0.12	0.12
	0.25	0.16	0.15	0.14
	0.50	0.21	0.18	0.17
	0.75	0.38	0.25	0.21
75%	0.0	0.20	0.20	0.18
	0.25	0.20	0.22	0.19
	0.50	0.20	0.24	0.21
	0.75	0.23	0.29	0.23

Table 5.4. Updated standard deviation of the standard deviation model parameter, ϕ_σ , evaluated with different methods.

Amount of Censored Data	Correlation between Adjacent Measurements	Numerical Simulation with $\bar{\phi}^*$ Maximizing Likelihood	Numerical Simulation with $\bar{\phi}^* = \bar{\mu}_\phi$	Analytical Approximation
0%	0.0	0.07	0.07	0.07
	0.25	0.08	0.07	0.08
	0.50	0.09	0.09	0.09
	0.75	0.13	0.13	0.12
25%	0.0	0.09	0.09	0.09
	0.25	0.09	0.09	0.09
	0.50	0.11	0.10	0.10
	0.75	0.15	0.13	0.13
50%	0.0	0.11	0.11	0.11
	0.25	0.12	0.11	0.11
	0.50	0.14	0.12	0.12
	0.75	0.25	0.16	0.15
75%	0.0	0.17	0.17	0.16
	0.25	0.17	0.17	0.16
	0.50	0.18	0.18	0.17
	0.75	0.21	0.21	0.20

Table 5.5. Updated standard deviation of correlation model parameter, ϕ_ρ , evaluated with different methods.

Amount of Censored Data	Correlation between Adjacent Measurements	Numerical Simulation with $\bar{\phi}^*$ Maximizing Likelihood	Numerical Simulation with $\bar{\phi}^* = \bar{\mu}_{\bar{\phi}}$	Analytical Approximation
0%	0.0	100	100	100
	0.25	0.28	0.28	0.29
	0.50	0.25	0.25	0.25
	0.75	0.31	0.30	0.29
25%	0.0	100	100	100
	0.25	0.32	0.30	0.31
	0.50	0.28	0.26	0.26
	0.75	0.33	0.30	0.29
50%	0.0	100	100	100
	0.25	0.40	0.34	0.36
	0.50	0.35	0.29	0.30
	0.75	0.52	0.34	0.33
75%	0.0	100	100	100
	0.25	0.57	0.45	0.49
	0.50	0.56	0.39	0.40
	0.75	0.86	0.45	0.43

5.4 EFFECT OF CENSORED DATA FOR NON-NORMALLY-DISTRIBUTED DATA

The approximate methods described in Section 5.3 for normally-distributed data were also tested for non-normally-distributed data. These approximate methods did not work for non-normally-distributed data, and therefore the only method available for evaluating the expected updated moments of model parameters for non-normally-distributed data is the numerical integration method described in Section 5.3.3.

To evaluate the effect of censored data with the case of non-normally-distributed data, a standard lognormal distribution was evaluated. The standard lognormal distribution is highly skewed, as shown in Figure 5.9. A standard lognormal distribution has the following properties:

$$\lambda = E(\ln X) = 0$$

$$\zeta^2 = \text{Var}(\ln X) = 1$$

The mean and standard deviation of the standard lognormal distribution are therefore 1.647 and 2.162, respectively. The simple model described in Section 5.2.1 was used to model the mean, standard deviation, and correlation coefficient between measurements. The values of ϕ_μ and ϕ_σ are therefore 1.647 and 0.771, respectively. The value of the correlation parameter, ϕ_ρ , depends on the desired correlation between measurements. A value of 0.1 was used for no correlation between measurements, and a value of 1.98 was used for a correlation of 0.25 between adjacent data points.

A fifth-order Hermite Polynomial was used to transform this non-normal distribution into a normal distribution (Section 3.3.7.1). The values for the fifth-order

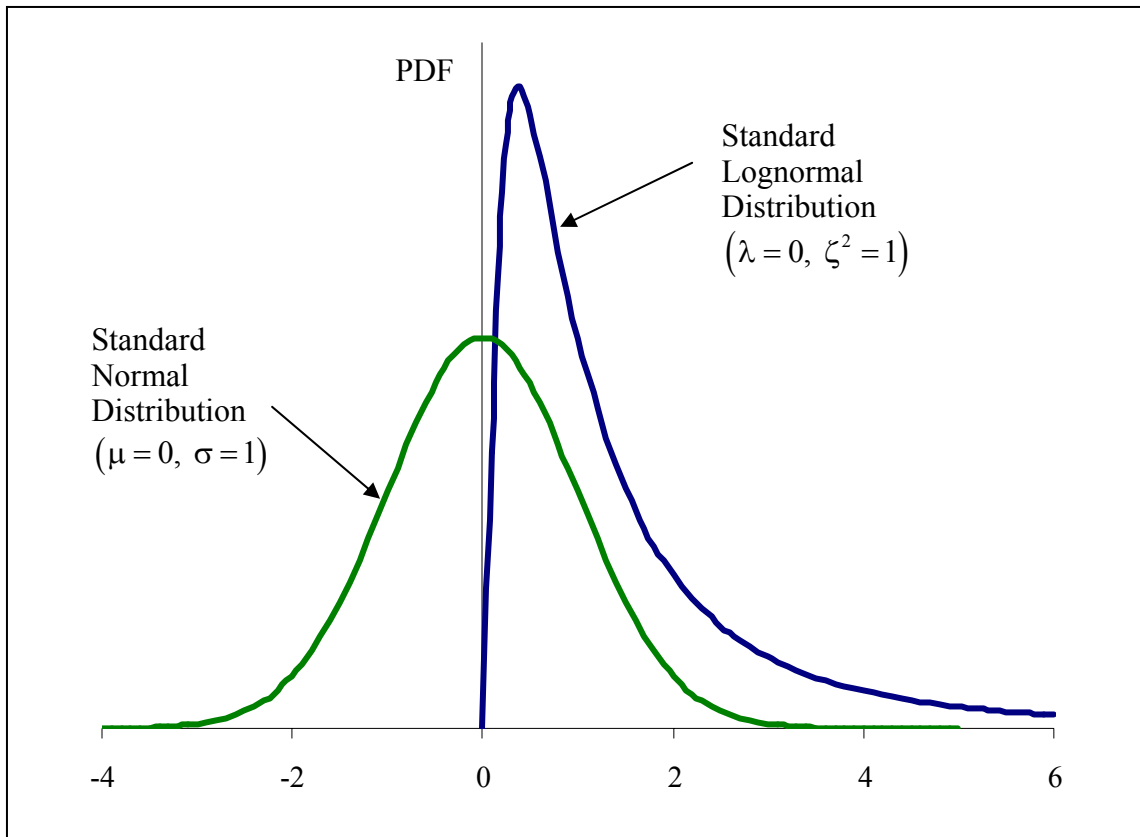


Figure 5.9. Comparison of standard normal distribution and standard lognormal distribution.

Hermite Polynomial coefficients for a standard lognormal distribution were found by Wang (2002), and these coefficients were used as additional model parameters:

$$\phi_{\psi_2} = \psi_2' = -1.003$$

$$\phi_{\psi_3} = \psi_3' = 0.916$$

$$\phi_{\psi_4} = \psi_4' = -0.645$$

$$\phi_{\psi_5} = \psi_5' = 0.252$$

Three cases were considered for the lognormal distribution: (1) statistically independent data with no censoring, (2) data with a correlation of 0.25 between adjacent points and no censored data, and (3) data with a correlation of 0.25 between adjacent points and 25 percent censored data. As for normally-distributed data, the estimated mean values of the model parameters were examined for bias and the effect of censored data on the standard deviations of the model parameters was determined.

The results for the mean values of the model parameters are shown in Table 5.6. The 95-percent confidence intervals for the mean values are also shown in this table. These results for the lognormal distributions are similar to the results for the normal distributions, with no bias in the estimated mean values of the model parameters for the mean, standard deviation, and correlation model parameters. The estimated values of the Hermite Polynomial coefficients tend to be slightly different than the true model values. This is due to the nature of the Hermite Polynomials, since different values for the coefficients can result in similarly shaped distributions. The standard normal inverses of the cumulative distribution functions for the lognormal distributions are shown in Figures 5.10 through 5.12. These figures show that the shape of the estimated distributions, which are determined by the Hermite Polynomial model parameters, follow the distribution of the true model almost exactly.

The probability distributions for the lognormal distributions, as shown in the standard normal inverse of the cumulative distribution, $\Phi^{-1}[F_Y(y)]$, in Figures 5.10 through 5.12 may be used to find percentile values. For example, the standard normal

Table 5.6. Estimated mean values and 95 percent confidence intervals for the mean values for lognormal distributions.

Model Parameter	True Model Values	Case 1: No Censored Data, $\rho_{adj}=0$	Case 2: No Censored Data, $\rho_{adj}=0.25$	Case 3: 25% Censored Data, $\rho_{adj}=0.25$
ϕ_{μ}	1.647	1.68 (1.64, 1.72)	1.66 (1.61, 1.70)	1.73 (1.67, 1.79)
ϕ_{σ}	0.771	0.76 (0.73, 0.80)	0.74 (0.71, 0.78)	0.78 (0.75, 0.81)
ϕ_{ρ}	0.1 for $\rho_{adj}=0$ 1.98 for $\rho_{adj}=0.25$	-8.11 (-8.61, -7.61)	1.99 (1.96, 2.02)	2.00 (1.95, 2.05)
ϕ_{ψ_2}	-1.003	-1.24 (-1.29, -1.19)	-1.23 (-1.28, -1.19)	-1.26 (-1.34, -1.18)
ϕ_{ψ_3}	0.916	0.91 (0.86, 0.95)	0.90 (0.86, 0.94)	0.94 (0.89, 0.99)
ϕ_{ψ_4}	-0.645	-1.05 (-1.22, -0.88)	-1.01 (-1.21, -0.81)	-0.92 (-1.21, -0.63)
ϕ_{ψ_5}	0.252	0.65 (0.34, 0.96)	0.64 (0.35, 0.93)	1.20 (0.83, 1.57)

inverse of 0.90 is 1.28. The 90th percentile value, $y_{0.90}$, is the value of y that corresponds to the $\Phi^{-1}[F_Y(y)]$ value of 1.28. The $y_{0.90}$ for Case 1 (Figure 5.10) is therefore 3.18.

The 95-percent confidence bounds on the estimated mean model values are also shown in Figures 5.10 through 5.12. For the $y_{0.90}$ value for Case 1, the lower 95-percent confidence bound is 2.69 and the upper bound is 4.27. In all three cases of the standard lognormal distribution the 95-percent confidence interval becomes wider in the right tail of the distribution. This means that the ability to predict a percentile value decreases as the percentile increases.

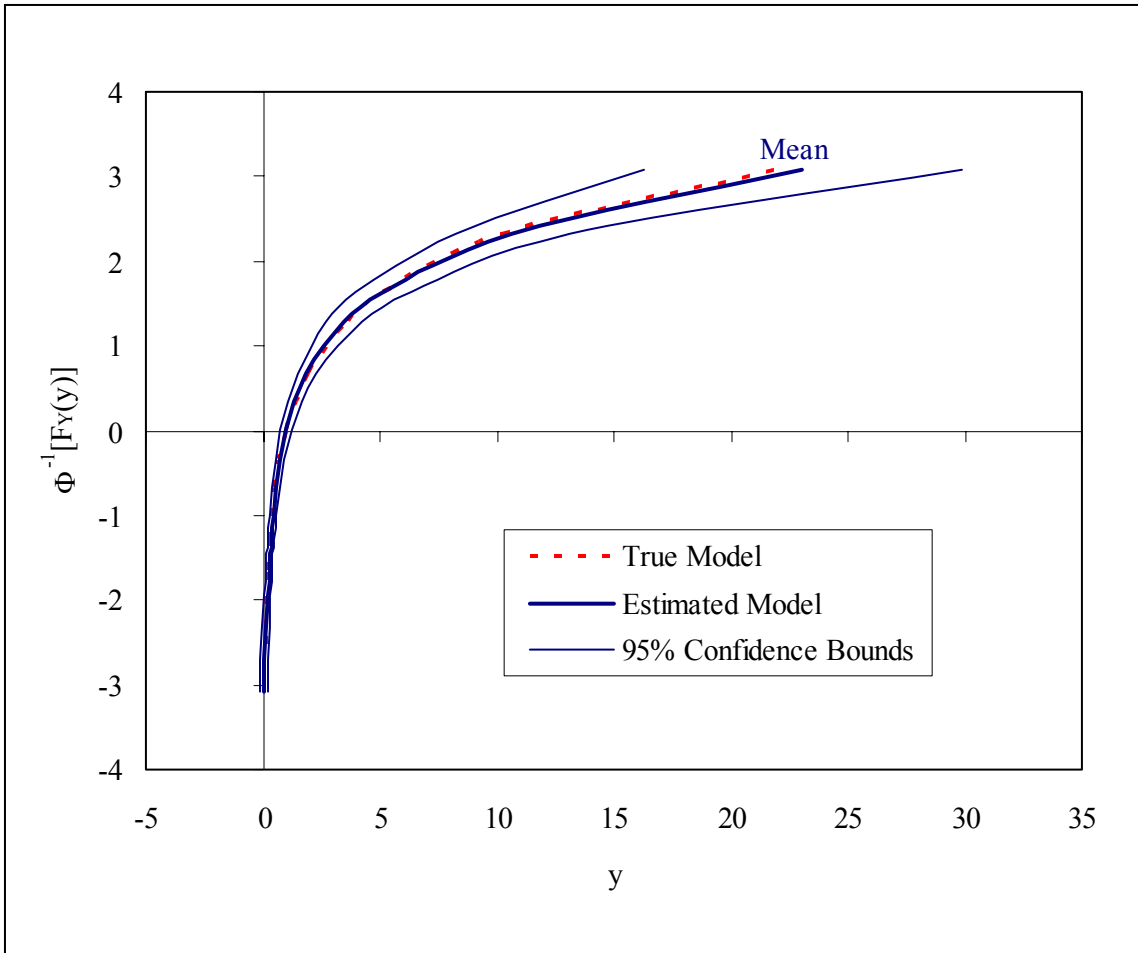


Figure 5.10. Probability distribution for Case 1, a standard lognormal distribution with no censored data and statistically independent data.

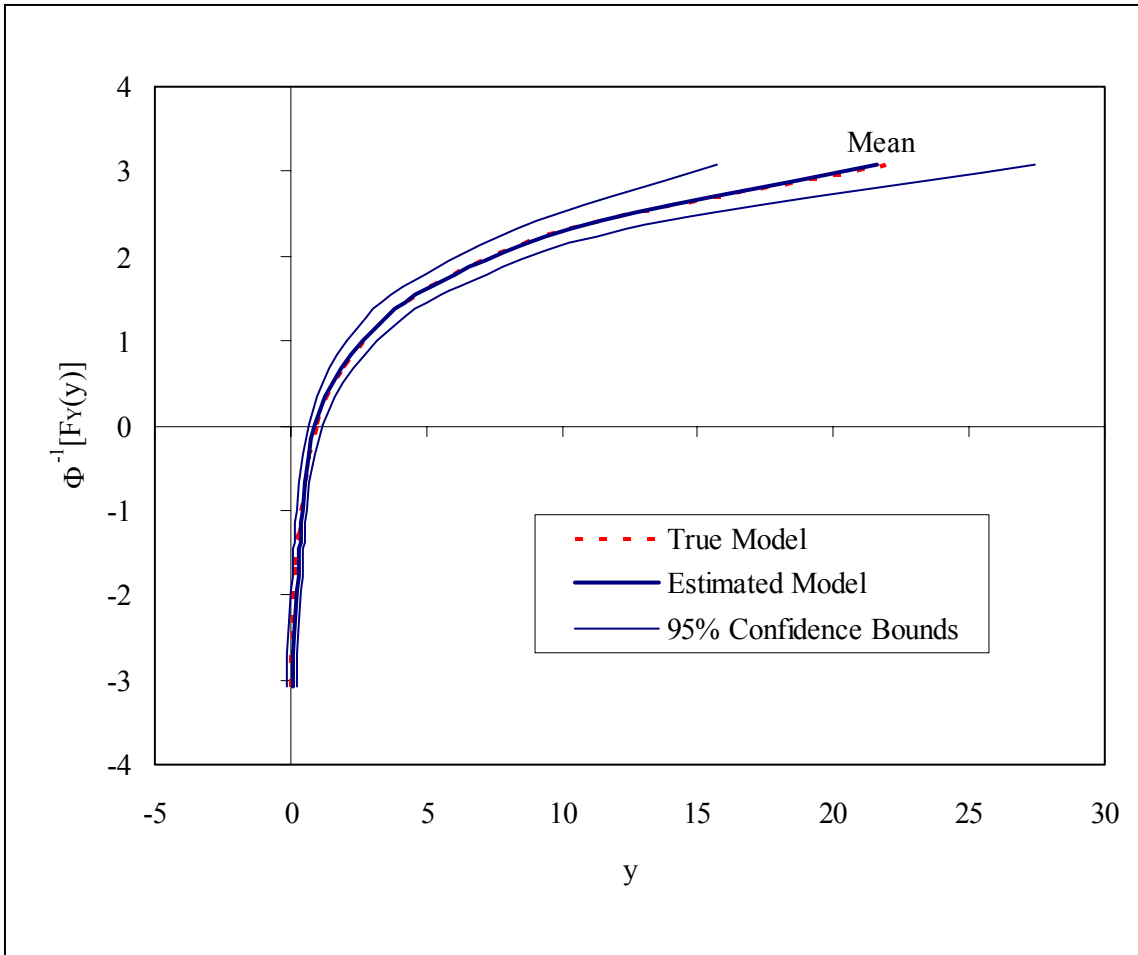


Figure 5.11. Probability distribution for Case 2, a standard lognormal distribution with no censored data and correlated data.

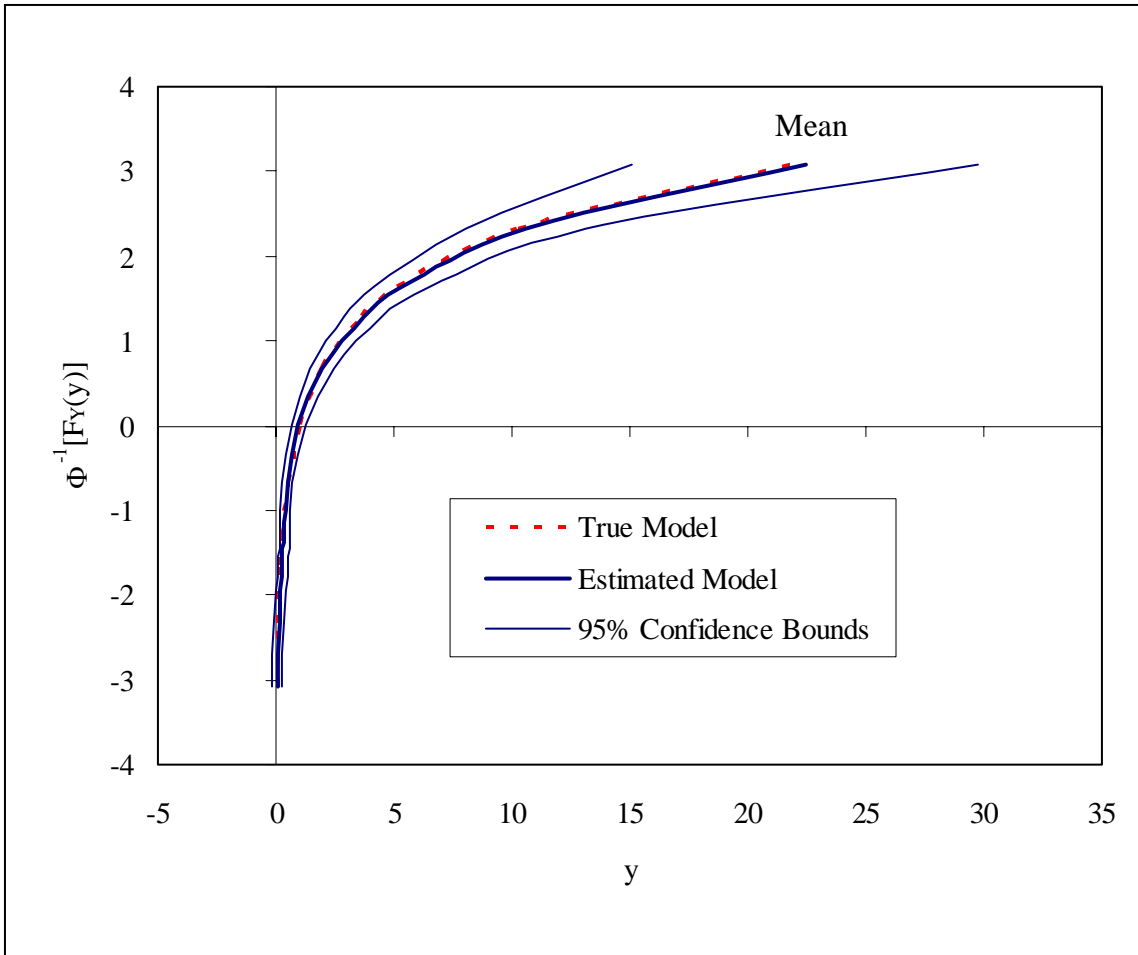


Figure 5.12. Probability distribution for Case 3, a standard lognormal distribution with censored and correlated data.

The confidence bounds for the 99th percentile value, $y_{0.99}$, are shown in Table 5.7 for the three lognormal cases. The width of the 95-percent confidence interval is smaller for Case 2 than for Case 1, indicating that correlated data increase the confidence in the percentile estimates. The width of the 95-percent confidence interval is greatest for Case 3, which is censored, correlated data. This indicates that censoring decreases the confidence in the percentile estimates.

Table 5.7. Confidence in 99th percentile estimates for the standard lognormal distribution.

	Case 1: No Censored Data, $\rho_{adj}=0$	Case 2: No Censored Data, $\rho_{adj}=0.25$	Case 3: 25% Censored Data, $\rho_{adj}=0.25$
99 th percentile value, $y_{0.99}$	10.68	10.34	10.61
Lower 95-percent confidence bound	8.23	8.30	8.09
Upper 95-percent confidence bound	13.14	12.38	13.13
Width of 95-percent confidence interval	4.91	4.07	5.03

5.5 SUMMARY

The effects of censoring on both normally-distributed and non-normally distributed data were discussed in this chapter. Censoring does not cause bias in the estimated mean values of the model parameters found with the FOSM Bayesian method. The amount learned about the model parameters from the data decreases as the amount of censoring increases, due to the uncertainty in the value of the censored data. Different methods for evaluating the expected updated variance in model parameters with censored data were compared. For normally-distributed data, the method that uses a Taylor series approximation for the natural logarithm of the likelihood function was found to be the most accurate and the most practical in terms of computation time. However, for non-normally-distributed data, this approximate method does not work and numerical integration must be used.

Chapter 6. Case Study Application – Model for Measured Contaminant Concentrations

6.1 INTRODUCTION

The French Limited site, a Superfund site located near Houston, Texas, was selected as an application for the FOSM Bayesian method developed for censored data. Censored data occur at this site in the form of groundwater concentrations that are reported as below the detection limit. These censored data play an important role at the site in determining the extent of contamination and the effect of remediation. The concentrations of benzene, a major contaminant of concern at the French Limited site, are modeled so that the model parameters may be calibrated with measurements from the site. In this chapter, background information is given about the French Limited site, including the history, hydrogeologic characteristics, investigation, and remediation of the site. The model used for the mean benzene concentrations before remediation is presented, along with the modifications to the model that account for the effects of remediation by source removal and biodegradation. The models used for the covariances and distribution of benzene concentrations in the groundwater at the site are also presented.

6.2 FRENCH LIMITED SITE

In this section, background information about the French limited site is presented, beginning with a general description of the site. The hydrogeology of the site is described, as well as the investigation and remediation efforts that have occurred at the site.

6.2.1 Site Description

The French Limited site is located in Harris County, Texas. The site and vicinity are shown in Figure 6.1. The main feature of the 22.5-acre site is a 7.3-acre lagoon, which was formed by sand-mining operations conducted from the late 1950s through 1965. The lagoon was then operated as a permitted, unlined waste disposal facility between 1966 and 1972. The facility received a variety of petrochemical and wood preservative wastes, as well as other unknown materials. Operators estimate that 80,000,000 gallons (96,000 m³) of waste were placed in the lagoon during the facility's active life. The wastes formed a sludge layer at the bottom of the lagoon with high concentrations of organic compounds and metals. The site was placed on the National Priority List in 1982 and was designated for remediation under the Comprehensive Environmental Response, Compensation, and Liability Act of 1980 (CERCLA), also known as "Superfund."

Contamination spread beyond the triangular-shaped boundaries of the site, particularly to the south. The responsible parties were given access rights to the properties south of the actual property boundaries of the French Limited site, with the access rights extending 30 years post-closure. For the remainder of this study, the term "site" will refer to the entire contaminated or monitored area within and beyond the actual property boundaries.

6.2.2 Site Hydrogeology

The French Limited site lies within the 100-year floodplain of the San Jacinto River. Floods occurred in 1969, 1973, 1979, and 1983 that resulted in overflowing of the

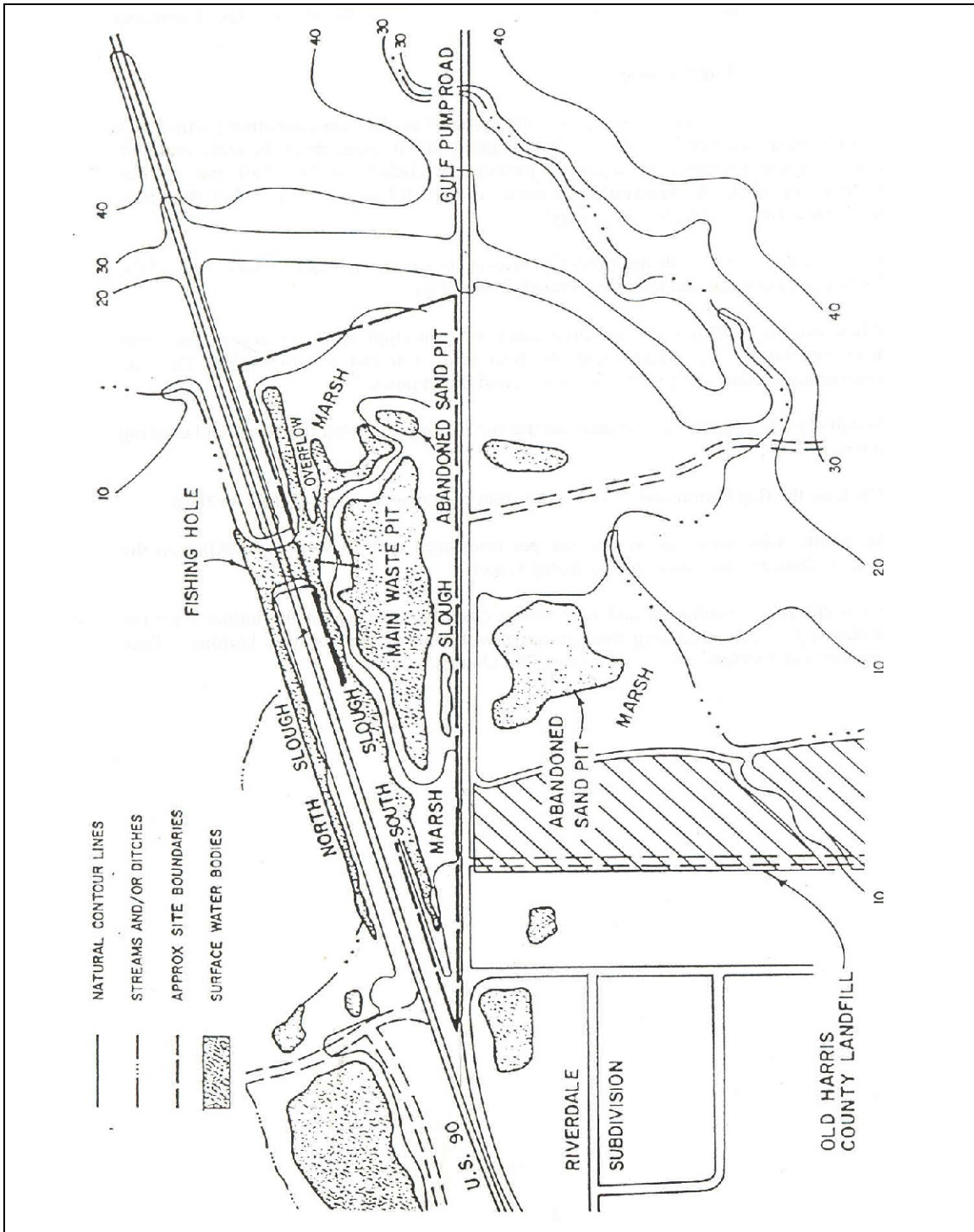


Figure 6.1. Map of French Limited site and vicinity (from Applied Hydrology Associates, 1989).

lagoon, releasing its contents into surrounding areas. A sheet-pile wall was constructed around the waste lagoon in 1989 to provide containment of the lagoon contents during flood events.

The site is located in an abandoned meander belt of the San Jacinto River, which contains alluvial deposits consisting of poorly consolidated sands, silty sands, gravels, and clay (Applied Hydrology Associates, 1989). The alluvial deposits range in depth from 6 to 17 m and are mostly saturated. Groundwater in this shallow aquifer system generally flows to the south. The Beaumont clay formation underlies the alluvial zone, forming a 20 to 30 m thick confining layer.

Although conditions throughout the site, both laterally and vertically, are quite heterogeneous, the upper alluvial zone has been divided into four distinct strata, from the surface downwards:

UNC – uncompacted stratum consisting mostly of loose silty sands

S1 – sandy stratum with some gravel

C1 – clay stratum

INT – interbedded silts, clays, and sands

The UNC, S1, and INT strata are essentially continuous over the French Limited site, while the C1 stratum is absent in some areas of the site.

6.2.3 Groundwater Investigation

Investigation of the French Limited site began in 1981. Between 1981 and 1989, approximately 40 monitoring wells were sampled periodically, and the samples were tested for a variety of contaminants. During the 1980s, benzene was the primary

contaminant of concern and was chosen as an indicator contaminant due to its high solubility, mobility, and carcinogenic character. Other contaminants found in the groundwater include toluene, vinyl chloride, acetone, 1,2-dichloroethane, arsenic, and lead.

Monitoring wells installed at the French Limited site are shown in Figure 6.2. During the 1980s, the entire upper alluvial zone was considered as one aquifer. Monitoring wells were screened over long intervals and often included multiple strata. Wells installed in the 1980s are labeled ERT, REI, and GW. During the 1990s, the S1 and INT strata were considered as separate aquifers. Monitoring wells installed during this time were screened over one of these strata, and were labeled accordingly with S1 or INT.

In 1992, a dense non-aqueous phase liquid (DNAPL) was discovered in three wells south of the lagoon. After further investigation, a sheet-pile containment wall was constructed around the DNAPL source area.

6.2.4 Site Remediation

Active remediation of the French Limited site occurred between January 1992 and December 1995. The main component of remediation consisted of bioremediation of the lagoon contents, which began in 1992 and was completed in 1993. The lagoon was then backfilled with clean soil in October 1994.

Active remediation of the groundwater to the south of the lagoon occurred between February 1992 and December 1995. The remediation method for the groundwater at the site was chosen based on the monitoring data from the ERT, REI, and GW wells. Traditional pump-and-treat remediation was performed using 54 withdrawal wells in the INT stratum and 48 withdrawal wells in the S1 stratum. Treated groundwater

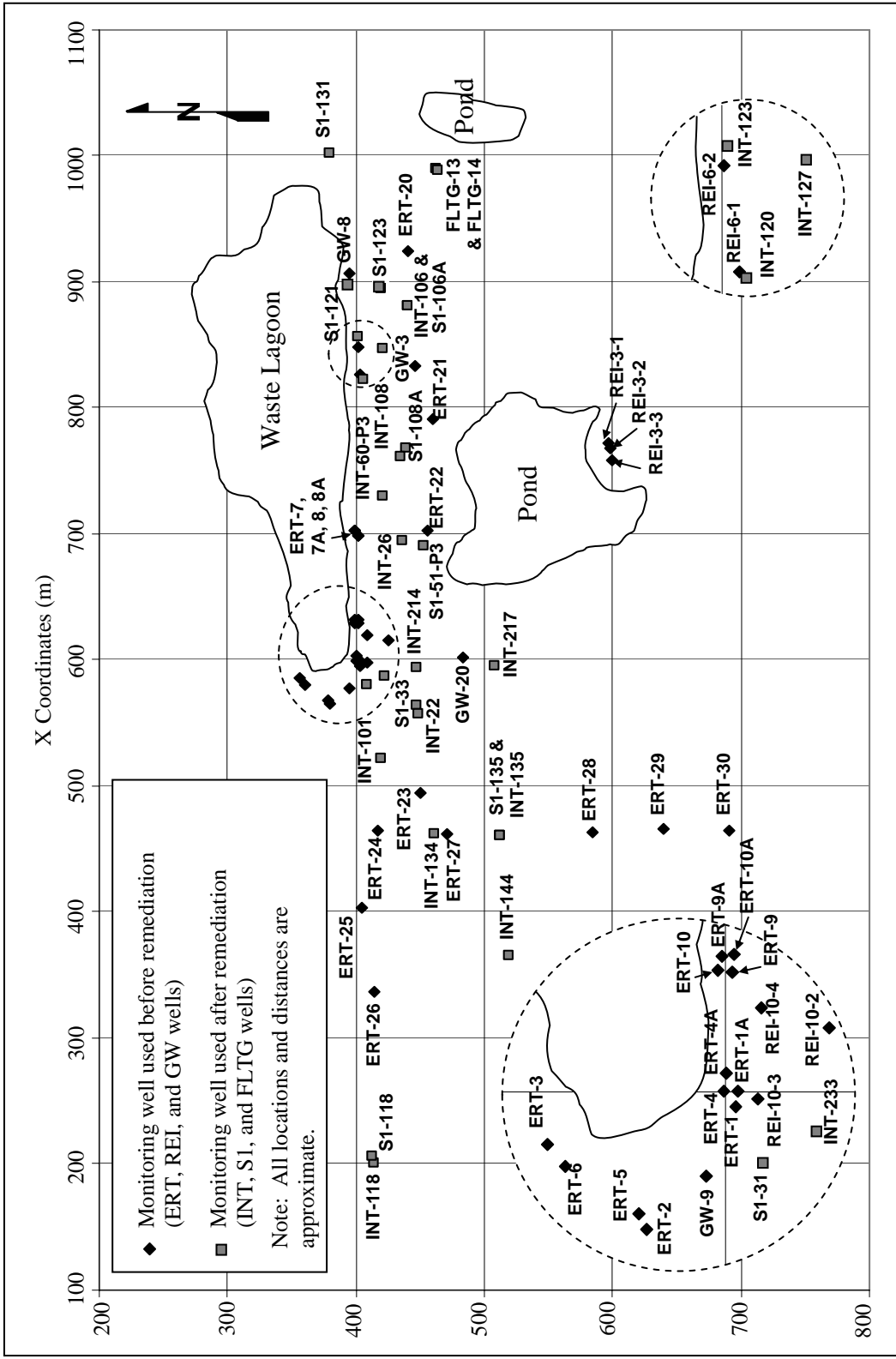


Figure 6.2. Monitoring wells at French Limited site.

was re-injected with 19 injection wells in the INT stratum and 9 wells in the S1 stratum. These injection wells also supplied oxygen, nitrogen, and potassium to the groundwater to promote biodegradation of the contaminants (ENSR 1991). All active remediation activities ended in December 1995.

Contamination remained in the shallow groundwater at the end of active remediation. Natural attenuation was chosen as the remediation method for the remaining contamination. The natural attenuation of the groundwater will be further discussed in Chapter 7.

6.3 MODEL FOR BENZENE CONCENTRATIONS

The model developed for the distribution of measured concentrations at the French Limited site is presented in this section. The model consists of three components: the mean, covariance, and distribution of the concentration measurements. The Horizontal Plane Source model (Galya 1987) was chosen to model the mean benzene concentrations at the site. The equations and parameters used in this model, as well as the modifications to the model to account for the effects of remediation on contaminant concentrations, are described. The model for the covariance of the data from the site, which considers correlations with measurement distance and time and also accounts for random errors in sampling, is then presented. Finally, the model for the distribution of the measurements is described. These models were developed based on the models used by McBrayer (1999) and Muchard (1997).

6.3.1 Model for Mean Concentrations

The mean contaminant concentrations in the groundwater at the French Limited site were modeled with a Horizontal Plane Source (HPS) model (Galya 1987). The probable source of contamination at the site was the waste lagoon, which covers a large area (7.3 acres). The plane source more accurately models this large probable contaminant source area than a point or line source. Also, the HPS model assumes constant aquifer properties and is therefore simple enough to be practically implemented in model calibration.

The concentration of a contaminant at any time and at any point in an aquifer is expressed as follows (Galya 1997):

$$C(x, y, z, t) = \frac{1}{nR} \int_{T_0}^{t_c} M_S(\tau) D(t_c - \tau) X_0(x_c, t_c - \tau) Y_0(y_c, t_c - \tau) Z_0(z_c, t_c - \tau) d\tau \quad (6.1)$$

The parameters used in the functions of this equation and throughout the rest of this chapter are listed in Table 6.1.

A parameter, θ , was introduced to the model so that the groundwater flow could be in any direction away from the plane source. The geometric parameters of the model are illustrated in Figure 6.3 and equations for calculating these parameters are as follows:

$$x_c = (x - X_s) \cos \theta + (y - Y_s) \sin \theta \quad (6.2)$$

$$y_c = -(x - X_s) \sin \theta + (y - Y_s) \cos \theta \quad (6.3)$$

$$z_c = Z_s - z \quad (6.4)$$

Table 6.1. Summary of parameters used in the Horizontal Plane Source model.

Parameter	Description
x	X-Coordinate at which the concentration is evaluated
y	Y-Coordinate at which the concentration is evaluated
z	Z-Coordinate at which the concentration is evaluated
t	Time at which the concentration is evaluated
X_s	X-Coordinate at center of plane source
Y_s	Y-Coordinate at center of plane source
Z_s	Z-Coordinate at plane source
T_0	Contaminant release start time
x_c	Longitudinal distance between source center and evaluation point
y_c	Transverse distance between source center and evaluation point
z_c	Vertical distance between plane source and evaluation point
t_c	Time between evaluation time and contaminant release start time
θ	Groundwater flow direction
τ	Time variable for integration
T_r	Time that remediation occurs
k	First-order decay coefficient for contaminant
k_1	First-order decay coefficient for contaminant before remediation
k_r	First-order decay coefficient for contaminant after remediation
$T_{1/2}$	Contaminant half-life
$T_{1/2,1}$	Contaminant half-life before remediation
$T_{1/2,r}$	Contaminant half-life after remediation
C_o	Contaminant concentration at source
L	Source length (in x-direction)
W	Source width (in y-direction)
B	Aquifer thickness
H_w	Well height
n	Aquifer porosity
R	Contaminant retardation Factor

Table 6.1 (continued)

v	Groundwater seepage velocity
a _L	Longitudinal dispersivity (parallel to direction of groundwater flow)
a _T	Transverse dispersivity (perpendicular to direction of groundwater flow)
a _V	Vertical dispersivity
E _r	Fraction of source remaining after remediation

In Equation 6.1, $M_S(\tau)$ refers to the mass release rate at time τ . For the French Limited site, the mass release rate was considered constant in the time period before remediation and in the time period after remediation. Johnson and Pankow (1992) give the following function for the surface-area average rate of mass release from a pool of solvent:

$$M_S = C_o n L W \sqrt{\frac{4a_v v^2}{\pi L}} \quad (6.5)$$

Although this equation was intended for mass release from a pool of solvent, the derivation of the equation is not unique to solvents and may be used for any contaminant release from a rectangular source into groundwater. Equation 6.5 was therefore used as the mass release rate for the contaminant source at the French Limited site.

The D term in Equation 6.1 is a function to represent the decay of contaminants due to biodegradation or chemical reactions. For first-order decay, the function is expressed in terms of the first-order decay coefficient, k:

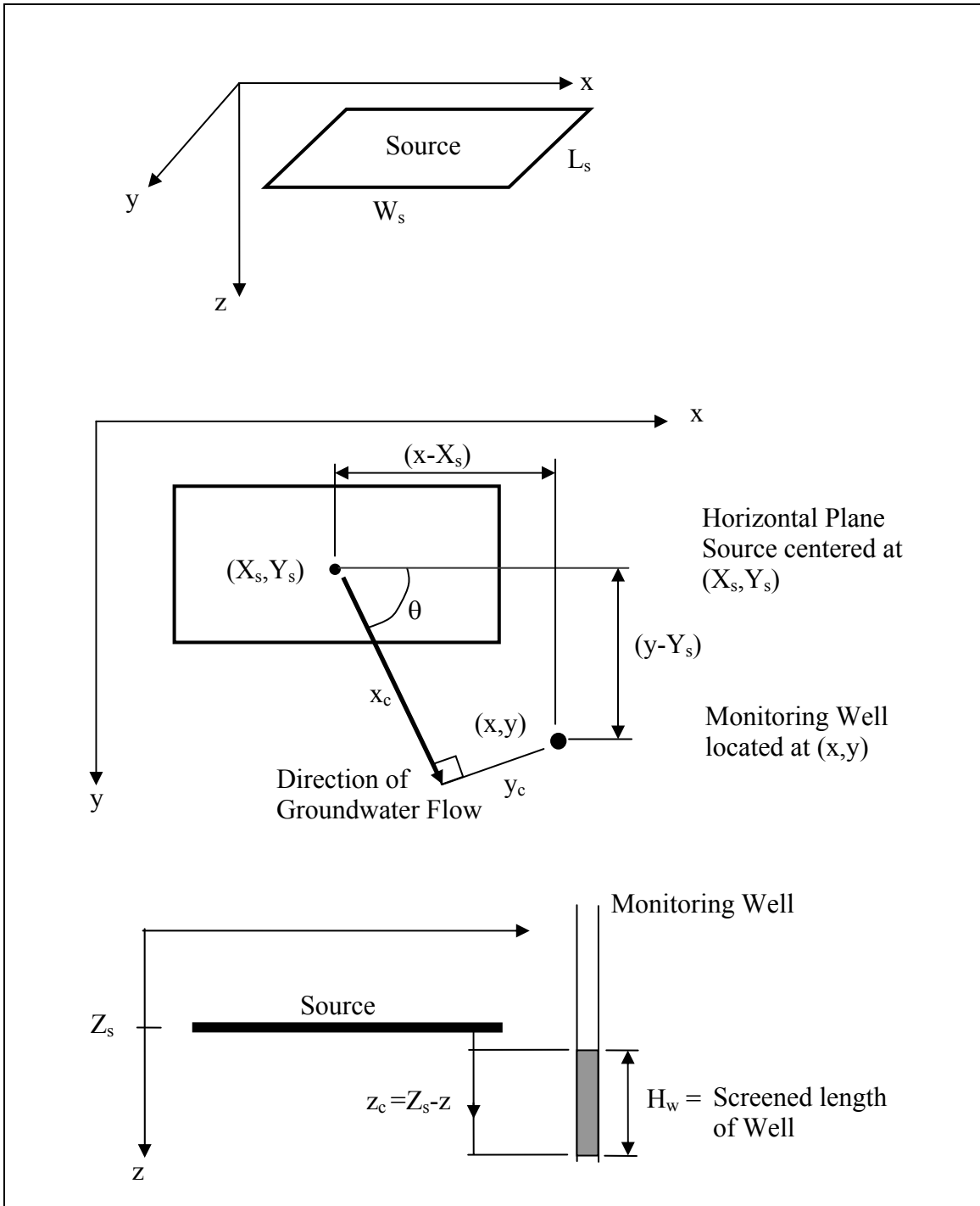


Figure 6.3. Geometric parameters of the Horizontal Plane Source model.

$$D = \exp(-kt_c) \quad (6.6)$$

where k is a function of the half-life of the contaminant:

$$k = \frac{\ln T_{1/2}}{2} \quad (6.7)$$

X_0 and Y_0 are Green's function solutions for a horizontal plane source, found by integrating a point source solution over the length and width of the plane source. The x -direction is the direction of groundwater flow, or longitudinal direction, while the y -direction is perpendicular to the groundwater flow, or the transverse direction. The Green's function solutions are presented by Galya as follows:

$$X_0 = \frac{1}{2L} \left[\operatorname{erf} \frac{\left(\frac{L}{2} + x_c - X_s - \frac{vt_c}{R} \right)}{\sqrt{\frac{4a_L vt_c}{R}}} + \operatorname{erf} \frac{\left(\frac{L}{2} - x_c + X_s + \frac{vt_c}{R} \right)}{\sqrt{\frac{4a_L vt_c}{R}}} \right] \quad (6.8)$$

$$Y_0 = \frac{1}{2W} \left[\operatorname{erf} \frac{\left(\frac{W}{2} + y_c - Y_s \right)}{\sqrt{\frac{4a_T vt_c}{R}}} + \operatorname{erf} \frac{\left(\frac{W}{2} - y_c + Y_s \right)}{\sqrt{\frac{4a_T vt}{R}}} \right] \quad (6.9)$$

The Z_0 term is the Green's function solution in the vertical direction for an aquifer of thickness b , as obtained by Carslaw and Jaeger (1959) by adding an infinite number of image sources:

$$Z_0 = \frac{1}{b} \left[1 + 2 \sum_{i=1}^{\infty} \exp\left(-\frac{i^2 \pi^2 a_v vt}{b^2 R}\right) \cos\left(\frac{i\pi z_c}{b}\right) \cos\left(\frac{i\pi Z_s}{b}\right) \right] \quad (6.10)$$

The number of terms used in the summation in the above equation may be determined as follows:

$$N_{\infty} = 1 + \left(\frac{b}{\pi}\right) \sqrt{\frac{25R}{a_v v(t-\tau)}} \quad (6.11)$$

The Galya model finds the contaminant concentration at a discrete point in the aquifer. Since monitoring wells are screened over a vertical interval, the concentration found in the well may be approximated by averaging the concentrations of the discrete points in the vertical interval of the well screen. This average is calculated by integrating the concentration along the screen interval of the well, H_w :

$$C(x, y, z, t) = \frac{1}{H_w n R} \int_0^{H_w} \int_{T_0}^{t_c} M_s(\tau) D(t_c - \tau) X_0(x_c, t_c - \tau) Y_0(y_c, t_c - \tau) Z_0(z_c, t_c - \tau) dt dz \quad (6.12)$$

The concept of the time variable for integration, τ , for the convolution integral of Equations 6.1 and 6.12 is illustrated in Figure 6.4. The integral is evaluated for τ values between the initial time of contaminant release, T_0 , to the evaluation time of the concentration, t_c . In Figure 6.4, three τ values are shown, whereas an infinite number of τ values would theoretically be used in the integration. At each time τ , a contaminant mass release rate from the source, $M_s(\tau)$, is determined. The travel time of the contaminant released at time τ is $(t_c - \tau)$. The advection and dispersion of the

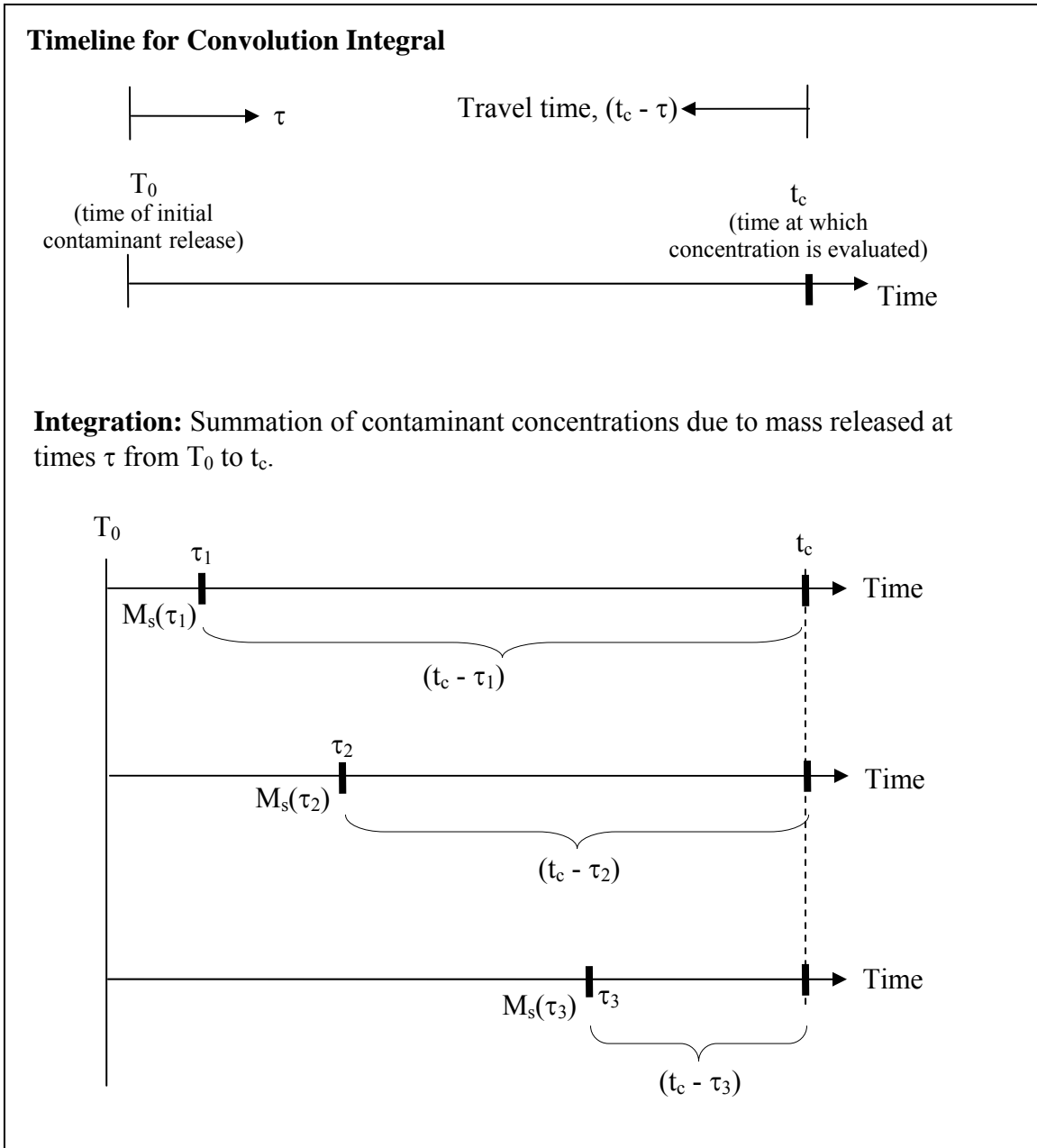


Figure 6.4. Conceptual illustration of convolution integral for calculating contaminant concentration.

contaminant mass released during time $d\tau$ is therefore calculated with the Green's function evaluated with the travel time, $(t_c - \tau)$. The decay of the contaminant mass released over $d\tau$ is calculated with the decay function for the travel time of the contaminant mass, $(t_c - \tau)$. By integrating from T_0 to t_c , the advection, dispersion, and decay of the contaminant released over that time are effectively summed to determine the contaminant concentration at a particular location and time. Since Equation 6.12 may not be integrated analytically, the Gauss-Kronrod Quadrature method for numerical integration was used for the integration.

As discussed in McBrayer (1999) and Muchard (1997), the approximations used in the FOSM Bayesian method are more exact with more linear models, and the natural logarithm of the model-predicted concentrations is more likely to be linear than the non-transformed concentrations. Also, using the natural logarithm of the concentration prevents predictions of negative concentrations. Therefore, the natural logarithms of the benzene concentration measurements from the French Limited site are calibrated with the natural logarithms of the concentrations modeled with Equation 6.12. The natural logarithm of a benzene measurement is denoted as Y_i :

$$Y_i = \ln \left[C(x_i, y_i, z_i, t_i) \right] \quad (6.13)$$

6.3.2 Model Parameters for Remediation Effects

This study considered the effects of remediation at the French Limited site. The groundwater model therefore needed to consider conditions both before and after remediation. Both the mass release rate, M_s , and the first-order decay coefficient, k , are expected to change after remediation. The subscript "1" will refer to conditions at the

site before remediation, and the subscript “r” will refer to conditions at the site after remediation.

The mass release rate before remediation, M_{s1} , is found with the mass release rate of Equation 6.5:

$$M_{s1} = C_o n L W \sqrt{\frac{4a_v v^2}{\pi L}} \quad (6.14)$$

A main component of the remediation of the French Limited site was bioremediation of the lagoon contents, which attempted to remove the source of contamination. A new parameter, E_r , was introduced to represent the effectiveness of the remediation in removing the contaminant source. This parameter represents the fraction of the source remaining after remediation. For example, if E_r is 0.10, then the mass release rate after remediation is reduced to only ten percent of the mass release rate before remediation. The mass release rate after remediation, M_{sr} , is therefore:

$$M_{sr} = E_r M_{s1} = E_r C_o n L W \sqrt{\frac{4a_v v^2}{\pi L}} \quad (6.15)$$

At the French Limited site, it was believed that bioremediation of the contaminants in the groundwater would increase after remediation. The first-order decay coefficient before remediation, k_1 , is determined by the half-life of the contaminant before remediation, $T_{1/2,1}$:

$$k_1 = \frac{\ln T_{1/2,1}}{2} \quad (6.16)$$

To account for the expected increased bioremediation after remediation, a contaminant half-life for the condition after remediation was introduced as $T_{1/2,r}$. The degradation after remediation is then:

$$k_r = \frac{\ln T_{1/2,r}}{2} \quad (6.17)$$

These remediation factors are incorporated in the convolution integral of Equation 6.12 by considering if the time at which the concentration is evaluated, t_c , and the value of the time variable for integration, τ , are before or after the time of remediation, T_r . The relation of these times to the remediation factors is shown in Figure 6.5. Since the mass release rate term in Equation 6.12 is a function of τ , the appropriate mass release rate to use while integrating is determined by whether or not τ is before or after the time of remediation:

$$M_s(\tau) = \begin{cases} M_{sl} & \text{if } \tau \leq T_r \\ M_{sr} & \text{if } \tau > T_r \end{cases} \quad (6.18)$$

The decay term in Equation 6.12 is a function of contaminant travel time, $(t_c - \tau)$. The first-order decay coefficient used in the $D(t_c - \tau)$ term must therefore be determined by whether or not the interval of $(t_c - \tau)$ is entirely before T_r , entirely after T_r , or spans T_r . If $(t_c - \tau)$ is entirely before T_r , k_1 is used in $D(t_c - \tau)$, while if $(t_c - \tau)$ is entirely after T_r , k_r is used in $D(t_c - \tau)$. When the span of $(t_c - \tau)$ includes T_r , the first-order decay coefficient used in $D(t_c - \tau)$ is a weighted average of k_1 and k_r . The first-order decay coefficient may therefore be determined as follows:

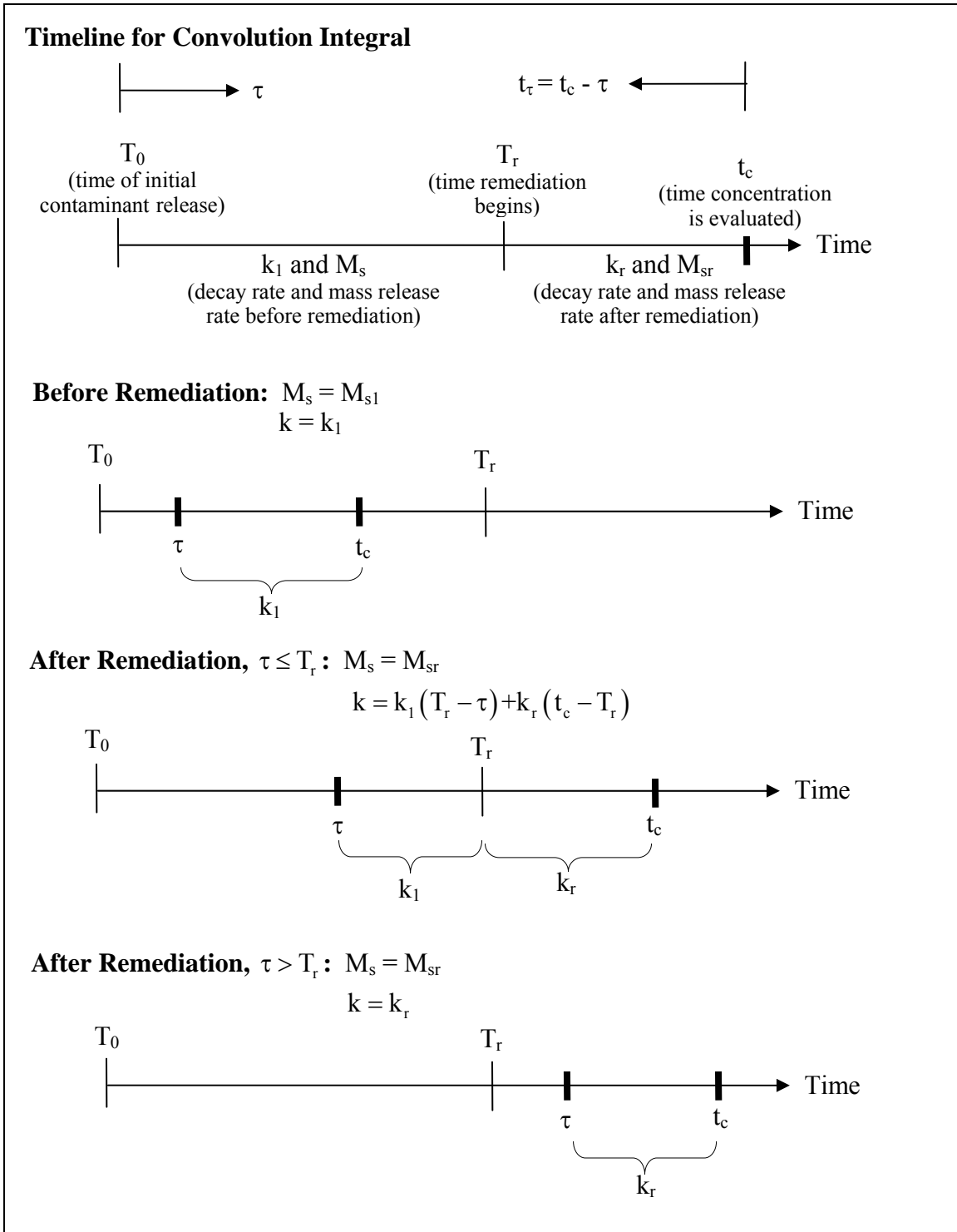


Figure 6.5. Illustration of remediation factors used to calculate contaminant concentration.

$$k = \begin{cases} k_l & \text{if } \tau \leq T_r \text{ and } t_c \leq T_r \\ k_l (T_r - \tau) + k_r (t_c - T_r) & \text{if } \tau \leq T_r \text{ and } t_c > T_r \\ k_r & \text{if } \tau > T_r \text{ and } t_c > T_r \end{cases} \quad (6.19)$$

6.3.3 Model for Covariance of Data

The covariance between the groundwater measurements is determined by the variance of each groundwater measurement and by the correlation between different measurements. Since the natural logarithm of the benzene measurements is calibrated with the natural logarithm of the modeled concentration (Section 6.3.1 and Equation 6.13), the covariances are calculated between the natural logarithm of measurements. The covariance between the natural logarithm of two of measurements, Y_i and Y_j , is found as follows:

$$\text{Cov}(Y_i, Y_j) = \rho_{i,j} \sqrt{\text{Var}(Y_i) \text{Var}(Y_j)} \quad (6.20)$$

The variance for each measurement is found as the variance in the natural logarithm of the concentration, Y_i :

$$\text{Var}(Y_i) = \delta^2 \Gamma^2(L_i) \quad (6.21)$$

The δ^2 term in this equation represents the uncertainty in the model-calculated concentrations. It is important to note that the variance for the natural logarithm of concentration is constant for a given value of δ . This means that the coefficient of

variation for the concentration itself (not transformed with the natural logarithm) will be approximately constant and the variance will increase with increasing concentration.

Since the wells are screened over a vertical interval and the concentrations are calculated by averaging over this interval (Equation 6.12), the variance in the natural logarithm of the concentration is smaller than it would be for a point measurement. A variance reduction factor is therefore used due to vertical averaging in the well (Vanmarcke 1983):

$$\Gamma^2(L_i) = \frac{\lambda_z^2}{2L_i^2} \left(\frac{2L_i}{\lambda_z} + \exp\left(-\frac{2L_i}{\lambda_z}\right) - 1 \right) \quad (6.22)$$

where:

L_i = length of well screen i

λ_z = vertical scale of fluctuation for a point measurement

The scale of fluctuation in the vertical dimension, and in other dimensions, is the separation distance at which the two measurements will both be consistently greater than or less than the model-predicted values.

Concentration measurements may be correlated with one another based on their separation with distance in the longitudinal (x), transverse (y), vertical (z), and temporal (t) dimensions. The correlation may be reduced because of random error (e). Also, measurements may be correlated on the basis of whether they were taken before or after remediation (r). A separable correlation structure (Vanmarcke 1983) is used to combine all of these possible measurement correlations:

$$\rho_{i,j} = \rho_x \rho_y \rho_z \rho_t \rho_e \rho_r \quad (6.23)$$

where:

$\rho_{i,j}$ = correlation between measurement i and measurement j

ρ_x = spatial correlation coefficient for the longitudinal direction

ρ_y = spatial correlation coefficient for the transverse direction

ρ_z = spatial correlation coefficient for the vertical direction

ρ_t = temporal correlation coefficient

ρ_e = correlation coefficient due to random error

ρ_r = correlation coefficient for measurements before/after remediation

The longitudinal, transverse, and temporal correlation coefficients were calculated with an exponential function that keeps the correlation coefficient between -1.0 and $+1.0$. The correlation depends on the distance between the two measurements in dimension D and the scale of fluctuation, λ_D , in that dimension:

$$\rho_D = \exp\left(-2 \frac{|\tau_D|}{\lambda_D}\right) \quad (6.24)$$

where:

ρ_D = spatial correlation coefficient for the longitudinal, transverse, or temporal dimension

τ_D = distance between the measurements in dimension D

λ_D = scale of fluctuation for the longitudinal, transverse, or temporal dimension

Figure 6.6 shows sample correlations for different scales of fluctuation according to separation distance or time between measurements. At the same separation between two measurements in distance or time, the correlation coefficient increases as the scale of fluctuation increases.

The vertical correlation coefficient used for the correlation between two screened wells is the correlation coefficient for two vertical averages defined by Vanmarcke (1983):

$$\rho_z = \frac{\sum_{k=0}^3 (-1)^k T_k \Gamma^2(T_k)}{2L_i L_j \sqrt{\Gamma^2(L_i) \Gamma^2(L_j)}} \quad (6.25)$$

where:

L_i = length of well screen i

L_j = length of well screen j

Γ^2 = variance reduction factor defined in Equation 5.17

T_0 = distance between bottom of screen i and top of screen j

T_1 = distance between top of screen i and top of screen j

T_2 = distance between top of screen i and bottom of screen j

T_3 = distance between bottom of screen i and bottom of screen j

The T_0 through T_3 terms of this equation are illustrated in Figure 6.7.

Random error due to natural variability in subsurface conditions, sampling variation, and measurement variations may occur. When two samples are taken at the same time from the same well, it is unusual for the concentrations to be identical. A reduction in the correlation between measurements is therefore included, so that the

Correlation with Horizontal Distance or Time

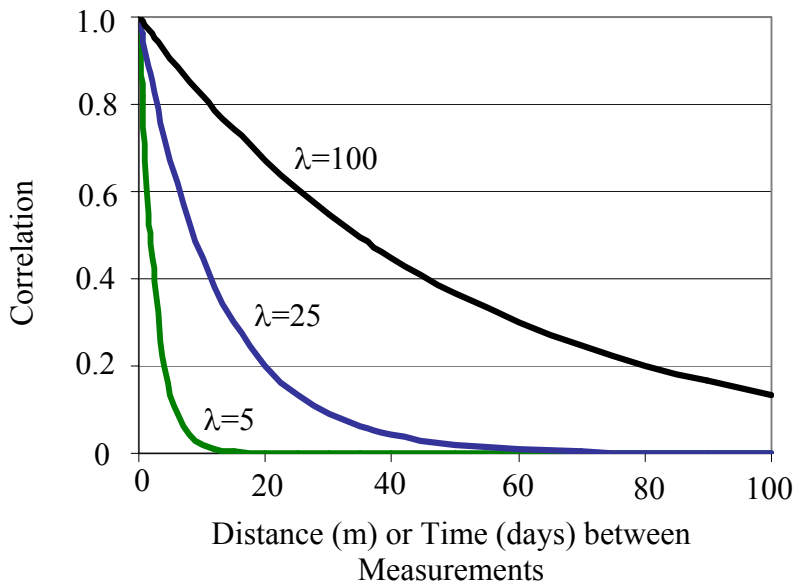
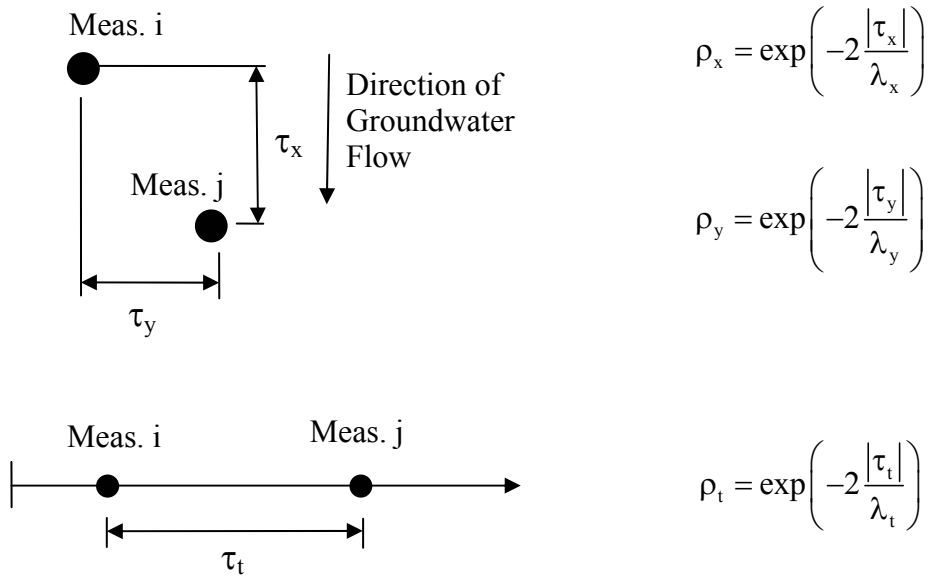


Figure 6.6. Correlation coefficients for longitudinal, transverse, and temporal dimensions.

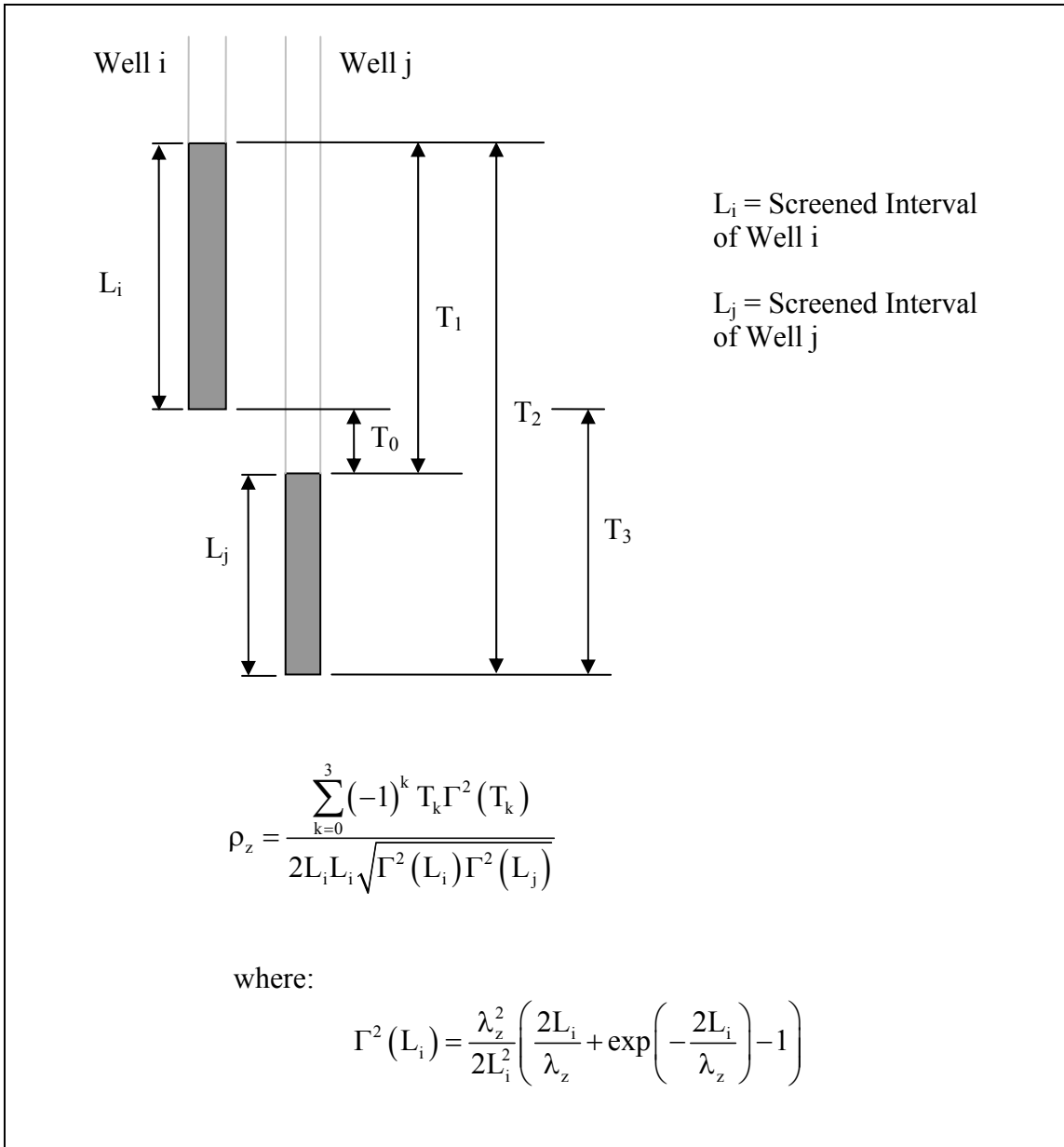


Figure 6.7. T parameters for vertical averaging correlation coefficient.

correlation may be less than 1.0 even if two measurements are taken at the same location and same time. An exponential function is used for this correlation:

$$\rho_e = \exp\left(-\frac{1}{\lambda_e}\right) \quad (6.26)$$

In this correlation function, λ_e determines the magnitude of the random error and is inversely proportional to the random error. A high value of λ_e gives a high correlation coefficient, indicating a low random error and a small reduction in correlation due to random error. At low values of λ_e , the correlation coefficient is small, indicating a large random error. The effect of λ_e on the correlation coefficient is illustrated in Figure 6.8.

Since the contamination conditions at the site are likely to be very different after remediation than before remediation, the correlation is reduced between a measurement that is made before remediation of the site and a measurement that is made after remediation of the site. The correlation is not reduced for measurements that are both before remediation or both after remediation. The resulting correlation function to account for remediation is:

$$\rho_r = \exp\left(-\frac{\tau_r}{\lambda_r}\right) \quad (6.27)$$

where:

$$\tau_r = \begin{cases} 0 & \text{if both measurements are before or after remediation} \\ 1 & \text{if one measurement is before remediation and one is after remediation} \end{cases}$$

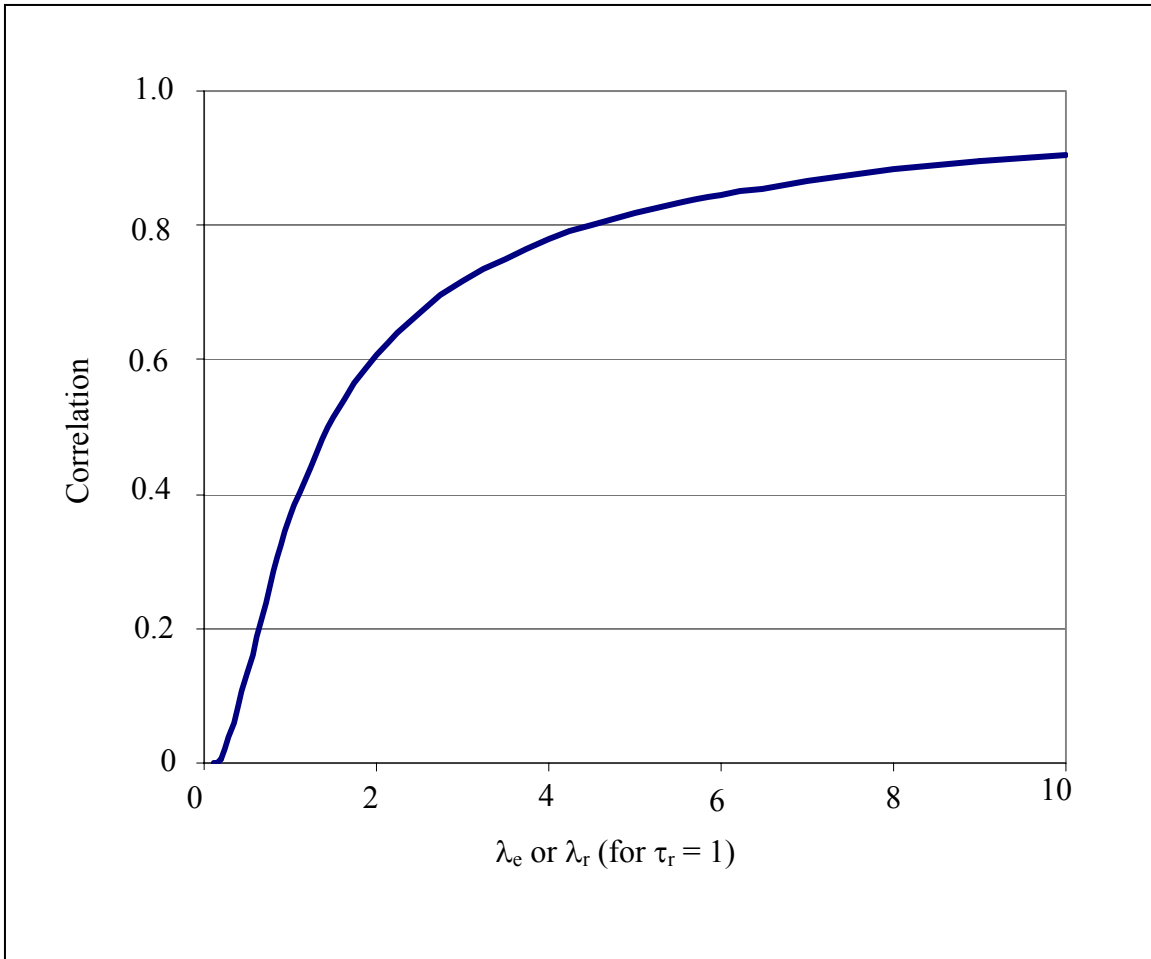


Figure 6.8. Correlation reduction due to random variability or remediation status.

When τ_r is 0, the correlation coefficient is 1.0. When τ_r is 1.0, the correlation coefficient will be between 0 and 1.0, as shown in Figure 6.8. The correlation between two points will therefore not be reduced by ρ_r when both measurements occur before or after remediation, but the correlation may be reduced if one measurement is before remediation and one is after remediation.

6.3.4 Distribution for Natural Logarithm of Measurements

The distribution of the natural logarithm of the benzene concentration measurements is modeled as a potentially non-normal distribution. A fifth-order Hermite Polynomial transform function (Section 3.4.7) was used to allow a non-normal distribution of the natural logarithm of the concentrations. Therefore, four additional model parameters were added: ψ'_2 through ψ'_5 .

6.4 SUMMARY

In this chapter, background information about the French Limited site was given. This site has extensive contamination from a variety of chemicals. Benzene was chosen as the contaminant to be studied for this application, due to the amount of concentration measurements available and its recalcitrant and carcinogenic characteristics. The Horizontal Plane Source model (Galya 1987) for concentration of a contaminant in an aquifer was chosen as the model for the mean benzene concentrations. This model includes steady advection, mixing in three dimensions, and degradation of the contaminant. Since data are available for both before and after remediation of the site, the groundwater model was modified to account for the effects of source reduction and enhanced bioremediation of the contaminant. The covariances of the data from the site were modeled, considering correlations with measurement distance and time and also accounting for random errors in sampling. Also, the distribution of the data was modeled so that the data could have a normal or a non-normal distribution.

Chapter 7. Case Study Application – Calibration of Groundwater Model

7.1 INTRODUCTION

In the previous chapter, the French Limited site was described and models were developed for the mean, variance, correlation, and distribution of the benzene concentrations in the groundwater at the site. In this chapter, these models are calibrated with the concentration measurements from the site using the FOSM Bayesian method for data analysis (including censored measurements and allowing for non-normal data distribution), and the results of the model calibration are discussed.

7.2 MODEL CALIBRATION

This section discusses the data used in the calibration, the model parameters calibrated, and the method of calibration. Data from the French Limited site were calibrated to the models in Chapter 6 for the mean, covariances, and distribution of contaminant concentrations in groundwater. The calibration was performed using a computer program for the FOSM Bayesian method for data analysis, incorporating the censored data and allowing the data to have a non-normal distribution. Benzene was chosen as the contaminant modeled because it was the major contaminant of concern at the site. As one of the most recalcitrant of the contaminants present at the site, benzene is a good indicator of the extent of contamination. Also, more benzene concentration measurements were available than for any other contaminant at the site.

7.2.1 Data from the French Limited Site

Data for the calibration consisted of benzene concentrations measured in samples from monitoring wells at the French Limited site. The well locations are shown in Figure 6.2.

Data were available from 36 wells that were sampled prior to remediation of the site. There were 233 total measurements from these wells, including 68 (29 percent) censored measurements. The sampling dates ranged between 1981 and 1989. These 36 wells were not sampled after remediation.

Active remediation of the groundwater at the site occurred from 1992 to 1995. The remediation of the groundwater consisted of withdrawal of groundwater for treatment, re-injection of treated groundwater, and injection of oxygen and nutrients to promote biodegradation. Concentration measurements taken during remediation were not used in the model calibration due to the disrupted groundwater flow during this time period.

For the post-remediation period, data were available from 28 wells that were sampled quarterly beginning in January 1996. The original post-remediation plan for the groundwater was to let natural attenuation complete the remediation process. However, contaminant concentrations did not decrease as quickly as expected. In April 1998, oxygen and nutrients were once again added to the aquifer to promote increased rates of biodegradation. The model calibration therefore used quarterly monitoring data through February 1998. Of the 281 post-remediation measurements used in the calibration, 196 (70 percent) were censored. A comparison of the total number of measurements and the number of censored measurements in the periods before and after remediation is shown in Figure 7.1.

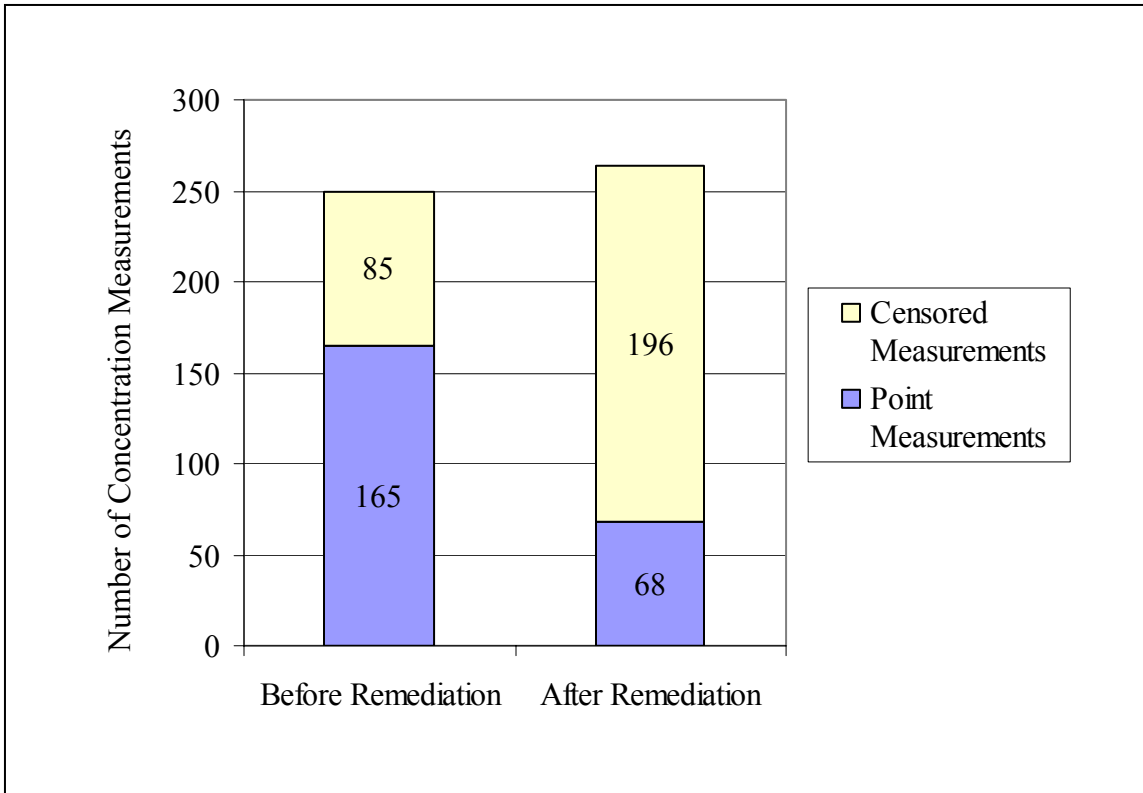


Figure 7.1. Summary of benzene concentration data available from the French Limited site.

The well locations and screened intervals for the wells used in this study are presented in Appendix E. The benzene concentration data used in the calibration are also presented in Appendix E and include the well locations, screened intervals of the wells, the sample dates, and measured concentrations or reported non-detection.

7.2.2 Model Parameters for Calibration

A total of 26 model parameters were calibrated with the natural logarithm of the benzene concentration data for the French Limited site. The model parameters calibrated

with the data include parameters for the HPS model to find the mean values of the natural logarithm of the concentration, and parameters for the variance in the natural logarithm of the concentrations. Parameters for the Hermite Polynomial transform function, which accounts for the non-normality of the data, were also calibrated.

Prior mean and standard deviation values for the mean and covariance model parameters were based on judgment, measurements from the site, and values found by McBrayer (1999). A large value was used for the standard deviation when the prior mean value was considered very uncertain. The prior values for the Hermite Polynomial parameters were set to zero, so that the prior distribution of the data for the natural logarithm of the concentration was a normal distribution. Large prior standard deviations were used for the covariance and Hermite Polynomial parameters because these parameters were considered very uncertain for the data set to be calibrated. The prior values and a brief definition of the calibrated parameters are given in Table 7.1.

For most of these model parameters, it is physically impossible for their value to be below zero. A lognormal distribution was therefore used to describe these model parameters, since the lognormal distribution does not allow negative values for a parameter. All parameters had a lognormal distribution except X_s , Y_s , Z_s , θ , and ϕ_2 through ϕ_5 . For these seven parameters, a normal distribution was used.

The parameters listed in Table 7.2 appear in the HPS model, or are necessary for calculating parameters in the HPS model, but were not calibrated. Initial attempts at calibrating these parameters showed that the model was not sensitive to these parameters and therefore these parameter values could be changed to physically unrealistic values. For example, based on soil properties found in borings, the porosity of the soil at the French Limited site should not be less than 0.15 or greater than 0.35. The aquifer thickness and water table elevation at the site are reasonably well-known from site

exploration, averaging about 34 m and -4.6 m, respectively. During the calibration process, the water table elevation would be moved to an elevation above the ground surface, or the aquifer thickness would become unreasonably small, without significantly influencing the model results. The initial contaminant release time was based on the time that waste materials were initially dumped in the lagoon at the French Limited site, and the remediation start time was based on the date that remediation of the lagoon began. The exact dates that waste disposal and remediation of the lagoon affected the groundwater at the site are unknown; however, the calibration process would adjust these dates to times before waste disposal or remediation activities began, which is not physically possible. The parameters listed in Table 7.2 were therefore kept constant throughout the calibration.

Two model parameters that were calibrated, source elevation (Z_s) and retardation (R), were initially kept constant at their prior values because they would also easily move to physically unrealistic values during the calibration process. However, once a reasonable calibration of the other model parameters was completed, these two model parameters could be added and calibrated.

Table 7.1. Prior values of model parameters used in calibration.

Model Parameter	Prior Mean Value	Prior Standard Deviation	Units	Definition of Parameter
Mean Model Parameters				
X_s	780	100	m	X-Coordinate of source center
Y_s	350	50	m	Y-Coordinate of source center
L_s	29.1	25	m	Source length
W_s	415.7	100	m	Source width
θ	90	10	degrees	Groundwater flow direction
C_o	15.8	100	g/m^3	Concentration at source
a_L	21.3	10	m	Longitudinal dispersivity
a_T	4.3	10	m	Transverse dispersivity
a_V	0.6	10	m	Vertical dispersivity
$T_{1/2}$	1825	10,000	days	Half-life before remediation
v	0.015	0.1	m/day	Seepage velocity
E_r	0.01	100	--	Effect of remediation on source
$T_{1/2r}$	365	1000	days	Half-life after remediation
R	3	3	--	Retardation
Z_S	-11	100	m MSL	Source elevation
Covariance Parameters				
δ	2.56	1000	$\ln(g/m^3)$	Component of variance of $\ln(C)$
λ_e	6.89	1000	--	Random variability in C
λ_t	54.6	1000	days	Temporal scale of fluctuation
λ_x	19.0	1000	m	Longitudinal scale of fluctuation
λ_y	20.7	1000	m	Transverse scale of fluctuation
λ_z	1.47	1000	m	Vertical scale of fluctuation
λ_r	0.22	1000	--	Variability due to remediation status
Data Distribution Parameters				
ψ_2	0	100	--	Second-order Hermite coefficient
ψ_3	0	100	--	Third-order Hermite coefficient
ψ_4	0	100	--	Fourth-order Hermite coefficient
ψ_5	0	100	--	Fifth-order Hermite coefficient

Table 7.2. Constant values used during calibration.

Constant	Value	Units	Definition of Constant
n	0.25	--	Porosity
b	34	m	Aquifer thickness
Z _{elev}	-4.6	m	Water table elevation
T ₀	6/30/1965	date	Initial contaminant release time
T _r	1/1/1992	date	Remediation start time

7.3 CALIBRATION PROCESS

The natural logarithms of the benzene concentrations from the French Limited site were calibrated with the natural logarithm of the horizontal plane source model (Equation 6.12) using a computer program written in Visual C++. The prior model parameters were first calibrated with the 233 measurements taken at the site prior to remediation. This smaller data set, rather than the entire data set of 514 measurements, was used initially to determine which model parameters should be kept constant and not calibrated. As discussed in Section 7.2.2, five model parameters (shown in Table 7.2) were kept constant during the calibration since the model was not sensitive to their values. Two additional model parameters (source elevation and retardation) were kept constant until the other model parameters were calibrated.

After determining which model parameters to calibrate, an iterative process was used, following the steps outlined in Section 3.4. Each iteration consists of testing different sets of model parameters to find the maximum likelihood, then calculating the second derivatives of the natural logarithm of the likelihood function. For the 233 measurements before remediation, each iteration took approximately 20 minutes to run on a Pentium Centrino personal computer. Seventeen iterations were performed to

determine a set of model parameters that came close to maximizing the likelihood function.

This set of model parameters was then used as the starting point for calibrating the entire set of 514 measurements, both before and after remediation of the site. The same iterative approach was used, with each iteration taking approximately 35 minutes to perform. Thirty iterations were performed automatically with the computer program, then the model parameter values were adjusted manually to try to find the maximum likelihood. None of the model parameter sets truly maximized the likelihood, as indicated by a negative definite matrix of the second derivative of the natural logarithm of the likelihood function (Section 3.4.5). This was probably because of discontinuities in the likelihood function in the vicinity of the maximum. Numerical integration was therefore used to find the first and second moments of the natural logarithm of the likelihood function, $\bar{\mu}_G$ and $[C_G]$ (Equations 3.18 and 3.19). The numerical integration was performed using a Monte Carlo simulation, with 5000 simulations of model parameter sets. This numerical integration took approximately one day to calculate.

7.4 CALIBRATION RESULTS

The results of the calibration of the benzene concentrations with the model for the mean and covariances of the measurements are presented in this section. The updated means and standard deviations of the model parameters found with the calibration are given, followed by discussions of the results. The model parameters used for calculating the mean benzene concentrations are compared to physical characteristics of the site and published values for the parameters. The model parameters for the covariances of the benzene concentrations are then examined to determine if they are physically reasonable, and the model parameters that describe the non-normal distribution of the measurements

are discussed. Finally, a comparison is made of the model-predicted and measured concentrations.

7.4.1 Updated Means and Standard Deviations of Model Parameters

The updated mean and standard deviation for the model parameters are shown in Table 7.3. For all of the parameters, the updated standard deviation is very small in comparison to the updated mean. This is because the $-G''$ values are large compared to the inverse of the prior covariance matrix, C_{ϕ}^{-1} . The updated standard deviations are therefore essentially the inverse of the $-G''$ matrix and the prior covariances contribute very little (Section 3.4.5). The updated mean values are also essentially the values for the parameters that maximize the natural logarithm of the likelihood function.

Table 7.3. Updated values of model parameters used in calibration.

Model Parameter	Updated Mean Value	Updated Standard Deviation	Units	Definition of Parameter
Mean Model Parameters				
X_s	755.8	32.1	m	X-Coordinate of source center
Y_s	341.9	19.4	m	Y-Coordinate of source center
L_s	79.1	25.0	m	Source length
W_s	401.9	79.8	m	Source width
θ	79.1	8.5	degrees	Groundwater flow direction
C_o	4.45	0.66	g/m^3	Concentration at source
a_L	17.02	4.12	m	Longitudinal dispersivity
a_T	12.83	4.16	m	Transverse dispersivity
a_V	0.26	0.04	m	Vertical dispersivity
$T_{1/2}$	2.2×10^9	1.8×10^{10}	days	Half-life before remediation
v	0.03	0.007	m/day	Seepage velocity
E_r	1.7×10^{-7}	6.16×10^{-7}	--	Effect of remediation on source
$T_{1/2r}$	544.3	145.8	days	Half-life after remediation
R	4.09	0.56	--	Retardation
Z_S	-7.12	0.43	m MSL	Source elevation
Covariance Parameters				
δ	30.1	4.98	$\ln(g/m^3)$	Component of variance of $\ln(C)$
λ_e	538.0	263.8	--	Random variability in C
λ_t	2528	827.2	days	Temporal scale of fluctuation
λ_x	0.006	0.004	m	Longitudinal scale of fluctuation
λ_y	0.008	0.004	m	Transverse scale of fluctuation
λ_z	0.10	0.029	m	Vertical scale of fluctuation
λ_r	8.3×10^{-5}	1.3×10^{-4}	--	Variability due to remediation status
Data Distribution Parameters				
ψ_2	0.082	0.003	--	Second-order Hermite coefficient
ψ_3	1.10	0.07	--	Third-order Hermite coefficient
ψ_4	-0.19	0.01	--	Fourth-order Hermite coefficient
ψ_5	-0.70	0.06	--	Fifth-order Hermite coefficient

7.4.2 Mean Model Parameters

The mean model parameters represent physical characteristics of the groundwater flow and contamination at the French Limited site. The model calibration gave reasonable results for these parameters, since the updated mean values for the parameters are within the physical limits for the characteristics they describe.

The parameters that describe the contamination source (X_s , Y_s , L_s , and W_s) place the updated horizontal plane source for the model roughly over the footprint of the waste lagoon, as shown in Figure 7.2. Although the plane source does not precisely represent the leaching of contaminants from the lagoon, the plane source is expected to be in the area of the lagoon since the highest measured benzene concentrations were measured near the lagoon. The updated mean for the concentration of benzene released at the source prior to remediation is 4.41 g/m^3 , which is well below the water solubility of 1750 g/m^3 .

The groundwater flow is described by the seepage velocity and the flow direction. The updated mean for seepage velocity is 0.03 m/day , which is on the same order of magnitude as the prior value of 0.015 m/day (Applied Hydrology Associates 1989). The general direction of groundwater flow at the site, based on groundwater contour maps, is due south. The updated mean for the flow direction is 79.1 degrees or 10.9 degrees east of due south. The relationship of this flow direction to the plane source is shown in Figure 7.2.

The updated mean dispersivity values are within recognized ranges. The updated longitudinal dispersivity, a_L , of 16.54 m is within the range of 1 to 100 m or more reported by Charbeneau (2000). The U.S. EPA (1986) suggests that the transverse dispersivity be estimated at one-third of a_L and the vertical dispersivity be estimated at

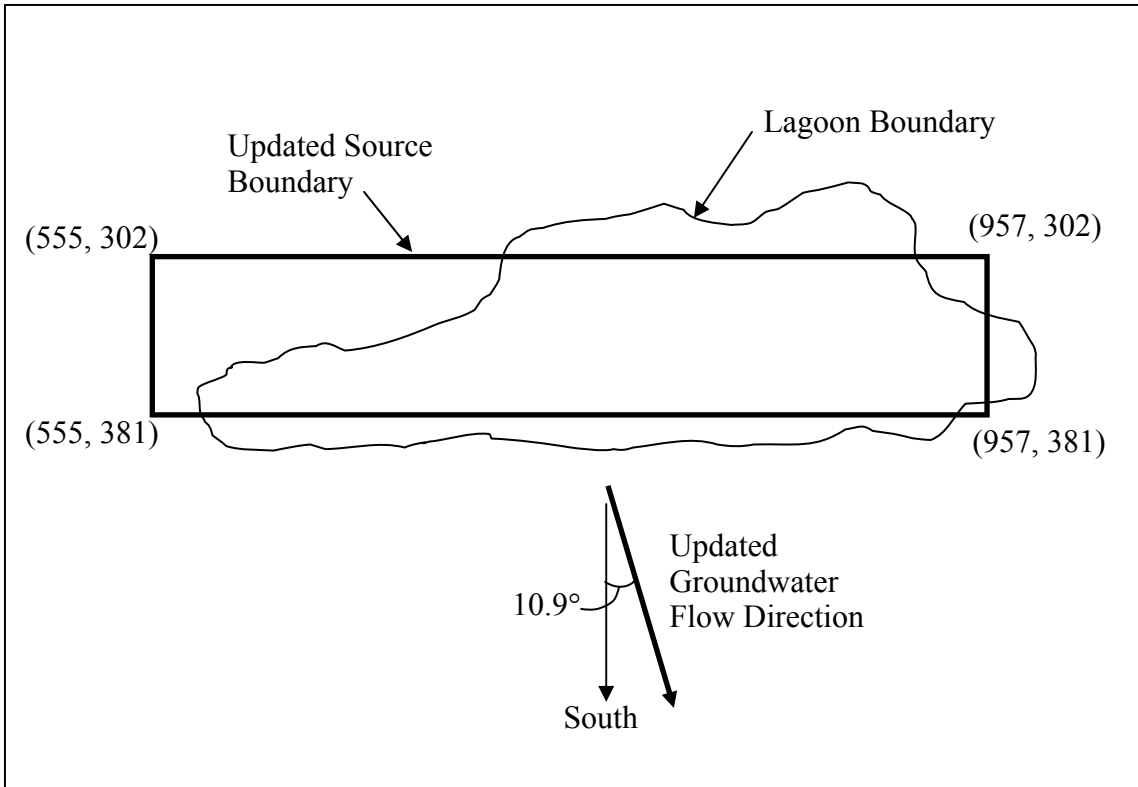


Figure 7.2. Updated source size, source location, and groundwater flow direction for the French Limited site.

0.0125 to 0.1 of a_L . The updated transverse dispersivity is about twice this estimate at 0.74 of a_L , while the updated vertical dispersivity of 0.015 of a_L is within the recommended range.

The updated mean of the half-life of benzene before remediation is 2.71×10^8 days, which is much larger than published values for benzene in soil of 10 to 730 days (Howard et al. 1991). This updated half-life indicates that the model is calibrated with no degradation of benzene occurring before remediation. This result is not surprising, due to the high concentrations of benzene and the low levels of dissolved oxygen measured at the site before remediation. Field studies have shown that at low levels of dissolved

oxygen, benzene degradation is slowest in the areas of highest contamination (i.e. Vroblesky and Chapelle 1994) and that benzene degrades slowly in anaerobic conditions (i.e. Kao et al. 1997).

Remediation efforts at the French Limited site included bioremediation of the lagoon contents, pump-and-treat of groundwater, and injection of oxygen and nutrients into the groundwater. The purpose of these efforts was to eliminate the sources of contamination and increase the degradation rate of contaminants in the groundwater. The updated mean value for the effect of remediation on the source was 1.04×10^{-7} , which means that the release rate of benzene decreased from 86.5 g/day to 9.0×10^{-6} g/day over the source area. This indicates that the source was effectively removed by the remediation. However, source removal was not complete at the actual French Limited site, since post-remediation monitoring revealed increasing benzene concentrations in some wells. The horizontal plane source used in the model is a large source area, and in reality there were probably scattered pockets of benzene contaminant sources throughout the site.

The updated mean of the half-life of benzene after remediation is 527 days, which is within the range of 10 to 730 days reported by Howard et al. (1991). The calibrated model therefore indicates that the degradation rate of benzene was increased through the remediation efforts.

7.4.3 Covariance Model Parameters

The updated mean value for δ , the constant component of the variance in the natural logarithm of concentration, is $30.1 \ln(\text{g}/\text{m}^3)$. The updated mean value for λ_z , used for calculating the vertical correlation coefficient, is 0.10. These two parameters are used to calculate the variance in the natural logarithm of concentration (Equation 6.21), which

considers the averaging that occurs over the screened interval of a well. For the largest screened length of a well at the French Limited site, 16.76 m, the variance in the natural logarithm of the concentration, $\text{Var}(Y_i)$, is $0.032 \ln(\text{g}/\text{m}^3)$. This results in standard deviation in the benzene concentration of approximately $1.0 \text{ g}/\text{m}^3$. For the smallest screened length of a well at the French Limited site, 1.52 m, the $\text{Var}(Y_i)$, is $3.67 \ln(\text{g}/\text{m}^3)$. This results in standard deviation in the benzene concentration of approximately $6.3 \text{ g}/\text{m}^3$. As the screened length of the well decreases, there is less averaging of the concentration over the length of the well, and therefore the variance in the measured concentration increases.

The updated mean value of λ_e , which represents the random error in measurements of concentration, is large at 483. This large value results in a high correlation coefficient of 0.998, which means that the random error is small and the total correlation between two data points will be reduced very little by the random error.

The correlation coefficient for time is shown in Figure 7.3. The correlation for measurements at the same location taken 30 days apart is 0.96. At 1 year and 2 year periods between measurements, the correlations are 0.63 and 0.39, respectively. These high correlations with time indicate that the difference between measured and model-calculated concentrations is consistent over time at a particular location. This could be indicative of the heterogeneities at the site. The HPS model assumes uniform conditions throughout the aquifer. However, the soil conditions in the alluvial channel that underlies the site are heterogeneous, and the groundwater may preferentially flow through channels with higher hydraulic conductivity. In such channels, the measured benzene concentrations are likely to be consistently greater than the model-predicted concentrations, while in areas of lower hydraulic conductivity, the measured concentrations are likely to be consistently less than the model-predicted concentrations.

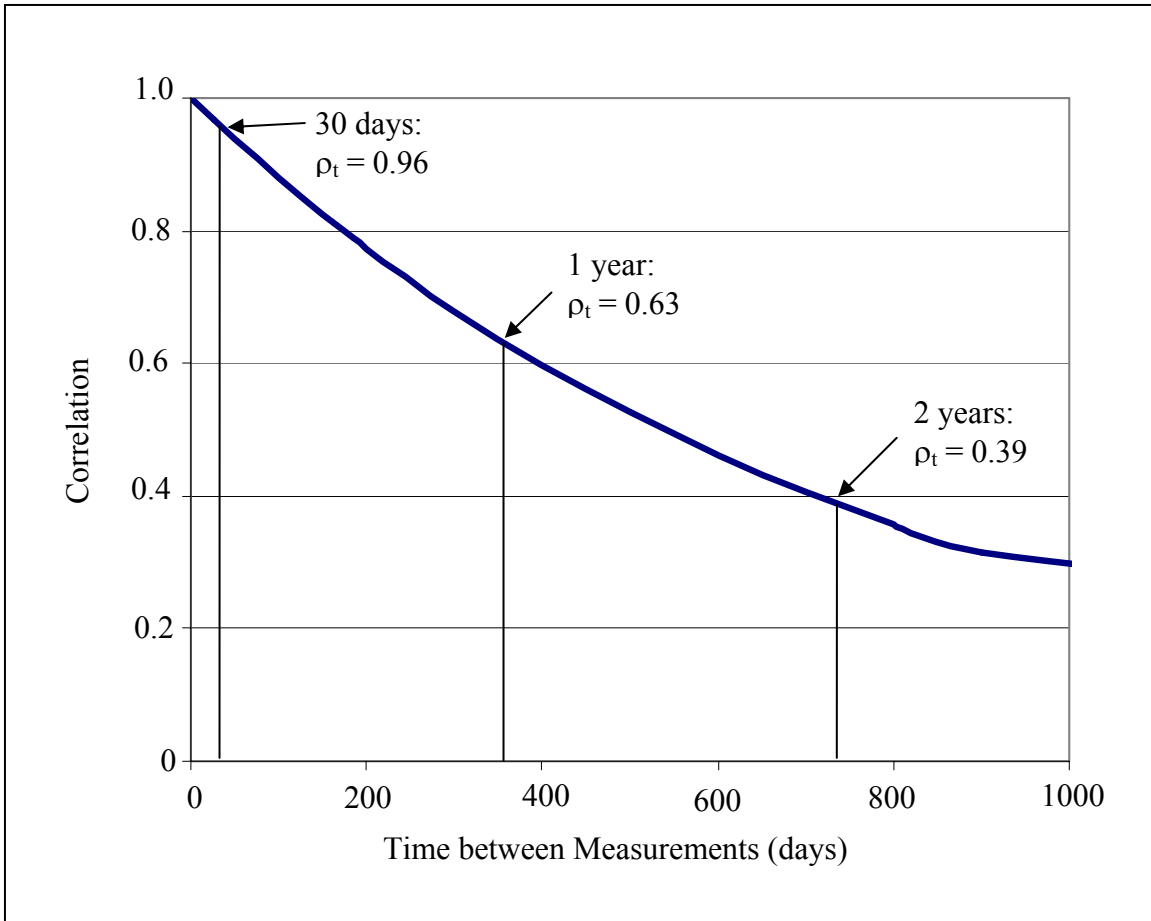


Figure 7.3. Calibrated correlation with time for French Limited site.

Model-predicted concentrations for two wells located within the scale of fluctuation are either consistently over or consistently under the measured concentrations. Therefore, large scales of fluctuation in these dimensions would mean that model-predicted concentrations at wells located far apart from one another would either be above or below the measured concentrations at multiple sampling times. This generally indicates a systematic error in the model, with predicted concentrations throughout the site either too high or too low. The updated scales of fluctuation for the French Limited site in the longitudinal and transverse dimensions, λ_x and λ_y , are both very small at 0.005

m. These small values mean that there was no correlation between measurements in these dimensions, which indicates that the systematic error in the model is low.

The small updated mean of λ_r , the parameter that determines the correlation between points before and after remediation, results in a correlation coefficient of zero. Measurements taken before remediation are therefore not correlated at all with measurements taken after remediation.

The different correlation coefficients are all multiplied to find the total correlation between measurements (Equation 6.23). Since the longitudinal and transverse correlations are zero except for wells located at the same x- and y-coordinates, correlations between measurements only occur for measurements taken at the same well at different times, or for measurements that are taken at two different wells with the same x- and y-coordinates but different vertically screened intervals. At a particular well, ρ_x , ρ_y , ρ_z , and ρ_r will all be equal to 1.0. Since ρ_e is equal to 0.998, the total correlation is dominated by ρ_t .

7.4.4 Data Distribution Parameters

The Hermite Polynomial parameters, ψ_2 through ψ_5 , determine the shape of the data distribution. The natural logarithm of the concentration measurements used for the model calibration are non-normally distributed, as shown in Figure 7.4. The x-axis of this plot is the conditioned means of the measurements normalized with the model-predicted mean and variance. The y-axis is the standard normal inverse of the cumulative density function (CDF). A normal distribution is a straight line on this plot, and for other distributions, the non-linearity of the inverse of the CDF indicates the degree of non-normality of the distribution.

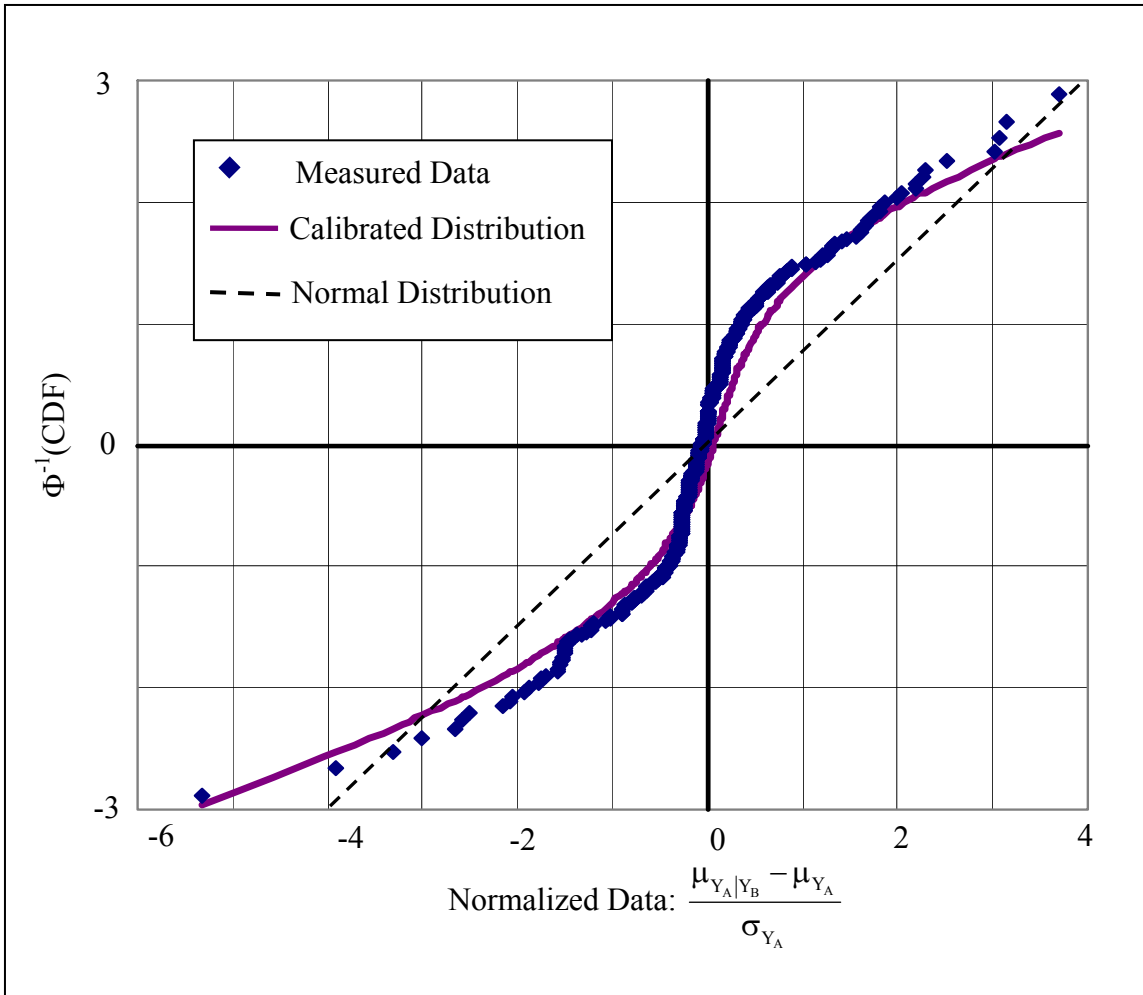


Figure 7.4. Measured data distribution compared to calibrated distribution.

The curve that is calibrated with the measurements using the Hermite Polynomial transform function fits the distribution of the measurements very well. This calibrated distribution is able to follow the shape of the measurement distribution near the mean value and also at the tails of the distribution. A normal distribution, which is a straight line on this graph, is also shown for reference. For this set of measurements, a normal distribution would have fit the measurements only at the mean and the upper tail of the

distribution (greater than three standard deviations away from the mean). The normal distribution would have neglected the actual distribution of the data at all other areas of the distribution. The contribution of the censored measurements, which are in the lower tail of the distribution, would therefore have been neglected and the updated model parameters would less accurately represent the measured data from the site.

7.4.5 Correlations between Model Parameters

The correlations between model parameters determine if changing one model parameter has a significant effect on another model parameter. The correlations between model parameters are shown in Figure 7.5. The most significant correlation, 0.90, was between the x-coordinate of the center of the plane source (X_s) and the width of the plane source (W_s). This means that if X_s is increased, the width of the source must also be increased to compensate for the effect on groundwater concentrations. The full width of the plane source that extends to the east at the site is therefore necessary for the model to explain the measured groundwater concentrations.

Another significant correlation, -0.74, was between the transverse dispersivity (α_T) and the vertical dispersivity (α_V). Therefore, if the transverse dispersivity increases, the vertical dispersivity must decrease for the model to find the same concentrations. Because the variance in the natural logarithm of the concentrations depends on both the constant component of variation (δ) and the correlation in the vertical direction (λ_z), as shown in Equation 6.21, these two parameters have a significant negative correlation, -0.75. This negative correlation allows the variance to explain variability in groundwater concentrations if one of the parameters is decreased, since the other parameter will then increase.

	X _s	Y _s	L _s	W _s	θ	C _o	a _L	a _T	a _V	T _{1/2}	v	E _r	T _{1/2r}
X _s	1												
Y _s	-0.21	1											
L _s	-0.23	-0.29	1										
W _s	0.90	-0.30	-0.16	1									
θ	-0.02	0.69	-0.46	-0.25	1								
C _o	0.24	-0.15	-0.34	0.06	0.16	1							
a _L	-0.10	-0.57	0.09	-0.07	-0.33	0.16	1						
a _T	0.07	-0.14	-0.18	-0.06	0.13	0.52	0.03	1					
a _V	-0.03	0.08	0.08	0.01	-0.05	-0.34	0.23	-0.74	1				
T _{1/2}	0.07	0.38	-0.23	0.04	0.27	0.01	-0.17	-0.04	-0.03	1			
v	-0.10	-0.37	-0.04	-0.01	-0.31	-0.34	0.15	-0.03	-0.18	0.05	1		
E _r	-0.12	-0.07	-0.24	0.01	-0.03	-0.19	0.03	-0.06	-0.08	0.40	0.49	1	
T _{1/2r}	-0.23	0.15	-0.23	-0.42	0.34	0.21	0.15	0.37	-0.09	0.07	0.06	-0.06	1
R	-0.05	-0.14	0.27	0.17	-0.46	-0.29	-0.10	-0.03	-0.18	-0.06	0.35	-0.05	-0.10
Z _s	0.02	0.20	0.18	0.13	-0.03	-0.35	-0.19	-0.29	0.15	0.02	-0.24	-0.18	-0.33
δ	0.53	0.20	-0.07	0.49	0.16	-0.16	-0.17	-0.19	0.31	-0.01	-0.27	-0.31	-0.06
λ _e	0.33	0.24	-0.13	0.28	0.27	-0.25	-0.17	-0.35	0.30	0.16	-0.03	0.15	-0.22
λ _t	-0.13	0.41	0.06	-0.09	0.03	-0.36	-0.08	-0.41	0.45	0.22	-0.20	-0.15	-0.03
λ _x	0.25	-0.05	-0.34	0.30	0.09	0.01	-0.05	-0.01	-0.13	0.39	0.40	0.53	-0.10
λ _y	0.04	-0.08	0.16	0.05	-0.23	-0.01	-0.03	0.00	0.19	-0.07	-0.28	-0.26	0.11
λ _z	-0.55	0.20	0.05	-0.56	0.07	0.01	-0.08	0.02	-0.14	0.01	0.01	0.14	0.05
λ _r	-0.11	0.12	-0.07	-0.18	0.22	-0.05	-0.08	0.05	-0.04	0.08	0.27	0.20	0.10
ψ ₂	0.08	-0.11	-0.17	0.08	-0.08	0.25	-0.09	0.22	-0.41	-0.07	0.26	-0.05	0.06
ψ ₃	0.34	0.16	-0.07	0.27	0.14	0.11	-0.04	0.08	0.11	-0.07	-0.35	-0.31	0.17
ψ ₄	-0.02	-0.12	-0.16	-0.16	0.11	0.27	0.33	0.02	0.22	-0.15	-0.14	-0.19	0.37
ψ ₅	-0.17	-0.25	-0.09	-0.25	0.13	0.22	0.29	0.03	0.08	-0.23	0.04	0.02	0.23

	R	Z _s	δ	λ _e	λ _t	λ _x	λ _y	λ _z	λ _r	ψ ₂	ψ ₃	ψ ₄	ψ ₅
R	1												
Z _s	0.21	1											
δ	-0.03	0.45	1										
λ _e	-0.18	0.27	0.37	1									
λ _t	0.13	0.39	0.34	0.06	1								
λ _x	-0.03	-0.08	-0.09	0.35	-0.12	1							
λ _y	0.17	0.11	0.11	-0.44	0.25	-0.46	1						
λ _z	-0.07	-0.20	-0.75	-0.09	0.06	0.02	-0.14	1					
λ _r	-0.06	-0.21	-0.28	0.26	-0.10	0.29	-0.34	0.37	1				
ψ ₂	0.22	-0.20	-0.07	0.02	-0.12	0.29	-0.31	0.03	-0.07	1			
ψ ₃	0.14	0.14	0.41	0.33	0.02	-0.20	0.17	-0.18	0.01	-0.09	1		
ψ ₄	-0.38	-0.28	0.00	-0.02	-0.15	-0.23	0.05	0.08	-0.13	-0.08	0.19	1	
ψ ₅	-0.34	-0.20	-0.20	-0.17	-0.37	-0.08	-0.06	0.02	0.07	-0.15	-0.24	0.39	1

Figure 7.5. Correlations between model parameters for the means and covariances of the benzene concentrations at the French Limited site.

7.4.6 Comparison of Model-Predicted and Measured Concentrations

Comparisons of model-predicted and measured benzene concentrations are shown in Figure 7.6 for a well sampled before remediation, ERT-21, and in Figure 7.7 for a well sampled after remediation, INT-101. Model-predicted and measured benzene concentrations for all of the wells at the French Limited site are shown in Appendix F. Two types of model-predicted concentrations were calculated. In the first type of model prediction, the updated model parameters are used in Equation 6.12, without conditioning on previous measurements, to calculate the concentrations at the well location for the sample times. In the second type of model prediction, the updated model parameters are used to calculate the concentrations along with the measurements from all wells collected before the sample time, as shown in Equation 4.18. This conditioning process accounts for censored measurements and for correlations between measurements.

Notice in both Figures 7.6 and 7.7 that the conditioned concentration for the first sampling date is equal to the unconditioned concentration. This is because there are no previous measurements on which to condition the first measurement. After this first measurement, the conditioned concentrations follow the measured concentrations closely due to the high correlation between measurements with time and the short time period between measurements. These conditioned concentrations indicate that the calibration was successful in fitting the measured concentrations to the model. These results also indicate that considering all collected measurements through the conditioning process provides better concentration predictions than simply using the determined values for model parameters.

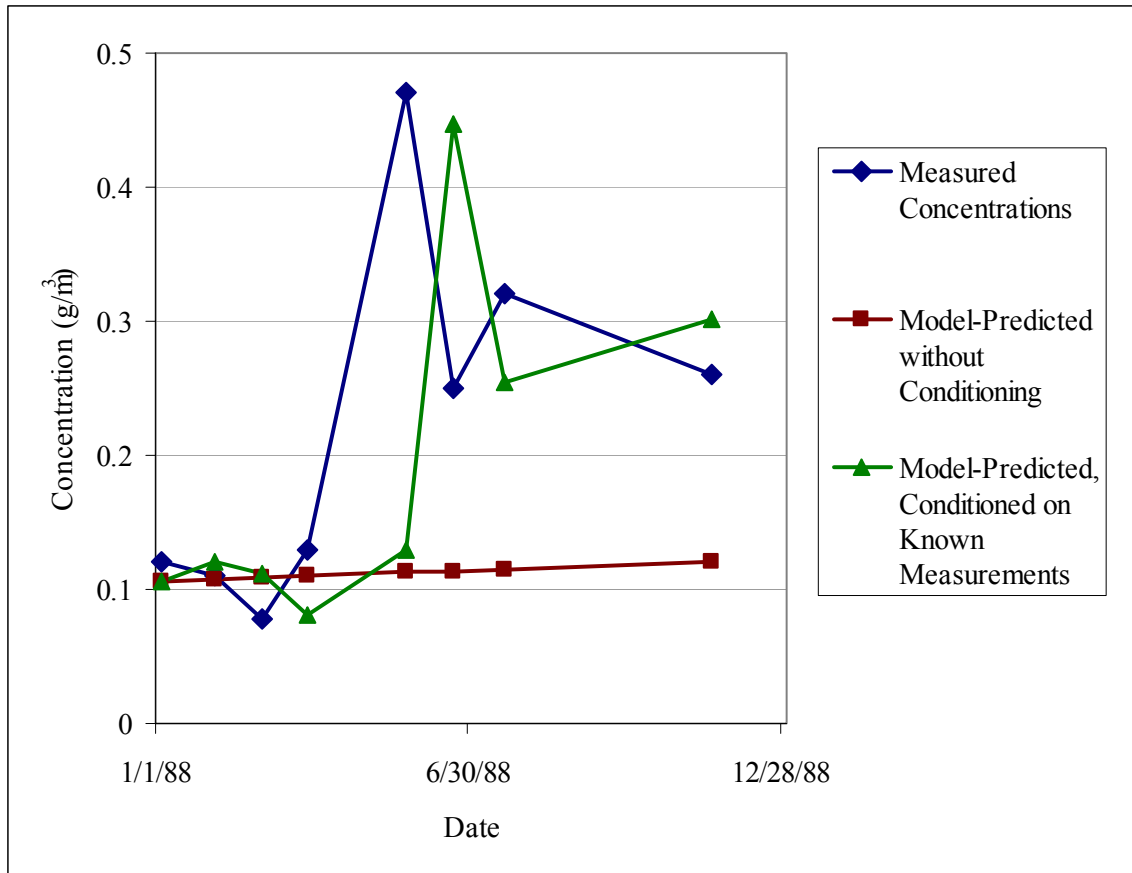


Figure 7.6. Comparison of measured and model-predicted concentrations for well ERT-21, sampled prior to remediation.

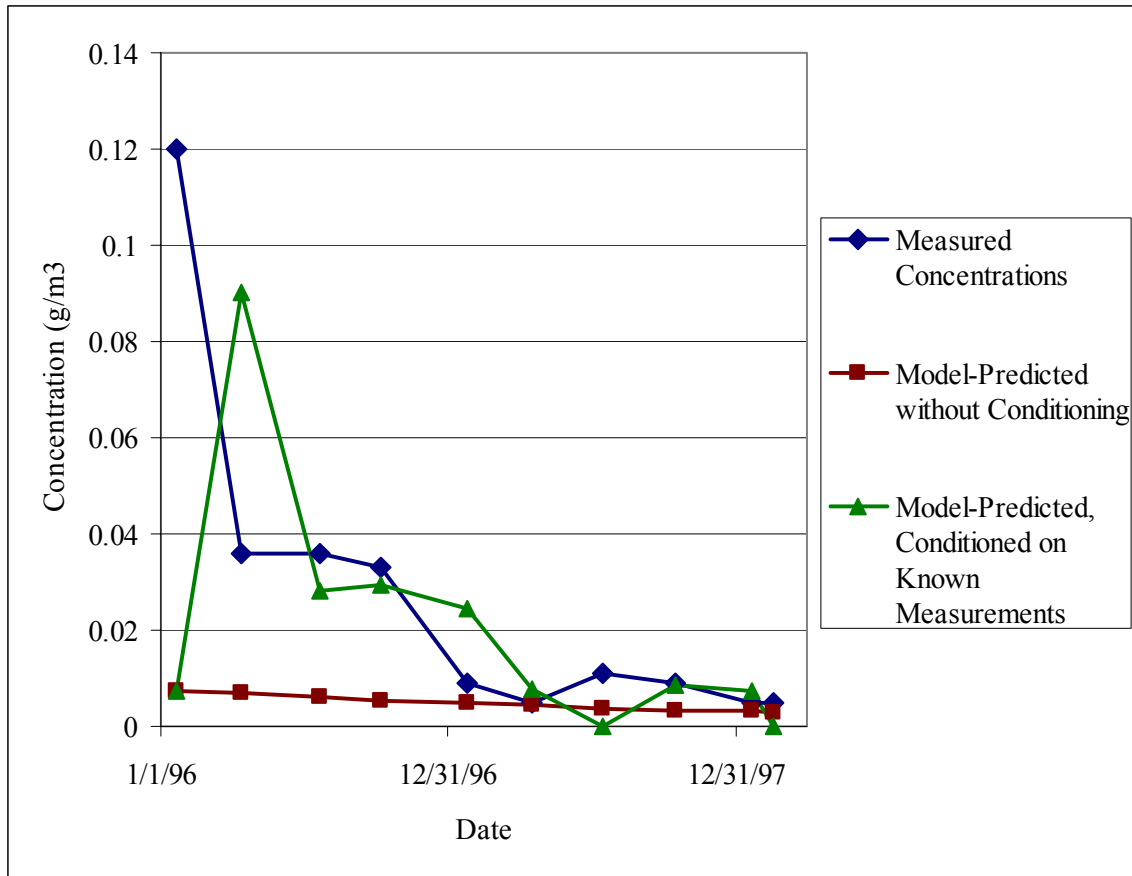


Figure 7.7. Comparison of measured and model-predicted concentrations for well INT-101, sampled after remediation.

7.5 CONCENTRATION PREDICTIONS

Using the calibrated model results to predict future concentrations is useful in making decisions regarding the remediation and monitoring of the site. The remedial objective for the groundwater at the French Limited site was to “reduce health hazards from the impact of waste materials in the upper alluvial aquifer groundwater” (Southwestern Environmental Consulting, Inc. 1996). For benzene, a known carcinogen, the criterion chosen for this objective was the 1.0×10^{-6} excess cancer risk Human Health Criteria. This EPA criterion is the extra risk of developing cancer due to exposure to a toxic substance incurred over the lifetime of an individual (U.S. EPA 2003b). Therefore, the benzene concentration that meets this criterion will cause less than one in a million extra cases of cancer in a population. The site closure plan stated that, “For all areas inside the site property line, groundwater recovery and treatment will be continued until modeling shows that natural attenuation will achieve these Human Health Criteria at the site property line in 10 years or less active remediation will continue until this criterion can be achieved at the site boundary through natural attenuation in 10 years or less and maintained below criteria thereafter in those areas outside the site boundary” (Southwestern Environmental Consulting, Inc. 1996). In this plan, the site boundary refers to the actual property line of the French Limited site.

At the time of site closure in 1996, groundwater modeling indicated that natural attenuation would indeed result in these standards being met in 10 years. Active remediation was therefore ended at this time. However, during the first three years of monitoring, benzene concentrations in some wells, such as INT-134 and S1-131, remained at elevated levels or perhaps even increased over time. Therefore, active remediation began again in April 1998.

For the model calibrated in this dissertation, predictions of future groundwater concentrations may be made. These predictions include not only the expected concentration, but also the uncertainty in that concentration, based on the uncertainty in the model parameters used to predict the concentration and the modeled variance of the concentration. Predictions of concentrations for two wells located at the French Limited property line, INT-26 and S1-108A, were made for 10 years after site closure, assuming no further active remediation occurred after site closure. The calculated benzene concentration to meet the 1.0×10^{-6} excess cancer risk criterion was 0.005 g/m^3 . This includes the risk from ingestion and dermal contact with benzene-contaminated water, and also inhalation of vapors produced during bathing and showering.

The probability distributions for the predicted benzene concentrations in wells INT-26 and S1-108A are shown in Figures 7.8 and 7.9, respectively. For well INT-26, the median concentration predicted for 10 years post-closure was 0.001 g/m^3 . While this median concentration is below the criterion concentration, the value is uncertain, and therefore the probability that the benzene concentration will be greater than 0.005 g/m^3 was calculated. The probability that the benzene concentration in INT-26 will be greater than 0.005 g/m^3 in 10 years is 22 percent. For well S1-108A, the median concentration predicted for 10 years post-closure was 0.0006 g/m^3 . Although this median concentration is well below the criterion concentration, the probability that the concentration at this well will be greater than 0.005 g/m^3 is 17 percent.

The predicted median benzene concentrations in wells INT-26 and S1-108A are below the criterion concentration, which would seem to indicate that no further active remediation is required and natural attenuation will result in acceptable concentrations at the site boundary in 10 years. However, when the uncertainty in these predicted concentrations is considered, the results of natural attenuation are less clear. There is a

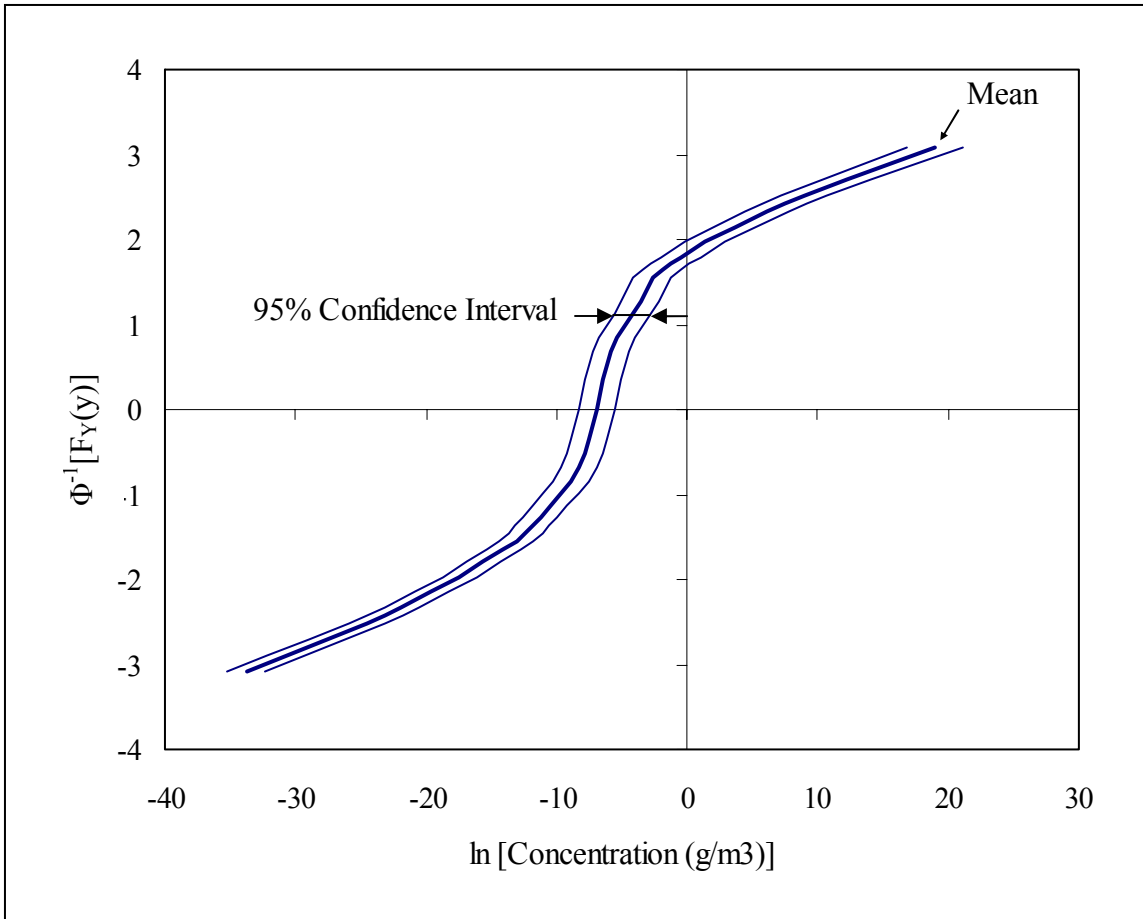


Figure 7.8. Probability distribution of predicted benzene concentration for well INT-26.

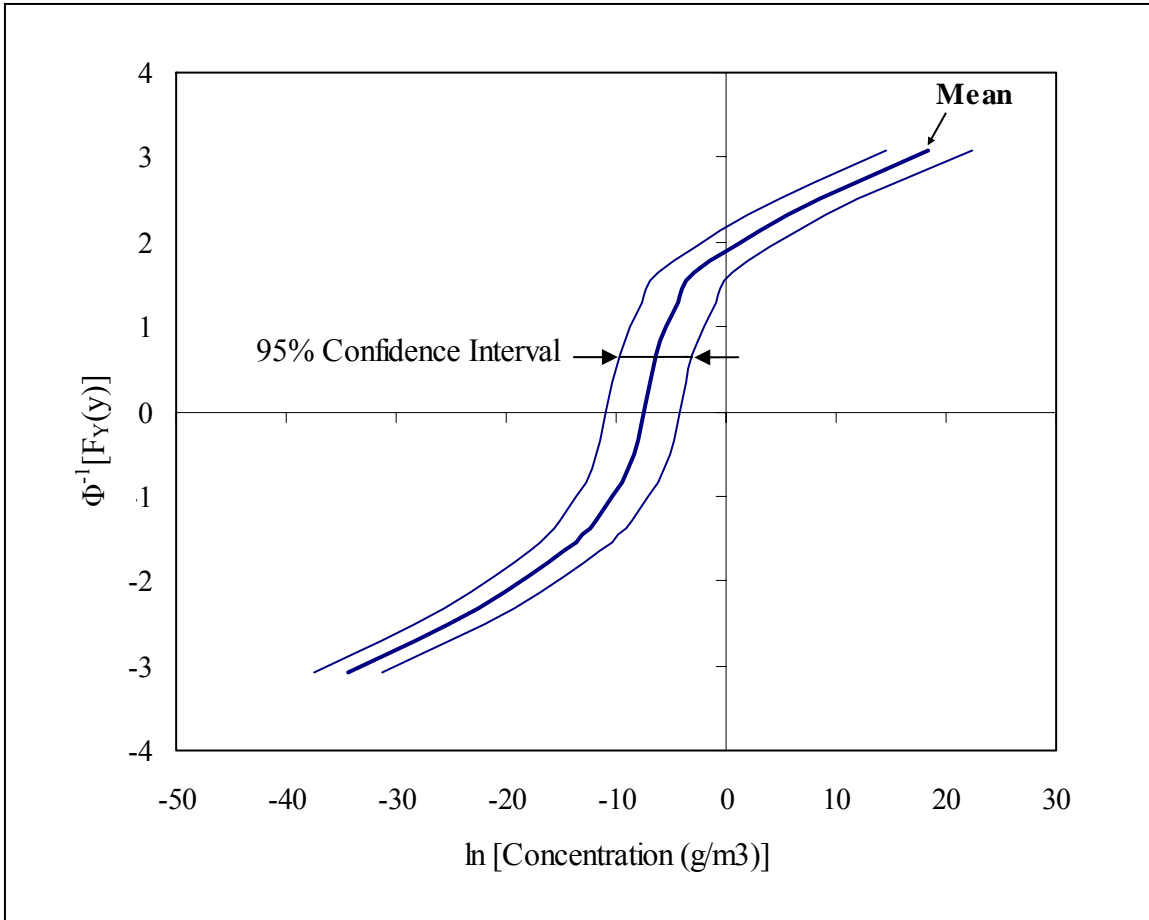


Figure 7.9. Probability distribution of predicted benzene concentration for well S1-108A.

high probability that the concentrations in these wells will be greater than the criterion concentration after 10 years of natural attenuation. If the criterion concentration is not met, then more remediation will be required. The high probabilities of not meeting the criterion should be considered along with the potential cost of future remediation of the site, which could be millions of dollars. The expected cost of future remediation is calculated by multiplying the probability that remediation will be needed (such as 22 percent for well INT-26) by the cost of remediation. This expected cost of future remediation can then be compared with the cost of obtaining more information about the contamination at the site, which could help reduce the uncertainty in the concentration predictions. Considering the probability that the concentrations may not meet the established criteria therefore allows more informed decisions to be made regarding the further remediation of the site.

7.6 SUMMARY

The set of benzene measurements that was calibrated for the French Limited site contained a significant amount of censored data in the form of concentrations that were reported as below the detection limit. The site was therefore a good application of the method developed for analyzing censored data. The results from the calibration were reasonable for the physical characteristics of the site. The calibration was also successful in fitting the non-normal distribution of the measurements. The FOSM Bayesian method was proven a useful method in considering all the complexities of the site: concentrations measured above and below the detection limit, the effects of remediation on the concentrations, measurements at many different times and locations, and correlations between concentrations that represent the heterogeneities at the site and the random errors in measurements.

Chapter 8. Conclusions

The objective of this research was to develop a method for including censored data in data analysis and test program design. An extension was developed for the FOSM Bayesian method that allows the inclusion of censored data that may be correlated and that may have a non-normal distribution. The method developed for data analysis was applied to a real contaminated site to calibrate benzene concentrations in the groundwater to a model describing the mean, standard deviation, correlation, and distribution of the concentration measurements. In this chapter, the research is summarized and the major conclusions reached from the work are presented, along with recommendations for future work.

8.1 METHOD DEVELOPED FOR ANALYZING CENSORED DATA

This research extended the FOSM Bayesian method (Gilbert 1999) to incorporate censored data into data analysis and test program design. The method uses a Hermite Polynomial transform function so that the data may have a normal distribution or a non-normal distribution. The extension to the FOSM Bayesian method was derived, then it was tested with simple models to verify the method and determine the most effective calculation technique for implementing the method. In this section, the conclusions about the method and recommendations for future development of the method are presented.

8.1.1 Conclusions

The FOSM Bayesian method finds updated model parameters based on data that have been collected or are expected with a test program. The conditional mean and

variance for a data point are required in calculating the likelihood of observing the data given a set of model parameters. For censored data, the moments of the censored region are used in calculating the conditional moments. When a data point has a non-normal distribution, the moments of the censored region are approximated with the moments of the equivalent censored region of a normal distribution. This approximation was determined to be reasonable for different non-normal distributions, including a highly skewed lognormal distribution and a uniform distribution.

A simple model for normally-distributed, statistically independent data with varying correlations between data points and varying amounts of censored data was used to determine the effects of censored data and to verify the method for test program design. The model consisted of three parameters, one each for the mean, standard deviation, and correlation of the data points. Increasing the size of the data set resulted in a decrease in the expected variance of the mean model parameter. However, the size of the data set was less important as the amount of censored data increased. This is because censored data provides less information about the model parameters than non-censored data.

The expected mean values of the model parameters for the simple model were very close to the true values of the model parameters for all levels of censored data. Therefore, no bias resulted from including censored data in the method. The expected standard deviations of the model parameters showed that as the level of censoring increases and as the correlation between data points increases, less information is provided by the data and the amount learned about the model parameters decreases. The mean and the standard deviation model parameters had a negative correlation at high levels of censored data, but had no correlation when there was no censored data. The

standard deviation and correlation model parameters were positively correlated at high levels of correlation between data points.

Several different methods were tried for implementing the method with expected, censored data for test program design. The most accurate methods were also the most computationally-intensive methods. A complete analytical approximation is the least computationally-intensive method, but the accuracy of the method was only acceptable for non-censored, statistically independent data with a normal distribution. For normally-distributed data, a Monte Carlo simulation using a Taylor series approximation for the likelihood function worked well. However, for non-normally-distributed data, no approximate methods worked and numerical integration was required.

When the method was used for data analysis with censored data, the Taylor series approximation for the likelihood function allowed the calibration of the model parameters with the data to proceed close to the maximum likelihood. But the model parameters calibrated with this method did not truly maximize the likelihood, as indicated by a negative definite matrix of the second derivative of the likelihood function. This was due to discontinuities in the likelihood function near the maximum, and numerical integration was therefore required to calculate the moments of the likelihood function.

8.1.2 Recommendations for Future Work

Future development of the FOSM Bayesian method for use with censored, non-normally-distributed data should focus on addressing the discontinuities in the likelihood function near the maximum so that numerical integration is not required. Approximate methods for test program design should also be developed so that Monte Carlo simulations are not required. An approximate method is particularly needed for use with

data that has a non-normal distribution, since numerical integration is currently required with these distributions.

8.2 APPLICATION OF NEW METHOD TO CONTAMINATED GROUNDWATER

To demonstrate the usefulness of the new methodology for analyzing censored, non-normally-distributed data, the method was applied to a complex civil engineering problem. The French Limited site, a Superfund site with contaminated groundwater, was chosen as a case study. Since this site has been thoroughly investigated, a large amount of groundwater concentration data and other information about the site was available. Contamination occurred at this site due to wastes being dumped into an unlined lagoon in the 1960s. Benzene was a major contaminant of concern at the site due to its high concentrations, recalcitrance, and carcinogenic quality. Investigation of the site began in the 1980s, and active remediation of the site occurred from 1991 through 1995. A total of 514 benzene concentration measurements were made before and after remediation from a total of 64 wells.

The concentration measurements were calibrated to a horizontal plane source model for the groundwater contamination. The variance of the measurements, correlation between measurements, and distribution of the measurements were also modeled. A total of 26 model parameters were calibrated with the concentration measurements using the FOSM Bayesian method. The method was then used to predict future benzene concentrations. In this section, the conclusions drawn from this case study and recommendations for future research are presented.

8.2.1 Conclusions

To model the mean benzene concentrations at the French Limited Site, a Horizontal Plane Source model (Galya 1987) was used. The model was amended to account for decreased contaminant source and increased contaminant biodegradation due to remediation efforts. The correlation between measurements was modeled to account for correlations in the longitudinal, transverse, vertical, and temporal dimensions, as well as correlation reductions due to random error and the effects of remediation. The distribution of the measurements was modeled with using a Hermite Polynomial transformation so that the distribution could be non-normal.

When the new method was used to calibrate the model parameters with the concentration measurements, reasonable results were obtained for the updated mean values of the model parameters. The updated mean values for the parameters that described the physical characteristics of the groundwater flow and the benzene contamination were all realistic, based on published values and specific information from investigation of the site. The updated source location and dimensions were similar to the footprint of the waste lagoon, and the groundwater velocity and flow direction were close to values found during site investigation. The dispersivity values were within published ranges. The extremely large half-life of benzene prior to remediation, 6×10^7 years, indicated that no degradation of benzene was occurring. This is consistent with studies that show very little degradation of benzene in areas of high concentration, particularly under anaerobic conditions, which represent the conditions at the French Limited site prior to remediation.

The remediation of the French Limited site consisted of removing the contaminant source, removing contaminated groundwater, and increasing biodegradation of the contaminant in the groundwater. The updated mean values of the remediation

parameters describe the success of these remediation efforts. The source removal was effective, as the benzene released from the source dropped from 86.5 g/day to only 9×10^{-6} g/day over the source area. The degradation of the benzene in the groundwater greatly increased after remediation, with a half-life after remediation of 544 days, due to the reduced contaminant concentrations in the groundwater and the introduction of dissolved oxygen and nutrients to promote biodegradation. Despite the source removal and increased degradation, the remediation was still not effective in eliminating contamination at the site, as seen in both measured and model-predicted concentrations. The remediation efforts did not account for sources of contaminant other than the lagoon, or the groundwater contamination that could not be completely removed with pump-and-treat.

The updated mean values for the correlation parameters indicated that the only significant correlation occurred between measurements at the same well at different times, or between two wells at the same location with different vertically screened intervals. Since there was no correlation between wells at different locations, the systematic error in the model was very low. The high correlation with time indicates consistency between the measured and model-calculated measurements over time at a particular location. This is probably due to the heterogeneities of the aquifer at the French Limited site. Preferential flow through channels with higher hydraulic conductivity results in measured concentrations that are consistently greater than or less than model-predicted concentrations.

The Hermite Polynomial transform function successfully modeled the non-normal distribution of the concentration measurements. The resulting distribution closely followed the measurements, and was more effective in modeling the lower tails of the distribution where censored data occur than a normal distribution.

The updated standard deviations of the model parameters were all small compared to the large prior standard deviations. This means that calibrating the model parameters with the data greatly reduced the uncertainty in the model parameters.

Although the uncertainty in the model parameters was reduced, the uncertainty in predicted concentrations was still high due to the modeled uncertainty and the remaining uncertainty in the model parameters. When predictions were made of benzene concentrations in two wells for 10 years after the active remediation of the site ended, the median concentrations were below the target benzene concentration. However, the probabilities that the concentrations would be above the target concentration were high, at approximately 20 percent for both wells. This means that even though the primary remediation effort of removing the contaminant source was successful, the contamination at the site was not completely remediated. The probability that concentrations would not meet the remediation criterion are useful in making decisions about whether further remediation or investigation of the site would be cost-effective.

The updated model parameters for the correlations between measurements are also useful in making decisions regarding the monitoring of the site. The high correlation with time at a particular location can be used to the sampling frequency at a well. Quarterly sampling was used at the French Limited site, but the correlation with time between two measurements taken 90 days apart is 0.93. Therefore, if a concentration is high in a well during one quarter, it is also very likely to be high the next quarter. Since the spatial correlation between wells is low, less frequent sampling at more wells might be more cost-effective and provide more information about the contamination of the site.

8.2.2 Recommendations for Future Work

The results of the groundwater model calibration should be used to make further predictions of the remediation performance at the French Limited site. The predictions should then be compared to the actual conditions at the site as described by post-remediation concentration measurements. Different monitoring plans for the contaminated groundwater site using the groundwater model calibration results should be analyzed to determine what type of monitoring plan is best based on the information it provides about the site and its cost and practicality.

The method used in this research should be compared to the more simple analysis methods for groundwater contamination that are commonly used in practice. The effect of the analysis method on the decisions made about the site should be determined, and the benefits of each method should be compared.

The method developed for this research should be applied to other contaminated groundwater sites to determine if the models and the method give consistently reasonable results for sites with different characteristics.

Appendix A. Derivation of Moments for Censored Normal Distribution

In this appendix, the mean and standard deviation for the censored and non-censored regions of a normally-distributed data point are derived. A normal distribution with a censored region and two non-censored regions is shown in Figure 4.1. The lower bound of the censored region is $y_{i,l}$ and the upper bound of the censored region is $y_{i,u}$. These bounds may have any value, including positive or negative infinity. Since only one data point is considered in this appendix, the lower and upper bounds of the censored region will be referred to as y_l and y_u , respectively, to simplify notation.

For a normal distribution, the probability density function (PDF) is:

$$f_Y(y) = \frac{1}{\sigma\sqrt{2\pi}} e^{-\frac{1}{2}\left(\frac{y-\mu}{\sigma}\right)^2} \quad (\text{A.1})$$

For any distribution type, the integral of the PDF, when evaluated between the upper and lower bounds of the PDF, must be equal to one. The censored region of a normal distribution is a truncated portion of the normal distribution. When finding the moments of a truncated distribution, the PDF of the truncated distribution must be divided by the area of the truncated portion of the full distribution. This allows the PDF of the truncated distribution to be equal to 1.0 when integrated between its upper and lower bounds. For a normal distribution censored between y_l and y_u , the area of the censored region is:

$$\begin{aligned}
\int_{y_1}^{y_u} \frac{1}{\sigma\sqrt{2\pi}} e^{-\frac{1}{2}\left(\frac{y-\mu}{\sigma}\right)^2} dy &= P(y_1 < Y \leq y_u) \\
&= \Phi\left(\frac{y_u - \mu}{\sigma}\right) - \Phi\left(\frac{y_1 - \mu}{\sigma}\right)
\end{aligned} \tag{A.2}$$

where μ and σ are the mean and standard deviation of the entire normal distribution (without censoring).

The area of the non-censored region is:

$$\begin{aligned}
\int_{-\infty}^{y_1} \frac{1}{\sigma\sqrt{2\pi}} e^{-\frac{1}{2}\left(\frac{y-\mu}{\sigma}\right)^2} dy + \int_{y_u}^{\infty} \frac{1}{\sigma\sqrt{2\pi}} e^{-\frac{1}{2}\left(\frac{y-\mu}{\sigma}\right)^2} dy &= P(Y \leq y_1 \cap Y > y_u) \\
&= P(Y \leq y_1) + P(Y > y_u) \\
&= 1 - P(y_1 < Y \leq y_u)
\end{aligned} \tag{A.3}$$

These areas will be used in the following derivations of the first and second moments of the censored and non-censored regions.

A.1 MEAN OF CENSORED REGION

The expected value of a random variable Y is found with the following integral (Ang and Tang 1975):

$$\mu_Y = \int_{-\infty}^{\infty} y \cdot f_Y(y) dy \tag{A.4}$$

where $f_Y(y)$ is the PDF of Y .

To find the mean of the censored region of a normal distribution, the integral in Equation A.4 is evaluated for a normal distribution between the upper and lower bounds of the censored region, then the result is divided by the area of the censored region. For the censored region defined by y_l and y_u , the mean is:

$$u_{Y,ul} = \left[\int_{y_l}^{y_u} y \frac{1}{\sigma\sqrt{2\pi}} e^{-\frac{1}{2}\left(\frac{y-\mu}{\sigma}\right)^2} dy \right] \frac{1}{P(y_l < Y \leq y_u)} \quad (\text{A.5})$$

The following variables are used to facilitate the integration of Equation A.5 by transforming the normal distribution into a standard normal distribution:

$$y' = \frac{y - \mu}{\sigma} \quad (\text{A.6})$$

$$dy' = \frac{dy}{\sigma} \quad (\text{A.7})$$

$$a' = \frac{a - \mu}{\sigma} \quad (\text{A.8})$$

$$b' = \frac{b - \mu}{\sigma} \quad (\text{A.9})$$

Rearranging Equation A.6:

$$y = \sigma y' + \mu \quad (\text{A.10})$$

and Equation A.7:

$$dy = \sigma dy' \quad (\text{A.11})$$

Substituting Equations A.6 through A.11 in Equation A.4:

$$u_{Y,ul} = \left[\int_{y_l}^{y_u} (\sigma y' + \mu) \frac{1}{\sqrt{2\pi}} e^{-\frac{1}{2}(y')^2} dy' \right] \frac{1}{P(y_l < Y \leq y_u)} \quad (\text{A.12})$$

Dividing the integral in the above equation into two parts:

$$\mu_{Y,ul} = \left[\mu \int_{y_l}^{y_u} \frac{1}{\sqrt{2\pi}} e^{-\frac{1}{2}(y')^2} dy' + \frac{\sigma}{\sqrt{2\pi}} \int_{y_l}^{y_u} y' e^{-\frac{1}{2}(y')^2} dy' \right] \frac{1}{P(y_l < Y \leq y_u)} \quad (\text{A.13})$$

The first integral of Equation A.13 is equal to $P(y_l < Y \leq y_u)$:

$$\begin{aligned} u_{Y,ul} &= \left[\mu P(y_l < Y \leq y_u) + \frac{\sigma}{\sqrt{2\pi}} \int_{y_l}^{y_u} y' e^{-\frac{1}{2}(y')^2} dy' \right] \frac{1}{P(y_l < Y \leq y_u)} \\ &= \mu + \left[\frac{\sigma}{\sqrt{2\pi}} \int_{y_l}^{y_u} y' e^{-\frac{1}{2}(y')^2} dy' \right] \frac{1}{P(y_l < Y \leq y_u)} \end{aligned} \quad (\text{A.14})$$

The following variables are defined to facilitate the integration of Equation A.14:

$$v = \frac{1}{2}(y')^2 \quad (\text{A.15})$$

$$dv = y' dy' \quad (\text{A.16})$$

$$v_l = \frac{1}{2}(y_l')^2 \quad (\text{A.17})$$

$$v_u = \frac{1}{2}(y_u')^2 \quad (\text{A.18})$$

Substituting Equation A.15 through A.18 into Equation A.14 results in:

$$\mu_{Y,ul} = \mu + \left[\frac{\sigma}{\sqrt{2\pi}} \int_{v_l}^{v_u} e^{-v} dv \right] \frac{1}{P(y_l < Y \leq y_u)} \quad (\text{A.19})$$

Integrating the above equation and evaluating the integral gives the following result:

$$\begin{aligned} \mu_{Y,ul} &= \mu + \left[\frac{\sigma}{\sqrt{2\pi}} (-e^{-v}) \Big|_{v_l}^{v_u} \right] \frac{1}{P(y_l < Y \leq y_u)} \\ &= \mu + \left[\frac{\sigma}{\sqrt{2\pi}} (-e^{-v_u} + e^{-v_l}) \right] \frac{1}{P(y_l < Y \leq y_u)} \end{aligned} \quad (\text{A.20})$$

Equation A.20 is then rewritten in the original terms:

$$\mu_{Y,ul} = \mu + \left[\frac{\sigma}{\sqrt{2\pi}} \left(e^{-\frac{1}{2}\left(\frac{y_l - \mu}{\sigma}\right)^2} - e^{-\frac{1}{2}\left(\frac{y_u - \mu}{\sigma}\right)^2} \right) \right] \frac{1}{P(y_l < Y \leq y_u)} \quad (\text{A.21})$$

This is the mean of a censored region of a normal distribution.

A.2 VARIANCE OF CENSORED REGION

The variance of a random variable Y is found with the following integral (Ang and Tang 1975):

$$\text{Var}(Y) = \int_{-\infty}^{\infty} (x - \mu_Y)^2 f_Y(y) dy \quad (\text{A.22})$$

which may also be written as:

$$\begin{aligned} \text{Var}(Y) &= E(Y^2) - \mu_Y^2 \\ &= \int_{-\infty}^{\infty} y^2 f_Y(y) dy - \mu_Y^2 \end{aligned} \quad (\text{A.23})$$

To find the variance of the censored region of a normal distribution, the integral in Equation A.23 is evaluated for a normal distribution between the upper and lower bounds of the censored region, then the result is divided by the area of the censored region. For the censored region defined by y_l and y_u , the variance is:

$$\sigma_{Y,ul}^2 = \left[\int_{y_l}^{y_u} y^2 \frac{1}{\sigma\sqrt{2\pi}} e^{-\frac{1}{2}\left(\frac{y-\mu}{\sigma}\right)^2} dy \right] \frac{1}{P(y_l < Y \leq y_u)} - \mu_{Y,ul}^2 \quad (\text{A.24})$$

The variables defined in Equations A.6 through A.11 are substituted into Equation A.24, resulting in the following:

$$\sigma_{Y,ul}^2 = \left[\int_{y_l}^{y_u} (\sigma y' + \mu)^2 \frac{1}{\sqrt{2\pi}} e^{-\frac{1}{2}(y')^2} dy' \right] \frac{1}{P(y_l < Y \leq y_u)} - \mu_{Y,ul}^2 \quad (\text{A.25})$$

Dividing the integral in the above equation into parts:

$$\begin{aligned}
\sigma_{y,ul}^2 &= \left[\int_{y'_i}^{y'_u} \sigma^2 (y')^2 \frac{1}{\sqrt{2\pi}} e^{-\frac{1}{2}(y')^2} dy' + \int_{y'_i}^{y'_u} 2\mu\sigma y' \frac{1}{\sqrt{2\pi}} e^{-\frac{1}{2}(y')^2} dy' \right. \\
&\quad \left. + \int_{y'_i}^{y'_u} \mu^2 \frac{1}{\sqrt{2\pi}} e^{-\frac{1}{2}(y')^2} dy' \right] \frac{1}{P(y_1 < Y \leq y_u)} - \mu_{y,ul}^2 \\
&= \left[\frac{\sigma^2}{\sqrt{2\pi}} \int_{y'_i}^{y'_u} (y')^2 e^{-\frac{1}{2}(y')^2} dy' + \frac{2\mu\sigma}{\sqrt{2\pi}} \int_{y'_i}^{y'_u} y' e^{-\frac{1}{2}(y')^2} dy' \right. \\
&\quad \left. + \mu^2 P(y_1 < Y \leq y_u) \right] \frac{1}{P(y_1 < Y \leq y_u)} - \mu_{y,ul}^2
\end{aligned} \tag{A.26}$$

The first integral in the above equation is evaluated as follows:

$$\begin{aligned}
\int_{y'_i}^{y'_u} (y')^2 e^{-\frac{1}{2}(y')^2} dy' &= -y'_u \left(e^{-\frac{1}{2}(y'_u)^2} \right) + y'_i \left(e^{-\frac{1}{2}(y'_i)^2} \right) \\
&\quad + \frac{\sqrt{2\pi}}{2} \operatorname{erf} \left(\frac{y'_u \sqrt{2}}{2} \right) - \frac{\sqrt{2\pi}}{2} \operatorname{erf} \left(\frac{y'_i \sqrt{2}}{2} \right) \\
&= -y'_u \left(e^{-\frac{1}{2}(y'_u)^2} \right) + y'_i \left(e^{-\frac{1}{2}(y'_i)^2} \right) + \sqrt{\frac{\pi}{2}} \left[\operatorname{erf} \left(\frac{y'_u}{\sqrt{2}} \right) - \operatorname{erf} \left(\frac{y'_i}{\sqrt{2}} \right) \right]
\end{aligned} \tag{A.27}$$

From the derivation for the mean of the censored region, the second integral in Equation A.24 is:

$$\int_{y_l}^{y_u} y' e^{-\frac{1}{2}(y')^2} dy' = -e^{-\frac{1}{2}(y_u')^2} + e^{-\frac{1}{2}(y_l')^2} \quad (\text{A.28})$$

The variance of the censored region is therefore:

$$\begin{aligned} \sigma_{Y,ul}^2 = & \mu_y^2 - \mu_{y,ul}^2 + \frac{2\mu\sigma}{P(y_l < Y \leq y_u)\sqrt{2\pi}} \left[-e^{-\frac{1}{2}\left(\frac{y_u-\mu}{\sigma}\right)^2} + e^{-\frac{1}{2}\left(\frac{y_l-\mu}{\sigma}\right)^2} \right] \\ & - \frac{\sigma^2}{P(y_l < Y \leq y_u)\sqrt{2\pi}} \left[\left(\frac{y_u-\mu}{\sigma}\right) e^{-\frac{1}{2}\left(\frac{y_u-\mu}{\sigma}\right)^2} + \left(\frac{y_l-\mu}{\sigma}\right) e^{-\frac{1}{2}\left(\frac{y_l-\mu}{\sigma}\right)^2} \right. \\ & \left. + \sqrt{\frac{\pi}{2}} \left[\operatorname{erf}\left(\frac{y_u-\mu}{\sigma\sqrt{2}}\right) - \operatorname{erf}\left(\frac{y_l-\mu}{\sigma\sqrt{2}}\right) \right] \right] \quad (\text{A.29}) \end{aligned}$$

A.3 MEAN OF NON-CENSORED REGION

The mean of the non-censored region, $\mu_{Y,NC}$, is found using the same derivation as for the censored region. However, the integral is evaluated over the non-censored region, from negative infinity to y_l and from y_u to positive infinity:

$$u_{Y,NC} = \left[\int_{-\infty}^{y_l} y \frac{1}{\sigma\sqrt{2\pi}} e^{-\frac{1}{2}\left(\frac{y-\mu}{\sigma}\right)^2} dy + \int_{y_u}^{\infty} y \frac{1}{\sigma\sqrt{2\pi}} e^{-\frac{1}{2}\left(\frac{y-\mu}{\sigma}\right)^2} dy \right] \frac{1}{1-P(y_l < Y \leq y_u)} \quad (\text{A.30})$$

Substituting Equations A.6 through A.11 into the equation above:

$$u_{Y,NC} = \left[\mu P(Y \leq y_1) + \frac{\sigma}{\sqrt{2\pi}} \int_{-\infty}^{y_1} y' e^{-\frac{1}{2}(y')^2} dy' \right. \\ \left. + \mu P(Y > y_u) + \frac{\sigma}{\sqrt{2\pi}} \int_{y_u}^{\infty} y' e^{-\frac{1}{2}(y')^2} dy' \right] \frac{1}{1 - P(y_1 < Y \leq y_u)} \quad (\text{A.31})$$

Combining the terms in Equation A.31 and simplifying:

$$u_{Y,NC} = \left[\mu(1 - P(y_1 < Y \leq y_u)) \right. \\ \left. + \frac{\sigma}{\sqrt{2\pi}} \left(\int_{-\infty}^{y_1} y' e^{-\frac{1}{2}(y')^2} dy' + \int_{y_u}^{\infty} y' e^{-\frac{1}{2}(y')^2} dy' \right) \right] \frac{1}{1 - P(y_1 < Y \leq y_u)} \quad (\text{A.32}) \\ = \mu + \frac{\sigma}{\sqrt{2\pi}} \left(\int_{-\infty}^{y_1} y' e^{-\frac{1}{2}(y')^2} dy' + \int_{y_u}^{\infty} y' e^{-\frac{1}{2}(y')^2} dy' \right) \frac{1}{1 - P(y_1 < Y \leq y_u)}$$

Substituting Equations A.15 through A.18 into the equation above:

$$\mu_{Y,NC} = \mu + \frac{\sigma}{\sqrt{2\pi}} \left(\int_{\infty}^{v_1} e^{-v} dv + \int_{v_u}^{\infty} e^{-v} dv \right) \frac{1}{1 - P(y_1 < Y \leq y_u)} \quad (\text{A.33})$$

Notice that the first integral in the equation above is now evaluated beginning at infinity, instead of negative infinity. Just as the upper bound of the integral is transformed to v_u by squaring it and dividing by two (Equation A.18), the lower value of integration is transformed to v_1 (Equation A.17): $0.5(-\infty)^2$, which is equal to infinity.

Integrating and evaluating the integrals in Equation A.33:

$$\begin{aligned}
\mu_{Y,NC} &= \mu + \frac{\sigma}{\sqrt{2\pi}} \left(\left(-e^{-v} \right) \Big|_{-\infty}^{y_1} + \left(-e^{-v} \right) \Big|_{y_u}^{\infty} \right) \frac{1}{1 - P(y_1 < Y \leq y_u)} \\
&= \mu + \frac{\sigma}{\sqrt{2\pi}} \left(\left(-e^{-v_1} + \cancel{e^{-\infty}} \right) + \left(-\cancel{e^{-\infty}} + e^{-v_u} \right) \right) \frac{1}{1 - P(y_1 < Y \leq y_u)} \quad (\text{A.34}) \\
&= \mu + \frac{\sigma}{\sqrt{2\pi}} \left(-e^{-v_1} + e^{-v_u} \right) \frac{1}{1 - P(y_1 < Y \leq y_u)}
\end{aligned}$$

The mean of the non-censored region is therefore:

$$\mu_{Y,NC} = \mu + \frac{\sigma}{\sqrt{2\pi}} \left(e^{-\frac{1}{2}\left(\frac{y_u - \mu}{\sigma}\right)^2} - e^{-\frac{1}{2}\left(\frac{y_1 - \mu}{\sigma}\right)^2} \right) \frac{1}{1 - P(y_1 < Y \leq y_u)} \quad (\text{A.35})$$

A.4 VARIANCE OF NON-CENSORED REGION

The variance of the non-censored region, $\sigma_{Y,NC}^2$, is found using the same derivation as for the censored region. However, the integral is evaluated over the non-censored region, from negative infinity to y_1 and from y_u to positive infinity:

$$\begin{aligned}
\sigma_{Y,NC}^2 &= \left[\int_{-\infty}^{y_1} y^2 \frac{1}{\sigma\sqrt{2\pi}} e^{-\frac{1}{2}\left(\frac{y-\mu}{\sigma}\right)^2} dy + \int_{y_u}^{\infty} y^2 \frac{1}{\sigma\sqrt{2\pi}} e^{-\frac{1}{2}\left(\frac{y-\mu}{\sigma}\right)^2} dy \right] \\
&\quad \cdot \frac{1}{1 - P(y_1 < Y \leq y_u)} - \mu_{y,NC}^2
\end{aligned} \quad (\text{A.36})$$

Substituting Equations A.6 through A.11 into the equation above:

$$\begin{aligned}
\sigma_{Y,ul}^2 = & \left[\frac{\sigma^2}{\sqrt{2\pi}} \int_{-\infty}^{y_1} (y')^2 e^{-\frac{1}{2}(y')^2} dy' + \frac{\sigma^2}{\sqrt{2\pi}} \int_{y_u}^{\infty} (y')^2 e^{-\frac{1}{2}(y')^2} dy' \right. \\
& \left. + \frac{2\mu\sigma}{\sqrt{2\pi}} \int_{-\infty}^{y_1} y' e^{-\frac{1}{2}(y')^2} dy' + \frac{2\mu\sigma}{\sqrt{2\pi}} \int_{y_u}^{\infty} y' e^{-\frac{1}{2}(y')^2} dy' \right] \frac{1}{1 - P(y_1 < Y \leq y_u)} \\
& + \mu_y^2 - \mu_{y,ul}^2
\end{aligned} \tag{A.37}$$

Integrating Equation A.37 and simplifying results in:

$$\begin{aligned}
\sigma_{Y,NC}^2 = & \mu_y^2 - \mu_{y,ul}^2 + \frac{2\mu\sigma}{[1 - P(y_1 < Y \leq y_u)]\sqrt{2\pi}} \left[-e^{-\frac{1}{2}\left(\frac{y_u - \mu}{\sigma}\right)^2} + e^{-\frac{1}{2}\left(\frac{y_1 - \mu}{\sigma}\right)^2} \right] \\
& - \frac{\sigma^2}{[1 - P(y_1 < Y \leq y_u)]\sqrt{2\pi}} \left[-(\infty) e^{-\frac{1}{2}\left(\frac{\infty - \mu}{\sigma}\right)^2} + \left(\frac{y_u - \mu}{\sigma}\right) e^{-\frac{1}{2}\left(\frac{y_u - \mu}{\sigma}\right)^2} \right. \\
& \left. - \left(\frac{y_1 - \mu}{\sigma}\right) e^{-\frac{1}{2}\left(\frac{y_1 - \mu}{\sigma}\right)^2} + (-\infty) e^{-\frac{1}{2}\left(\frac{-\infty - \mu}{\sigma}\right)^2} \right. \\
& \left. + \frac{\sqrt{2\pi}}{2} \left[\text{erf}\left(\frac{\infty}{\sqrt{2}}\right) - \text{erf}\left(\frac{y_u - \mu}{\sigma\sqrt{2}}\right) \right. \right. \\
& \left. \left. + \text{erf}\left(\frac{y_1 - \mu}{\sigma\sqrt{2}}\right) - \text{erf}\left(\frac{-\infty}{\sqrt{2}}\right) \right] \right]
\end{aligned} \tag{A.38}$$

The variance of the non-censored region is therefore:

$$\begin{aligned}
\sigma_{Y,NC}^2 = & \mu_y^2 - \mu_{y,ul}^2 + \frac{2\mu\sigma}{[1-P(y_l < Y \leq y_u)]\sqrt{2\pi}} \left[-e^{-\frac{1}{2}\left(\frac{y_u-\mu}{\sigma}\right)^2} + e^{-\frac{1}{2}\left(\frac{y_l-\mu}{\sigma}\right)^2} \right] \\
& - \frac{\sigma^2}{[1-P(y_l < Y \leq y_u)]\sqrt{2\pi}} \left[\left(\frac{y_u-\mu}{\sigma}\right) e^{-\frac{1}{2}\left(\frac{y_u-\mu}{\sigma}\right)^2} - \left(\frac{y_l-\mu}{\sigma}\right) e^{-\frac{1}{2}\left(\frac{y_l-\mu}{\sigma}\right)^2} \right] \quad (A.39) \\
& + \frac{\sigma^2}{2[1-P(y_l < Y \leq y_u)]} \left[\operatorname{erf}\left(\frac{y_l-\mu}{\sigma\sqrt{2}}\right) - \operatorname{erf}\left(\frac{y_u-\mu}{\sigma\sqrt{2}}\right) + 2 \right]
\end{aligned}$$

A.5 ALTERNATIVE EXPRESSIONS FOR MOMENTS OF NON-CENSORED REGION

The moments for the non-censored region may be expressed in terms of the moments of the censored region and the moments of the total distribution (the distribution with no censored region).

The mean is analogous to the centroidal distance (Ang and Tang 1975). Similarly, the variance is analogous to the central moment of inertia. When a distribution is censored, the moments are analogous to a shape with a piece missing, which may be calculated as a composite shape made up of a number of parts. The centroidal distance for a composite shape, $x_{\text{composite}}$, is:

$$x_{\text{composite}} = \frac{\sum_{\text{all parts}} (\text{Area of Part}) \cdot (\text{Centroid of Part})}{\sum_{\text{all parts}} \text{Area of Part}} \quad (A.40)$$

The area for a part of the composite shape is the same as the probability of a region of the distribution. The mean of the distribution is the same as the centroid of an area:

$$\mu_{\text{composite}} = \frac{\sum_{\text{all regions}} P(\text{region}) \cdot \mu_{\text{region}}}{\sum_{\text{all regions}} P(\text{region})} \quad (\text{A.41})$$

Therefore, the mean of the non-censored region for a distribution with a censored region bounded by y_l and y_u , is:

$$\mu_{Y,\text{NC}} = \frac{\mu_Y P(-\infty < Y \leq \infty) - \mu_{Y,\text{ul}} P(y_l < Y \leq y_u)}{P(-\infty < Y \leq \infty) - P(y_l < Y \leq y_u)} \quad (\text{A.42})$$

which reduces to:

$$\mu_{Y,\text{NC}} = \frac{\mu_Y - \mu_{Y,\text{ul}} P(y_l < Y \leq y_u)}{1 - P(y_l < Y \leq y_u)} \quad (\text{A.43})$$

The centroidal moment of inertia for a composite shape is found as follows:

$$I_{\text{composite}} = \sum_{\text{all parts}} \left[I_{\text{part}} + \text{Area of Part} \cdot (\text{Centroid of Part} - \text{Centroid of Composite})^2 \right] \quad (\text{A.44})$$

For a distribution with multiple regions, the variance is:

$$\sigma_{\text{composite}}^2 = \sum_{\text{all regions}} \sigma_{\text{region}}^2 + P(\text{region}) \cdot (\mu_{\text{region}} - \mu_{\text{composite}})^2 \quad (\text{A.45})$$

For a censored region bounded by y_l and y_u , the variance of the non-censored region is therefore:

$$\sigma_{\text{NC}}^2 = (\mu_Y - \mu_{Y,ul})^2 + \frac{\sigma_Y^2 - \sigma_{Y,ul}^2}{1 - P(y_l < Y \leq y_u)} \quad (\text{A.46})$$

Appendix B. Example Calculation of Conditional Moments

This appendix presents an example calculation of the conditional moments of a data point (Equations 4.18 and 4.19). For this example, a measurement will be conditioned on three previous measurements. Therefore, Measurement 4 will be conditioned on Measurements 1, 2, and 3. The measurements are shown in Table B1.

Table B1. Values for Measurements 1 through 4.

Measurement	Model-predicted mean value, μ_Y	Measured Value, y	Mean of Censored Region if Censored, $\mu_{Y,ul}$	Variance of Censored Region if Censored, $\sigma_{Y,ul}$
1	7	Censored	3.96	11.25
2	18	22	--	--
3	8	10	--	--
4	3	Not yet measured	2.42	2.54

For this example, the standard deviation of all four measurements is 2.0, and the correlation between all measurements is 0.50. The censored measurements are censored below 5.0, and this censoring level is used to calculate the mean and variance of the censored region.

The conditional mean is found as follows (Equation 4.18):

$$\mu_{Y_A|Y_B} = \mu_{Y_A} + \left\{ \left[C_{Y_{BB}} \right]^{-1} \left[C_{Y_{AB}} \right] \right\}^T \{ \bar{y}_B - \bar{\mu}_{Y_B} \} \quad (B.1)$$

Since the subscript “A” refers to the measurement that is being conditioned on the known measurements, “A” refers to Measurement 4. Since the subscript “B” refers to the known measurements, “B” refers to Measurements 1, 2, and 3.

The covariance between two measurements is:

$$\text{COV}_{i,j} = C_{i,j} = \rho_{i,j} \sigma_i \sigma_j \quad (\text{B.2})$$

The covariance matrices in equation B.1 are calculated as follows:

$$[C_{\text{BB}}] = \begin{bmatrix} 1(2)(2) & 0.5(2)(2) & 0.5(2)(2) \\ 0.5(2)(2) & 1(2)(2) & 0.5(2)(2) \\ 0.5(2)(2) & 0.5(2)(2) & 1(2)(2) \end{bmatrix} \quad (\text{B.3})$$

$$= \begin{bmatrix} 4 & 2 & 2 \\ 2 & 4 & 2 \\ 2 & 2 & 4 \end{bmatrix}$$

$$[C_{\text{AB}}] = \begin{Bmatrix} 0.5(2)(2) \\ 0.5(2)(2) \\ 0.5(2)(2) \end{Bmatrix} \quad (\text{B.4})$$

$$= \begin{Bmatrix} 2 \\ 2 \\ 2 \end{Bmatrix}$$

Using the values for Measurements 1 through 4 in Equation B.1 results in:

$$\begin{aligned}\mu_{Y_A|Y_B} &= 3 + \left\{ \begin{bmatrix} 4 & 2 & 2 \\ 2 & 4 & 2 \\ 2 & 2 & 4 \end{bmatrix}^{-1} \begin{bmatrix} 2 \\ 2 \\ 2 \end{bmatrix} \right\}^T \begin{bmatrix} 3.96 - 7 \\ 22 - 18 \\ 10 - 8 \end{bmatrix} \\ &= 3.74\end{aligned}\tag{B.5}$$

The conditional mean of Measurement 4, conditioned on Measurements 1 through 3, is therefore equal to 3.74. This conditional mean is greater than the model-predicted value of 3 for Measurement 4, because Measurement 4 is correlated with Measurements 1 through 3, and Measurements 2 and 3 have values much greater than 3.

The conditional variance is found as follows (Equation 4.19):

$$\begin{aligned}\sigma_{Y_A|Y_B}^2 &= \sigma_{Y_A}^2 - \left\{ \begin{bmatrix} C_{Y_{AB}} \end{bmatrix}^T \begin{bmatrix} C_{Y_{BB}} \end{bmatrix}^{-1} \begin{bmatrix} C_{Y_{AB}} \end{bmatrix} \right\} \\ &\quad + \left\{ \begin{bmatrix} C_{Y_{BB}} \end{bmatrix}^{-1} \begin{bmatrix} C_{Y_{AB}} \end{bmatrix} \right\}^T \begin{bmatrix} C_{Y_{BBul}} \end{bmatrix} \left\{ \begin{bmatrix} C_{Y_{BB}} \end{bmatrix}^{-1} \begin{bmatrix} C_{Y_{AB}} \end{bmatrix} \right\}\end{aligned}\tag{B.6}$$

The $C_{Y_{BBul}}$ term in Equation B.6 adds extra variability for censored data. If the data point is not censored, the standard deviation used in the covariance is zero. If the data point is censored, the standard deviation of the censored region is used in the covariance. This term is calculated as follows for Measurements 1 through 3:

$$\begin{aligned}\begin{bmatrix} C_{Y_{BBul}} \end{bmatrix} &= \begin{bmatrix} 1(3.35)(3.35) & 0.5(3.35)(0) & 0.5(3.35)(0) \\ 0.5(0)(0) & 1(0)(0) & 0.5(0)(0) \\ 0.5(0)(0) & 0.5(0)(0) & 1(0)(0) \end{bmatrix} \\ &= \begin{bmatrix} 11.25 & 0 & 0 \\ 0 & 0 & 0 \\ 0 & 0 & 0 \end{bmatrix}\end{aligned}\tag{B.7}$$

Using the values for Measurements 1 through 4 in Equation B.6 results in:

$$\begin{aligned}
 \sigma_{Y_A|Y_B}^2 &= 2^2 - \left\{ \begin{matrix} \left[\begin{matrix} 2 \\ 2 \\ 2 \end{matrix} \right]^T \begin{bmatrix} 4 & 2 & 2 \\ 2 & 4 & 2 \\ 2 & 2 & 4 \end{bmatrix}^{-1} \begin{bmatrix} 2 \\ 2 \\ 2 \end{bmatrix} \end{matrix} \right\} \\
 &+ \left\{ \begin{matrix} \begin{bmatrix} 4 & 2 & 2 \\ 2 & 4 & 2 \\ 2 & 2 & 4 \end{bmatrix}^{-1} \begin{bmatrix} 2 \\ 2 \\ 2 \end{bmatrix} \end{matrix} \right\}^T \begin{bmatrix} 11.25 & 0 & 0 \\ 0 & 0 & 0 \\ 0 & 0 & 0 \end{bmatrix} \left\{ \begin{matrix} \begin{bmatrix} 4 & 2 & 2 \\ 2 & 4 & 2 \\ 2 & 2 & 4 \end{bmatrix}^{-1} \begin{bmatrix} 2 \\ 2 \\ 2 \end{bmatrix} \end{matrix} \right\} \quad (\text{B.8}) \\
 &= 4 - 1.5 + 0.7 \\
 &= 3.2
 \end{aligned}$$

The conditional mean of Measurement 4, conditioned on Measurements 1 through 3, is therefore 3.2. This is less than the variance of 4 that predicted for this measurement, since conditioning the variance on the other three measurements reduces the variability for this measurement.

Notice that if the correlation between Measurement 4 and any of the other measurements was zero, then those measurements would not contribute to the conditional mean and variance of Measurement 4. Only the measurements that are correlated with the measurement being conditioned will affect the conditional moments.

Appendix C. Derivation of Analytical Method

In this appendix, the complete analytical method of Section 5.3.3 is derived for a normally-distributed data point. This method is used to evaluate the expected value of the second derivative of the likelihood function (Equation 4.38), which is used in updating the covariance of the model parameters (Equation 4.34). As stated in Section 5.3.3, two assumptions are made in this method. The first assumption is that the set of model parameter values used for the Taylor series expansion point, $\bar{\phi}^*$, do not depend on the data and are equal to the prior mean values of the model parameters, $\bar{\mu}_\phi$. The second assumption is that data points that are expected to be censored are equal to the mean of the censored region of that data point, $\mu_{Y_i, ul}$, when calculating the conditional moments of the data.

For each expected data point, the probability that the point will be censored and the probability that the point will not be censored are considered. The expected value of the second derivative of the likelihood function in this method is therefore calculated as follows:

$$\begin{aligned}
 E_Y \left(\frac{\partial^2 \mathbf{g}}{\partial \phi_1 \partial \phi_j} \right) &= E_Y \left(\frac{\partial^2 \mathbf{g}_C}{\partial \phi_1 \partial \phi_j} \right) P(y_1 < Y \leq y_u) \\
 &\quad + E_Y \left(\frac{\partial^2 \mathbf{g}_{NC}}{\partial \phi_1 \partial \phi_j} \right) [1 - P(y_1 < Y \leq y_u)]
 \end{aligned}
 \tag{C.1}$$

where:

\mathbf{g}_C = the likelihood function if the data point is expected to be censored

\mathbf{g}_{NC} = the likelihood function if the data point is not expected to be censored

$P(y_l < Y \leq y_u)$ = the probability that the data point is censored

$[1 - P(y_l < Y \leq y_u)]$ = the probability that the data point is not censored

When a data point is non-censored, the likelihood function is the multivariate normal distribution. The second derivative of the multivariate normal distribution for one data point is (Muchard 1997):

$$\begin{aligned}
\frac{\partial^2 g_{NC}}{\partial \phi_i \partial \phi_j} = & \left[\frac{1}{2} \frac{1}{C_Y^2} \frac{\partial C_Y}{\partial \phi_i} \frac{\partial C_Y}{\partial \phi_j} - \frac{1}{2} \frac{1}{C_Y} \frac{\partial^2 C_Y}{\partial \phi_i \partial \phi_j} + \frac{\mu_Y}{C_Y^2} \frac{\partial \mu_Y}{\partial \phi_i} \frac{\partial C_Y}{\partial \phi_j} - \frac{1}{C_Y} \frac{\partial \mu_Y}{\partial \phi_i} \frac{\partial \mu_Y}{\partial \phi_j} \right. \\
& \left. - \frac{\mu_Y}{C_Y} \frac{\partial^2 \mu_Y}{\partial \phi_i \partial \phi_j} - \frac{\mu_Y^2}{C_Y^3} \frac{\partial C_Y}{\partial \phi_i} \frac{\partial C_Y}{\partial \phi_j} + \frac{\mu_Y}{C_Y^2} \frac{\partial C_Y}{\partial \phi_i} \frac{\partial \mu_Y}{\partial \phi_j} + \frac{1}{2} \frac{\mu_Y^2}{C_Y^2} \frac{\partial^2 C_Y}{\partial \phi_i \partial \phi_j} \right] \\
& + y \left[-\frac{1}{C_Y^2} \frac{\partial \mu_Y}{\partial \phi_i} \frac{\partial C_Y}{\partial \phi_j} + \frac{1}{C_Y} \frac{\partial^2 \mu_Y}{\partial \phi_i \partial \phi_j} + 2 \frac{\mu_Y}{C_Y^3} \frac{\partial C_Y}{\partial \phi_i} \frac{\partial C_Y}{\partial \phi_j} \right. \\
& \left. - \frac{1}{C_Y^2} \frac{\partial C_Y}{\partial \phi_i} \frac{\partial \mu_Y}{\partial \phi_j} - \frac{\mu_Y}{C_Y^2} \frac{\partial^2 C_Y}{\partial \phi_i \partial \phi_j} \right] \\
& + y^2 \left[-\frac{1}{C_Y^3} \frac{\partial C_Y}{\partial \phi_i} \frac{\partial C_Y}{\partial \phi_j} + \frac{1}{2} \frac{1}{C_Y^2} \frac{\partial^2 C_Y}{\partial \phi_i \partial \phi_j} \right] \tag{C.2}
\end{aligned}$$

where μ_Y is the modeled mean of the data point, C_Y is the modeled variance of the data point, and the derivatives are evaluated at $\bar{\phi} = \mu_{\bar{\phi}}$.

Equation C.1 may be re-written as follows:

$$\frac{\partial^2 g_{NC}}{\partial \phi_i \partial \phi_j} = a + by + cy^2 \tag{C.3}$$

where:

$$\begin{aligned}
 a = & \frac{1}{2} \frac{1}{C_Y^2} \frac{\partial C_Y}{\partial \phi_i} \frac{\partial C_Y}{\partial \phi_j} - \frac{1}{2} \frac{1}{C_Y} \frac{\partial^2 C_Y}{\partial \phi_i \partial \phi_j} + \frac{\mu_Y}{C_Y^2} \frac{\partial \mu_Y}{\partial \phi_i} \frac{\partial C_Y}{\partial \phi_j} \\
 & - \frac{1}{C_Y} \frac{\partial \mu_Y}{\partial \phi_i} \frac{\partial \mu_Y}{\partial \phi_j} - \frac{\mu_Y}{C_Y} \frac{\partial^2 \mu_Y}{\partial \phi_i \partial \phi_j} - \frac{\mu_Y^2}{C_Y^3} \frac{\partial C_Y}{\partial \phi_i} \frac{\partial C_Y}{\partial \phi_j} \\
 & + \frac{\mu_Y}{C_Y^2} \frac{\partial C_Y}{\partial \phi_i} \frac{\partial \mu_Y}{\partial \phi_j} + \frac{1}{2} \frac{\mu_Y^2}{C_Y^2} \frac{\partial^2 C_Y}{\partial \phi_i \partial \phi_j}
 \end{aligned}$$

$$\begin{aligned}
 b = & -\frac{1}{C_Y^2} \frac{\partial \mu_Y}{\partial \phi_i} \frac{\partial C_Y}{\partial \phi_j} + \frac{1}{C_Y} \frac{\partial^2 \mu_Y}{\partial \phi_i \partial \phi_j} + 2 \frac{\mu_Y}{C_Y^3} \frac{\partial C_Y}{\partial \phi_i} \frac{\partial C_Y}{\partial \phi_j} \\
 & - \frac{1}{C_Y^2} \frac{\partial C_Y}{\partial \phi_i} \frac{\partial \mu_Y}{\partial \phi_j} - \frac{\mu_Y}{C_Y^2} \frac{\partial^2 C_Y}{\partial \phi_i \partial \phi_j}
 \end{aligned}$$

$$c = -\frac{1}{C_Y^3} \frac{\partial C_Y}{\partial \phi_i} \frac{\partial C_Y}{\partial \phi_j} + \frac{1}{2} \frac{1}{C_Y^2} \frac{\partial^2 C_Y}{\partial \phi_i \partial \phi_j}$$

The expected value of the second derivative of the likelihood function for the non-censored region is then:

$$E_Y \left(\frac{\partial^2 \mathbf{g}_{NC}}{\partial \phi_i \partial \phi_j} \right) = \int_{-\infty}^{y_l} (a + by + cy^2) f_Y(y) dy + \int_{y_u}^{\infty} (a + by + cy^2) f_Y(y) dy \quad (C.4)$$

where $f_Y(y)$ is the probability density function of the normal distribution.

Separating the terms in the integrals above:

$$\begin{aligned}
E_Y \left(\frac{\partial^2 g_{NC}}{\partial \phi_i \partial \phi_j} \right) &= a \int_{-\infty}^{y_1} f_Y(y) dy + a \int_{y_u}^{\infty} f_Y(y) dy \\
&+ b \int_{-\infty}^{y_1} y \cdot f_Y(y) dy + b \int_{y_u}^{\infty} y \cdot f_Y(y) dy \\
&+ c \int_{-\infty}^{y_1} y^2 f_Y(y) dy + c \int_{y_u}^{\infty} y^2 f_Y(y) dy
\end{aligned} \tag{C.5}$$

Integrating Equation C.5 and evaluating the integrals results in the following:

$$\begin{aligned}
E_Y \left(\frac{\partial^2 g_{NC}}{\partial \phi_i \partial \phi_j} \right) &= a \left[P(y \leq y_1 \cup y \geq y_u) \right] \\
&+ b \left[E(Y)_1 + E(Y)_u \right] P(y \leq y_1 \cup y \geq y_u) \\
&+ c \left[E(Y^2)_1 + E(Y^2)_u \right] P(y \leq y_1 \cup y \geq y_u)
\end{aligned} \tag{C.6}$$

where:

$P(y \leq y_1 \cup y \geq y_u)$ = the probability that y is in the non-censored regions

$E(Y)_1$ = mean of the non-censored region with $y \leq y_1$

$E(Y)_u$ = mean of the non-censored region with $y \geq y_u$

$E(Y^2)_1$ = expected value of Y^2 for the $y \leq y_1$ portion of the non-censored region

$E(Y^2)_u$ = expected value of Y^2 for the $y \geq y_u$ portion of the non-censored region

The expected value of Y for the non-censored regions is:

$$E(Y)_1 + E(Y)_u = \mu_{Y,NC} \tag{C.7}$$

where $\mu_{Y,NC}$ is given in Equation A.35.

The expected value of Y^2 (Ang and Tang 1976) is:

$$\begin{aligned} E(Y^2) &= \text{Var}(Y) + E(Y)^2 \\ &= \sigma_Y^2 + \mu_Y^2 \end{aligned} \tag{C.8}$$

The expected value of Y^2 for the non-censored region is therefore the sum of the variance of the non-censored region (Equation A.40) and the square of the mean of the non-censored region (Equation A.35):

$$E(Y^2)_1 + E(Y^2)_u = \sigma_{Y,NC}^2 + \mu_{Y,NC}^2 \tag{C.9}$$

For a censored measurement, the second derivative of the likelihood function is:

$$\begin{aligned} \frac{\partial^2 \mathbf{g}_C}{\partial \phi_i \partial \phi_j} &= -\frac{1}{[\Phi(\mathbf{u}_u) - \Phi(\mathbf{u}_1)]^2} \left[f_{U_u}(\mathbf{u}_u) \frac{\partial \mathbf{u}_u}{\partial \phi_i} - f_{U_1}(\mathbf{u}_1) \frac{\partial \mathbf{u}_1}{\partial \phi_i} \right] \\ &\quad \left[f_{U_u}(\mathbf{u}_u) \frac{\partial \mathbf{u}_u}{\partial \phi_j} - f_{U_1}(\mathbf{u}_1) \frac{\partial \mathbf{u}_1}{\partial \phi_j} \right] \\ &\quad + \frac{1}{[\Phi(\mathbf{u}_u) - \Phi(\mathbf{u}_1)]} \left[-\mathbf{u}_u \cdot f_{U_u}(\mathbf{u}_u) \frac{\partial \mathbf{u}_u}{\partial \phi_j} \frac{\partial \mathbf{u}_u}{\partial \phi_i} + f_{U_u}(\mathbf{u}_u) \frac{\partial^2 \mathbf{u}_u}{\partial \phi_i \partial \phi_j} \right. \\ &\quad \left. + \mathbf{u}_1 \cdot f_{U_1}(\mathbf{u}_1) \frac{\partial \mathbf{u}_1}{\partial \phi_j} \frac{\partial \mathbf{u}_1}{\partial \phi_i} + f_{U_1}(\mathbf{u}_1) \frac{\partial^2 \mathbf{u}_1}{\partial \phi_i \partial \phi_j} \right] \end{aligned} \tag{C.10}$$

where:

$$\mathbf{u}_u = \frac{y_u - \mu_{y|Y_B}}{\sigma_{y|Y_B}}$$

$$\mathbf{u}_l = \frac{y_l - \mu_{y|Y_B}}{\sigma_{y|Y_B}}$$

$$f_{U_u}(\mathbf{u}_u) = \frac{1}{\sqrt{2\pi}} e^{-\frac{1}{2} \left(\frac{y_u - \mu_{y|Y_B}}{\sigma_{y|Y_B}} \right)^2}$$

$$f_{U_u}(\mathbf{u}_u) = \frac{1}{\sqrt{2\pi}} e^{-\frac{1}{2} \left(\frac{y_u - \mu_{y|Y_B}}{\sigma_{y|Y_B}} \right)^2}$$

and $\mu_{y|Y_B}$ and $\sigma_{y|Y_B}$ are the conditional moments of Y derived in Section 4.4.1.2. The derivatives in Equation C.11 are evaluated at the prior mean values of the model parameters, $\bar{\mu}_\phi$.

The second derivative of the natural logarithm of the likelihood function for a censored measurement in Equation C.11 does not depend on the data point, y . Therefore, the expected value of the second derivative of the natural logarithm of the likelihood function for a censored measurement is:

$$E_Y \left(\frac{\partial^2 \mathbf{g}_C}{\partial \phi_i \partial \phi_j} \right) = \frac{\partial^2 \mathbf{g}_C}{\partial \phi_i \partial \phi_j} \quad (\text{C.11})$$

Equations C.6 and C.11 are then substituted into Equation C.1 to find the expected second derivative of the natural logarithm of the likelihood function.

Appendix D. Complete Results for Comparison of Methods to Calculate $E(-G'')$

This appendix contains the results for the numerical simulations described in Chapter 5 for calculating the expected value of the negative second derivative of the natural logarithm of the likelihood function, $E_{\bar{Y}}\left(\frac{\partial^2 g}{\partial \phi_i \partial \phi_j} \Big|_{\bar{\phi}^*}\right)$, which is abbreviated as $E(-G'')$. The evaluation point of $E(-G'')$, $\bar{\phi}^*$, was found with two different methods: using the prior mean model parameters so that $\bar{\phi}^* = \bar{\mu}_{\bar{\phi}}$, and finding $\bar{\phi}^*$ to maximize the likelihood function. The mean, standard deviation, and 90 percent confidence interval bounds are given for each simulation conducted for each method.

Table D1. Results of numerical simulations with $\bar{\phi}^* = \bar{\mu}_{\bar{\phi}}$ for no censored data.

Correlation between adjacent data points	i	j	Mean	Standard Deviation	90% Confidence Interval
0	0	0	100.00	0	100 - 100
	0	1	0.13	-20.06	-0.91 - 1.18
	1	1	201.05	-28.55	199.57 - 202.54
	0	2	0.00	0	0 - 0
	1	2	0.00	0	0 - 0
	2	2	0.00	0	0 - 0
0.25	0	0	60.22	-1.53E-05	60.22 - 60.22
	0	1	0.13	-15.59	-0.68 - 0.94
	1	1	201.05	-28.55	199.57 - 202.54
	0	2	0.02	-5.67	-0.28 - 0.31
	1	2	-18.17	-7.79	-18.57 - -17.76
	2	2	14.52	-5.07	14.26 - 14.78
0.5	0	0	33.97	0.00E+00	33.97 - 33.97
	0	1	0.13	-11.74	-0.48 - 0.74
	1	1	201.05	-28.55	199.57 - 202.54
	0	2	0.02	-5.27	-0.26 - 0.29
	1	2	-45.63	-10.39	-46.17 - -45.09
	2	2	26.66	-6.59	26.31 - 27.00
0.75	0	0	15.12	-2.69E-06	15.12 - 15.12
	0	1	0.12	-7.87	-0.29 - 0.53
	1	1	201.05	-28.55	199.57 - 202.54
	0	2	0.01	-3.66	-0.18 - 0.20
	1	2	-73.36	-12.27	-74.00 - -72.72
	2	2	37.89	-7.03	37.53 - 38.26

Table D2. Results of numerical simulations with $\bar{\phi}^* = \bar{\mu}_{\bar{\phi}}$ for 25 percent censored data.

Correlation between adjacent data points	i	j	Mean	Standard Deviation	90% Confidence Interval
0	0	0	93.94	-1.03	93.88 - 93.99
	0	1	19.23	-17.19	18.33 - 20.12
	1	1	137.95	-21.58	136.83 - 139.07
	0	2	0.00	0	0 - 0
	1	2	0.00	0	0 - 0
	2	2	0.00	0	0 - 0
0.25	0	0	58.35	-0.56	58.32 - 58.37
	0	1	11.64	-13.40	10.95 - 12.34
	1	1	137.33	-22.28	136.17 - 138.49
	0	2	-0.99	-5.36	-1.27 - -0.71
	1	2	-11.92	-5.61	-12.21 - -11.63
	2	2	12.53	-4.06	12.32 - 12.75
0.5	0	0	34.18	-0.37	34.16 - 34.20
	0	1	6.09	-10.26	5.56 - 6.63
	1	1	138.53	-24.08	137.28 - 139.78
	0	2	-1.76	-5.25	-2.03 - -1.49
	1	2	-30.28	-7.90	-30.69 - -29.87
	2	2	21.72	-5.06	21.46 - 21.98
0.75	0	0	16.08	-0.37	16.06 - 16.10
	0	1	1.79	-7.25	1.41 - 2.17
	1	1	141.08	-27.98	139.62 - 142.54
	0	2	-1.49	-3.99	-1.69 - -1.28
	1	2	-49.40	-11.42	-49.99 - -48.80
	2	2	28.41	-5.82	28.10 - 28.71

Table D3. Results of numerical simulations with $\bar{\phi}^* = \bar{\mu}_{\bar{\phi}}$ for 50 percent censored data.

Correlation between adjacent data points	i	j	Mean	Standard Deviation	90% Confidence Interval
0	0	0	81.87	-1.80	81.78 - 81.96
	0	1	40.33	-14.97	39.56 - 41.11
	1	1	100.66	-22.78	99.48 - 101.84
	0	2	0.00	0	0 - 0
	1	2	0.00	0	0 - 0
	2	2	0.00	0	0 - 0
0.25	0	0	53.81	-1.23	53.74 - 53.87
	0	1	26.04	-11.82	25.43 - 26.66
	1	1	94.43	-22.70	93.25 - 95.62
	0	2	-1.55	-4.63	-1.79 - -1.31
	1	2	-7.31	-4.20	-7.53 - -7.10
	2	2	9.30	-3.06	9.14 - 9.46
0.5	0	0	33.25	-0.85	33.21 - 33.30
	0	1	14.98	-9.14	14.50 - 15.45
	1	1	90.87	-24.20	89.61 - 92.13
	0	2	-2.81	-4.60	-3.05 - -2.57
	1	2	-18.50	-5.27	-18.77 - -18.22
	2	2	15.37	-4.10	15.16 - 15.59
0.75	0	0	16.47	-0.59	16.43 - 16.50
	0	1	5.91	-6.50	5.57 - 6.24
	1	1	89.32	-29.11	87.80 - 90.83
	0	2	-2.25	-3.69	-2.45 - -2.06
	1	2	-30.00	-9.02	-30.47 - -29.53
	2	2	18.59	-5.36	18.31 - 18.87

Table D4. Results of numerical simulations with $\bar{\phi}^* = \bar{\mu}_{\bar{\phi}}$ for 75 percent censored data.

Correlation between adjacent data points	i	j	Mean	Standard Deviation	90% Confidence Interval
0	0	0	59.97	-2.34	59.85 - 60.09
	0	1	55.70	-12.71	55.04 - 56.37
	1	1	87.98	-23.19	86.78 - 89.19
	0	2	0.00	0	0 - 0
	1	2	0.00	0	0 - 0
	2	2	0.00	0	0 - 0
0.25	0	0	43.43	-1.97	43.32 - 43.53
	0	1	40.04	-10.75	39.48 - 40.60
	1	1	73.69	-22.24	72.53 - 74.85
	0	2	-1.40	-3.31	-1.57 - -1.23
	1	2	-3.74	-3.49	-3.92 - -3.56
	2	2	5.10	-2.14	4.99 - 5.21
0.5	0	0	28.96	-1.59	28.88 - 29.05
	0	1	25.78	-8.71	25.33 - 26.23
	1	1	60.86	-22.21	59.71 - 62.02
	0	2	-2.53	-3.49	-2.71 - -2.35
	1	2	-9.07	-3.21	-9.24 - -8.90
	2	2	8.05	-3.05	7.89 - 8.21
0.75	0	0	15.25	-1.19	15.19 - 15.32
	0	1	12.09	-6.45	11.75 - 12.42
	1	1	49.42	-24.96	48.12 - 50.72
	0	2	-1.99	-2.83	-2.14 - -1.85
	1	2	-13.94	-4.97	-14.20 - -13.68
	2	2	8.99	-4.19	8.77 - 9.21

Table D5. Results of numerical simulations with $\bar{\phi}^*$ maximizing the likelihood function for no censored data.

Correlation between adjacent data points	i	j	Mean	Standard Deviation	90% Confidence Interval
0	0	0	102.53	-14.14	101.79 - 103.26
	0	1	0.00	-0.04	0.00 - 0.00
	1	1	200.00	-0.06	200.00 - 200.01
	0	2	0.00	0	0 - 0
	1	2	0.00	0	0 - 0
	2	2	0.00	0	0 - 0
0.25	0	0	65.56	-16.44	64.71 - 66.42
	0	1	0.00	-0.02	0.00 - 0.00
	1	1	200.02	-0.06	200.01 - 200.02
	0	2	-0.02	-0.52	-0.05 - 0.00
	1	2	-17.85	-7.91	-18.26 - -17.44
	2	2	13.51	-4.65	13.26 - 13.75
0.5	0	0	39.33	-13.79	38.62 - 40.05
	0	1	0.00	-0.02	0.00 - 0.00
	1	1	200.01	-0.07	200.00 - 200.01
	0	2	-0.04	-0.64	-0.07 - 0.00
	1	2	-43.46	-9.03	-43.92 - -42.99
	2	2	25.44	-3.80	25.25 - 25.64
0.75	0	0	20.88	-10.31	20.34 - 21.41
	0	1	0.00	-0.01	0.00 - 0.00
	1	1	200.00	-0.07	200.00 - 200.01
	0	2	-0.05	-0.68	-0.08 - -0.01
	1	2	-69.97	-7.22	-70.34 - -69.59
	2	2	36.31	-3.09	36.15 - 36.47

Table D6. Results of numerical simulations with $\bar{\phi}^*$ maximizing the likelihood function for 25 percent censored data.

Correlation between adjacent data points	i	j	Mean	Standard Deviation	90% Confidence Interval
0	0	0	96.56	-17.06	95.67 - 97.45
	0	1	19.07	-2.47	18.94 - 19.20
	1	1	137.31	-8.16	136.89 - 137.74
	0	2	0.00	0	0 - 0
	1	2	0.00	0	0 - 0
	2	2	0.00	0	0 - 0
0.25	0	0	63.38	-18.14	62.44 - 64.32
	0	1	12.09	-3.31	11.92 - 12.26
	1	1	136.76	-9.86	136.24 - 137.27
	0	2	-0.96	-0.75	-1.00 - -0.92
	1	2	-11.81	-6.26	-12.13 - -11.48
	2	2	11.55	-4.40	11.32 - 11.78
0.5	0	0	39.09	-15.65	38.27 - 39.90
	0	1	6.48	-2.93	6.33 - 6.63
	1	1	138.40	-13.69	137.69 - 139.11
	0	2	-1.73	-0.91	-1.78 - -1.68
	1	2	-29.09	-7.65	-29.49 - -28.69
	2	2	20.81	-3.31	20.64 - 20.98
0.75	0	0	22.03	-11.19	21.45 - 22.61
	0	1	2.32	-1.61	2.24 - 2.41
	1	1	141.83	-18.07	140.89 - 142.77
	0	2	-1.65	-1.23	-1.71 - -1.59
	1	2	-47.59	-7.76	-48.00 - -47.19
	2	2	27.73	-3.24	27.56 - 27.90

Table D7. Results of numerical simulations with $\bar{\phi}^*$ maximizing the likelihood function for 50 percent censored data.

Correlation between adjacent data points	i	j	Mean	Standard Deviation	90% Confidence Interval
0	0	0	85.88	-20.17	84.83 - 86.93
	0	1	40.23	-3.92	40.03 - 40.44
	1	1	100.48	-4.73	100.23 - 100.72
	0	2	0.00	0	0 - 0
	1	2	0.00	0	0 - 0
	2	2	0.00	0	0 - 0
0.25	0	0	59.73	-20.28	58.67 - 60.78
	0	1	27.34	-6.68	26.99 - 27.68
	1	1	95.08	-7.78	94.68 - 95.49
	0	2	-1.50	-0.98	-1.55 - -1.45
	1	2	-7.53	-4.45	-7.77 - -7.30
	2	2	8.47	-3.51	8.29 - 8.66
0.5	0	0	39.14	-15.06	38.36 - 39.92
	0	1	16.65	-6.04	16.34 - 16.97
	1	1	91.95	-11.90	91.33 - 92.57
	0	2	-2.64	-1.06	-2.70 - -2.59
	1	2	-18.07	-5.66	-18.37 - -17.78
	2	2	14.71	-2.95	14.55 - 14.86
0.75	0	0	23.73	-12.55	23.07 - 24.38
	0	1	8.37	-4.96	8.11 - 8.63
	1	1	92.26	-18.69	91.29 - 93.23
	0	2	-2.35	-1.38	-2.42 - -2.28
	1	2	-29.56	-8.27	-29.99 - -29.13
	2	2	18.54	-4.08	18.33 - 18.76

Table D8. Results of numerical simulations with $\bar{\phi}^*$ maximizing the likelihood function for 75 percent censored data.

Correlation between adjacent data points	i	j	Mean	Standard Deviation	90% Confidence Interval
0	0	0	66.90	-24.55	65.62 - 68.17
	0	1	56.95	-8.76	56.50 - 57.41
	1	1	87.45	-0.81	87.40 - 87.49
	0	2	0.00	0	0 - 0
	1	2	0.00	0	0 - 0
	2	2	0.00	0	0 - 0
0.25	0	0	50.93	-23.88	49.68 - 52.17
	0	1	42.79	-12.53	42.14 - 43.44
	1	1	75.09	-7.80	74.68 - 75.49
	0	2	-1.31	-0.94	-1.36 - -1.27
	1	2	-3.94	-2.99	-4.10 - -3.78
	2	2	4.43	-2.56	4.30 - 4.56
0.5	0	0	37.57	-24.32	36.31 - 38.84
	0	1	30.00	-12.64	29.34 - 30.65
	1	1	64.46	-7.65	64.06 - 64.86
	0	2	-2.27	-0.95	-2.32 - -2.22
	1	2	-8.88	-3.46	-9.06 - -8.70
	2	2	7.58	-2.06	7.47 - 7.69
0.75	0	0	26.47	-21.74	25.34 - 27.60
	0	1	19.09	-10.32	18.56 - 19.63
	1	1	56.92	-11.19	56.34 - 57.50
	0	2	-1.87	-1.44	-1.95 - -1.80
	1	2	-13.87	-5.81	-14.18 - -13.57
	2	2	9.22	-3.37	9.04 - 9.39

Appendix E. Groundwater Monitoring Data from French Limited Site

The data from the French Limited site that were used in the model calibration in Chapter 6 are presented in this appendix. The well coordinates and screened intervals are listed in Tables E1 and E2. The locations of the wells are plotted in Figure 6.4. Table E3 contains the benzene concentrations measured at the wells, or the reported detection limits for censored measurements, sorted by the sampling date. The benzene concentrations are plotted for each well in Appendix F, along with model-predicted concentrations.

Table E1. Wells at the French Limited site sampled before remediation.

Well Name	Well Location		Screened Interval of Well	
	X-Coordinate (m)	Y-Coordinate (m)	Elevation at Top of Screen (m)	Elevation at Bottom of Screen (m)
ERT-1	595.4	403.0	-1.46	-10.61
ERT-1A	599.2	403.7	3.02	-1.55
ERT-2	564.9	380.1	-0.49	-10.39
ERT-3	586.3	355.7	-1.04	-9.57
ERT-4	599.2	399.9	-1.28	-9.66
ERT-4A	603.0	399.9	2.87	-1.71
ERT-5	568.0	378.6	-1.19	-10.33
ERT-6	580.2	360.3	-1.22	-10.36
ERT-7	699.0	401.4	-1.16	-9.69
ERT-7A	702.1	398.4	2.80	-1.77
ERT-8	699.0	401.4	-1.68	-10.67
ERT-8A	702.1	398.4	2.77	-1.80
ERT-9	628.9	401.4	-2.19	-11.34
ERT-9A	632.0	402.2	2.96	-1.62
ERT-10	628.9	398.4	-1.59	-10.73
ERT-10A	632.0	399.2	2.96	-1.62
ERT-20	924.6	441.1	1.28	-9.39
ERT-21	790.5	459.4	1.04	-9.63
ERT-22	702.1	456.3	0.49	-11.70
ERT-23	494.8	450.2	-0.76	-12.95
ERT-24	464.4	416.7	0.00	-10.67
ERT-25	403.4	404.5	1.52	-10.67
ERT-26	336.3	413.6	0.97	-11.21
ERT-27	461.3	471.5	1.92	-10.27
ERT-28	462.8	584.3	2.99	-13.78
ERT-29	465.9	639.2	2.96	-12.28
ERT-30	464.3	691.0	2.38	-11.34
GW-3	833.1	445.6	1.89	-4.21
GW-8	906.3	395.3	1.13	-1.92
GW-9	577.1	395.3	0.58	-2.47
GW-20	601.5	483.7	1.83	-4.27
REI-3-1	772.2	596.5	-9.39	-12.44
REI-3-2	767.6	598.0	-5.40	-6.92
REI-3-3	758.5	599.6	0.55	-3.72
REI-6-1	827.1	403.0	-5.43	-11.52
REI-6-2	848.4	401.4	2.50	-3.60
REI-10-2	615.2	425.8	-6.49	-10.70
REI-10-3	597.7	409.1	-7.16	-10.30
REI-10-4	619.8	409.1	-6.40	-10.30

Table E2. Wells at the French Limited site sampled after remediation.

Well Name	Well Location		Screened Interval of Well	
	X-Coordinate (m)	Y-Coordinate (m)	Elevation at Top of Screen (m)	Elevation at Bottom of Screen (m)
FLTG-14	990.1	463.9	2.29	-3.81
INT-22	564.7	447.7	-7.25	-11.83
INT-26	695.6	435.8	-6.83	-11.40
INT-60-P-3	731.9	421.1	-8.99	-12.04
INT-101	523.8	419.7	-10.00	-13.05
INT-106	881.9	441.1	-8.87	-11.92
INT-108	769.2	439.5	-7.25	-10.30
INT-118	202.5	413.8	-6.20	-9.20
INT-120	823.6	406.0	-9.30	-12.25
INT-123	858.4	402.3	-9.30	-12.25
INT-127	848.4	421.4	-10.55	-13.50
INT-134	462.8	461.3	-4.85	-10.94
INT-135	462.2	512.7	-5.85	-11.95
INT-144	366.7	520.0	-8.56	-11.61
INT-214	595.3	447.2	-4.97	-11.06
INT-217	596.3	508.1	-6.71	-12.80
INT-233	588.6	423.0	-8.02	-14.11
S1-31	582.1	409.1	-1.68	-4.72
S1-33	558.8	448.7	-0.24	-3.29
S1-51-P-3	691.4	453.3	-1.34	-4.39
S1-106A	881.9	441.1	-1.55	-4.60
S1-108A	762.2	435.0	-0.24	-4.82
S1-118	207.5	412.8	1.37	-3.20
S1-121	901.7	395.3	-1.31	-4.27
S1-123	896.3	420.0	-3.35	-6.31
S1-131	999.9	380.1	-2.93	-5.88
S1-135	462.2	512.7	1.16	-1.89

Table E3. Benzene concentration measurements at the French Limited site. (For point measurements, the measured concentration is given. For censored measurements, the detection limit is given.)

Well Name	Sample Date	Point or Censored Measurement	Benzene Concentration or Detection Limit (g/m3)
GW-8	11/14/1981	Point	0.148
GW-8	4/14/1983	Point	0.18
GW-9	4/14/1983	Point	0.1
GW-20	11/14/1983	Point	0.006
GW-3	11/28/1983	Point	0.022
REI-6-2	7/2/1984	Point	0.121
REI-3-1	7/16/1984	Censored	0.005
REI-3-2	7/16/1984	Censored	0.005
REI-3-3	7/16/1984	Censored	0.005
REI-6-1	7/16/1984	Point	2.5
GW-3	7/16/1984	Censored	0.005
ERT-1	4/20/1987	Point	1.4
ERT-2	4/20/1987	Point	1.1
ERT-3	4/20/1987	Point	0.31
ERT-4	4/19/1987	Point	0.96
ERT-5	4/19/1987	Point	0.69
ERT-6	4/27/1987	Point	0.69
REI-10-2	8/31/1987	Point	5.3
REI-10-4	8/31/1987	Point	6.1
REI-10-2	9/27/1987	Point	6.2
REI-10-3	9/27/1987	Point	0.28
REI-10-4	9/27/1987	Point	4.2
ERT-7	11/5/1987	Point	0.97
ERT-8	11/6/1987	Point	1.7
ERT-7A	11/19/1987	Point	0.03
ERT-8A	11/19/1987	Point	0.01
ERT-9	11/19/1987	Point	1.8
ERT-9A	11/19/1987	Point	0.51
ERT-10	11/19/1987	Point	2.3
ERT-10A	11/19/1987	Point	0.54

Table E3. (continued)

Well Name	Sample Date	Point or Censored Measurement	Benzene Concentration or Detection Limit (g/m3)
ERT-1	1/4/1988	Point	1.3
ERT-1A	1/4/1988	Point	1.1
ERT-4A	1/4/1988	Point	0.61
ERT-7	1/4/1988	Point	0.16
ERT-7A	1/4/1988	Point	0.026
ERT-8	1/4/1988	Point	2
ERT-8A	1/4/1988	Point	0.018
ERT-9	1/4/1988	Point	2.9
ERT-9A	1/4/1988	Point	1.3
ERT-10	1/4/1988	Point	4.3
ERT-20	1/4/1988	Point	2.3
ERT-21	1/4/1988	Point	0.12
ERT-22	1/4/1988	Point	0.53
ERT-23	1/4/1988	Censored	0.005
ERT-24	1/4/1988	Censored	0.01
REI-3-3	1/4/1988	Censored	0.01
REI-10-2	1/4/1988	Point	6.6
REI-10-3	1/4/1988	Censored	0.01
REI-10-4	1/4/1988	Point	4.9
ERT-1	2/4/1988	Point	1.9
ERT-1A	2/4/1988	Point	1.1
ERT-2	2/4/1988	Point	0.84
ERT-3	2/4/1988	Point	0.7
ERT-4A	2/4/1988	Point	1.3
ERT-5	2/4/1988	Point	1.7
ERT-6	2/4/1988	Point	0.93
ERT-7	2/4/1988	Point	0.059
ERT-7A	2/4/1988	Point	0.045
ERT-8	2/4/1988	Point	2
ERT-8A	2/4/1988	Point	0.022
ERT-9	2/4/1988	Point	3.6
ERT-9A	2/4/1988	Point	1.1
ERT-10	2/4/1988	Point	3.3
ERT-20	2/4/1988	Point	2.2
ERT-21	2/4/1988	Point	0.11
ERT-22	2/4/1988	Point	0.95
ERT-23	2/4/1988	Censored	0.005
ERT-24	2/5/1988	Censored	0.01

Table E3. (continued)

Well Name	Sample Date	Point or Censored Measurement	Benzene Concentration or Detection Limit (g/m3)
REI-10-2	2/4/1988	Point	4.6
REI-10-3	2/4/1988	Point	1.6
REI-10-4	2/4/1988	Point	4.4
ERT-1	3/3/1988	Point	1.3
ERT-1A	3/3/1988	Point	0.91
ERT-2	3/3/1988	Point	1.2
ERT-3	3/3/1988	Point	0.49
ERT-4A	3/3/1988	Point	1.4
ERT-5	3/3/1988	Point	1.6
ERT-6	3/3/1988	Point	1.1
ERT-7	3/3/1988	Point	0.065
ERT-7A	3/3/1988	Point	0.003
ERT-8A	3/3/1988	Point	0.005
ERT-9	3/3/1988	Point	2.7
ERT-9A	3/3/1988	Point	0.96
ERT-10	3/3/1988	Point	3.8
ERT-20	3/3/1988	Point	1.8
ERT-21	3/3/1988	Point	0.078
ERT-22	3/3/1988	Point	1
ERT-23	3/3/1988	Censored	0.005
ERT-24	3/3/1988	Censored	0.005
REI-10-2	3/3/1988	Point	5.1
REI-10-3	3/3/1988	Point	0.49
REI-10-4	3/3/1988	Point	0.25
ERT-1	3/29/1988	Point	1.2
ERT-1A	3/29/1988	Point	0.93
ERT-2	3/29/1988	Point	0.28
ERT-3	3/29/1988	Point	0.58
ERT-4A	3/29/1988	Point	1.1
ERT-5	3/29/1988	Point	1.4
ERT-6	3/29/1988	Point	0.86
ERT-7	3/29/1988	Point	0.044
ERT-7A	3/29/1988	Point	0.02
ERT-8	3/29/1988	Point	0.98
ERT-8A	3/29/1988	Point	0.018
ERT-9	3/29/1988	Point	3.1
ERT-9A	3/29/1988	Point	0.61

Table E3. (continued)

Well Name	Sample Date	Point or Censored Measurement	Benzene Concentration or Detection Limit (g/m3)
ERT-10	3/29/1988	Point	3.5
ERT-20	3/29/1988	Point	2.5
ERT-21	3/29/1988	Point	0.13
ERT-22	3/29/1988	Point	1
ERT-24	3/29/1988	Censored	0.005
ERT-25	3/29/1988	Censored	0.005
ERT-27	3/29/1988	Censored	0.005
ERT-28	3/29/1988	Censored	0.005
ERT-29	3/29/1988	Censored	0.005
ERT-30	3/29/1988	Censored	0.005
REI-10-2	3/29/1988	Point	5.1
REI-10-3	3/29/1988	Point	2.2
REI-10-4	3/29/1988	Point	0.41
ERT-25	4/5/1988	Censored	0.005
ERT-26	4/5/1988	Censored	0.005
ERT-27	4/5/1988	Censored	0.005
ERT-28	4/5/1988	Censored	0.005
ERT-29	4/5/1988	Censored	0.005
ERT-30	4/5/1988	Censored	0.005
ERT-24	4/27/1988	Censored	0.005
ERT-25	4/27/1988	Censored	0.005
ERT-26	4/27/1988	Censored	0.005
ERT-27	4/27/1988	Censored	0.005
ERT-28	4/27/1988	Censored	0.005
ERT-29	4/27/1988	Censored	0.005
ERT-30	4/27/1988	Censored	0.005
ERT-1	5/25/1988	Point	1.7
ERT-2	5/25/1988	Point	1.4
ERT-3	5/25/1988	Point	0.6
ERT-5	5/25/1988	Point	1.5
ERT-6	5/25/1988	Point	0.17
ERT-7	5/25/1988	Point	0.088
ERT-8	5/25/1988	Point	0.98
ERT-9	5/25/1988	Point	3.6
ERT-10	5/25/1988	Point	3.4
ERT-20	5/25/1988	Point	2.5
ERT-21	5/25/1988	Point	0.47
ERT-22	5/25/1988	Point	0.84

Table E3. (continued)

Well Name	Sample Date	Point or Censored Measurement	Benzene Concentration or Detection Limit (g/m3)
ERT-23	5/25/1988	Censored	0.005
ERT-24	5/25/1988	Censored	0.005
ERT-25	5/25/1988	Censored	0.005
ERT-26	5/25/1988	Censored	0.005
ERT-27	5/25/1988	Censored	0.005
ERT-28	5/25/1988	Censored	0.005
ERT-29	5/25/1988	Censored	0.005
ERT-30	5/25/1988	Censored	0.005
REI-10-2	5/25/1988	Point	5.6
REI-10-3	5/25/1988	Point	2.6
REI-10-4	5/25/1988	Point	3.4
ERT-1	6/22/1988	Point	1.2
ERT-2	6/22/1988	Point	1.3
ERT-3	6/22/1988	Point	0.7
ERT-5	6/22/1988	Point	0.89
ERT-6	6/22/1988	Point	0.82
ERT-7	6/22/1988	Point	0.088
ERT-8	6/22/1988	Point	0.82
ERT-9	6/22/1988	Point	3.2
ERT-10	6/22/1988	Point	3.2
ERT-20	6/22/1988	Point	2.4
ERT-21	6/22/1988	Point	0.25
ERT-22	6/22/1988	Point	0.89
ERT-23	6/22/1988	Censored	0.005
ERT-24	6/22/1988	Censored	0.005
ERT-25	6/22/1988	Censored	0.005
ERT-26	6/22/1988	Censored	0.005
ERT-27	6/22/1988	Censored	0.005
ERT-28	6/22/1988	Censored	0.005
ERT-29	6/22/1988	Censored	0.005
ERT-30	6/22/1988	Censored	0.005
REI-10-2	6/22/1988	Point	4.8
REI-10-3	6/22/1988	Point	2.5
REI-10-4	6/22/1988	Point	3.1

Table E3. (continued)

Well Name	Sample Date	Point or Censored Measurement	Benzene Concentration or Detection Limit (g/m3)
ERT-1	7/21/1988	Point	2.1
ERT-1A	7/21/1988	Point	0.1
ERT-2	7/21/1988	Point	1.3
ERT-3	7/21/1988	Point	0.93
ERT-4A	7/21/1988	Point	0.2
ERT-5	7/21/1988	Point	1.3
ERT-6	7/21/1988	Point	0.74
ERT-7	7/21/1988	Point	0.39
ERT-7A	7/21/1988	Point	0.04
ERT-8	7/21/1988	Point	0.67
ERT-8A	7/21/1988	Point	0.007
ERT-9	7/21/1988	Point	3.5
ERT-9A	7/21/1988	Point	2.6
ERT-10	7/21/1988	Point	3
ERT-20	7/21/1988	Point	2.3
ERT-21	7/21/1988	Point	0.32
ERT-22	7/21/1988	Point	1.1
ERT-23	7/21/1988	Censored	0.005
ERT-24	7/21/1988	Censored	0.005
ERT-25	7/21/1988	Censored	0.005
ERT-26	7/21/1988	Censored	0.005
ERT-27	7/21/1988	Censored	0.005
ERT-28	7/21/1988	Censored	0.005
ERT-29	7/21/1988	Censored	0.005
ERT-30	7/21/1988	Censored	0.005
REI-10-2	7/21/1988	Point	6.5
REI-10-3	7/21/1988	Point	2.6
REI-10-4	7/21/1988	Point	4.5
ERT-1	11/15/1988	Point	2
ERT-2	11/18/1988	Point	1.1
ERT-3	11/18/1988	Point	1
ERT-8	11/18/1988	Point	1.3
ERT-10	11/18/1988	Point	3.8
ERT-20	11/18/1988	Point	1.8
ERT-21	11/18/1988	Point	0.26
ERT-22	11/18/1988	Point	1

Table E3. (continued)

Well Name	Sample Date	Point or Censored Measurement	Benzene Concentration or Detection Limit (g/m ³)
ERT-23	11/18/1988	Censored	0.005
ERT-24	11/18/1988	Censored	0.005
ERT-25	11/18/1988	Censored	0.005
ERT-26	11/18/1988	Censored	0.005
ERT-27	11/18/1988	Censored	0.005
ERT-28	11/18/1988	Censored	0.005
ERT-29	11/18/1988	Censored	0.005
ERT-30	11/18/1988	Censored	0.005
REI-10-3	11/18/1988	Point	2.4
REI-10-4	11/18/1988	Point	3.9
ERT-1	12/7/1989	Point	1.8
ERT-2	12/7/1989	Point	1.0
ERT-3	12/7/1989	Point	1.1
ERT-8	12/7/1989	Point	0.9
ERT-10	12/7/1989	Point	3.2
ERT-23	12/7/1989	Censored	0.005
ERT-24	12/7/1989	Censored	0.005
ERT-27	12/7/1989	Censored	0.005
ERT-28	12/7/1989	Censored	0.005
ERT-29	12/7/1989	Censored	0.005
INT-118	1/15/1996	Censored	0.0003
INT-144	1/15/1996	Censored	0.0003
S1-106A	1/15/1996	Censored	0.0003
S1-108A	1/15/1996	Censored	0.0003
S1-118	1/15/1996	Censored	0.0003
S1-135	1/15/1996	Censored	0.0003
FLTG-13	1/16/1996	Censored	0.0003
FLTG-14	1/16/1996	Censored	0.0003
INT-108	1/16/1996	Censored	0.0003
INT-217	1/16/1996	Point	0.022
S1-33	1/16/1996	Censored	0.0003
INT-22	1/17/1996	Point	0.044
INT-26	1/17/1996	Point	0.18
INT-106	1/17/1996	Censored	0.0003
INT-135	1/17/1996	Censored	0.0003
S1-31	1/17/1996	Censored	0.0003

Table E3. (continued)

Well Name	Sample Date	Point or Censored Measurement	Benzene Concentration or Detection Limit (g/m3)
INT-60-P-3	1/18/1996	Censored	0.0003
INT-134	1/18/1996	Point	0.034
INT-214	1/18/1996	Censored	0.0003
S1-51-P-3	1/18/1996	Censored	0.0003
S1-121	1/18/1996	Censored	0.0003
INT-101	1/22/1996	Point	0.12
INT-127	1/22/1996	Point	0.15
INT-120	1/23/1996	Censored	0.015
INT-123	1/23/1996	Censored	0.0003
INT-233	1/23/1996	Point	0.74
S1-123	1/23/1996	Censored	0.0003
S1-131	1/23/1996	Point	0.008
FLTG-13	4/12/1996	Censored	0.0003
FLTG-14	4/12/1996	Point	0.007
INT-22	4/12/1996	Censored	0.0003
INT-26	4/12/1996	Point	0.098
INT-60-P-3	4/12/1996	Point	0.025
INT-101	4/12/1996	Point	0.036
INT-106	4/12/1996	Point	0.006
INT-108	4/12/1996	Censored	0.0003
INT-118	4/12/1996	Censored	0.0003
INT-120	4/12/1996	Point	0.005
INT-123	4/12/1996	Censored	0.0006
INT-127	4/12/1996	Point	0.16
INT-134	4/12/1996	Point	0.027
INT-135	4/12/1996	Censored	0.0003
INT-144	4/12/1996	Censored	0.0003
INT-214	4/12/1996	Censored	0.0003
INT-217	4/12/1996	Point	0.051
INT-233	4/12/1996	Point	0.37
S1-31	4/12/1996	Censored	0.0003
S1-33	4/12/1996	Censored	0.0003
S1-51-P-3	4/12/1996	Censored	0.0003
S1-106A	4/12/1996	Censored	0.0003

Table E3. (continued)

Well Name	Sample Date	Point or Censored Measurement	Benzene Concentration or Detection Limit (g/m3)
S1-108A	4/12/1996	Point	0.004
S1-118	4/12/1996	Censored	0.0003
S1-121	4/12/1996	Point	0.005
S1-123	4/12/1996	Censored	0.003
S1-131	4/12/1996	Point	0.021
S1-135	4/12/1996	Point	0.003
FLTG-13	7/22/1996	Censored	0.0003
FLTG-14	7/22/1996	Censored	0.0003
INT-22	7/22/1996	Censored	0.0003
INT-26	7/22/1996	Point	0.1
INT-60-P-3	7/22/1996	Censored	0.0003
INT-101	7/22/1996	Point	0.036
INT-106	7/22/1996	Point	0.004
INT-108	7/22/1996	Censored	0.0003
INT-118	7/22/1996	Censored	0.0003
INT-120	7/22/1996	Point	0.003
INT-123	7/22/1996	Point	0.002
INT-127	7/22/1996	Point	0.17
INT-134	7/22/1996	Point	0.054
INT-135	7/22/1996	Censored	0.0003
INT-144	7/22/1996	Censored	0.0003
INT-214	7/22/1996	Censored	0.0003
INT-217	7/22/1996	Point	0.016
INT-233	7/22/1996	Point	0.35
S1-31	7/22/1996	Censored	0.0003
S1-33	7/22/1996	Censored	0.0003
S1-51-P-3	7/22/1996	Censored	0.0003
S1-106A	7/22/1996	Censored	0.0003
S1-108A	7/22/1996	Censored	0.0003
S1-118	7/22/1996	Censored	0.0003
S1-121	7/22/1996	Point	0.004
S1-123	7/22/1996	Censored	0.003
S1-131	7/22/1996	Point	0.031
S1-135	7/22/1996	Censored	0.0003
S1-118	10/4/1996	Censored	0.005
S1-135	10/4/1996	Censored	0.005
FLTG-13	10/7/1996	Censored	0.005
FLTG-14	10/7/1996	Censored	0.005

Table E3. (continued)

Well Name	Sample Date	Point or Censored Measurement	Benzene Concentration or Detection Limit (g/m3)
INT-22	10/7/1996	Point	0.004
INT-26	10/7/1996	Point	0.075
INT-60-P-3	10/7/1996	Censored	0.005
INT-101	10/7/1996	Point	0.033
INT-106	10/7/1996	Point	0.01
INT-108	10/7/1996	Censored	0.005
INT-118	10/7/1996	Censored	0.005
INT-120	10/7/1996	Point	0.005
INT-123	10/7/1996	Point	0.005
INT-127	10/7/1996	Point	0.2
INT-134	10/7/1996	Point	0.056
INT-135	10/7/1996	Censored	0.005
INT-144	10/7/1996	Censored	0.005
INT-214	10/7/1996	Censored	0.005
INT-217	10/7/1996	Point	0.022
INT-233	10/7/1996	Point	0.5
S1-31	10/7/1996	Censored	0.005
S1-33	10/7/1996	Censored	0.005
S1-51-P-3	10/7/1996	Censored	0.005
S1-106A	10/7/1996	Censored	0.005
S1-108A	10/7/1996	Censored	0.005
S1-121	10/7/1996	Censored	0.005
S1-123	10/7/1996	Censored	0.005
S1-131	10/7/1996	Point	0.032
FLTG-13	1/24/1997	Censored	0.002
FLTG-14	1/24/1997	Censored	0.005
INT-22	1/24/1997	Censored	0.005
INT-26	1/24/1997	Point	0.024
INT-60-P-3	1/24/1997	Censored	0.005
INT-101	1/24/1997	Point	0.009
INT-106	1/24/1997	Point	0.005
INT-108	1/24/1997	Censored	0.005
INT-118	1/24/1997	Censored	0.005
INT-120	1/24/1997	Censored	0.004
INT-123	1/24/1997	Point	0.028
INT-127	1/24/1997	Point	0.18
INT-134	1/24/1997	Point	0.044

Table E3. (continued)

Well Name	Sample Date	Point or Censored Measurement	Benzene Concentration or Detection Limit (g/m3)
INT-135	1/24/1997	Censored	0.005
INT-144	1/24/1997	Censored	0.005
INT-214	1/24/1997	Censored	0.005
INT-217	1/24/1997	Point	0.018
INT-233	1/24/1997	Censored	0.005
S1-31	1/24/1997	Censored	0.005
S1-33	1/24/1997	Censored	0.005
S1-51-P-3	1/24/1997	Censored	0.005
S1-106A	1/24/1997	Censored	0.005
S1-108A	1/24/1997	Censored	0.005
S1-118	1/24/1997	Censored	0.005
S1-121	1/24/1997	Censored	0.005
S1-123	1/24/1997	Censored	0.005
S1-131	1/24/1997	Censored	0.003
S1-135	1/24/1997	Censored	0.005
FLTG-13	4/14/1997	Censored	0.005
FLTG-14	4/14/1997	Censored	0.005
INT-60-P-3	4/14/1997	Censored	0.005
INT-108	4/14/1997	Censored	0.005
INT-118	4/14/1997	Censored	0.005
INT-135	4/14/1997	Censored	0.005
INT-144	4/14/1997	Censored	0.005
INT-214	4/14/1997	Censored	0.005
S1-31	4/14/1997	Censored	0.005
S1-33	4/14/1997	Censored	0.005
S1-51-P-3	4/14/1997	Censored	0.005
INT-22	4/15/1997	Censored	0.005
INT-101	4/15/1997	Censored	0.005
INT-106	4/15/1997	Censored	0.005
INT-120	4/15/1997	Point	0.013
INT-217	4/15/1997	Censored	0.005
S1-106A	4/15/1997	Censored	0.005
S1-108A	4/15/1997	Censored	0.005
S1-118	4/15/1997	Censored	0.005
S1-121	4/15/1997	Point	0.012
S1-123	4/15/1997	Censored	0.005
S1-131	4/15/1997	Censored	0.004
S1-135	4/15/1997	Censored	0.005

Table E3. (continued)

Well Name	Sample Date	Point or Censored Measurement	Benzene Concentration or Detection Limit (g/m3)
INT-26	4/16/1997	Point	0.024
INT-123	4/16/1997	Censored	0.005
INT-127	4/16/1997	Point	0.065
INT-134	4/16/1997	Point	0.019
INT-233	4/16/1997	Point	0.1
FLTG-13	7/14/1997	Censored	0.005
FLTG-14	7/14/1997	Censored	0.005
INT-60-P-3	7/14/1997	Censored	0.005
INT-108	7/14/1997	Censored	0.005
INT-118	7/14/1997	Censored	0.005
INT-135	7/14/1997	Censored	0.005
INT-22	7/15/1997	Censored	0.005
INT-144	7/15/1997	Censored	0.005
INT-214	7/15/1997	Censored	0.005
S1-31	7/15/1997	Censored	0.005
S1-33	7/15/1997	Censored	0.005
S1-51-P-3	7/15/1997	Censored	0.005
S1-106A	7/15/1997	Point	0.008
S1-108A	7/15/1997	Censored	0.005
S1-118	7/15/1997	Censored	0.005
S1-121	7/15/1997	Censored	0.003
S1-123	7/15/1997	Point	0.069
S1-131	7/15/1997	Point	0.021
S1-135	7/15/1997	Censored	0.005
INT-26	7/16/1997	Point	0.038
INT-101	7/16/1997	Point	0.011
INT-106	7/16/1997	Censored	0.005
INT-120	7/16/1997	Censored	0.004
INT-123	7/16/1997	Censored	0.005
INT-127	7/16/1997	Point	0.067
INT-134	7/16/1997	Point	0.03
INT-217	7/16/1997	Point	0.016
INT-233	7/16/1997	Point	0.18
FLTG-13	10/14/1997	Censored	0.005
FLTG-14	10/14/1997	Censored	0.005

Table E3. (continued)

Well Name	Sample Date	Point or Censored Measurement	Benzene Concentration or Detection Limit (g/m3)
INT-22	10/14/1997	Censored	0.005
INT-26	10/14/1997	Point	0.089
INT-101	10/14/1997	Point	0.009
INT-108	10/14/1997	Censored	0.005
INT-118	10/14/1997	Censored	0.005
INT-134	10/14/1997	Point	0.033
INT-135	10/14/1997	Censored	0.005
INT-144	10/14/1997	Censored	0.005
INT-214	10/14/1997	Censored	0.005
S1-33	10/14/1997	Censored	0.005
S1-51-P-3	10/14/1997	Censored	0.005
S1-108A	10/14/1997	Censored	0.005
S1-118	10/14/1997	Censored	0.005
S1-135	10/14/1997	Censored	0.005
INT-60-P-3	10/15/1997	Censored	0.005
INT-106	10/15/1997	Censored	0.003
INT-120	10/15/1997	Point	0.044
INT-123	10/15/1997	Censored	0.005
INT-127	10/15/1997	Censored	0.005
INT-217	10/15/1997	Point	0.014
INT-233	10/15/1997	Point	0.23
S1-31	10/15/1997	Censored	0.005
S1-106A	10/15/1997	Censored	0.005
S1-123	10/15/1997	Censored	0.025
S1-131	10/15/1997	Point	0.021
S1-123	10/31/1997	Censored	2.5
S1-121	11/5/1997	Censored	0.005
FLTG-13	1/19/1998	Censored	0.005
INT-60-P-3	1/19/1998	Censored	0.005
INT-108	1/19/1998	Censored	0.005
INT-118	1/19/1998	Censored	0.005
INT-135	1/19/1998	Censored	0.005
INT-144	1/19/1998	Censored	0.005
INT-214	1/19/1998	Censored	0.005
S1-31	1/19/1998	Censored	0.005
S1-33	1/19/1998	Censored	0.005
S1-51-P-3	1/19/1998	Censored	0.005

Table E3. (continued)

Well Name	Sample Date	Point or Censored Measurement	Benzene Concentration or Detection Limit (g/m ³)
FLTG-14	1/20/1998	Censored	0.005
INT-22	1/20/1998	Censored	0.005
S1-106A	1/20/1998	Censored	0.005
S1-108A	1/20/1998	Censored	0.005
S1-118	1/20/1998	Censored	0.005
S1-121	1/20/1998	Censored	0.002
S1-123	1/20/1998	Censored	0.005
S1-135	1/20/1998	Censored	0.005
INT-26	1/21/1998	Point	0.005
INT-101	1/21/1998	Censored	0.005
INT-106	1/21/1998	Censored	0.005
INT-120	1/21/1998	Point	0.009
INT-217	1/21/1998	Censored	0.002
S1-131	1/21/1998	Point	0.006
INT-123	1/22/1998	Censored	0.01
INT-127	1/22/1998	Censored	0.005
INT-134	1/22/1998	Point	0.025
INT-233	1/22/1998	Point	0.24
INT-108	2/12/1998	Censored	0.005
INT-135	2/12/1998	Censored	0.005
INT-214	2/12/1998	Censored	0.005
S1-33	2/12/1998	Censored	0.005
S1-108A	2/12/1998	Censored	0.005
S1-135	2/12/1998	Censored	0.005
FLTG-14	2/13/1998	Censored	0.005
INT-22	2/13/1998	Censored	0.005
INT-118	2/13/1998	Censored	0.005
INT-144	2/13/1998	Censored	0.005
S1-31	2/13/1998	Censored	0.005
S1-51-P-3	2/13/1998	Censored	0.005
S1-118	2/13/1998	Censored	0.005
S1-121	2/13/1998	Censored	0.002
FLTG-13	2/15/1998	Censored	0.005
INT-60-P-3	2/15/1998	Censored	0.005
S1-106A	2/15/1998	Point	0.006

Table E3. (continued)

Well Name	Sample Date	Point or Censored Measurement	Benzene Concentration or Detection Limit (g/m3)
INT-26	2/17/1998	Point	0.049
INT-101	2/17/1998	Point	0.005
INT-106	2/17/1998	Censored	0.005
INT-217	2/17/1998	Point	0.011
S1-131	2/17/1998	Point	0.058
INT-120	2/18/1998	Censored	0.006
INT-127	2/18/1998	Point	0.005
INT-134	2/18/1998	Point	0.041
INT-233	2/18/1998	Point	0.24
S1-123	2/18/1998	Point	0.25
INT-123	2/19/1998	Censored	0.005

Appendix F. Measured and Calculated Groundwater Concentrations

This appendix contains graphs of the measured and model-predicted benzene concentrations for all of the wells at the French Limited site that were sampled both before and after remediation. As discussed in Section 7.4.6, the model-predicted concentrations are calculated in two ways: with or without conditioning on the previous measurements. Without conditioning, the concentration is calculated with the groundwater model with the updated model parameters. With conditioning, the previously measured concentrations are combined with the calculated concentration, as shown in Equation 4.18. In all of the graphs in this appendix, the measured concentrations that were censored are plotted at the reported detection limit. These points are shown on the graphs with the data marker outlined.

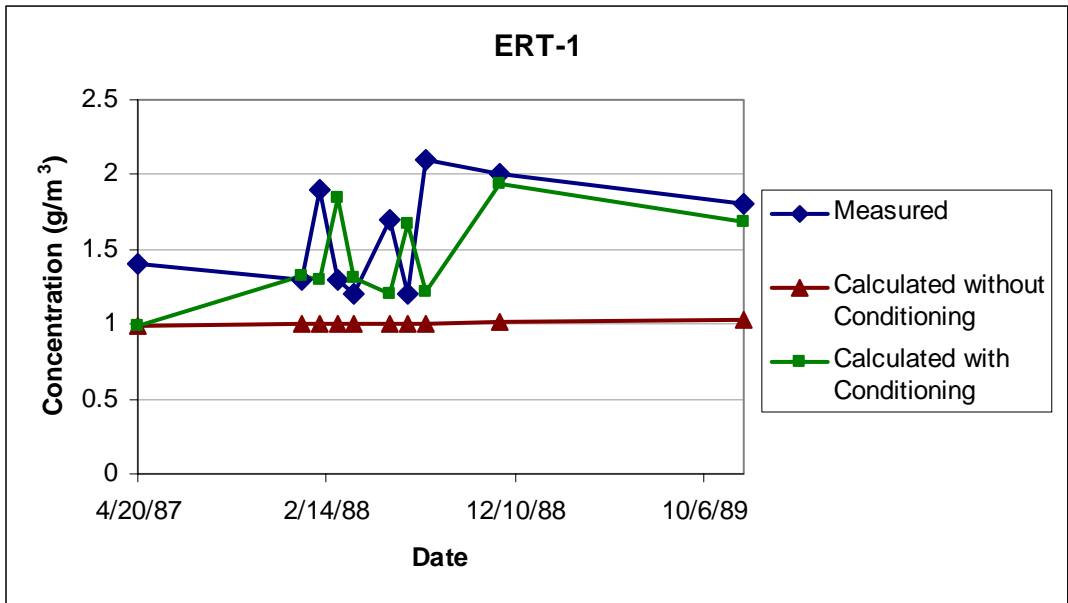


Figure F1. Comparison of measured and calculated benzene concentrations for well ERT-1.

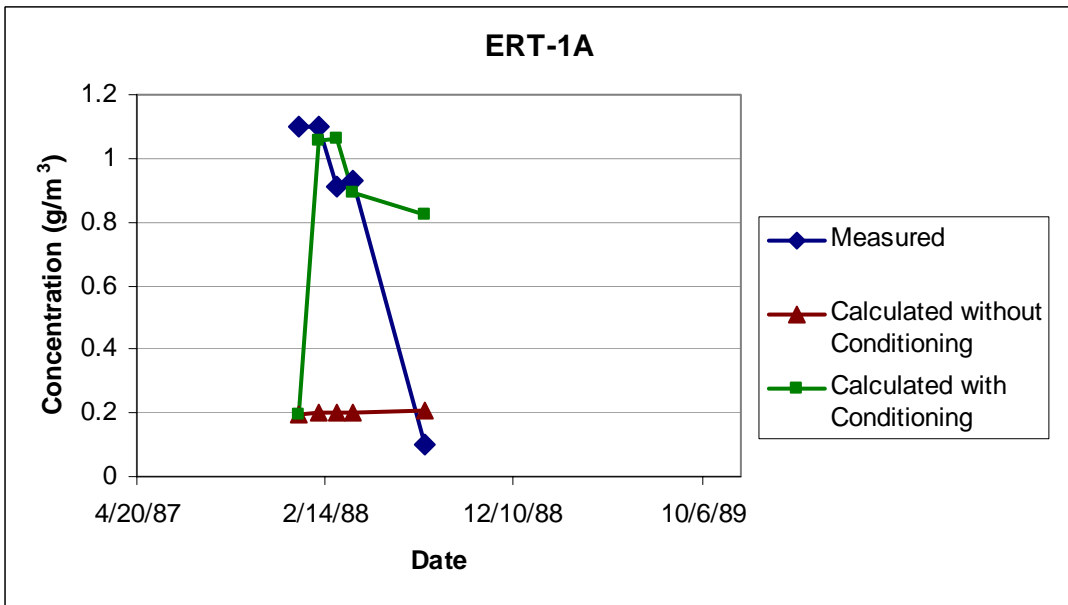


Figure F2. Comparison of measured and calculated benzene concentrations for well ERT-1A.

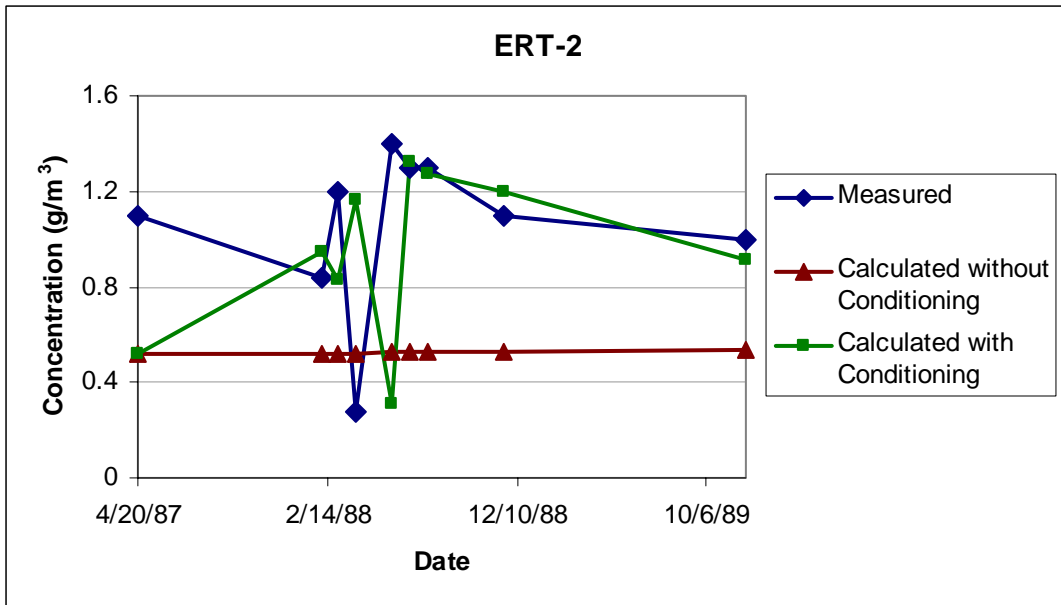


Figure F3. Comparison of measured and calculated benzene concentrations for well ERT-2.

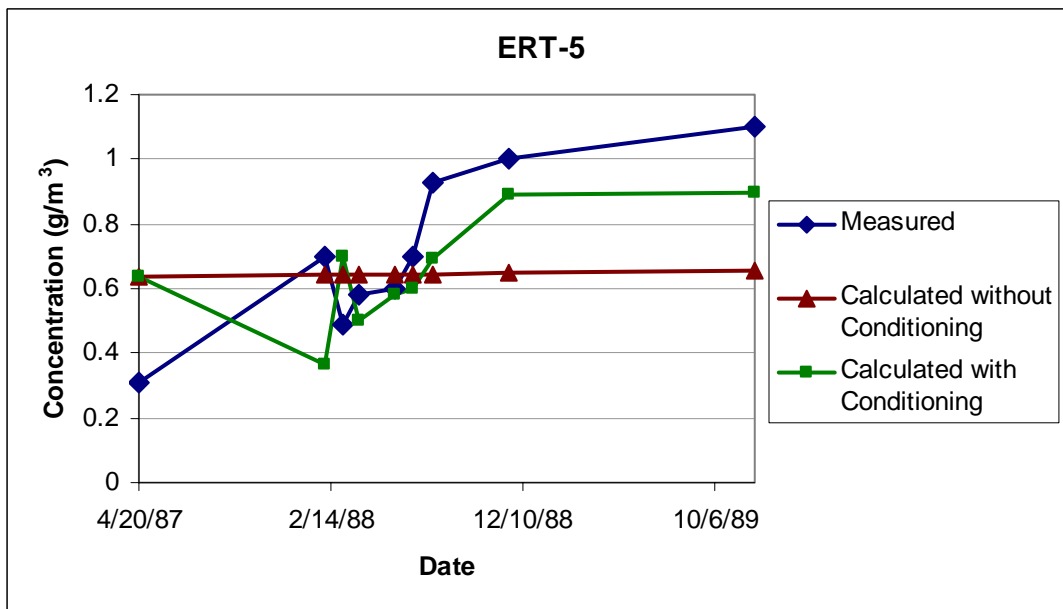


Figure F4. Comparison of measured and calculated benzene concentrations for well ERT-5.

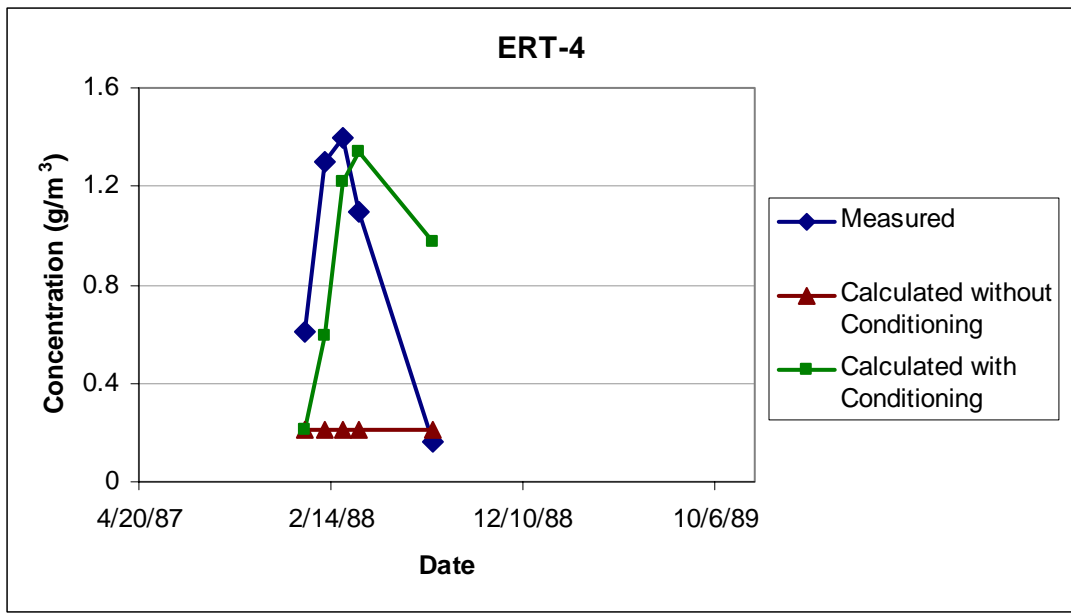


Figure F5. Comparison of measured and calculated benzene concentrations for well ERT-4.

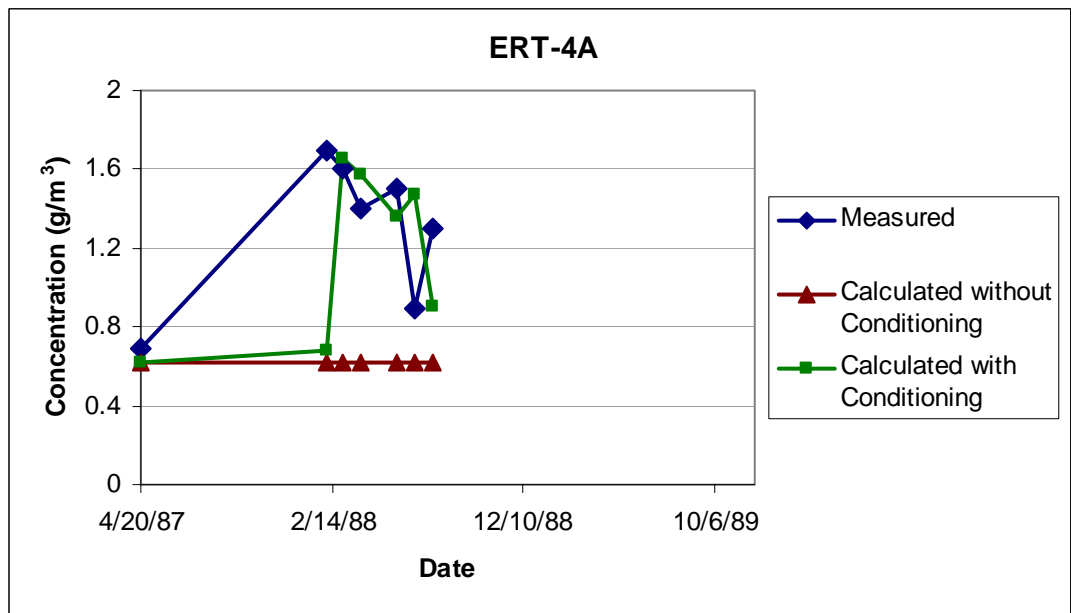


Figure F6. Comparison of measured and calculated benzene concentrations for well ERT-4A.

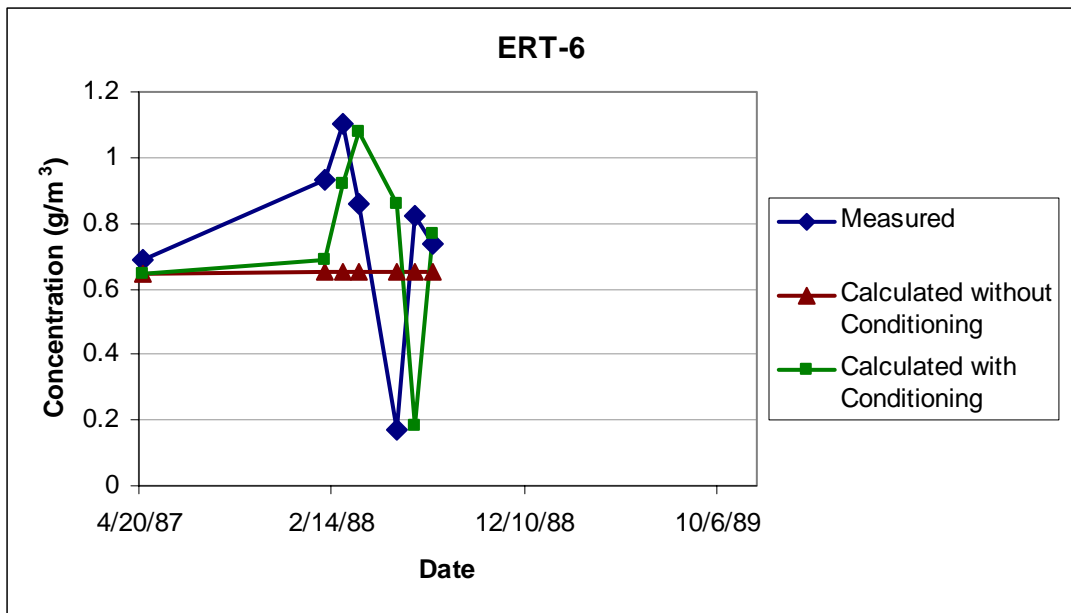


Figure F7. Comparison of measured and calculated benzene concentrations for well ERT-6.

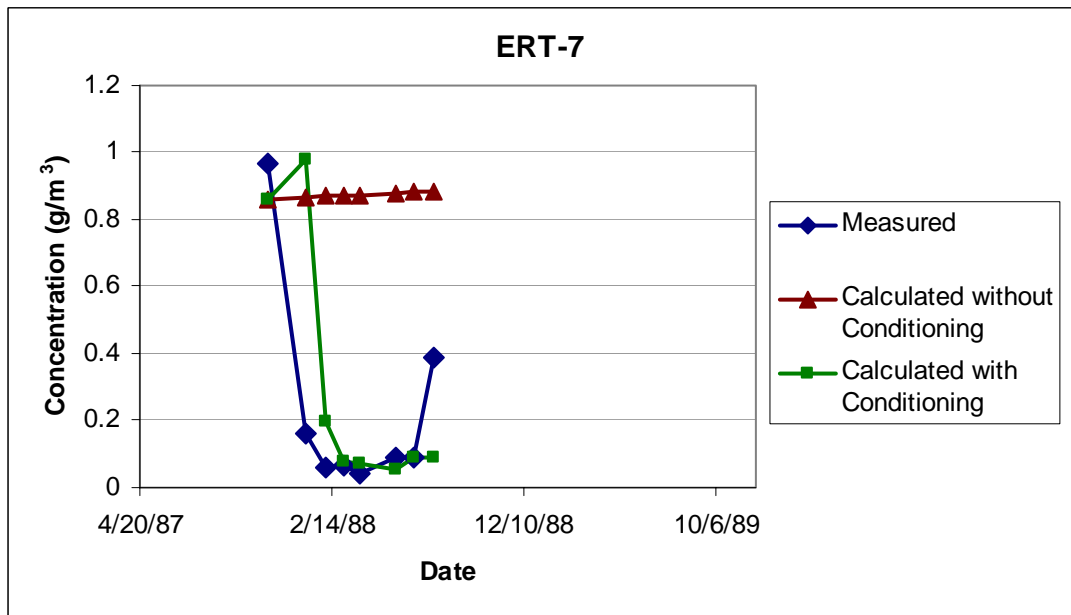


Figure F8. Comparison of measured and calculated benzene concentrations for well ERT-7.

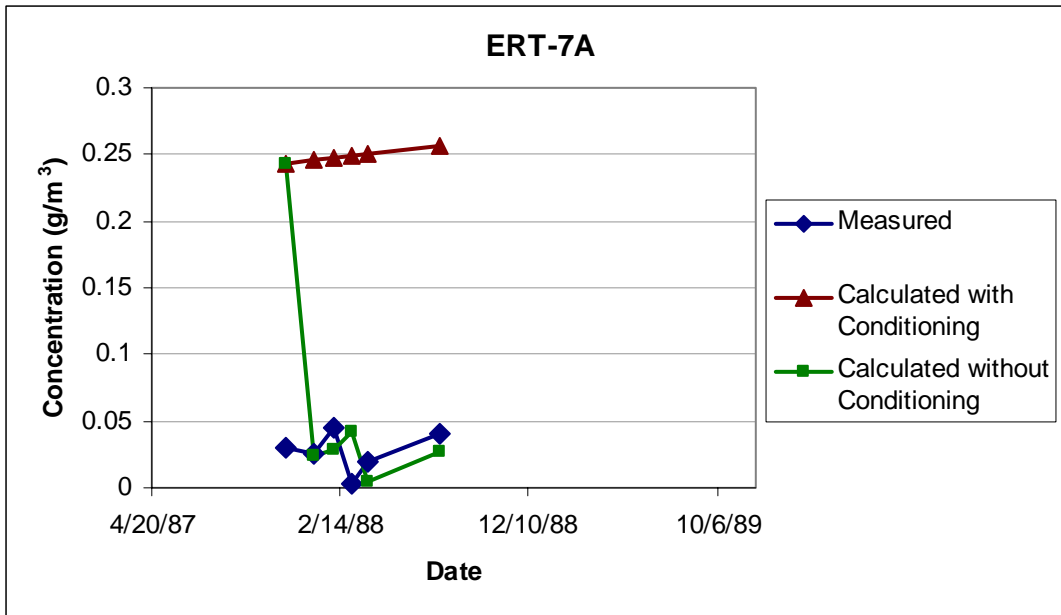


Figure F9. Comparison of measured and calculated benzene concentrations for well ERT-7A.

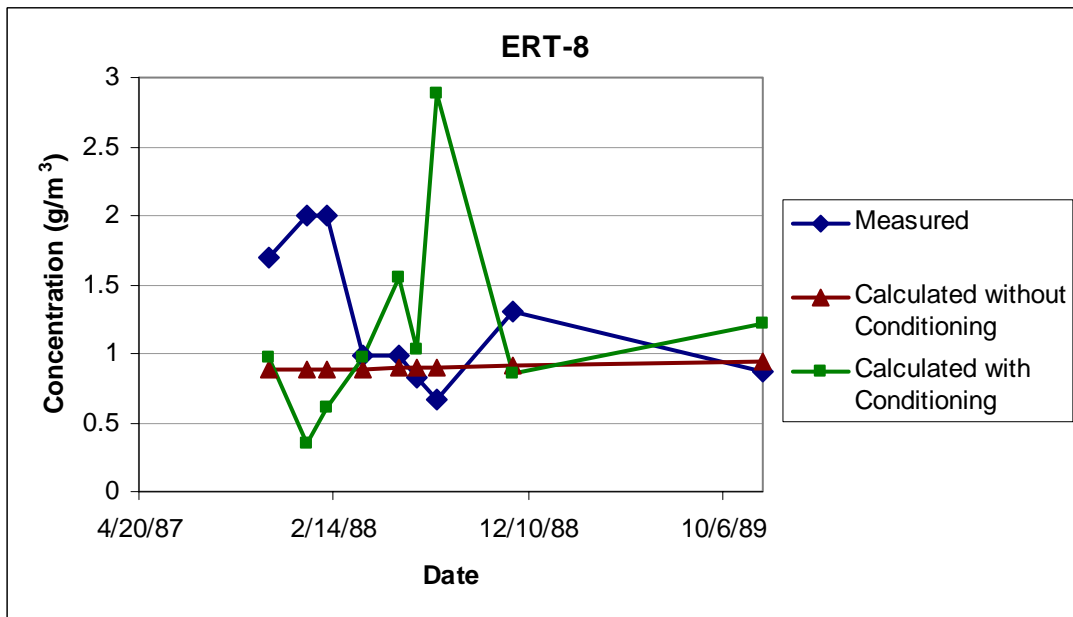


Figure F10. Comparison of measured and calculated benzene concentrations for well ERT-8.

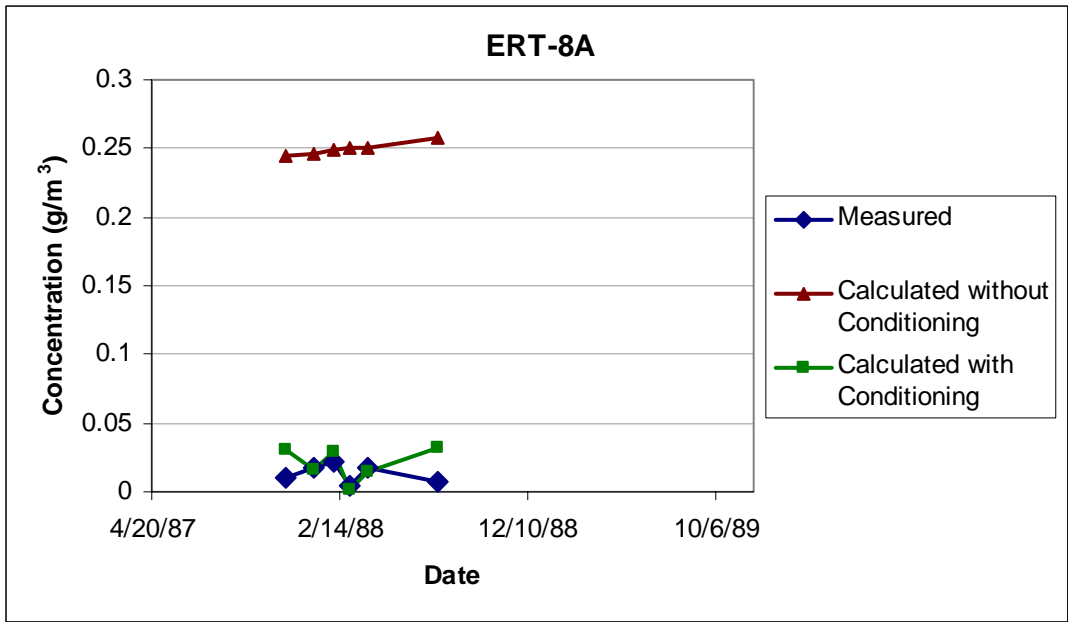


Figure F11. Comparison of measured and calculated benzene concentrations for well ERT-8A.

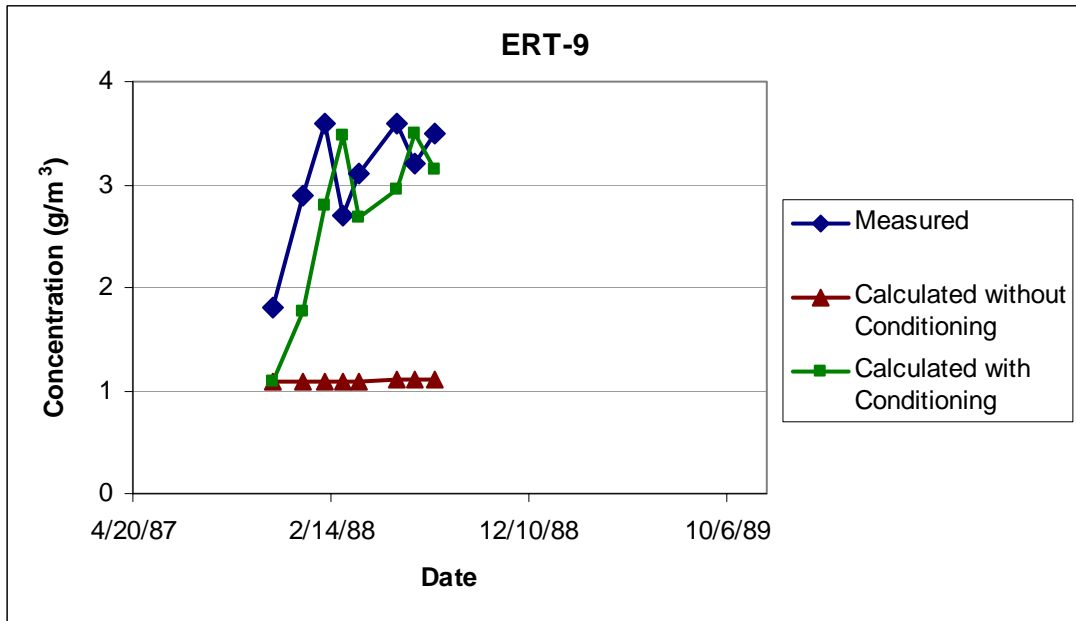


Figure F12. Comparison of measured and calculated benzene concentrations for well ERT-9.

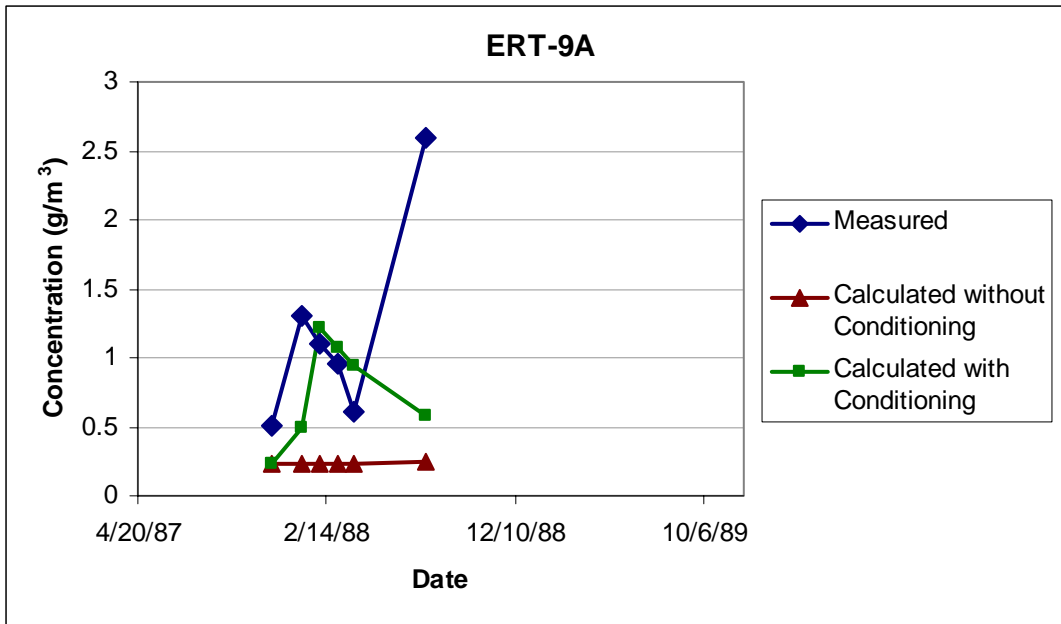


Figure F13. Comparison of measured and calculated benzene concentrations for well ERT-9A.

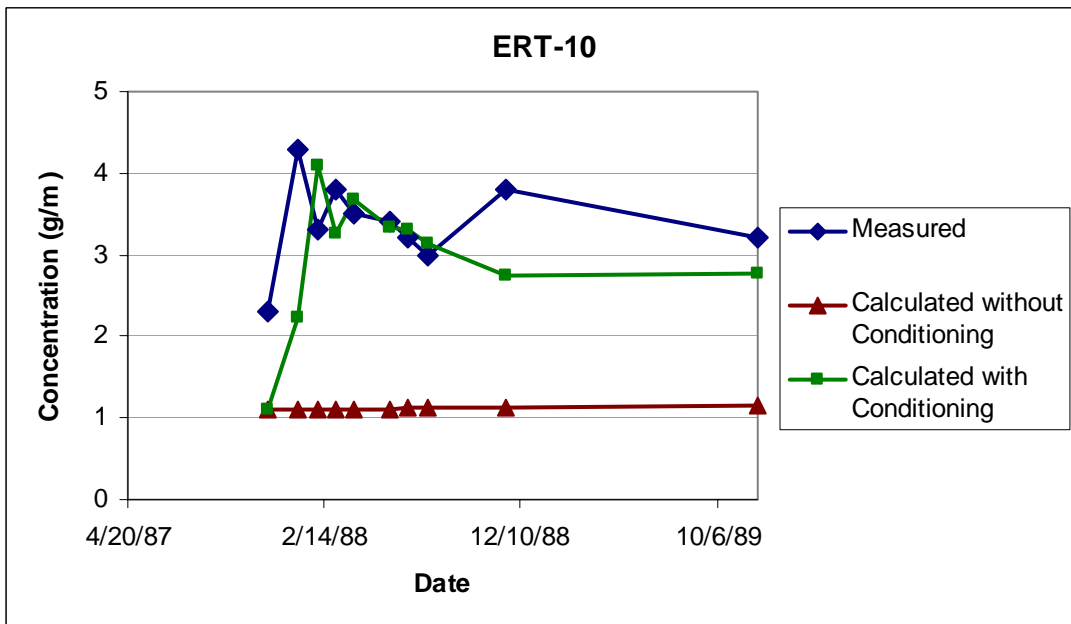


Figure F14. Comparison of measured and calculated benzene concentrations for well ERT-10.

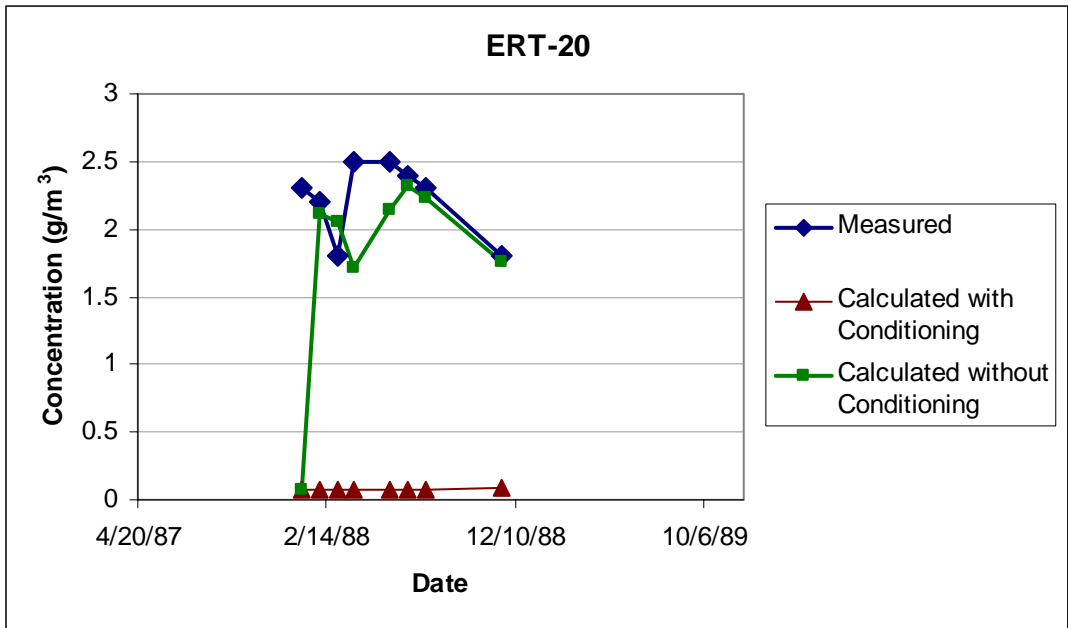


Figure F15. Comparison of measured and calculated benzene concentrations for well ERT-20.

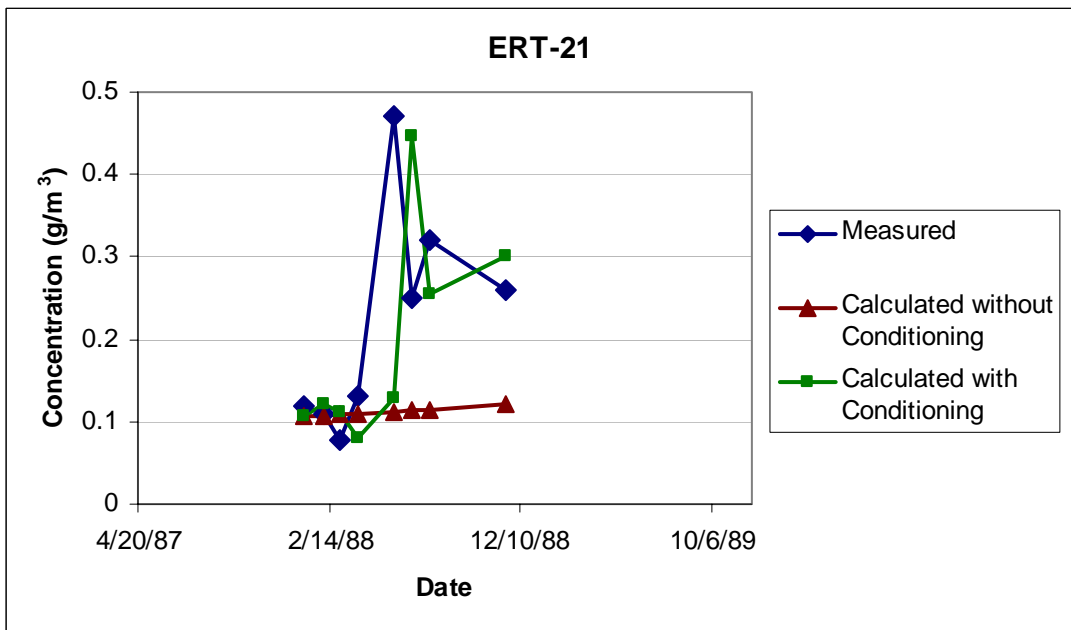


Figure F16. Comparison of measured and calculated benzene concentrations for well ERT-21.

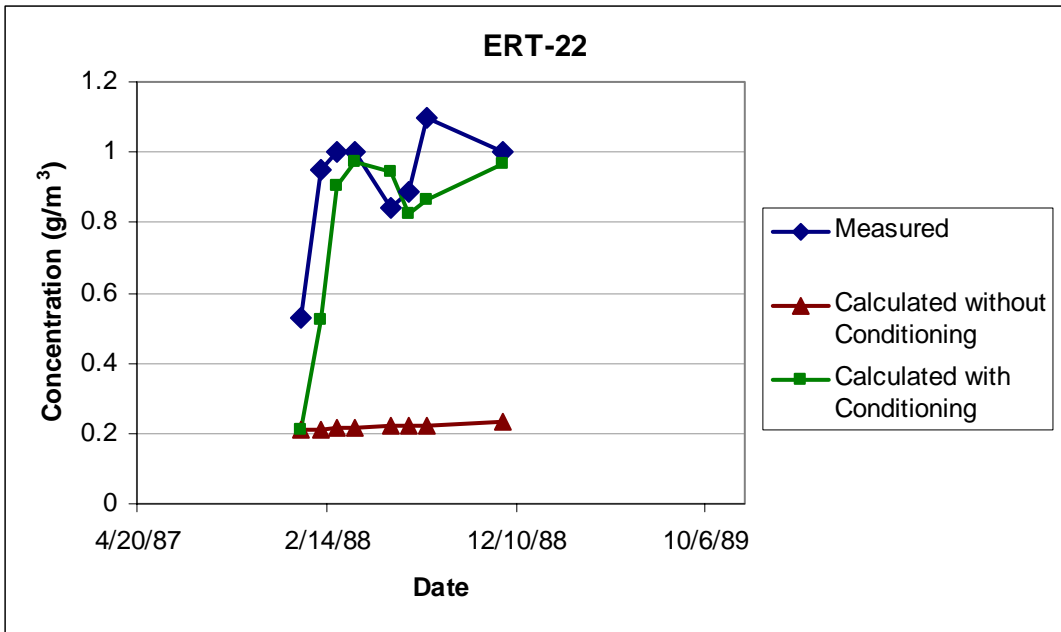


Figure F17. Comparison of measured and calculated benzene concentrations for well ERT-22.

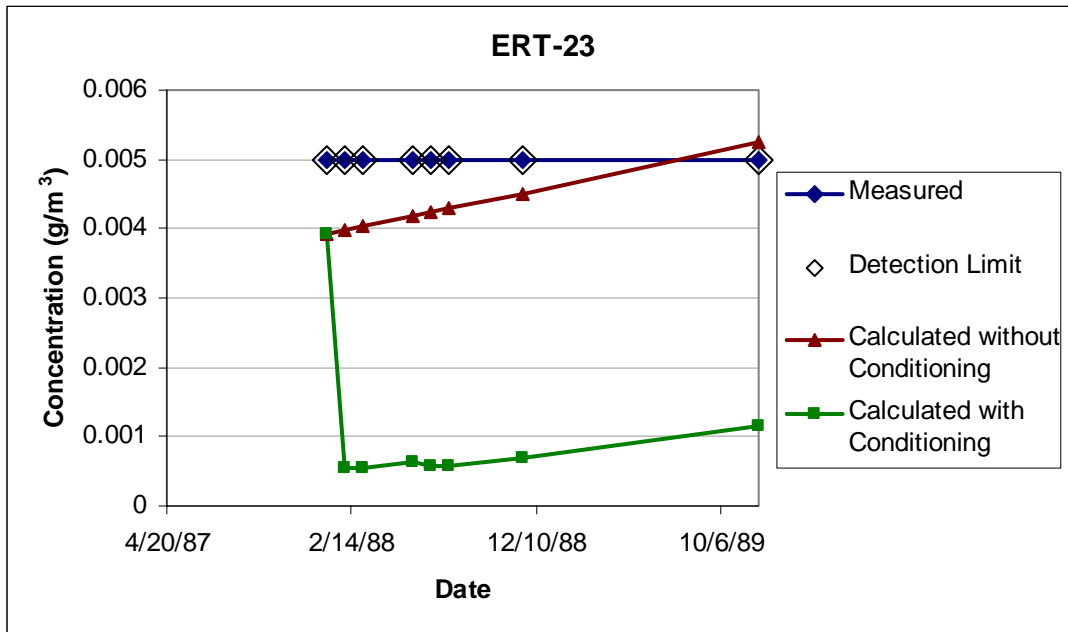


Figure F18. Comparison of measured and calculated benzene concentrations for well ERT-23.

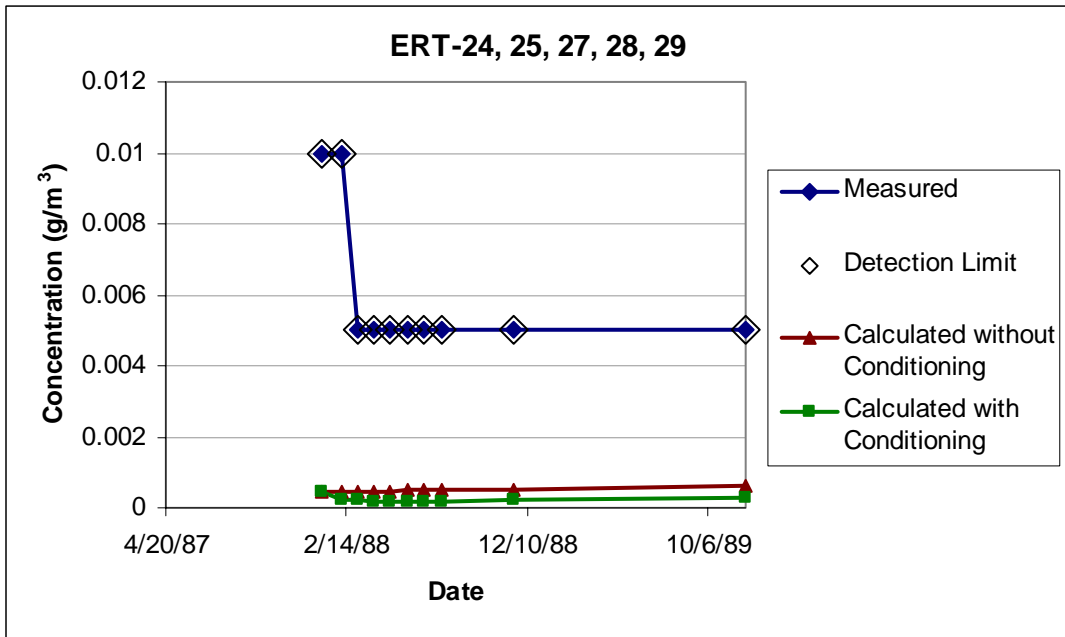
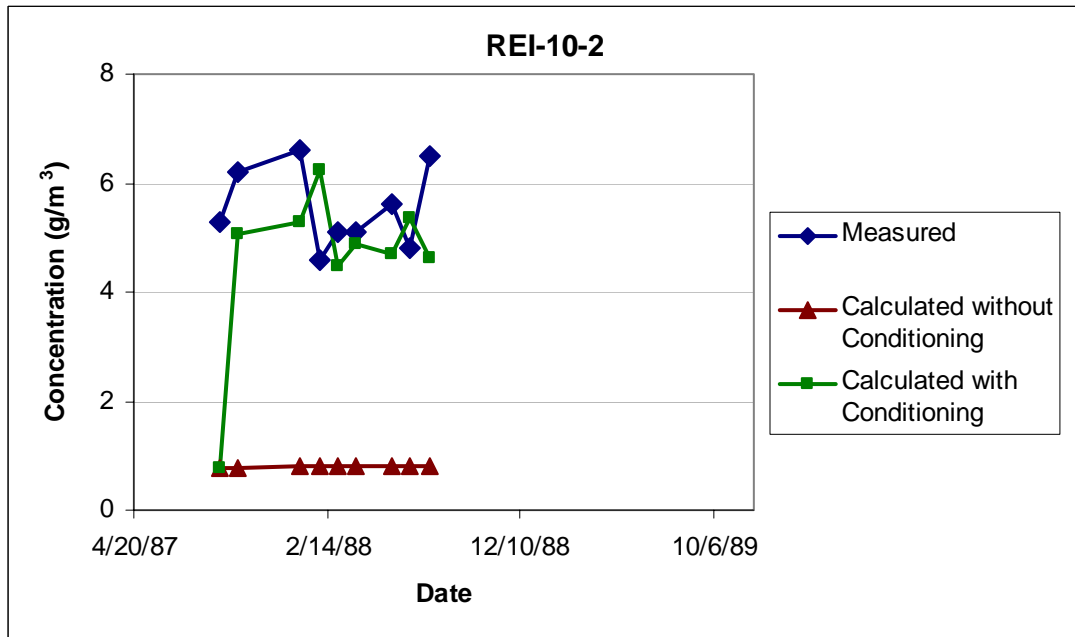


Figure F19. Comparison of measured and calculated benzene concentrations for wells ERT-24, ERT-25, ERT-27, ERT-28, and ERT-29.



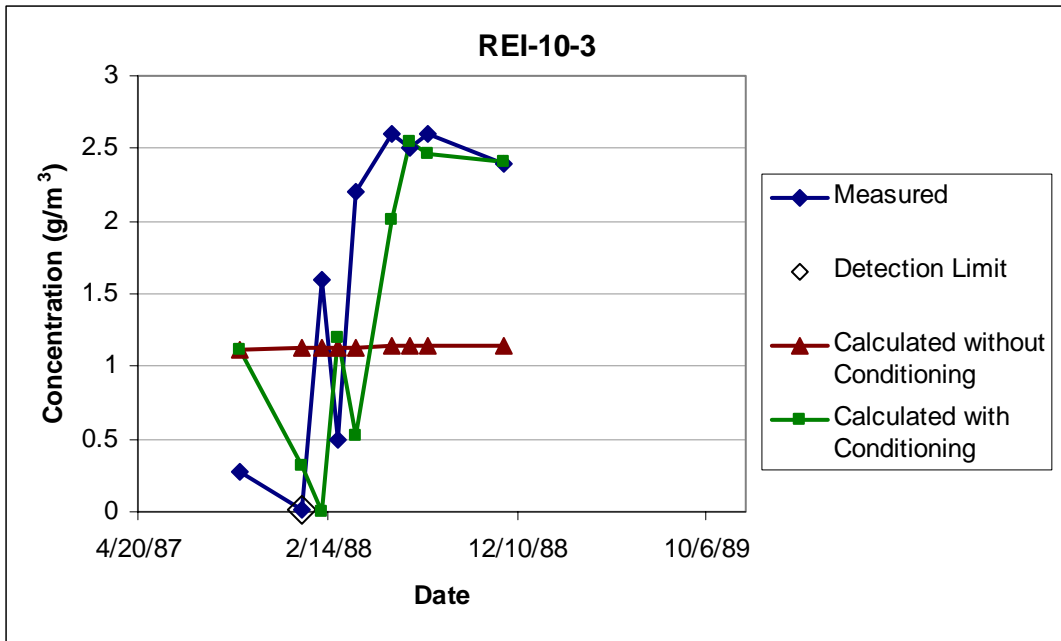


Figure F21. Comparison of measured and calculated benzene concentrations for well REI-10-3.

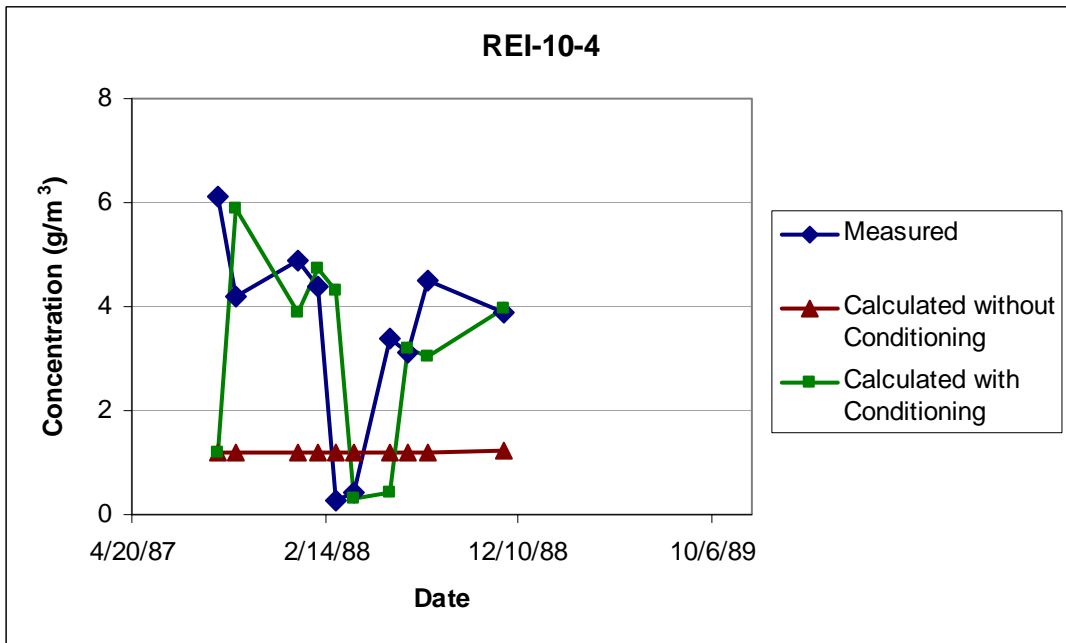


Figure F22. Comparison of measured and calculated benzene concentrations for well REI-10-4.

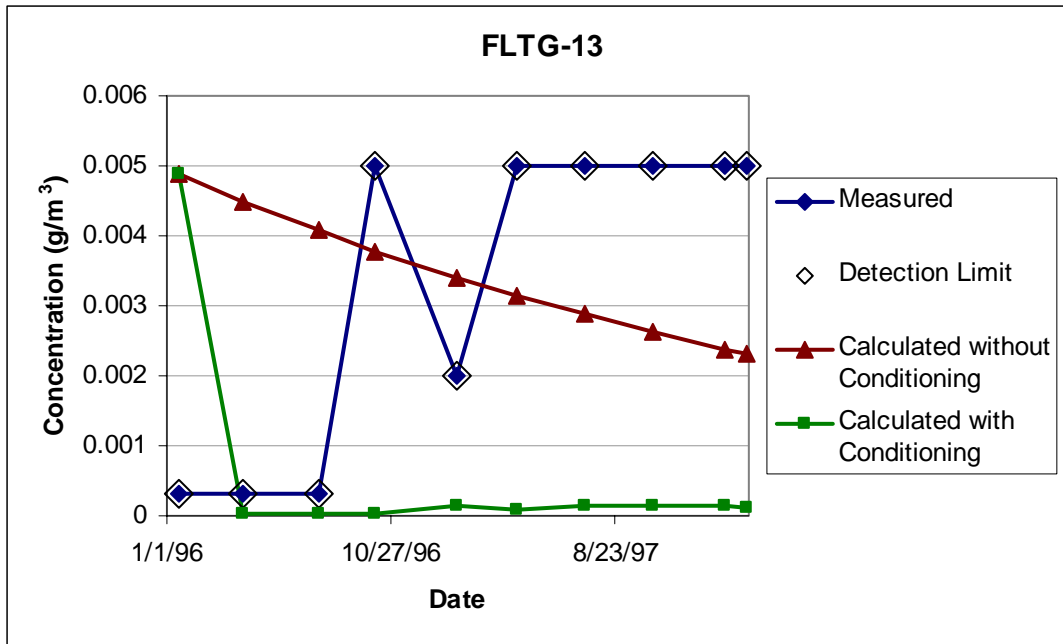


Figure F23. Comparison of measured and calculated benzene concentrations for well FLTG-13.

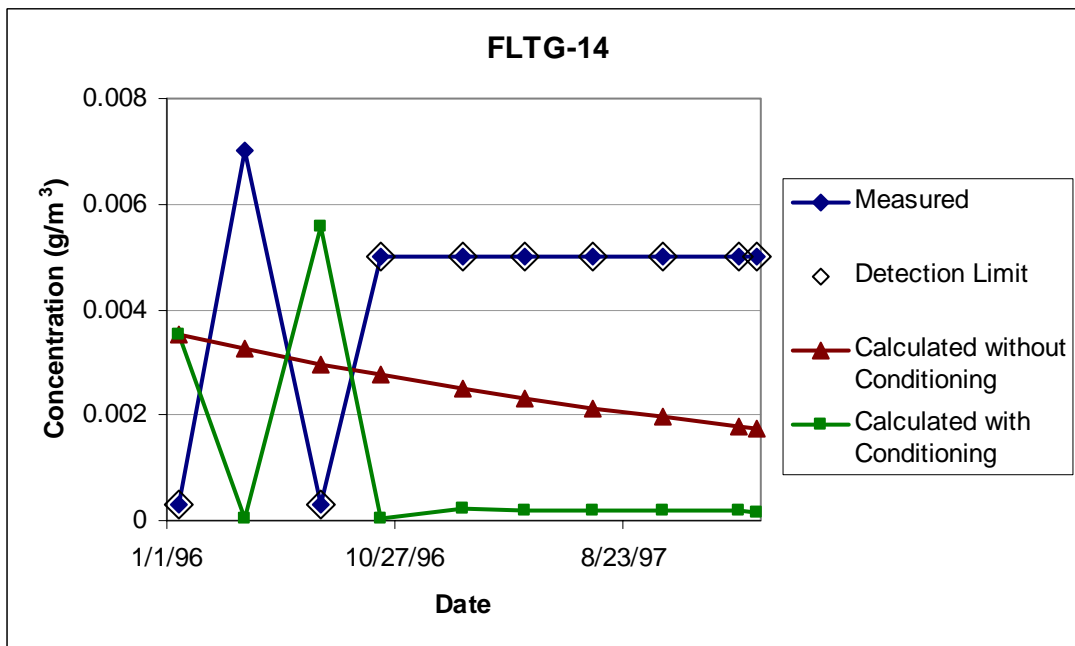


Figure F24. Comparison of measured and calculated benzene concentrations for well FLTG-14.

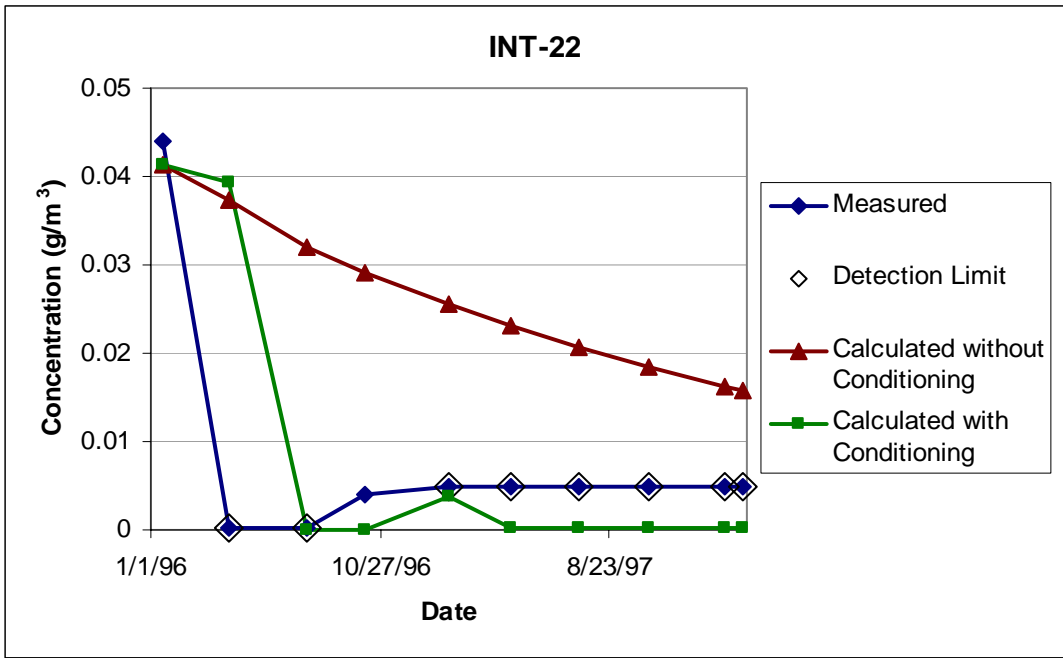


Figure F25. Comparison of measured and calculated benzene concentrations for well INT-22.

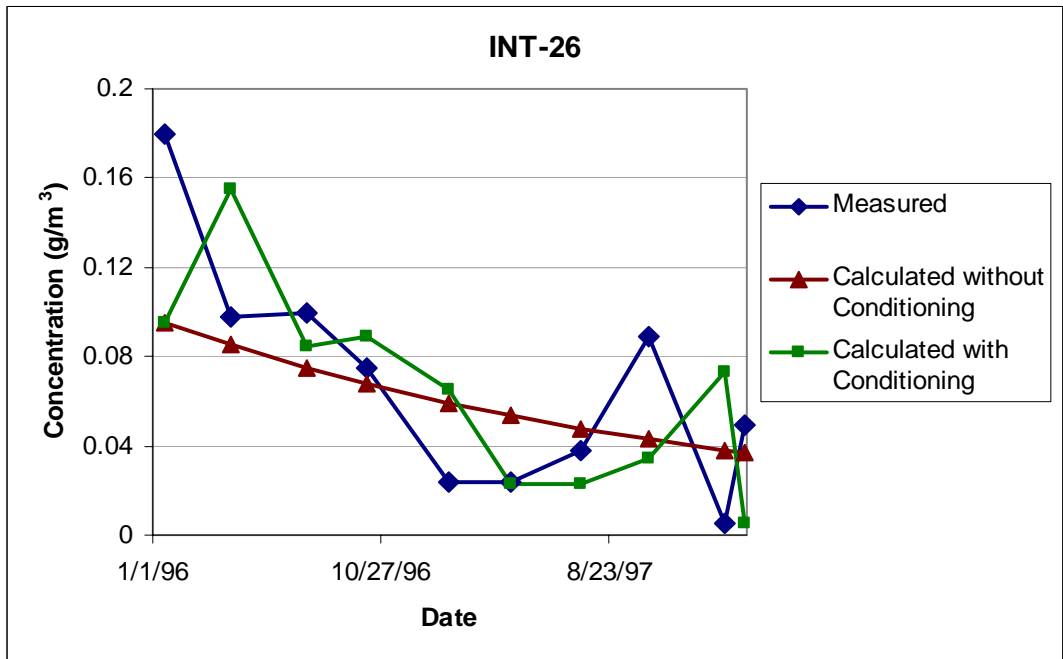


Figure F26. Comparison of measured and calculated benzene concentrations for well INT-26.

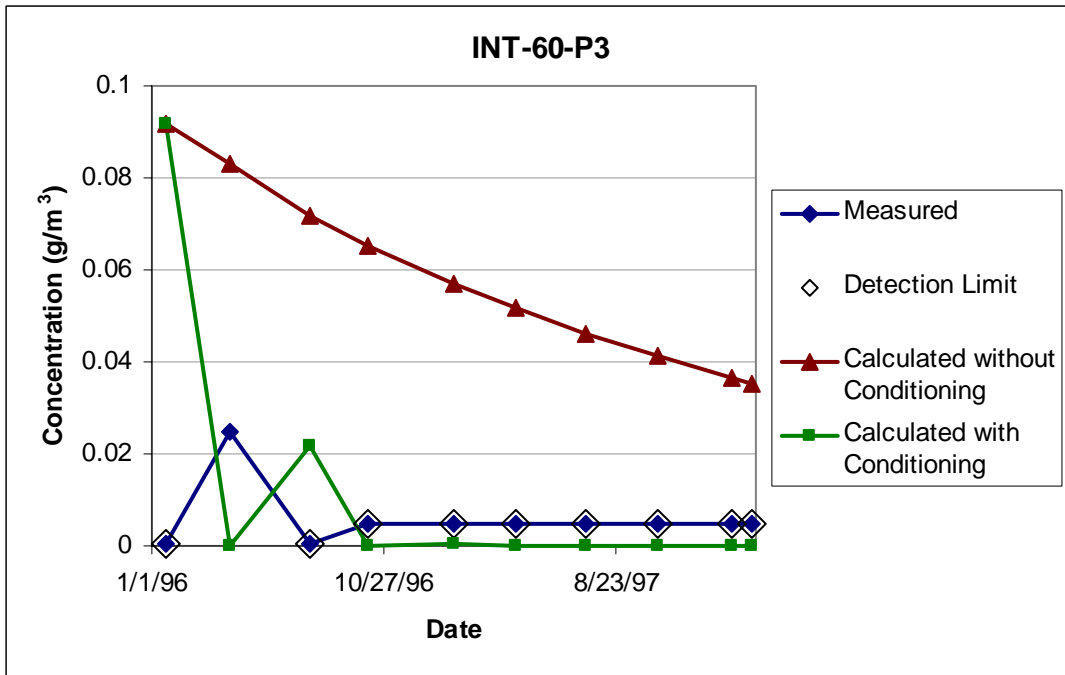


Figure F27. Comparison of measured and calculated benzene concentrations for well INT-60-P3.

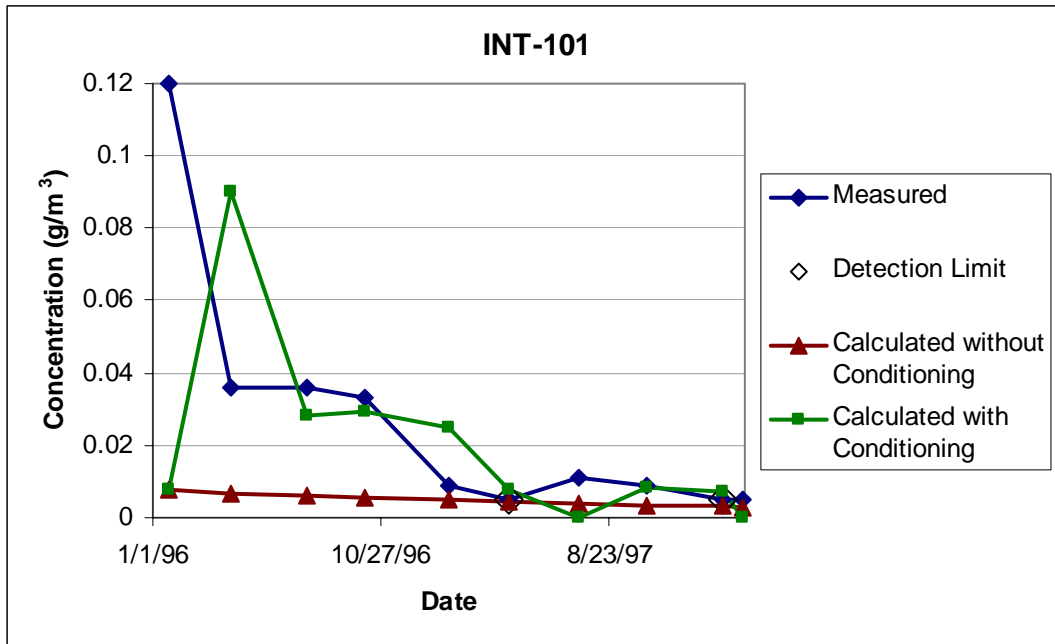


Figure F28. Comparison of measured and calculated benzene concentrations for well INT-101.

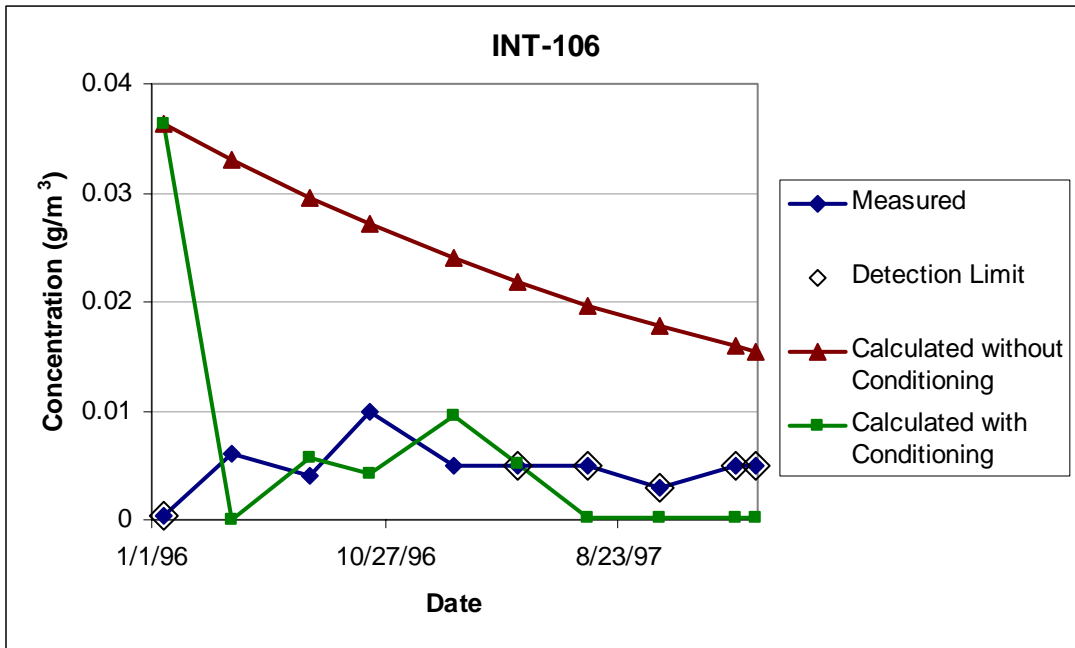


Figure F29. Comparison of measured and calculated benzene concentrations for well INT-106.

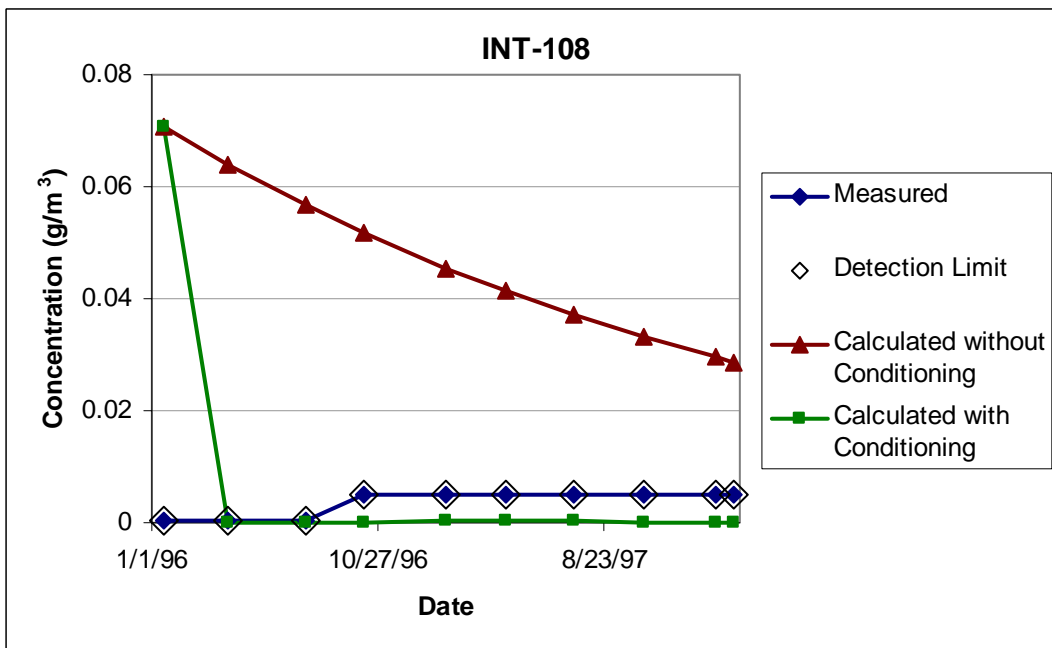


Figure F30. Comparison of measured and calculated benzene concentrations for well INT-108.

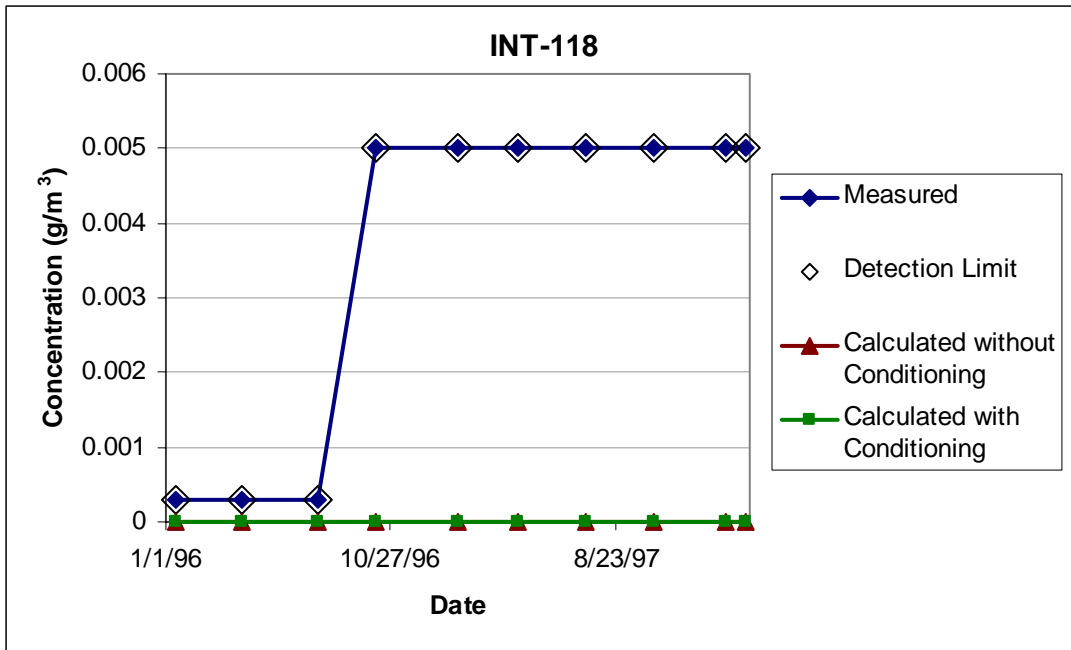


Figure F31. Comparison of measured and calculated benzene concentrations for well INT-118.

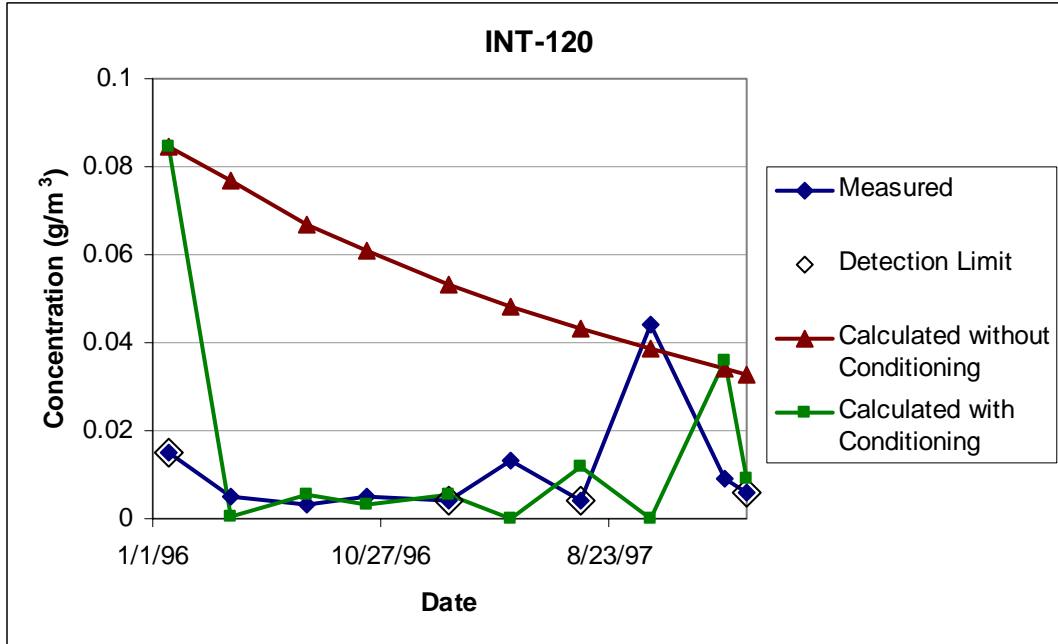


Figure F32. Comparison of measured and calculated benzene concentrations for well INT-120.

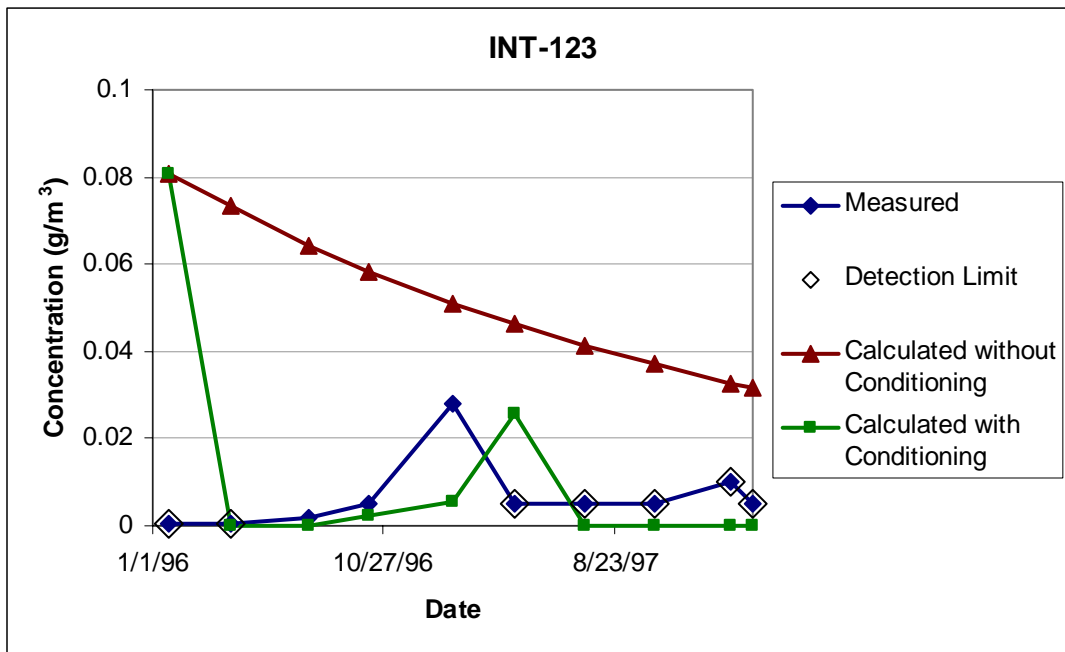


Figure F33. Comparison of measured and calculated benzene concentrations for well INT-123.

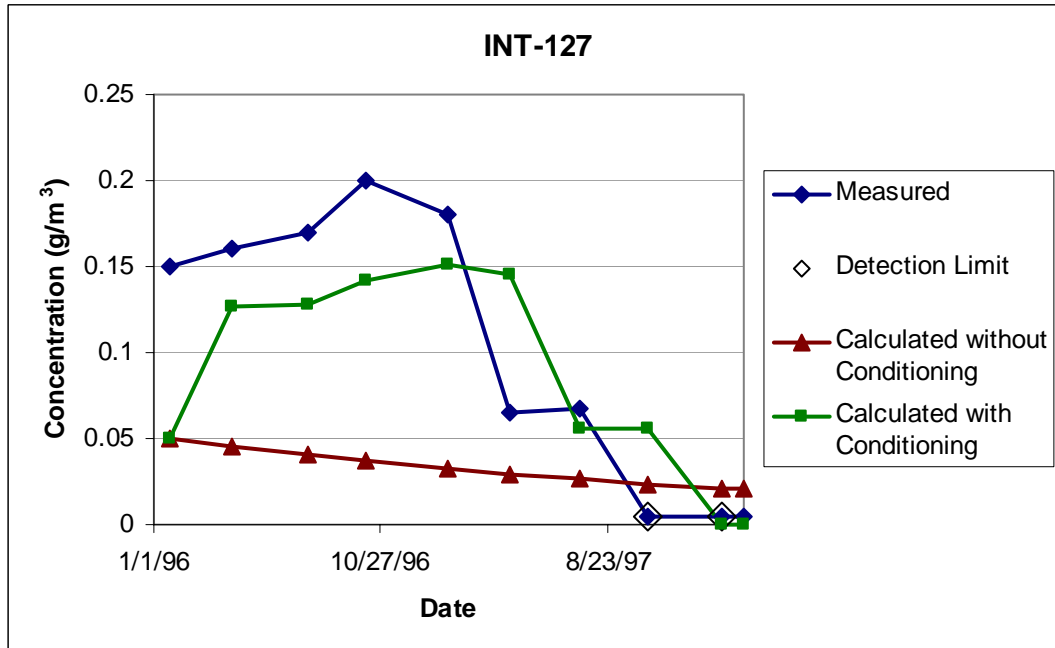


Figure F34. Comparison of measured and calculated benzene concentrations for well INT-127.

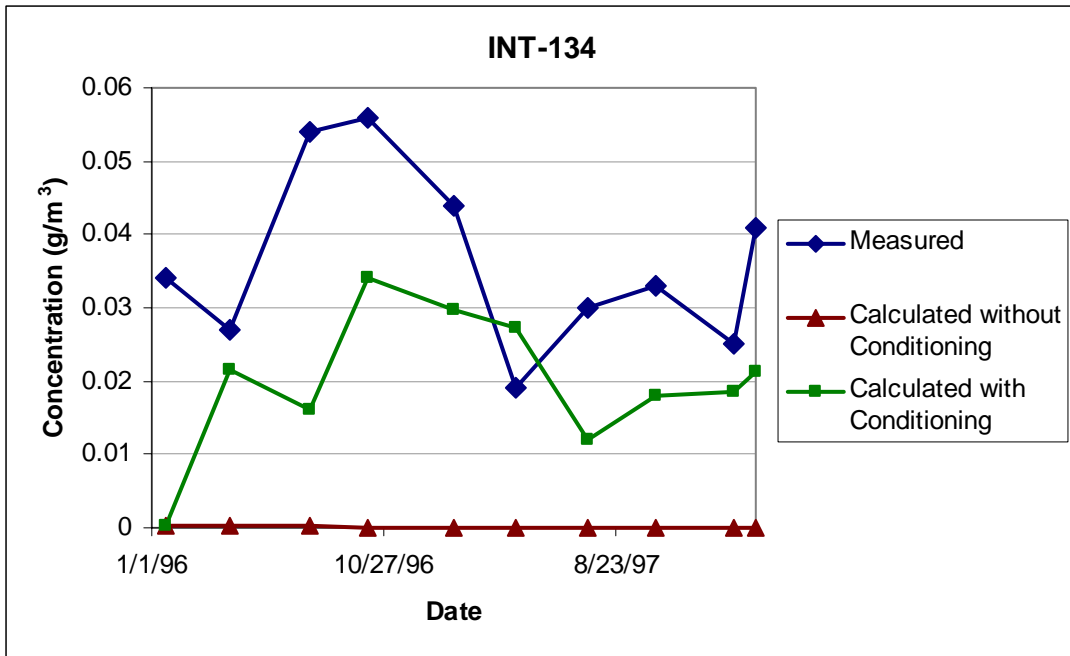


Figure F35. Comparison of measured and calculated benzene concentrations for well INT-134.

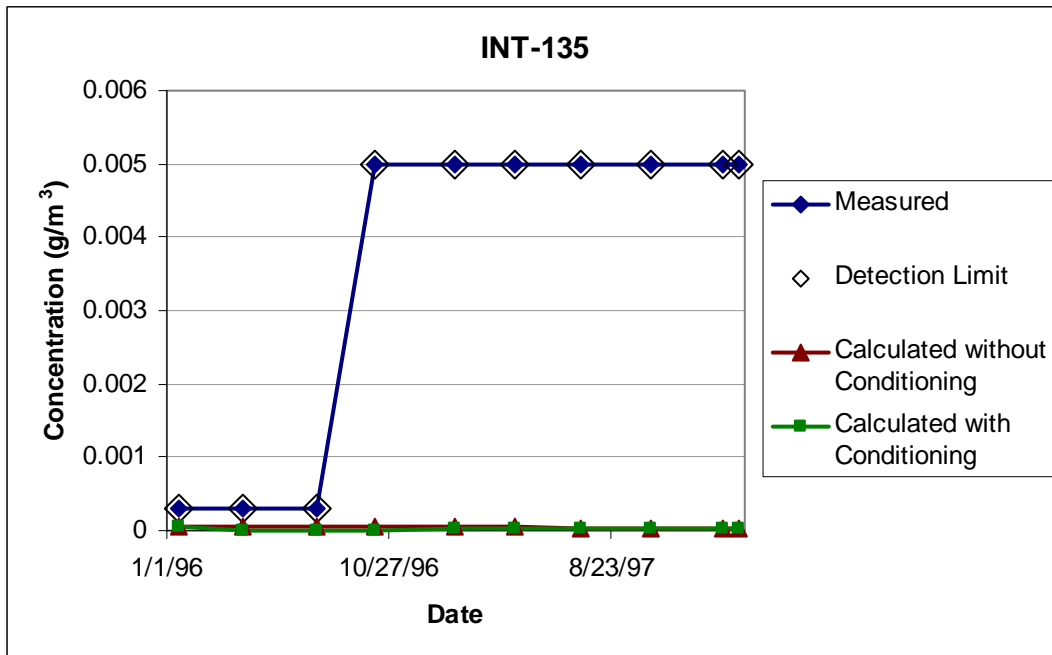


Figure F36. Comparison of measured and calculated benzene concentrations for well INT-135.

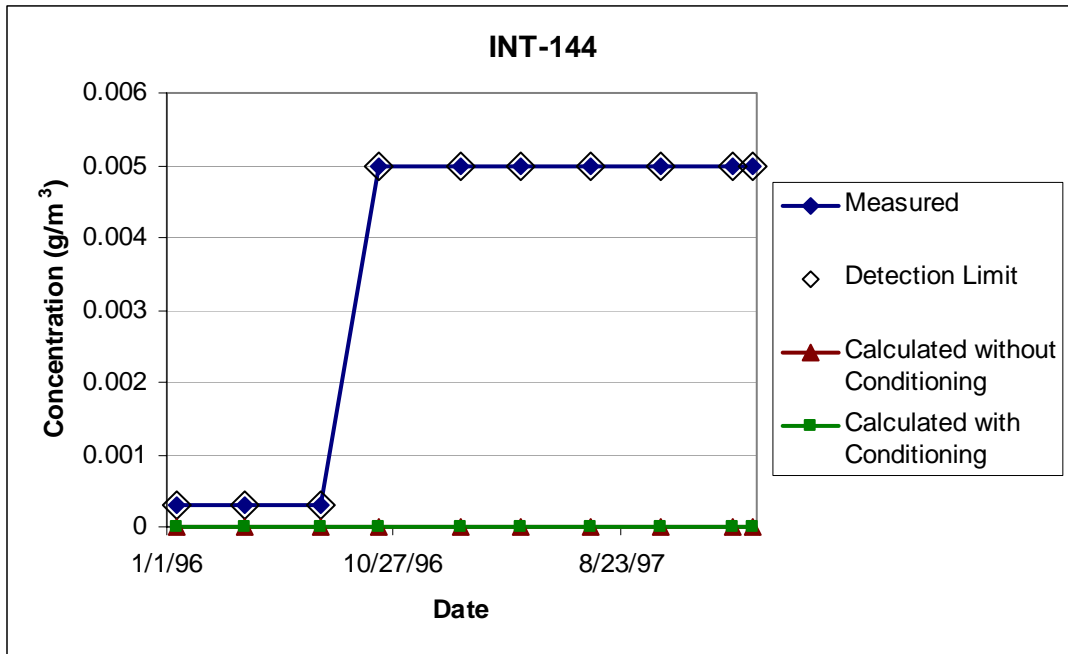


Figure F37. Comparison of measured and calculated benzene concentrations for well INT-144.

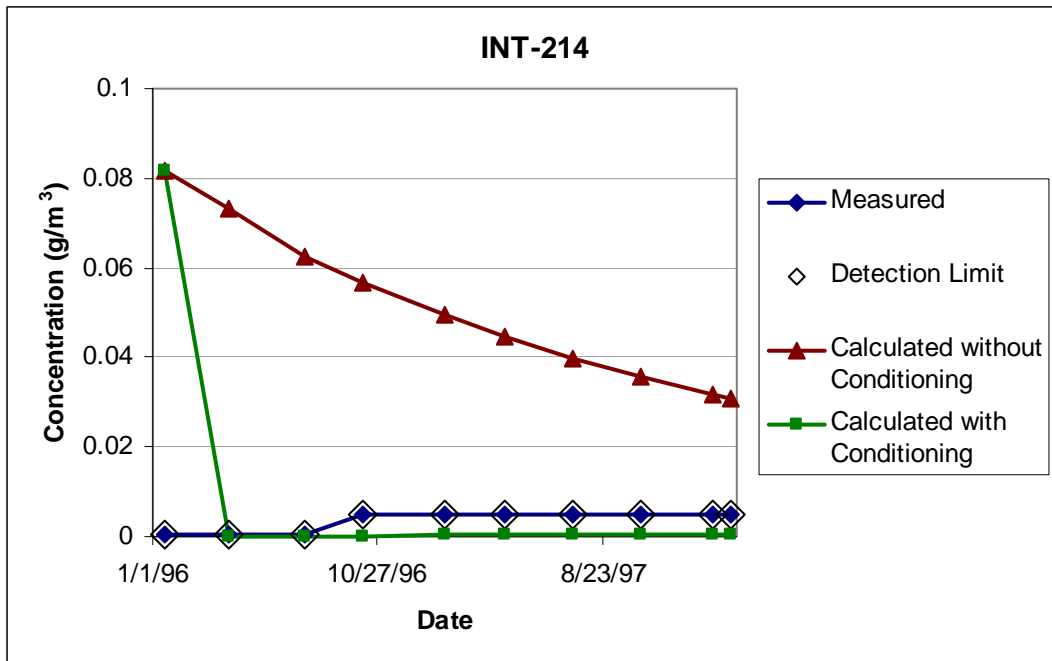


Figure F38. Comparison of measured and calculated benzene concentrations for well INT-214.

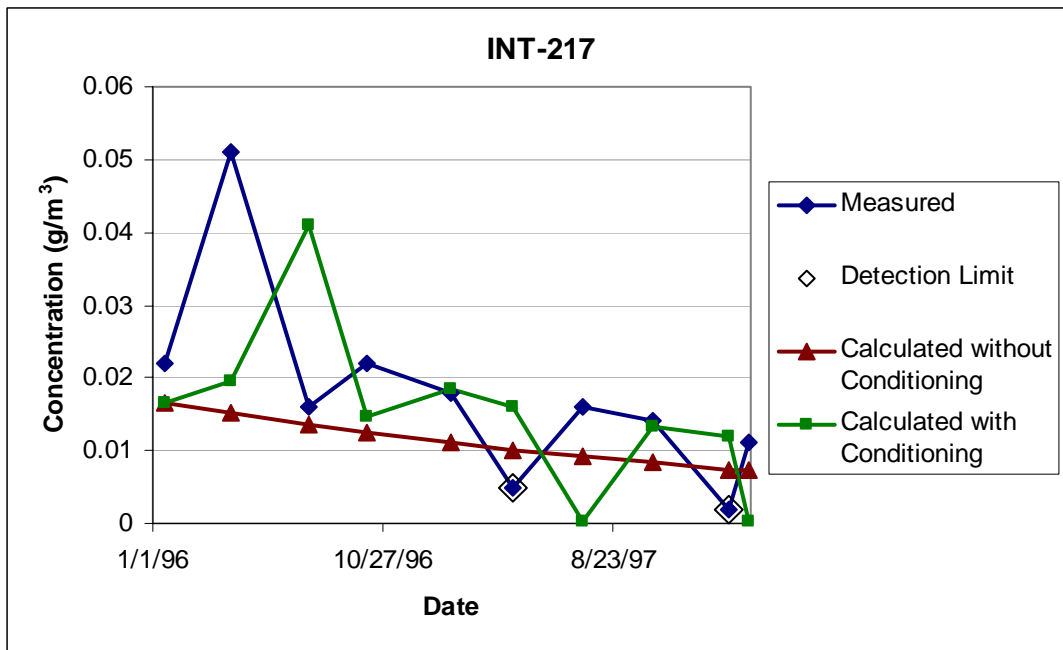


Figure F39. Comparison of measured and calculated benzene concentrations for well INT-217.

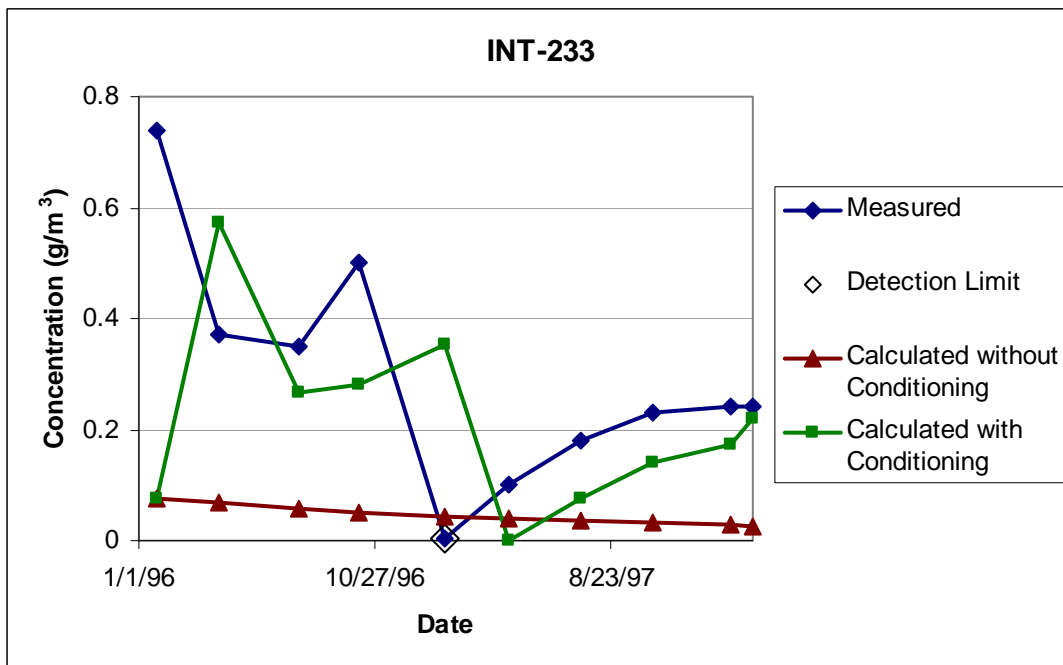


Figure F40. Comparison of measured and calculated benzene concentrations for well INT-233.

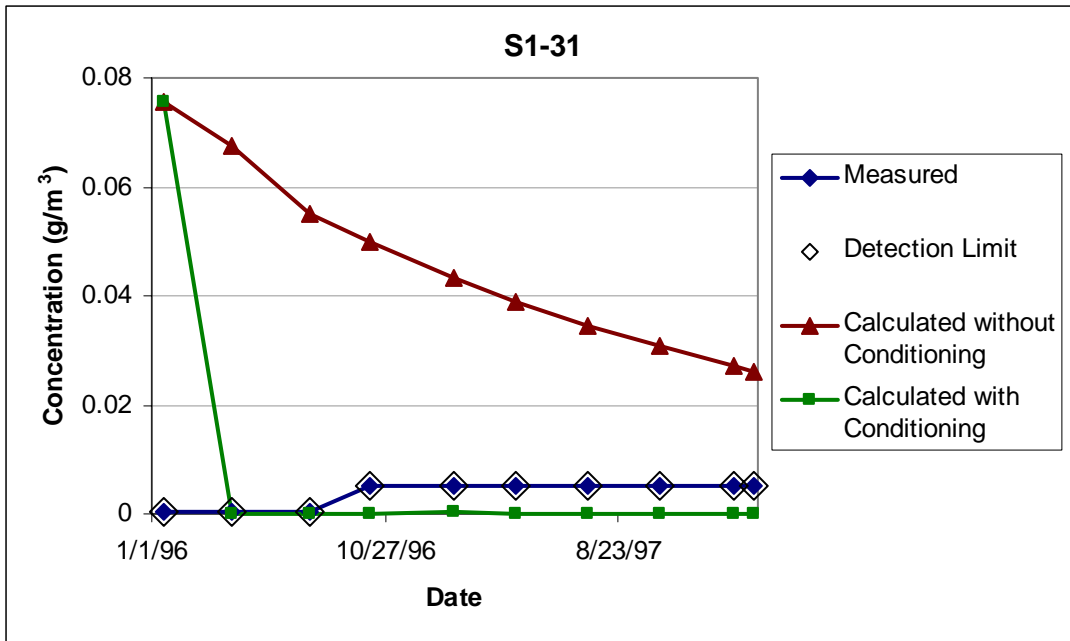


Figure F41. Comparison of measured and calculated benzene concentrations for well S1-31.

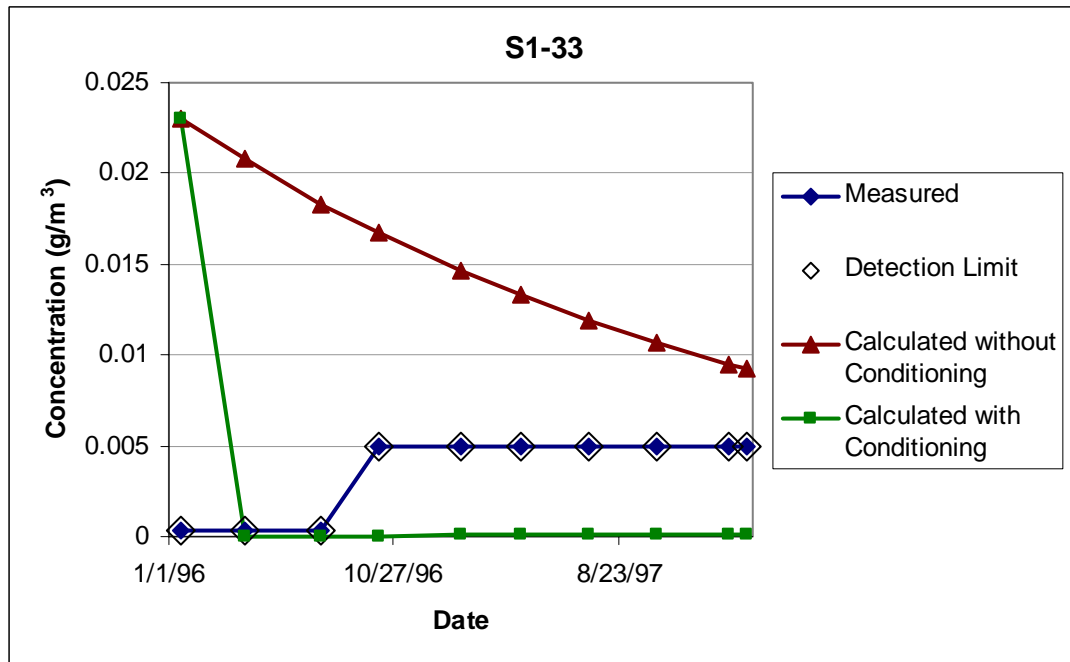


Figure F42. Comparison of measured and calculated benzene concentrations for well S1-33.

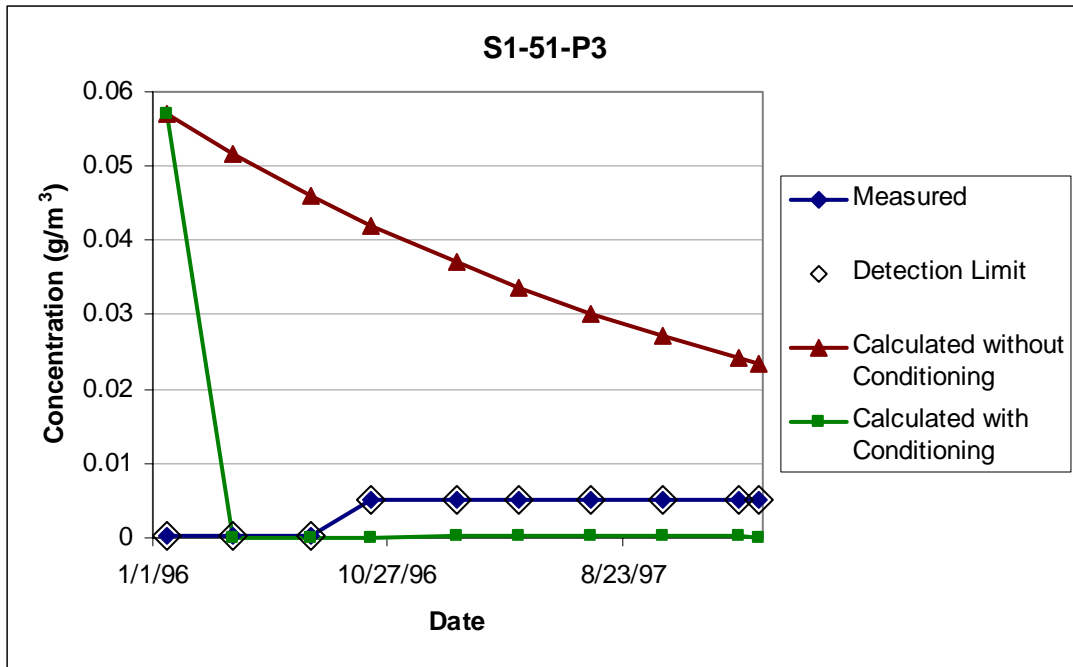


Figure F43. Comparison of measured and calculated benzene concentrations for well S1-51-P3.

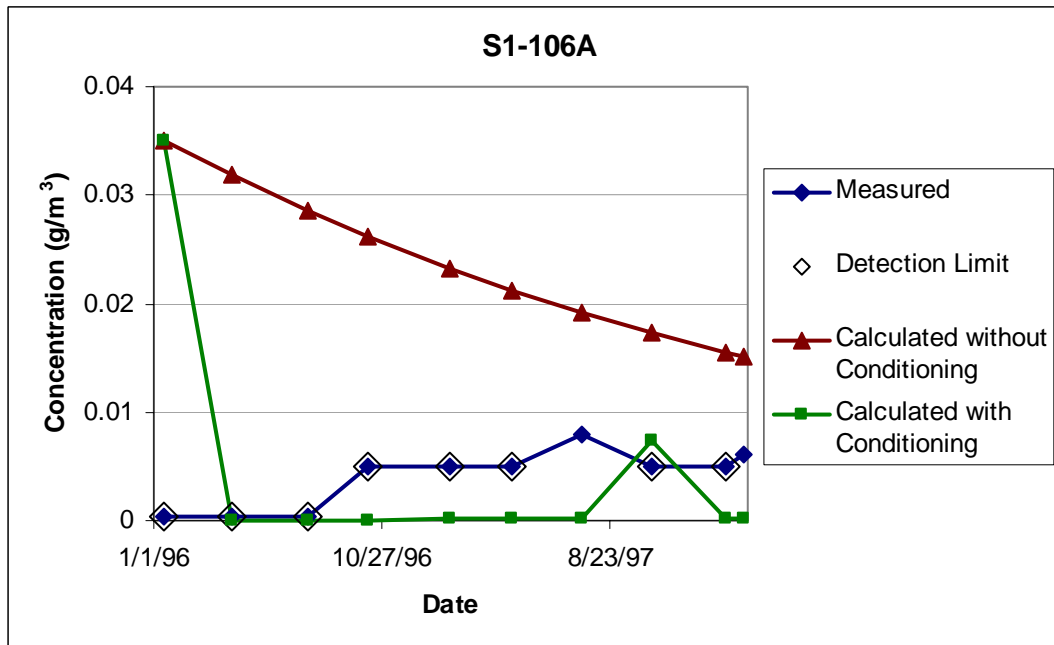


Figure F44. Comparison of measured and calculated benzene concentrations for well S1-106A.

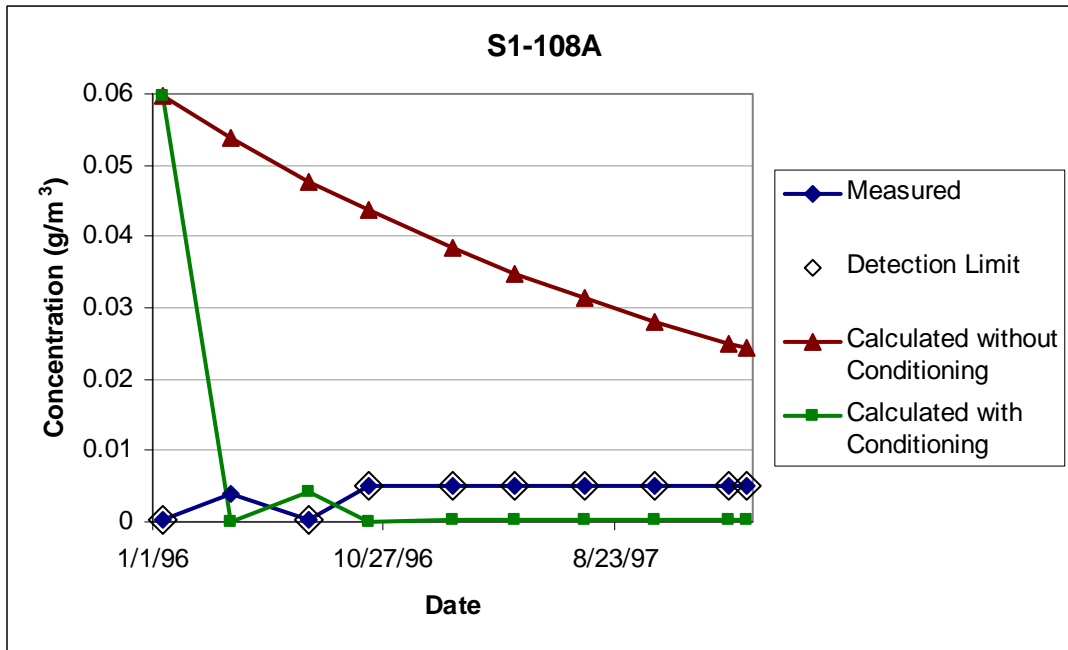


Figure F45. Comparison of measured and calculated benzene concentrations for well S1-108A.

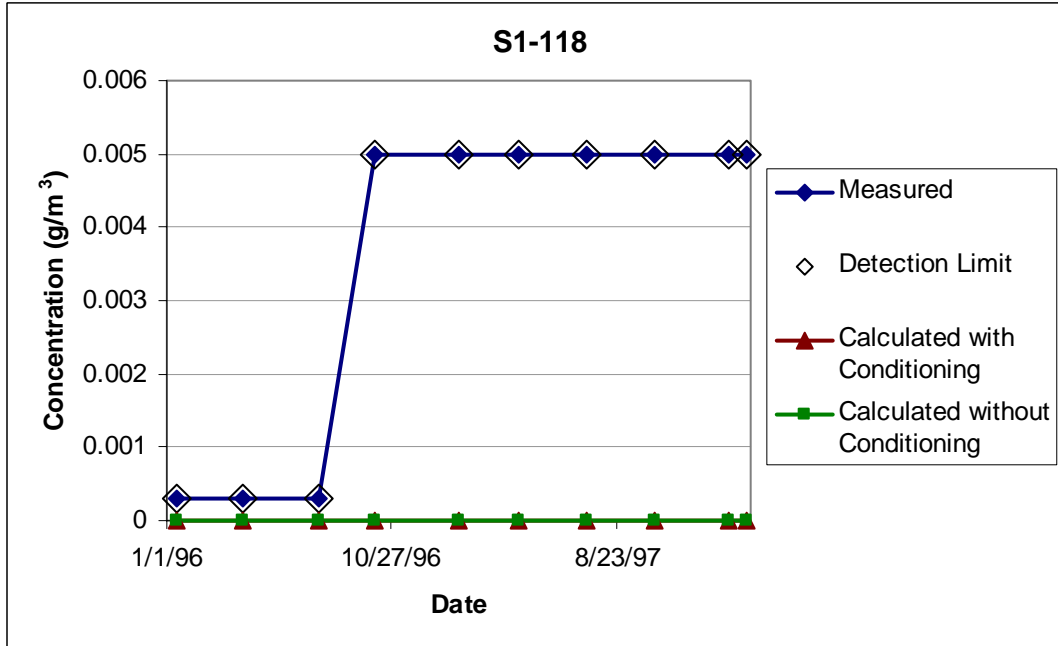


Figure F46. Comparison of measured and calculated benzene concentrations for well S1-118.

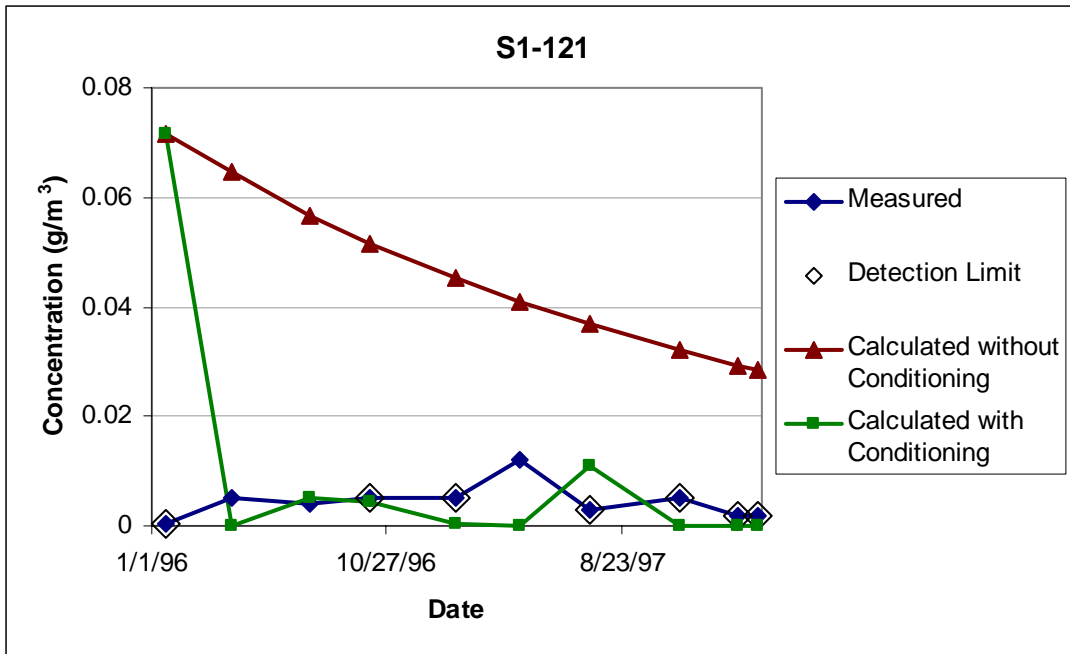


Figure F47. Comparison of measured and calculated benzene concentrations for well S1-121.

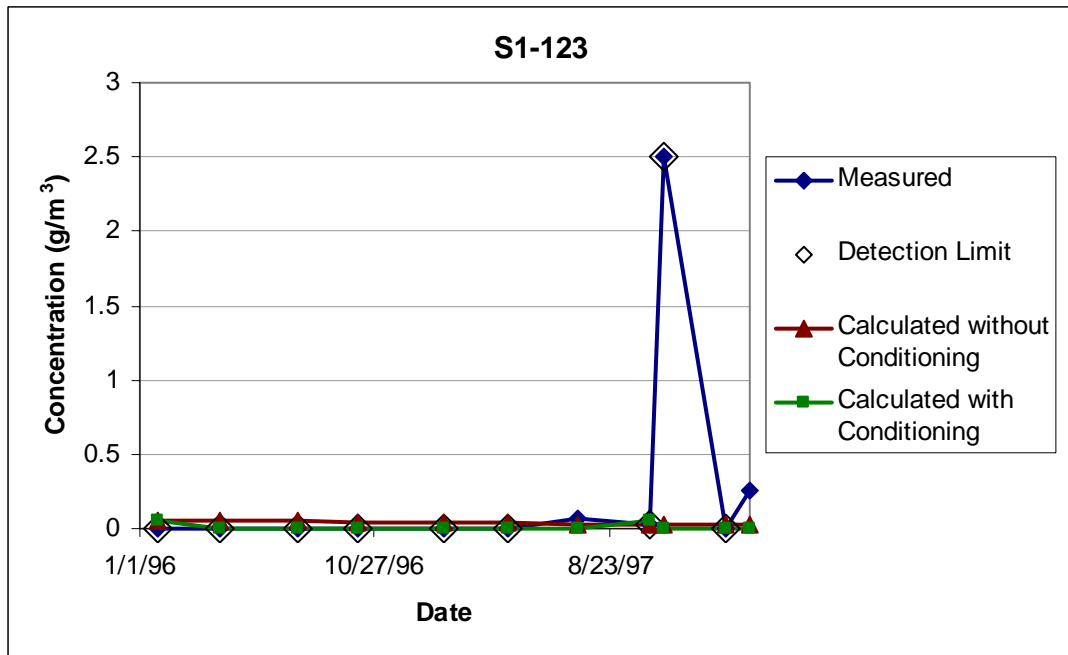


Figure F48. Comparison of measured and calculated benzene concentrations for well S1-123.

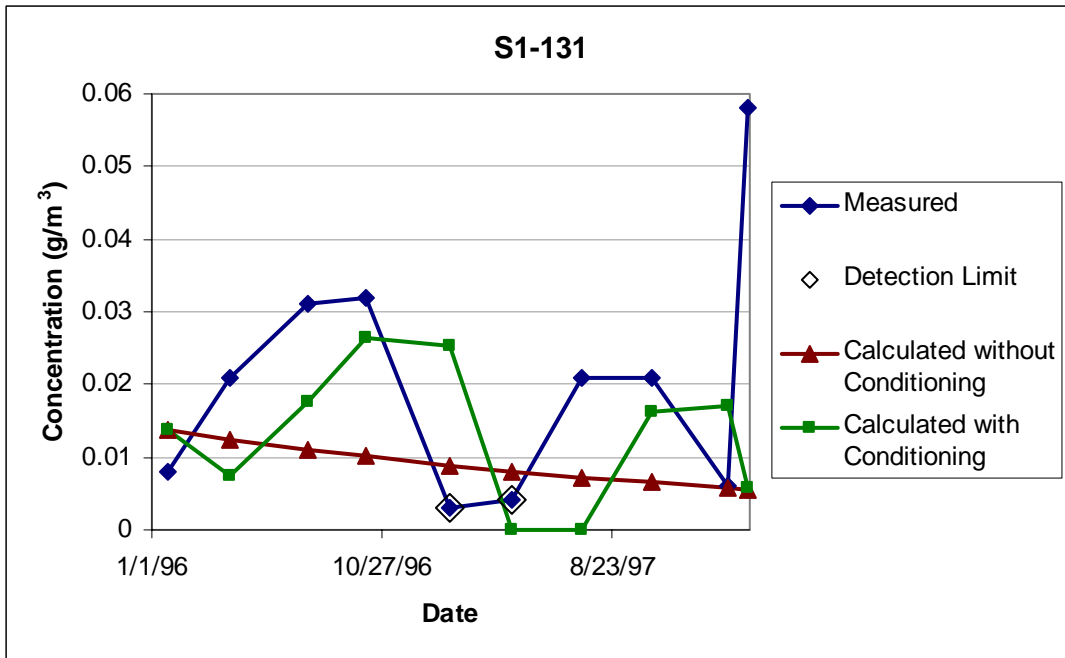


Figure F49. Comparison of measured and calculated benzene concentrations for well S1-131.

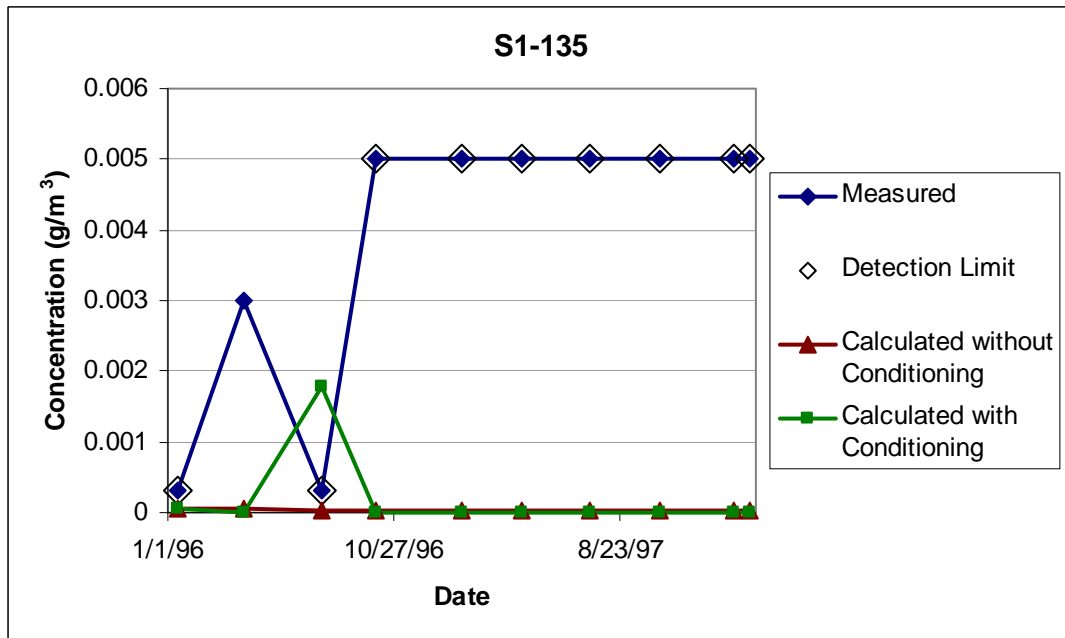


Figure F50. Comparison of measured and calculated benzene concentrations for well S1-135.

References

- Ang, A.H-S., and Tang, W.H. (1975) *Probability Concepts in Engineering Planning and Design, Volume 1 – Basic Principles*, John Wiley & Sons, Inc., New York, NY, 408 pp.
- Applied Hydrology Associates (1989) “French Limited Site Hydrogeologic Characterization Report”, Report to the French Limited Task Group.
- Applied Hydrology Associates (1996) “Natural Attenuation Modeling Progress Report, 4th Quarter, 1996”, Report submitted to U.S. Environmental Protection Agency, Region 6.
- Applied Hydrology Associates (1998) “Groundwater Sampling Report, 1st Quarter, 1998”, Report submitted to U.S. Environmental Protection Agency, Region 6.
- Berthouex, P.M. (1993) “A Study of the Precision of Lead Measurements at Concentrations Near the Method Limit of Detection”, *Water Environment Research*, Vol. 65, No. 5, pp. 620-629.
- Carrera, J., and Neuman, S.P. (1986) “Estimation of Aquifer Parameters under Transient and Steady-State Conditions, 1. Maximum Likelihood Method Incorporating Prior Information”, Vol. 22, No. 2, pp. 199-210.
- Carslaw, H.S. and Jaeger, J.C. (1959) *Conduction of Heat in Solids*, Oxford University Press, New York, 510 pp. (as cited by Galya 1997).
- Charbeneau, R.J. (2000) *Groundwater Hydraulics and Pollutant Transport*, Prentice-Hall, Inc., Upper Saddle River, NJ, 593 pp.
- El-Shaarawi, A.H., and Esterby, S.R. (1992) “Replacement of Censored Observations by a Constant: An Evaluation”, *Water Resources*, Vol. 26, No. 6, pp. 835-844.
- ENSR Consulting and Engineering (1991) “Shallow Aquifer and Subsoil Remediation Facilities Design Report”, Report to U.S. Environmental Protection Agency, Region 6, and Texas Water Commission.
- Fu, G. and Tang, Jianguo (1995) “Risk-Based Proof-Load Requirements for Bridge Evaluation”, *Journal of Structural Engineering*, Vol. 121, No. 3, pp. 542-556.
- Fujino, Y., and Lind, N.C. (1977) “Proof-Load Factors and Reliability”, *Journal of the Structural Division, Proceedings of the American Society of Civil Engineers*, Vol. 103, No. ST4, pp. 853-871.

- Galya, D.P. (1987) "A Horizontal Plane Source Model for Ground-Water Transport", *Ground Water*, Vol. 25, No. 6, pp. 733-739.
- Gilbert, R.B. (1999) "First-Order, Second-Moment Bayesian Method for Data Analysis in Decision Making," Geotechnical Engineering Center Report, Dept. of Civil Engineering, The University of Texas at Austin, Austin, TX, 50 pp.
- Gilbert, R.B., and Wang, D. (2003) "Framework for Extending the First-Order, Second-Moment Bayesian Method (SMBM) to Non-Normal Data", Draft Geotechnical Engineering Center Report, Dept. of Civil Engineering, The University of Texas at Austin, Austin, TX, 47 pp.
- Gilliom, R.J., and Helsel, D.R. (1986) "Estimation of Distributional Parameters for Censored Trace Level Water Quality Data. 1. Estimation Techniques", *Water Resources Research*, Vol. 22, No. 2, pp. 135-146.
- Greene, W.H. (1997) *Econometric Analysis*, Prentice-Hall, Inc., Upper Saddle River, NJ, 1075 pp.
- Gupta, V.K., and Sorooshian, S. (1985) "The Relationship between Data and the Precision of Parameter Estimates of Hydrologic Models", *Journal of Hydrology*, Vol. 81, pp. 57-77.
- Haas, C.N., and Scheff, P.A. (1990) "Estimation of Averages in Truncated Samples", *Environmental Science and Technology*, Vol. 24, No. 6, pp. 912-919.
- Howard, P.H. Boethling, R.S., Jarvis, W.F., Meylan, W.M., and Michalenko, E.M. (1991) *Handbook of Environmental Degradation Rates*, Lewis Publishers, Inc., Chelsea, MI, 725 pp.
- Journel, A.G., and Huijbregts, C.J. (1978) *Mining Geostatistics*, Academic Press, Inc., New York, NY, 600 pp.
- Kao, J., Howard, K., Mitchell, B., and Hinson, T. (1997) "Evaluation of Intrinsic Bioremediation of BTEX Contamination in Groundwater: A Case Study", International Conference on Advances in Ground-Water Hydrology – A Decade in Progress, Tampa, FL, pp. 36-46.
- Liu, S., Yen, S.T., and Kolpin, D.W. (1996) "Atrazine Concentrations in Near-Surface Aquifers: A Censored Regression Approach", *Journal of Environmental Quality*, Vol. 25, September-October, pp. 992-999.
- McBrayer, M.C. (1999) "Calibration of Groundwater Flow Models for Modeling and Teaching", Dissertation, The University of Texas at Austin, 403 pp.

- Muchard, S.M. (1997) "Estimating Groundwater Transport Parameters with a Second-Moment Bayesian Method", Master of Science Thesis, The University of Texas at Austin, 182 pp.
- Nowak, A.S., and Tharmabala, T. (1988) "Bridge Reliability Evaluation Using Load Tests", *Journal of Structural Engineering*, Vol. 114, No. 10, pp. 2268-2279.
- Porter, P.S., Ward, R.C., and Bell, H.F. (1988) "The Detection Limit", *Environmental Science and Technology*, Vol. 22, No. 8, pp. 856-861.
- Rodriguez, S.G.H., Henriques, C.C.D., Ellwanger, G.B., and de Lima, E.C.P. "Structural Reliability with Truncated Probability Distributions", *Proceedings of the International Conference on Offshore Mechanics and Arctic Engineering*, OMAE, July 5-9, 1998, Lisbon, Portugal, 6 pp.
- Southwestern Environmental Consulting, Inc. (1996) "Site Closure Plan, French Limited Project", Report to the U.S. Environmental Protection Agency and the Texas Natural Resource Conservation Commission.
- Steward, M.G. and Val, D.V. (1999) "Role of Load History in Reliability-Based Decision Analysis of Aging Bridges", *Journal of Structural Engineering*, Vol. 125, No. 7, pp. 776-783.
- Umble, E.J., Seaman, J.W., and Martz, H.F. (1999) "Distribution-free Bayesian Approach for Determining the Joint Probability of Failure of Materials Subject to Multiple Proof Loads", *Technometrics*, Vol. 41, No. 3, pp. 183-191.
- U.S. Environmental Protection Agency (2003a) "*The Environmental Protection Agency Code of Federal Regulations Title 40: Protection of Environment*", September 4, 2003, <<http://www.epa.gov/epahome/cfr40.htm>>.
- U.S. Environmental Protection Agency (2003b) "*Integrated Risk Information System*", December 22, 2003, <<http://www.epa.gov/iris/>>.
- Vanmarcke, E.H. (1983) *Random Fields: Analysis and Synthesis*, The MIT Press, Cambridge, MA, 382 pp.
- Vroblesky, D.A., and Chapelle, F.H. (1994) "Temporal and Spatial Changes of Terminal Electron-Accepting Processes in a Petroleum Hydrocarbon-Contaminated Aquifer and the Significance for Contaminant Biodegradation", *Water Resources Research*, Vol. 30, No. 5, pp. 1561-1570.
- Wagner, B.J. (1992) "Simultaneous Parameter Estimation and Contaminant Source Characterization for Coupled Groundwater Flow and Contaminant Transport Modelling", *Journal of Hydrology*, Vol. 135, pp. 275-303.

Wang, D. (2002) "Development of a Method for Model Calibration with Non-Normal Data", Dissertation, The University of Texas at Austin, 265 pp.

Vita

Cynthia Ann Finley was born to Barbara A. and James R. Finley in Houston, Texas on May 1, 1973. After graduating from Bothell High School, Bothell, Washington, in 1991, she attended Texas A&M University in College Station, Texas, and majored in civil engineering. She spent summers as an undergraduate working at Geotech Consultants, Inc. in Bellevue, Washington, Structural Design Associates in Lynnwood, Washington, and Clark Johnson Engineers in Bellevue, Washington. After earning a Bachelor of Science degree, magna cum laude, in May 1995, she began graduate studies at the University of Washington in September 1995. She earned her Master of Science in Civil Engineering in June 1997. Ms. Finley entered the University of Texas at Austin in August 1996 to begin work on her Ph.D. She spent the summer of 2000 at the Hong Kong University of Science and Technology.

Permanent address: P.O. Box 1051, Kittitas WA 98934

This dissertation was typed by the author.